AN INVESTIGATION OF THE ABERRANT EXPRESSION AND ACTIVATION OF RECEPTOR TYROSINE KINASES IN HODGKIN'S LYMPHOMA

BY

FATHIMA ZUMLA CADER

A thesis submitted to

The University of Birmingham

for the degree of

DOCTOR OF PHILOSOPHY

School of Cancer Sciences

University of Birmingham

June 2011

ABSTRACT

Multiple receptor tyrosine kinases (RTK) have been shown to be over-expressed in the malignant Hodgkin Reed-Sternberg (HRS) cells of Hodgkin lymphoma (HL). However, the activation status of many of these RTKs has not been studied. Furthermore, the contribution of aberrant RTK activation to the pathogenesis of HL is currently unknown.

In chapter three, I have shown using a human phospho-receptor tyrosine kinase array that HL cells are characterised by the activation of multiple RTK. I have confirmed the over-expression and activation in HRS cells of two of these RTK, MET and RON and provided preliminary evidence that MET is negatively regulated by LRIG1 in these cells.

In chapter four, I have shown for the first time that DDR1 is over-expressed in primary HRS cells. Furthermore, I have shown that in many cases, DDR1-expressing HRS cells are intimately associated with collagen, the ligand for DDR1. However, knockdown of DDR1 in a HL cell line in which DDR1 appeared to be constitutively phosphorylated revealed no detectable change in phenotype and few transcriptional changes. While exploring possible reasons for this, I identified that HL cells express multiple DDR1 isoforms including several novel transcripts.

Finally, in chapter five, I have shown that HL cells are sensitive to the RTK inhibitor, dasatinib. Furthermore, consistent with the aberrant activation of multiple RTKs in HL cells, I observed that these cells were also sensitive to lestaurtinib and dovitinib, two next generation multiple-target RTK inhibitors.

ACKNOWLEDGMENTS

I would like to thank my supervisors Professor Paul Murray, Dr Martina Vockerodt and Dr Pamela Kearns for all their time, patience and expert advice over the years. I would also like to acknowledge other members of the Murray/Woodman group both past and present. In particular, Dr Shikha Bose and Dr Jennifer Anderton not only supported me through my time in the lab but have been friends through the highs and lows. A special mention also goes to Ezster Nagy who has helped me with FACS analysis. I have been fortunate to work amongst truly wonderful people, and I am grateful for the opportunities provided by the PhD programme.

Over the years, my family have supported me in all my endeavours and provided me with the opportunities that have taken me to where I am today. Above all else, I want to thank my Mum and Dad whose love and support has seen me through all my trials and tribulations.

Finally, I would like to thank Leukaemia and Lymphoma Research who generously funded this project, and the Children's Cancer and Leukaemia Group for providing samples.

CONTENTS

LIST OF FIGURES

LIST OF TABLES

LIST OF COMMON ABBREVIATIONS

ASV	alternative splice variant
BART	BAM HIA rightward transcript
BCR	B cell receptor
BL	Burkitt's lymphoma
bp	base pair
cDNA	complementary DNA
DDR1	discoidin domain receptor 1
DMSO	dimethyl sulphoxide
DNA	deoxyribonucleic acid
EBER	Epstein-Barr encoded RNA
EBNA	Epstein-Barr nuclear antigen
EBNA-LP	EBNA leader protein
EBV	Epstein-Barr virus
ECM	extracellular matrix
FCS	fetal calf serum
FITC	fluorescein isothiocyanate
GAPDH	glyseraldehyde-3-phosphate dehydrogenase
GC	germinal centre
HL	Hodgkin's lymphoma
HRS	Hodgkin and Reed-Sternberg
IHC	immunohistochemistry
IM	infectious mononucleosis
IP	immunoprecipitation
JAK	janus kinase

LP	lymphocyte predominant
LMP	latent membrane protein
MC	mixed cellularity
miRNA	micro-RNAs
mRNA	messenger-RNA
NF-κB	nuclear factor kappa –light chain- enhancer of activated B cells
NLPHL	nodular lymphocyte predominant HL
NPC	nasopharyngeal carcinoma
NS	nodular sclerosis
PBS	phosphate-buffered saline
PCR	polymerase chain reaction
PI3K	phospho-inositide 3 kinase
PTLD	post-transplant lymphoproliferative disease
RNA	ribonucleic acid
RON	recepteur d'origine nantais
RT-PCR	reverse transcriptase polymerase chain reaction
STAT	signal transducer and activator of transcription
WHO	World Health Organization

CHAPTER 1

Introduction

1.1 Hodgkin's lymphoma

1.1.1 Introduction

Hodgkin's disease was first recognised as a clinical entity by Thomas Hodgkin in 1832. His report was based on the post-mortem description of several cases presenting with cervical lymphadenopathy, night sweats and cachexia[1]. It was over 60 years later that Dorothy Reed and Carl Sternberg identified the large malignant mononuclear and binucleated cells, now referred to as the Hodgkin and Reed-Sternberg cells (HRS)[2]. The disease was renamed Hodgkin's lymphoma (HL) when the neoplastic and lymphoid origin of HRS cells became apparent[3]. HL is unlike any other malignancy as, in most cases, the pathognomonic HRS cells and its variants only constitute approximately 1% of the cell population and are surrounded by a non-neoplastic infiltrate of T and B cells, eosinophils, neutrophils, plasma cells, histiocytes, fibroblasts and extracellular matrix(ECM)[4].

1.1.2 Classification

The diverse histological expression of HL has led to difficulties in its diagnosis and classification. HL is sub-classified according to the World Health Organisation (WHO) scheme which is based on biology, clinical features, morphology, immunophenotype and composition of the infiltrate[3]. HL exists as two distinct disease entities: classical HL (cHL) and nodular lymphocyte predominant HL (NLPHL). Within cHL there are four subtypes: nodular sclerosis (NS), mixed cellularity (MC), lymphocyte depleted (LD) and lymphocyte rich (LR) HL. These subtypes differ according to their clinical features, growth pattern, presence of fibrosis and composition of the cellular background but not in their immunophenotype or genetic features[5-8].

The HRS cells of cHL are large with abundant cytoplasm and can have two or more oval lobulated nuclei containing prominent "owl-eye" eosinophilic nucleoli with perinuclear clearing observed on haematoxylin and eosin (H&E) stain. Variants include the mononuclear Hodgkin cells and 'lacunar cells' characteristic of the NSHL form where the cytoplasm shrinks during fixation and tissue processing, leaving an empty space around the nucleus. Some HRS cells contain dense cytoplasm and pyknotic nuclei and are referred to as 'mummified cells' (Figure 1.1)[3].

NSHL is the commonest form of cHL in the western world accounting for approximately 70% of all cases[9]. It is characterised by nodules containing HRS cells separated by dense collagen bands. These collagen bands are largely absent in MCHL, instead the lymph node architecture is obliterated by a diffuse infiltrate, which can vary greatly in composition[3]. LRHL is similar to NLPHL but is distinguished by a morphology and immunophenotype consistent with cHL[5;10]. LDHL is the rarest cHL subtype, accounting for less than 1% of cases worldwide. It is the least well understood of all subtypes and consequently has undergone several re-classifications but a unifying feature is the presence of numerous HRS cells and fewer background lymphocytes in the inflammatory infiltrate [10;11].

NLPHL represents only 5% of all HL. Unlike classical HRS cells, the malignant cells of NLPHL referred to as lymphocyte predominant (LP) cells, are smaller and express CD20, a B cell marker but often lack the cell surface markers CD30 and CD15 characteristic of cHL [3;12].

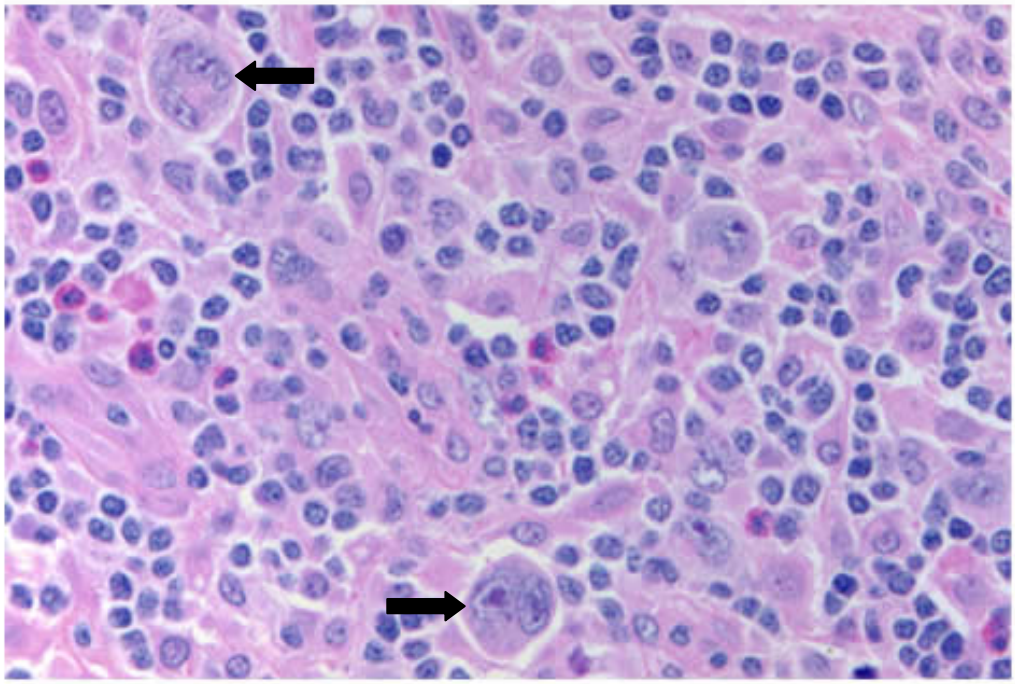

Figure 1.1 H&E stain of classical Hodgkin's lymphoma. Multinucleated HRS cells (black arrows) are seen in a cellular background rich in lymphocytes and containing some histiocytes and eosinophils[13].

1.1.3 Epidemiology of paediatric HL

The complex epidemiology of HL suggests several different factors are involved in the development of HL. In North America and European countries, HL accounts for approximately 6% of all childhood cancers with an incidence of 4.5-6.0 per million. By comparison, the incidence of paediatric HL in developing countries exceeds 7 per million[14]. In 1966, MacMahon identified a bimodal pattern of HL incidence in the USA characterised by an increasing incidence in childhood which peaks in young adults and a second peak in adults between 45-55 years[15]. Geographical variation was further analysed by Correa and O'Connor, who described three patterns of HL incidence that were related to economic development and urbanization. Pattern I, prevailing in developing countries, has incidence peaks in early childhood with 70% of paediatric HL occurring in children under 10 years. This pattern also has a second peak of HL incidence in adults over 60 years. MC and LD subtypes are most common in these populations. Pattern III, found in urban areas of developed nations, has a low incidence in childhood but shows a peak in young adults (15-30 years) and is usually of the NS subtype. Pattern II is an intermediate pattern between type I and III and is found in the rural regions of developed countries[16].

MacMahon initially hypothesised that an infectious agent was responsible for the early peak in HL incidence observed in young adults. This possibility is supported by several pieces of evidence. First, there is a peak in HL incidence in young adults and of the NS subtype from February to March[17-19]. Second, HL incidence shows a space-time clustering in young adults with small groups of patients presenting within one year who live within 1 km of each other[20;21]. Third, the epidemiology of HL was proposed to follow the poliovirus model which predicts the same infectious agent causes childhood HL and HL of young adults who develop

disease as a consequence of delayed infection. Consistent with this, children from low socioeconomic households with large sibships have an increased incidence of childhood HL while households with higher parental income and education level show an increased risk of developing HL during early adulthood[22]. The infectious agent suggested to be involved in HL pathogenesis was the Epstein Barr virus (EBV). The association of EBV with HL will be discussed in detail in section 1.3.

Familial studies show a 3 to 9 fold increased risk of developing cHL in first degree relatives[23]. Although this maybe a result of environmental influences, a genetic component is supported by a high concordance in monozygotic twins who have a 99-fold increased risk of HL compared to dizygotic twins[24]. In view of these genetic and viral links, the human leukocyte antigen (HLA) gene loci have been considered to be a possible site for a susceptibility gene for HL. The HLA class I region in particular, B5, B8, B18 and A1, has been reported to be associated with 60-70% of familial HL[25]. Furthermore, individuals carrying the class I alleles HLA-A *0101 and HLA-A*0201 appear to have a modified response to viral infection which may be an important determinant of EBV-related HL[26].

Class II antigens have been implicated in both the predisposition to HL and disease resistance. An association with the DPB1*0301 allele was proposed but an extended analysis of multiple HLA class II loci (e.g. DRB1, DQA1, DQB1, and DPB1) discounted an independent role of DPB1. Klitz *et al*., conducted an unmatched case control study and reported that in the NS subtype (but not other subtypes) the DRB1*1501, DQB1*0602, and DRB1*1104 alleles confer risk, while DRB1*1601, DRB1*0404, and DQB1*0303 alleles are protective[27-30].

A recent genome-wide association study of HL not only confirmed a strong HLA association and also identified three new susceptibility loci at 2p16.1 (*REL*), 8q24.21 (*PVT1*) and 10p14 (*GATA3*)[31]. Both the *REL* and *GATA3* genes encode proteins that are important in the pathogenesis of HL. PVT1 expression is as yet unreported in HL, however 20% of Burkitt's lymphoma (BL) harbour t(2;8) or t(8;22) translocations which involve the *PVT1* locus. Little is known about the function of *PVT1* but it has been reported to encode several microRNAs as well as induce T cell lymphomas in mice[32].

1.1.4 Clinical Presentation and Staging of HL

In 75% of patients with HL, the presenting feature is a painless peripheral lymphadenopathy typically involving the lymph nodes in the cervical chain. Patients with mediastinal lymphadenopathy may present with shortness of breath, cough, or rarely (if the mediastinal mass is bulky) with superior vena cava syndrome or tracheal compression[33]. More advanced disease may present as unexplained fever, weight loss or night sweats, termed 'B symptoms' and are recognised as poor prognostic factors in the Ann Arbor staging system[34]. The Ann Arbor staging was modified in 1989 to the so-called 'Cotswold revision', to account for the grade of disease (Table 1.1)[35].

Table 1.1 The Cotswold revision of Ann Arbor staging system[36].

STAGE	DEFINITION
I	Involvement of a single lymph node region or lymphoid structure (e.g. spleen, thymus, Waldeyer's ring)
II	Involvement of two or more lymph node regions on the same side of the diaphragm (the mediastinum is a single site, hilar lymph nodes are lateralised); the number of anatomic sites should be indicated by suffix (e.g. II_3)
III	Involvement of lymph node regions or structures on both sides of the diaphragm
III_1	With or without splenic, hilar, celiac or portal nodes
III_2	With para-aortic, iliac or mesenteric nodes
IV	Diffuse or disseminated involvement of one or more extranodal organs with or without associated lymph node involvement

	DESIGNATION APPLICABLE TO ANY STAGE
A	No symptoms
B	Fever (Temperature >38^{o}C), drenching night sweats, unexplained weight loss >10% in preceding 6 months
X	Bulky disease; widening of mediastinum by more than $^{1}/_{3}$ or the presence of a nodal mass with maximum dimension >10cm
E	Involvement of a single extranodal site that is contiguous or proximal to the known nodal site
CS	Clinical stage
PS	Pathological stage

1.1.5 Risk stratification and current treatment of paediatric HL

Conventional treatment of paediatric HL with combination chemotherapy, radiotherapy or both can achieve high cure rates. Early regimes were based on adult treatment schedules, but despite good survival outcomes it was apparent that children were more vulnerable to the sequelae of therapy[37-41]. Current regimes are tailored using risk stratification where the major poor prognostic factors are stage, B symptoms and bulky disease. An elevated erythrocyte sedimentation rate (ESR) also indicates a poor prognosis but is not included in risk adaptation[42;43].

The radio-sensitivity of HL was recognised as early as 1957 when Kaplan suggested that approximately 40 Gy of irradiation was an optimal curative dose. His pioneering work is still the basis of modern radiotherapy[44]. Radiotherapy, although highly effective in early stage disease, had significant acute complications as well as late effects in long-term survivors[41;45-47]. The treatment strategy for HL changed in 1964 with the introduction of MOPP combination therapy, which consists of mustargen (mustine), oncovin (vincristine), procarbazine and prednisone. MOPP therapy achieved dramatic results in advanced HL. Following the success of MOPP in adults, in 1967, Carbone and colleagues trialled this regime in children and reported similar effects in paediatric HL[48]. Subsequent studies used different combinations but none were superior until the introduction in 1974 of ABVD, a new four drug combination of adriamycin (doxorubicin), bleomycin, vinblastine and dacarbazine[42;49;50].

Although these regimes enabled treatment to be less radiotherapy dependent, the intensive chemotherapy was also associated with significant acute and late toxicity. Consequently, combined therapies have evolved to reduce toxicity while maintaining the excellent cure

rates. Over the last 20 years, risk adapted strategies utilizing prognostic factors, response to treatment and improved imaging techniques have guided clinical trials[51-53].

At present, in the UK paediatric patients with cHL are enrolled in a clinical trial, Euronet-PHL-C1. In this trial all patients receive two cycles of OEPA (vincristine, etoposide, prednisolone and doxorubicin) followed by a positron emission tomography (PET) scan to assess response. Group one: patients may either have no further treatment or, if disease persists, radiotherapy. Group two and three: patients are randomised to receive either COPP (prednisolone, procarbazine, vincristine and cyclophosphamide) or COPDAC (prednisolone, dacarbazine, vincristine and cyclophosphamide) +/- radiotherapy. There are three main aims of Euronet-PHL-C1: to establish in selected patients if chemotherapy alone is as good as chemotherapy and radiotherapy, to determine if dacarbazine and procarbazine are equally effective and to assess the long-term effects of these drugs on fertility. This trial also includes salvage strategies for relapsed and refractory HL to evaluate the role of further radiotherapy versus allogeneic stem cell transplant (ASCT)[54;55].

1.1.6 Prognosis and late effects

Overall, childhood HL is a curable disease with a five-year survival of 95% and 80% for early and advanced disease, respectively (reviewed in reference 33). However, primary progressive HL which remains refractory has a very poor outcome. Approximately 10% of early stage and up to 25% of advanced stage cHL relapse after first line therapy[56]. Yet, cure can still be achieved with salvage therapy with all relapsed and refractory patients receiving salvage chemotherapy plus potentially further treatment. The best curative options are still being evaluated and current choices include an ASCT +/- involved field radiotherapy. Any additional treatment entails significant risk to the patient, for example an ASCT has a non-

relapse mortality of over 20% [57-59]. In order to improve outcomes in this subset of HL patients, new therapies must be sought.

In long-term survivors of HL the complications of chemotherapy and radiotherapy have become more apparent. The most serious complications are chemotherapy-associated and radiation-associated secondary malignancy[45;46;60], infertility[61] and cardio-toxicity[62;63]. Second cancers are a leading cause of death, such that 15 years after the end of treatment, mortality related to late effects exceeds that of the original disease. Patients who received radiotherapy to the chest wall have a 7-18 fold increased risk of breast cancer[45]. Children are particularly vulnerable because receiving treatment at a young age strongly influences the risk and type of second malignancy.

All current data on the long-term sequelae of HL treatment is based on past regimes and contemporary schedules may have a different toxicity profile. It is imperative that novel treatment schedules are developed to increase overall survival in poor responders and to decrease morbidity and improve quality of life in long-term survivors.

1.2 The molecular biology of Hodgkin's lymphoma

1.2.1 Normal B cell development

The B cell is an essential part of the adaptive immune response generating antibodies and providing immune memory. Immature B cells are produced in the bone marrow and undergo several stages of development and differentiation.

An antibody molecule is composed of two identical light (L) and two identical heavy (H) chains, and the genes encoding them are found in the 'V' (Variable) and 'C' (Constant) regions. In the heavy-chain 'V' region there are three segments; V, D and J, which recombine

randomly, in a process called VDJ recombination. Similar rearrangements occur in the light-chain 'V' region except that there are only two segments involved; V and J. Immunoglobulin gene rearrangement introduces diversification to producing a unique variable domain in the immunoglobulin genes which encodes the B cell receptor of each individual B cell[64].

B cells bearing these immunoglobulins or antibodies are then released into the periphery where they encounter antigens. Upon binding of antigen to the B cell receptor (BCR), the B cell becomes activated. In T cell-dependent B cell development, activated B cells migrate to the B cell follicles of secondary lymphoid organs such as lymph nodes, spleen and Peyer's patches. Within these specialized structures the B cells receive a second co-stimulatory signal from antigen-specific T cells. The B cells then enter the next stage of differentiation and start to vigorously proliferate leading to the development of germinal centres (GC). GC are histological structures that in addition to B cells contain T cells and follicular dendritic cells (FDC), which are essential for subsequent B cell selection (Figure 1.2)[65].

Alongside B cell clonal expansion, the process of somatic hyper-mutation (SHM) begins in the GC. During SHM, random point mutations, deletions and duplications are introduced into the B cell receptor to increase antigen affinity. These variants are tested and those with high affinity for antigen are selected while those with poor affinity or disadvantageous mutations undergo apoptosis[66]. The proliferation of GC B cells takes place in the dark zone where they are referred to as centroblasts. In the light zone the GC B cells undergo selection and are referred to as centrocytes. GC B cells migrate between the light zone and dark zone undergoing several rounds of proliferation and selection[67].

B cells may also undergo class switch recombination (CSR), whereby parts of the antibody heavy chain locus are removed from the chromosome, and the gene segments surrounding

the deleted section are re-joined to retain a functional antibody gene that produces antibody of a different isotype. B cells produce IgM and IgD but require CSR for the production of IgA, IgE and IgG. CSR does not alter antigen affinity but does enable B cells to interact with different molecules[64]. Cells that successfully emerge from the GC can differentiate into either memory B cells, which provide for a rapid strong response to the next antigen encounter, or plasma cells which secrete antibody (Figure 1.2).

1.2.2 B cell transcription factors

The process of B cell development is regulated by transcription factors which determine cell fate. The first stage of B cell development in the bone marrow has two main checkpoints. The first, regulated by PU.1 in association with other factors, occurs at the bifurcation of the myeloid and B lymphoid cell lineages. Low expression of PU.1 favours B cell differentiation while high expression promotes differentiation to the myeloid line[68]. The second checkpoint is prior to VDJ rearrangement during the transition from the pro-B cell to the pre-B cell stage and is influenced by E2A and its isoforms, E12 and E47 as well as early B cell factor 1 (EBF1), and paired box gene 5(PAX5/BSAP) [69-72].

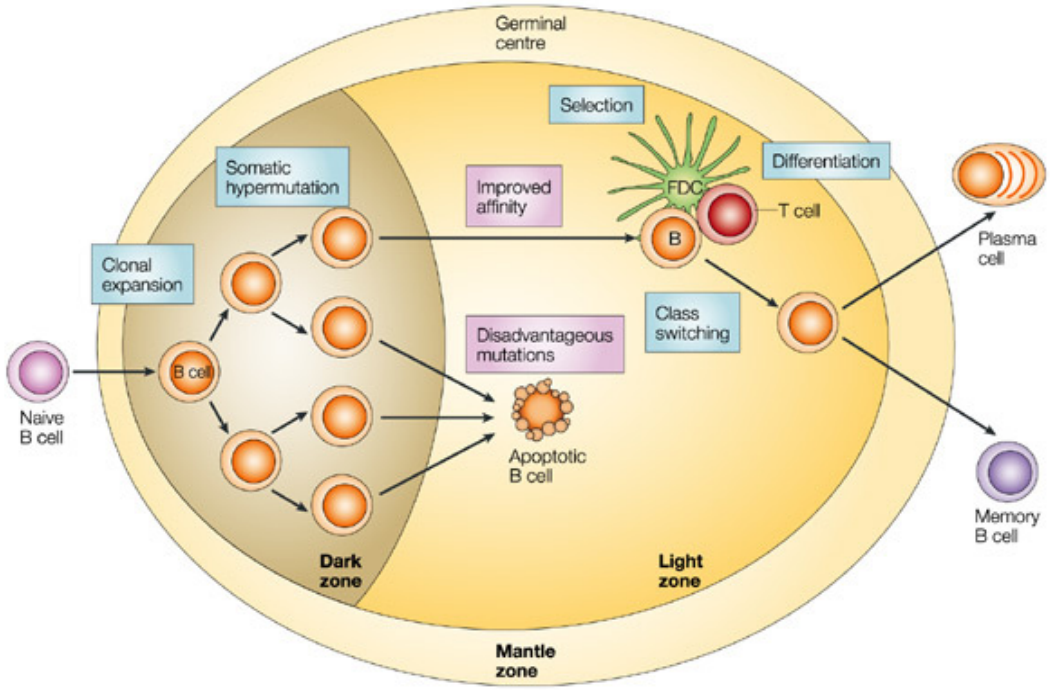

Figure 1.2 B cell development in the germinal centre. A naïve B cell encounters antigen and migrates to lymphoid follicles. Upon T cell stimulation, the B cell undergoes clonal expansion and SHM within the dark zone of the germinal centre. Selected B cells migrate to the light zone and are affinity tested. High affinity B cells are selected for further differentiation while poor affinity B cells are elininated by apoptosis. (Reproduced from Kuppers[73])

E2A contributes to the maintenance of the haemopoietic stem cell pool and is required for the expression of EBF1, Pax5 and initiation of the B cell programme. Both E12 and E47 are present in lymphoid progenitors but E47 alone is required for specification of the B cell lineage[74]. The role of EBF1 is less clear but its loss results in early arrest of B cell differentiation prior to immunoglobulin recombination. Furthermore, ectopic expression of EBF1 can overcome blocks in B cell differentiation in mice deficient in E2A and PU.1[70]. PAX5 is a key commitment factor that maintains B cell identity through the activation of B cell specific genes while repressing genes associated with other lineages[71]. The importance of PAX5 is demonstrated in mouse models where conditional ablation of *PAX5* in mature B cells resulted in reversal of differentiation to progenitors which subsequently gave rise to functional T cells[75].

These three transcription factors interact with each other and are regulated by feedback mechanisms involving inhibitor of DNA binding/differentiation (Id) proteins which are negative regulators of B cell transcription factors. Under physiological conditions, a negative feedback loop is maintained whereby E2A activates Id2 expression while EBF1 down-regulates Id2 to maintain E2A activity[76]. Similarly a feedback loop exists between EBF1 and PAX5. *EBF1* gene expression is regulated via two distinct promoter regions, the distal promoter by EBF1 and E2A and the proximal one by PAX5 and PU.1. *In vitro* studies demonstrated that the binding of EBF1 to a region in *PAX5* promoter results in the activation of PAX5. Furthermore, the forced expression of PAX5 in thymocytes results in activation of the B cell differentiation programme including *EBF1* transcription. Id2 has also been shown to interact with PAX5 antagonizing its function. These interactions are summarised in Figure 1.3[77].

Progression to the next stage of B cell differentiation occurs after antigen encounter. Early studies have identified that octamer binding sites on the V gene promoter regions are essential for immunoglobulin transcription. There are two proteins that can bind to these octamer sites; Oct1 which is ubiquitously expressed in various cell types and Oct2 which has a more limited expression. Oct2 confers B cell specificity in the presence of its co-activator BOB-1. Mice lacking Oct2 have normal B cell precursors but fewer IgM^+ B cells[78]. While mice lacking BOB-1 have no GCs, poor B cell maturation and reduced circulating B cells[79].

The GC reaction is driven by B cell lymphoma 6 (BCL6) which is highly expressed in GC B cells and is required for GC formation[80]. A crucial function of BCL6 is to repress B lymphocyte induced maturation protein 1 (BLIMP1). BLIMP1 initiates a cascade required for the terminal differentiation of B cells into plasma cells (PC). By repressing BLIMP1 expression, Bcl6 ensures that PC differentiation does not occur prematurely in GC B cells. Following the GC reaction BLIMP1 then induces repression of PAX5 and BCL6 such that B cells are unable to return to an earlier stage of differentiation[80;81].

Many of these transcription factors have crucial roles at multiple stages of differentiation. For example, although PU.1 is generally recognised as an early transcriptional regulator, it is also up-regulated in centroblasts, recruits Bcl6 to repress gene expression in GC B cells and is important for SHM[82]. Figure 1.4 illustrates the expression of some of the important molecules involved in B cell development.

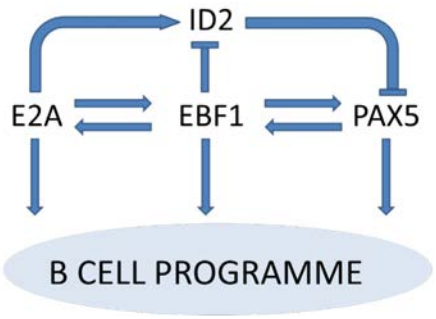

Figure 1.3 Schematic of the interaction between three key B cell transcription factors and Id2. The expression of E2A, EBF1 and Pax5 is regulated by feedback loops and the inhibitor ID2 which interact to promote the B cell transcription programme.

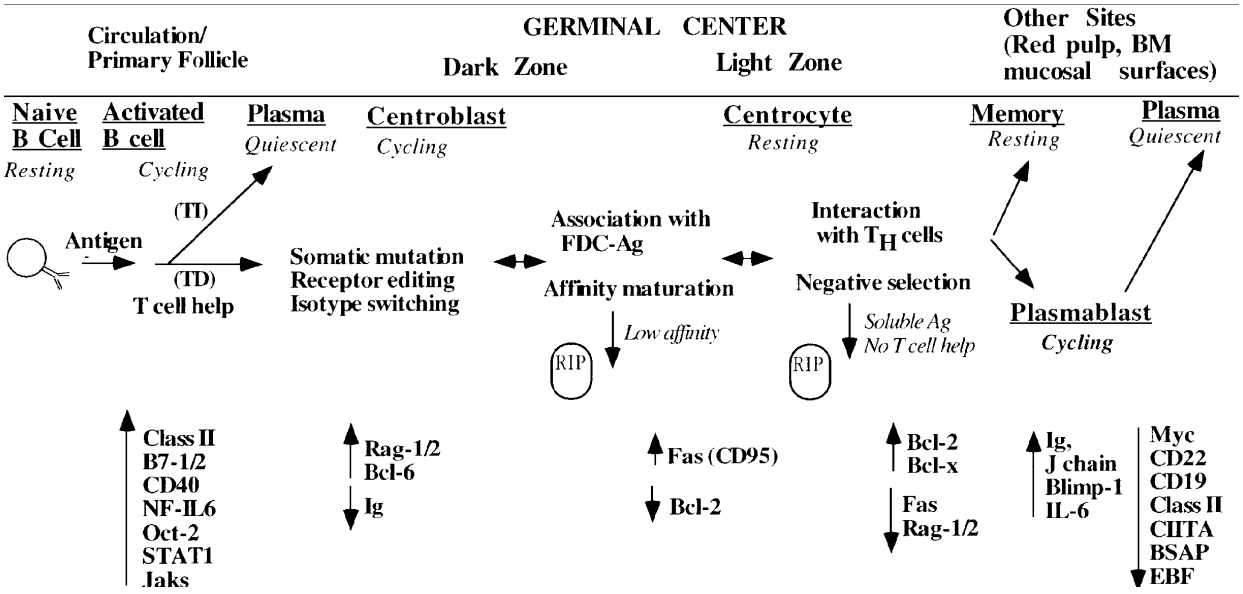

Figure 1.4 Schematic of important molecules in B cell differentiation. A number of different molecules become activated and others down-regulated as the B cell becomes differentiated. (Reproduced from Henderson and Calame[83])

1.2.3 The cellular origin of HRS cells

While the LP cells of NLPHL express several B cell markers including markers of a GC phenotype, HRS cells of cHL lack many B cell markers and express markers typical of other haematopoietic lineages[3]. This has made the identification of the normal cellular counterpart of the HRS cell of cHL elusive until recently. Analysis of single HRS cells micro-dissected from tissue section has shown that nearly all HRS cells carry clonally rearranged and somatically mutated immunoglobulin V gene indicating their origin as B cells that have undergone a GC reaction[84-87].

Furthermore, it has been shown that HRS cells do not express functional surface immunoglobulin and a quarter of cHL cases harbour crippling mutations[88]. A separate study found that although 75% of micro-dissected HRS cells retain coding sequence for an intact immunoglobulin, transcription ability is silenced[87]. Under physiological conditions B cells with non-functional immunoglobulins are removed by apoptosis, implying that the presumed progenitors of HRS cells are GC B cells that have escaped apoptosis[88]. In contrast, L&H cells contain functional immunoglobulins and a proportion of L&H cells show evidence of ongoing SHM and antigen selection suggesting they are derived from a stage intermediate between GC and memory B cells[89].

In a small proportion of HL cases, HRS cells express multiple T cell markers, CD3, granzyme B, perforin and T-cell intracellular antigen[90]. This could reflect a T cell lymphoma co-expressing CD30 and CD15 thereby mimicking HL or a B cell aberrantly expressing T cell markers or indeed be HL of truly T cell origin[91;92]. The latter possibility is supported by the following evidence. First, detection of clonal T cell receptor gene rearrangements but not immunoglobulin rearrangements in a small minority of HL cases[93]. Second, gene expression

analysis of HDLM-2, a HL cell line with T cell receptor rearrangements, shows HDLM-2 displays a gene expression profile akin to other B cell derived HL cell lines rather than cell lines derived from T cell lymphomas[94].

1.2.4 B cell reprogramming in cHL

Experimental models have demonstrated plasticity in lymphoid cells whereby alterations in transcription factors can profoundly affect the differentiated state. For example, PAX5 $^{-/-}$ pro-B cells are able to differentiate into functional macrophages, dendritic cells, osteoclasts and natural killer cells[95]. HRS cells show an extraordinary loss of B cell identity[96], the mechanisms of which are only beginning to be appreciated.

Of the key transcription factors, PU.1 expression is usually high in GC B cells but is consistently absent in HRS cells but interestingly PU.1 expression is a feature of L&H cells[97]. Although E2A, EBF1 and PAX5 are expressed to different degrees in primary HRS cells in most cases, their function is compromised. For example, a study by Mathas *et al.,* found the level of E2A expression in HRS cells to be similar to GC B cell derived cell lines. Despite normal expression, E2A function is impaired in HL cell lines by an up-regulation of two inhibitors of E2A activity; Id2 and activated B cell factor 1 (ABF-1). Id2 interacts with E2A to prevent DNA binding while ABF-1 specifically suppresses the E2A isoform, E47, by forming non-functional hetero-dimeric complexes. *In vitro* over-expression of both ABF-1 and Id2 decreases E2A activity compared with ABF-1 over-expression alone[98;99]. This study also demonstrated that inhibition of E2A results in the down-regulation of E2A-dependent B cell specific genes and may account for some of the transcriptional silencing seen in HRS cells. In contrast to E2A, EBF1 is expressed only at a low level and although PAX5 is expressed there is a down regulation of many of its target genes[98].

Not only is the B cell transcriptional programme repressed in HRS cells but transcription factors of other lineages are highly activated, for example the T cell transcription factors Notch 1 and GATA3. The oncogenic role of aberrant Notch expression is well defined in T cell malignancies but is less clear in B cell malignancies[100-102]. In HL, HRS cells not only express the Notch 1 receptor and its ligand jagged 1 (jg1) but also down-regulate the Notch 1 inhibitor, deltex1. The non-neoplastic cells of the microenvironment express only jg1. Raising the possibility that the activation of Notch 1 in HRS cells results from both autocrine and paracrine pathways[101]. It has been reported that in normal lymphoid tissue Notch receptors are expressed by GC B cells and Notch ligands by FDC. Moreover, it has been demonstrated *in vitro* that jg1 can rescue GC B cells from apoptosis and conversely blockade of Notch signalling reduced GC B survival in the presence of FDC[103]. Contrary to work showing tumour promoting properties of Notch signalling, another study noted that constitutive activation of all Notch receptors in a range of B cell derived cell lines actually leads to growth arrest and apoptosis [104]. A study of Notch1 expression in HRS cells observed that Notch 1 antagonises E2A and EBF1 contributing to suppression of the B cell phenotype[101]. In the same study, both PAX5 and Notch 1 were noted to be expressed but where there was a low expression of PAX5, Notch 1 was highly expressed. The converse was also noted but PAX5 did not appear to directly repress Notch 1 transcriptional activity [101].

In a proportion of cHL, the lack of BCR expression may be accounted for by the presence of crippling immunoglobulin mutations. Yet, in some instances the HRS cell contains an intact and functional immunoglobulin gene but still there is no BCR expression. One explanation comes from studies which show that in the majority of cases, HRS cells are deficient in both Oct2 and co-activator BOB-1 expression. However, expression of these transcription factors

cannot restore loss of immunoglobulin gene expression in HL cell lines [105-107]. Suggesting further inactivation of BCR signalling components may occur for example through epigenetic mechanisms such as methylation of the immunoglobulin heavy chain promoter[108]. Other markers of B cell identity such CD19 and CD79b are also down-regulated by epigenetic mechanisms. The treatment of HL cell lines with a demethylating agent has been shown to restore gene expression of these markers as well as PU.1 and BOB-1 [108;109].

1.2.5 Deregulated signalling pathways

Deregulated signalling is a feature of HRS cells which in some cases arise secondary to genetic alterations (Table 1.2). There now follows a description of several of these signalling pathways and their involvement in the pathogenesis of HL.

1.2.5.1 Nuclear factor kappa -light chain- enhancer of activated B cells (NF-κB)

The NF-κB/Rel family consists of five members (p50, p52, p65 [RelA], c-Rel, and RelB), which can form various homo-dimeric or hetero-dimeric complexes. In normal B cells, the inactive NF-κB complex resides in the cytoplasm bound to inhibitor of NF-κB (IκB) proteins. Activation of the NF-κB subunit causes phosphorylation of IκB proteins resulting in the degradation of IκB proteins. This phosphorylation is orchestrated by the IκB kinase (IκK) complex which contains two protein kinases, IκKα and IκKβ. Release of the NF-κB subunits permits translocation to the nucleus where the complex exerts its effect on downstream targets. The blocking of NF-κB activity *in vitro* leads to the apoptosis of HRS cells indicating a critical role for NF-κB in HRS cell survival. The constitutive activation of NF-κB activity in HL is mediated by the deregulation of different REL/NF-κB transcription factors[110-113]. Mutations of genes in the classical (canonical) NF-κB pathway can result in gain-of-function through the up-

regulation of *REL* and inactivation of IκB[114-116]. Other genetic abnormalities affecting the NF-κB pathway include TNFα-induced protein 3 (*TNFAIP3*) which encodes A20, a negative regulator of NF-κB. Loss-of-function mutations in *TNFAIP3* are found in 60% of EBV-negative HL. In the same study not only was the frequency of mutation lower in EBV-positive HL (12.5%) but also destructive mutations were confined to EBV-negative cases[117].

NF-κB can also be activated through the alternative (non-canonical) pathway via members of the tumour necrosis factor (TNF) family, CD40, CD30 and receptor activator of NF-κB (RANK). The over-expression of CD30 and CD40 are the hallmark of HRS cells. Whereas, the non-neoplastic cells expressing CD40 ligand (CD40L) surround the HRS cells and are thought to contribute to the activation of NF-κB[118;119]. The role of CD30 ligand (CD30L) is less clear as the activation of NF-κB appears to be largely CD30L independent[120;121]. However, *in vitro* a CD30-CD30L interaction between eosinophils and HDLM-2, a HL cell line, has been shown to promote the proliferation of these cells [122]. Activation of CD30, CD40 and RANK also mediates the phosphorylation of other signalling pathways, for example the mitogen-activated kinase (MEK/ERK) pathway [123] .

Table 1.2 Genetic mutations associated with HL. (Reproduced from Kuppers[89])

GENE	MUTATION	PATHWAY	FREQUENCY (%)
REL	Gains, amplification	NF-κB	50
NFKBIA	Point mutations, deletions	NF-κB	20
NFKBIE	Point mutations, deletions	NF-κB	15
TNFAIP3	Point mutations, deletions	NF-κB	40 (60% EBV-neg)
BCL3	Gains, translocations	NF-κB	10
JAK2	Gains, amplifications	JAK-STAT	40
SOCS1	Point mutations, deletions	JAK-STAT	45
TP53	Point mutations, deletions	P53	10
MDM2	Gains	P53	60
CD95	Point mutations	FAS	10

1.2.5.2 Janus kinase (JAK)-signal transducer and activator of transcription (STAT)

The JAK-STAT pathway also plays a critical role in the pathogenesis of HL. A variety of cytokines and growth factors can bind to their corresponding receptors on the HRS cell surface and can activate JAK, which in turn phosphorylates STAT proteins on specific tyrosine residues. The STAT proteins then dimerize and translocate to the nucleus initiating the transcription of target genes. The JAK-STAT pathway is negatively regulated by the suppressor of cytokine signalling 1 (SOCS1) which can bind to and inactivate JAK. Inactivation of SOCS1 through genomic gain and mutations of *JAK2* are frequently seen in HRS cells contributing to the constitutive activation of JAK-STAT pathway[124-126]. Even in the absence of these mutations, STAT3, STAT5a, STAT5b and STAT6 have all been shown to be constitutively active in HRS cells[112;127;128]. An alternative mechanism appears to involve interleukins (IL) secreted by HRS cells which engage receptors on the same cell; for example IL13-IL13R for STAT6 and IL21-IL21R for STAT5a, STAT5b and STAT3[129-131]. STATs can also be activated by receptor tyrosine kinases (RTKs) and although the aberrant activation of RTKs has been described in HL (discussed later in section 1.5) they have not been demonstrated to activate STATs in HRS cells.

1.2.5.3 Phospho-inositide 3 kinase (PI3K)

PI3K is constitutively activated in HRS cells and its inhibition results in reduced cell viability[132]. Under normal conditions PI3K becomes activated by RTKs or other cell-surface receptors, resulting in increased production of the membrane lipid phospho-inositol (3,4,5)P_3 (PIP_3) from phospho-inositol(4,5)P_2 (PIP_2). The level of PIP_3 is negatively controlled by the phosphatase and tensin homolog (PTEN), which converts PIP_3 back to PIP_2. Akt, which is the main effector of PI3K, binds PIP_3 at the plasma membrane. The binding of PIP_3 leads to

the phosphorylation of Akt at Ser-473 in its regulatory domain and subsequent activation[133]. The HRS cells of primary tumour samples not only expressed high levels of activated Akt but also display phosphorylation of downstream targets of Akt activation. These targets include a number of molecules important in apoptosis e.g. GSK-3, 4E-BP1, and p70 S6 kinase[132]. In HL cell lines, PTEN is expressed but its function is abrogated as a result of phosphorylation of the C-terminal tail[133].

1.2.6 The role of the cellular microenvironment in tumour survival

The microenvironment is considered essential for the growth and survival of HRS cells as demonstrated by the difficulty in establishing cell lines and the scarcity of HRS cells in the peripheral blood of patients. Moreover, when HRS cells metastasize to non-lymphoid organs they embed themselves in their typical microenvironment[134]. The microenvironment of HL is formed by the production of cytokines and chemokines which attract a reactive infiltrate which promotes and maintains tumour growth (Figure 1.5). In addition to the infiltrate of non-neoplastic T and B cells, eosinophils, macrophages, mast cells and fibroblasts, HL is often characterised by an ECM dominated by collagen[3].

The network of cytokines and chemokines produced by HRS cells is reinforced by the non-neoplastic cells of the microenvironment. For example, HRS cells can directly attract CD4+ T helper cells, eosinophils and mast cells through the production of chemokine ligand 5 (CCL5/RANTES). HRS cells can also induce fibroblasts to secrete CCL5 and eotaxin which together can further recruit CD4+ T helper cells and eosinophils. HRS cells do not produce eotaxin but can stimulate fibroblasts to do so through IL13 and TNFα signalling. CCL5 also has a direct effect on HRS cell survival and proliferation [135-137].

The microenvironment also has an important role in modulating the immune response to HRS cells. The infiltrate contains a large fraction of Regulatory T cells (Tregs) and T helper cells which are thought to suppress cytotoxic T cells (CTL) [(138)]. Tregs are recruited not only by HRS cells but also by surrounding non-neoplastic cells secreting IL-7[(139)]. The exact role of T cells in the microenvironment of HL still needs clarification as there is some suggestion that high numbers of Tregs are associated with a better prognosis. This observation might be a consequence of HRS cell suppression cells by Tregs[(140)]. HRS cells also produce immunosuppressive cytokines such as IL10, transforming growth factor (TGFβ) and galectin 1 which inhibit T effector function[(141)].

CTLs can become 'exhausted' which is a phenomenon that involves both a reduction in the numbers of CTLs and their responsiveness. Programmed death 1 ligand (PD-1L) has been shown to be necessary for the maintenance of T-cell exhaustion in a chronic-infection mouse model of lymphocytic choriomeningitis virus (LCMV). PD-1 was greatly up-regulated on CTLs in response to LCMV, and its expression was maintained during chronic infection Moreover, this study demonstrated the function of 'exhausted T cells' could be restored by blockade of PD-1-PD-1L interaction [(142)]. HRS cells have been shown to express PD-1 L and CTLs in the infiltrate to express PD-1. In HL, the expression of PD-1L has been identified as a negative prognostic factor[(143)].

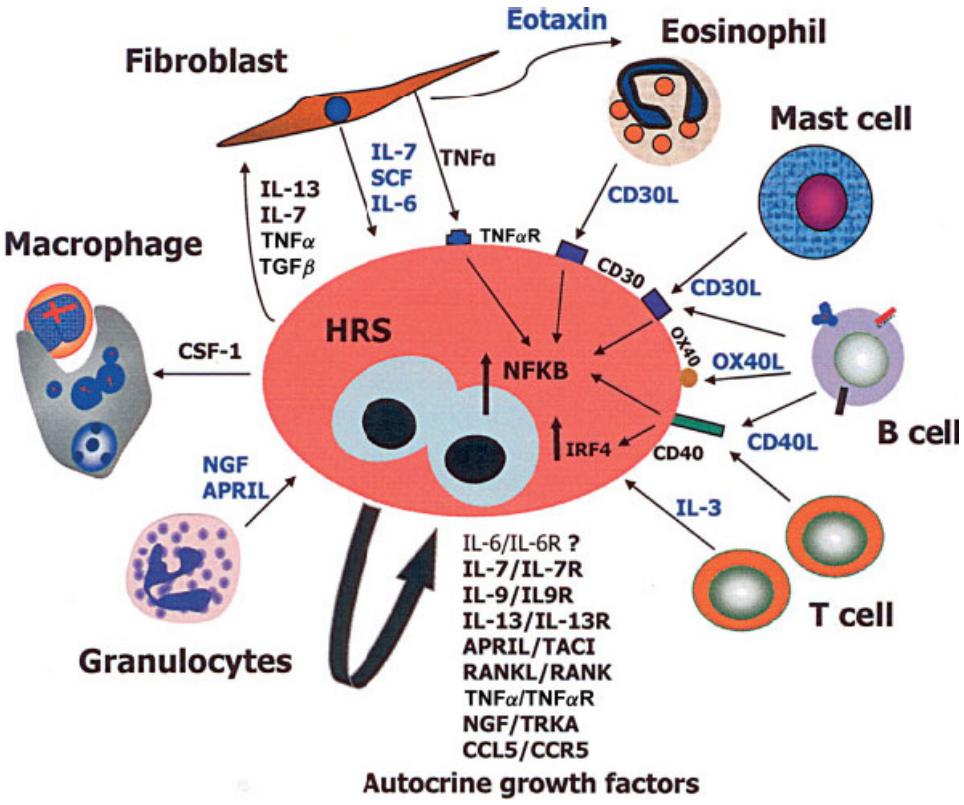

Figure 1.5 Cross-talk of HRS with the surrounding cells. The production of chemokines and cytokines recruit cells to the tumour microenvironment. HRS cells are able to interact with these cells via soluble mediators which in addition to autocrine growth factors promotes HRS proliferation and survival (Reproduced from Aldinucci *et al.*,[141])

1.2.7 The non-cellular component of the HL microenvironment

Various components within the stroma are altered in carcinogenesis. For example, in mice, PTEN ablation in stromal fibroblasts results in remodelling of the ECM, changes to the vasculature and conversion to a tumour promoting phenotype[144]. In the past, HL has been confused with inflammatory disorders and indeed changes seen in the microenvironment of HL mimic those seen during the process of wound healing. The exact nature of this response is different between HL subtypes. Gene expression profiling showed that MCHL resembled the inflammatory phase of wound healing. In contrast, NSHL shared similarities to the remodelling phase with the fibrosis seen in HL resembling scar tissue and is characterized by the overproduction and deposition of type I and III collagen by fibroblasts[145]. A previous study showed that blood vessels strongly expressing type IV collagen were numerous in NSHL and localised within the cellular nodules but were relatively scanty in LPHL, MCHL, and LDHL[146].

Collagens provide more than mere mechanical scaffold and are able to communicate using cell surface receptors. There are two main types of receptors which can bind to collagen, integrins and discoidin domain receptors[147]. Both can independently trigger numerous cellular responses including cell adhesion, migration and proliferation. Several cancers including breast and prostate have an elevated and altered collagen expression which is associated with metastases and poor outcome[148].

1.3 Hodgkin's Lymphoma and Epstein-Barr virus

1.3.1 Introduction

The Epstein-Barr virus (EBV) is a highly prevalent herpes virus that persists life-long in normal humans by colonising memory B cells. EBV infection usually occurs in childhood and is either asymptomatic or presents as a mild viral illness. The acquisition of EBV in late adolescence and adulthood can cause infectious mononucleosis which manifests as fever, malaise and lymphadenopathy[149]. EBV is ubiquitous and in a recent study, antibodies to EBV were detectable in over 95% of healthy young women[150]. In some individuals EBV can contribute to the development of lymphomas such as Burkitt's lymphoma (BL), Hodgkin's lymphoma (HL), or post-transplant lymphomas (PTLD) as well as epithelial cancers which include nasopharyngeal carcinoma (NPC) [149].

CTLs are particularly important in the recognition and elimination of EBV-infected cells. CTLs recognise virus-derived peptides that are presented by the infected cell in association with MHC class I. Individuals whose virus-specific immunity is compromised are at a higher risk for the development of virus-associated cancers. This is exemplified by an increase in post-transplant lymphoproliferative disease caused by EBV infection in transplant patients, often treated by decreasing the level of immunosuppression[151;152]. In paediatric HL, there is an association between HL and acquired immunodeficiency with studies reporting up to 90% of HL patients positive for HIV also have EBV positive HRS cells[153]. Yet virus-associated cancers also arise in immunocompetent individuals suggesting that the virus-infected tumour cell or its progenitor can escape the normal virus-specific immune responses.

1.3.2 Defining a virus-associated cancer

A tumour is referred to as 'virus-associated' when the virus genome or its products (i.e. RNA, protein) are detectable within the tumour cells[154]. The most widely used method to detect EBV is *in situ* hybridisation for the highly abundant Epstein-Barr encoded RNAs (EBERs); non-coding RNAs which are expressed in all forms of latent EBV infection. In the majority of EBV-associated tumours it is possible to show that the EBV genome is monoclonal. When EBV infects a cell the linear genome circularizes by fusion of the terminal repeats giving rise to a fusion sequence unique to each infected cell. The detection of only one fusion sequence in a tissue sample demonstrates monoclonality; in other words all the EBV-infected cells originated from a single EBV-infected cell[155;156].

1.3.3 EBV and the origin of B cell lymphomas

EBV is orally transmitted, and infectious virus can be detected at low levels in oropharyngeal secretions from healthy EBV-seropositive individuals. Early in the course of primary infection, EBV infects B-lymphocytes, possibly within the epithelium of the naso- and oro-pharyngeal mucosa. It is not clear whether naïve, memory or GC B cells, or all of these cell types, are the target of initial infection. In asymptomatic carriers, EBV resides in memory B cells which provide the long-term reservoir for EBV as a latent infection. Infected memory B cells lack expression of most viral genes (referred to as latency 0, see Figure 1.6) and are therefore not recognised by EBV-specific T cells. An exception is the EBV viral protein LMP2A which can be detected during latency 0. Activation of EBV-infected memory B cells can lead to their differentiation to plasma cells, a process that might switch on the lytic cycle of EBV and produce new viral particles which are shed into the saliva[157;158].

Our understanding of the role of EBV in B cell transformation comes mainly from the study of lymphoblastoid cell lines (LCL); immortalised cell lines which are generated by EBV infection of normal B cells *in vitro*. In LCLs, six nuclear proteins, referred to as the Epstein-Barr nuclear antigens (EBNAs 1, 2, 3A, 3B, 3C and EBNA-leader protein), two proteins found in the cell membrane of infected cells known as the latent membrane proteins (LMPs), two non-translated RNA molecules known as the Epstein-Barr virus encoded RNAs (EBERs) as well as the BamHi-A rightward transcripts (BARTs) are expressed[154]. Although originally thought to be protein-coding, several EBV miRNA are now known to be expressed from the BART region of the viral genome[159]. The use of recombinant EBV lacking individual latent genes has confirmed the absolute requirement for EBNA2 and LMP1 in the *in vitro* transformation of B cells, and has highlighted an important role for EBNA-LP, EBNA3A and EBNA3C in this process[160]. EBNA1 is consistently expressed in virus-associated tumours and although infection of primary B cells with EBNA1-negative EBV can generate LCLs the transforming efficiency is 10,000 fold less than in the presence of EBNA1[161].

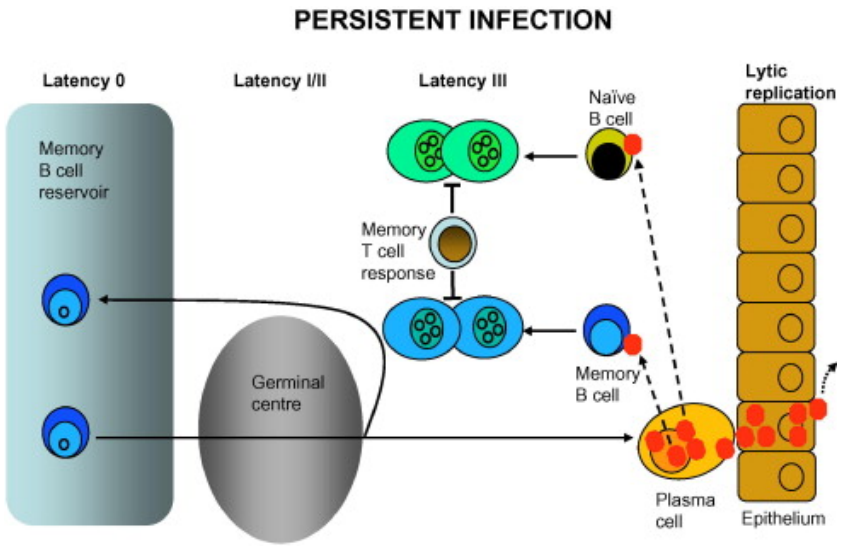

Figure 1.6 A schematic for latency and persistent EBV infection. Memory B cells lacking expression of most viral genes provide a long term reservoir of EBV. Activation of infected memory B cells can switch to the lytic cycle producing new viral particles (Reproduced from Cader *et al.,*[149]).

Table 1.3 The major forms of viral latency associated with EBV-positive malignancies.

LATENCY	VIRAL GENES EXPRESSED
I	EBNA1 EBERs, BARTs
II	EBNA1 EBERs, BARTs LMP1, LMP2A, & LMP2B
III	EBNA1, EBNA2, EBNA3A, EBNA3B, EBNA3C & EBNA-LP EBERs, BARTs LMP1, LMP2A, & LMP2B

B cells at the GC stage of differentiation are especially prone to neoplastic transformation. This is mainly because B cells undergoing SHM and CSR are particularly susceptible to oncogenic mutations, including chromosome translocations. As mentioned previously, GC B cells bearing disadvantageous mutations would be expected to undergo apoptosis but in HL such cells must have escaped that fate. Crippling immunoglobulin gene mutations (found in 25% of cases) appear to be exclusive to EBV-positive HL, suggesting that EBV is necessary to override apoptotic signals in GC B cells harboring deleterious immunoglobulin gene mutations[162]. In support of this, two additional groups have shown that EBV is capable of immortalising BCR-negative B cells[162-164]. More recently it has been shown that LMP2A is required for the *in vitro* transformation of BCR-negative GC B cells[165].

There is *in vivo* evidence, that expression of both LMP1 and LMP2A in B cells induces lymphomas with a B cell phenotype. This could represent an important mechanism for the transformation of B cells because LMP1 and LMP2A have been shown to substitute in part for the function of two molecules that are critical for GC B cell survival; LMP1 shares many features in common with a constitutively active CD40 receptor, while LMP2A mimics a BCR[166;167]. Most of the phenotypic changes seen in EBV-infected B cells are orchestrated through LMP1, a dominant oncogene through its activation of the NF-κB pathway. LMP1 can also deregulate PI3K, JAK-STAT and p38 signalling[154;168]. LMP2A competes with the BCR to bind the syk and lyn tyrosine kinases, thereby modulating the activity of these tyrosine kinases[169;170]. Transgenic mice models have confirmed that both LMP1 and LMP2A can contribute to B cell lymphomagenesis, but to-date none of these mouse models have been able to recapitulate the phenotype of any of the EBV-associated lymphomas that occur in humans[166;168].

In B cells from LMP2A transgenic mice it was observed that there was a decreased expression of many genes associated with normal B cell development as well as reduced levels of the transcription factors that regulate their expression[171]. Recently, Vockerodt *et al.,* showed that LMP1 expression in normal human GC B cells could induce a similar loss of B cell identity including the down-regulation of BCR components [172].

1.3.4 EBV and immune modulation in HL

EBV seems capable of contributing to the immune escape of HRS cells. For example, the production of IL10 which suppresses CTL function has been observed in 66% of EBV-positive cases compared to only 16% of EBV-negative cases [173]. EBV infection has also been shown to induce CCL5 and CCL3 which recruit T-helper cells [141]. The EBV encoded EBNA1 has been shown to up-regulate of CCL20 in HRS cells which can recruit Tregs to the tumour microenvironment[174].

1.4 Receptor Tyrosine kinases

1.4.1 Introduction

The human genome contains 58 receptor tyrosine kinases (RTKs), sub-classified into 20 families according to the nature of structural domains located within the extracellular region (Figure 1.7). All RTKs have an extracellular portion, to which the cognate ligand binds, a single pass transmembrane helix and a cytoplasmic portion that contains a protein tyrosine kinase domain, a regulatory carboxy-tail and juxtamembrane region. RTKs are highly conserved through evolution underpinning their importance to eukaryotic cells. The aberrant expression and activation of RTKs has been linked to pathogenesis of many diseases and inherited genetic syndromes[175].

1.4.2 Activation

Early work on RTKs proposed a straightforward mechanism of activation in which the receptor exists as monomers on the cell surface and ligand binding induces dimerization resulting in autophosphorylation and activation of the receptor. Subsequent studies suggest this model is too simplistic with different RTKs employing different strategies for activation[175].

Activation principally involves one of four mechanisms (Figure 1.8). The first mechanism 'ligand mediated' is exemplified by TrkA where the bivalent ligand simultaneously interacts with 2 receptor molecules cross linking them resulting in receptor dimerization without direct contact of extracellular domains[176].

In the second mechanism the ligand also binds and cross links two receptors but without altering the binding surface. Instead, a different region of the receptor undergoes a conformational change. For example, the extracellular domain of KIT consists of 5 immunoglobulin domains (D1-D5). The ligand, stem cell factor (SCF) binds to D1-D3 which causes a structural change in D4 and D5 resulting in receptor activation. Oncogenic gain-of-function mutations are often found in D5 leading to persistence of active conformation hence constitutive activation[177;178].

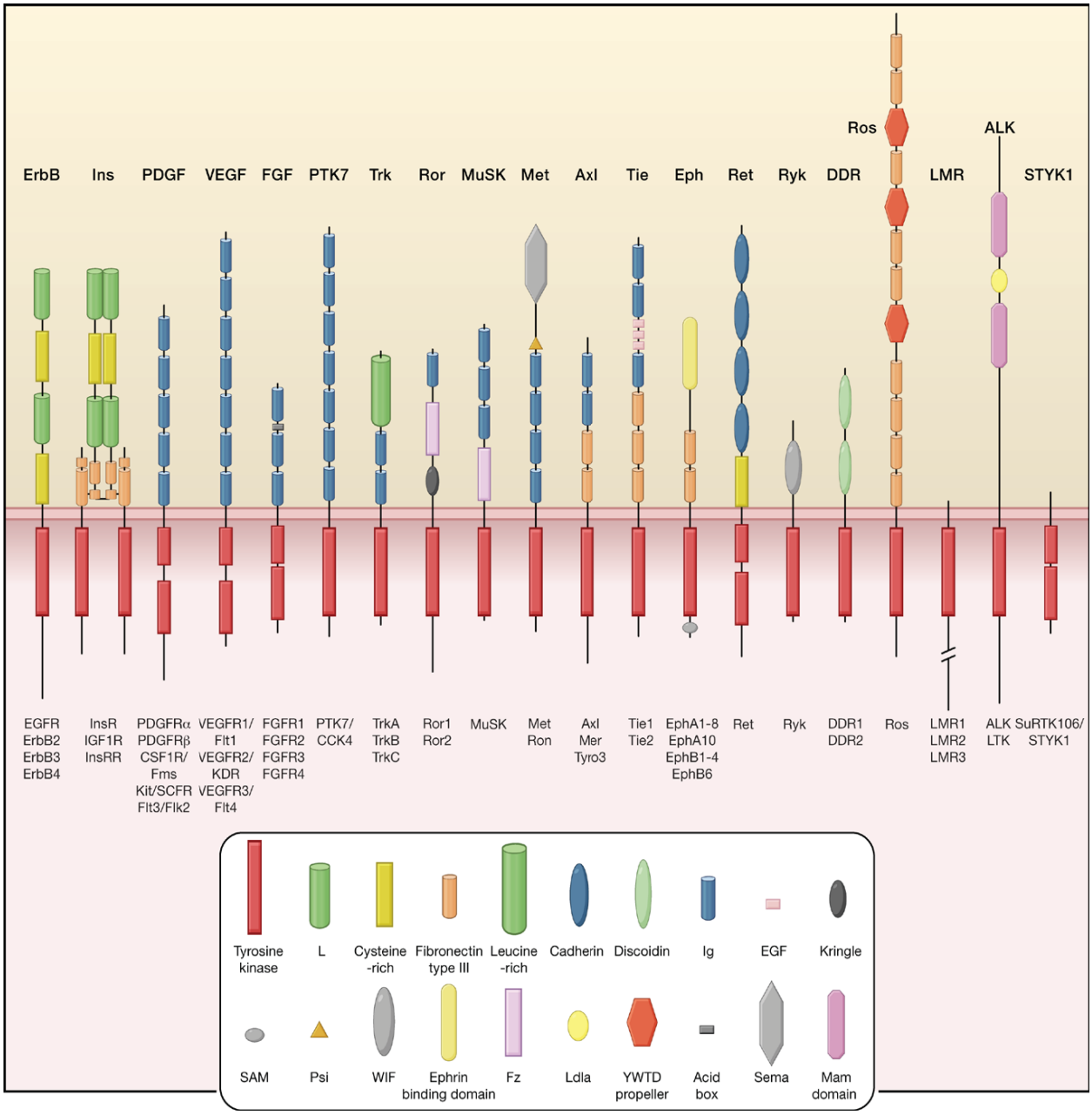

Figure 1.7 A diagrammatic representation of the different extracellular domains used to sub-classify RTKs. (Reproduced from Lennon and Schlessinger[175])

The third mechanism involves bivalent ligand binding, direct receptor-receptor contacts and an accessory molecule. The fibroblast growth factor receptor (FGFR) family uses this mechanism where heparin is an essential accessory molecule simultaneously contacting both ligand and receptor dimers. Interactions between FGF, FGFR and heparin stabilises the FGFR dimer activating the receptor[179].

Receptors of epidermal growth factor receptor family EGFR family use a fourth mechanism which is entirely 'receptor mediated' where the activating ligands make no direct contribution to the dimerization interface. Simultaneous ligand binding to two sites on the same receptor, Di and Diii drives conformational change by exposing a previously occluded dimerization site on the Dii domain [180].

1.4.3 Regulation

The intracellular kinase domain of RTKs consists of an N-lobe, a C-lobe and an 'activation loop'. The activation loop is a key structural element in the regulation of catalytic activity which is not positioned optimally in the unphosphorylated state. In the active state all RTKs adopt a similar configuration allowing phosphoryl transfer. In contrast, at rest there is wide variation in receptor structure between inactive RTKs reflecting their diverse regulatory mechanisms[175].

There are three main autoinhibitory mechanisms, inhibition of activation loop, C-terminal inhibition and juxtamembrane autoinhibition[181], examples of each are given below.

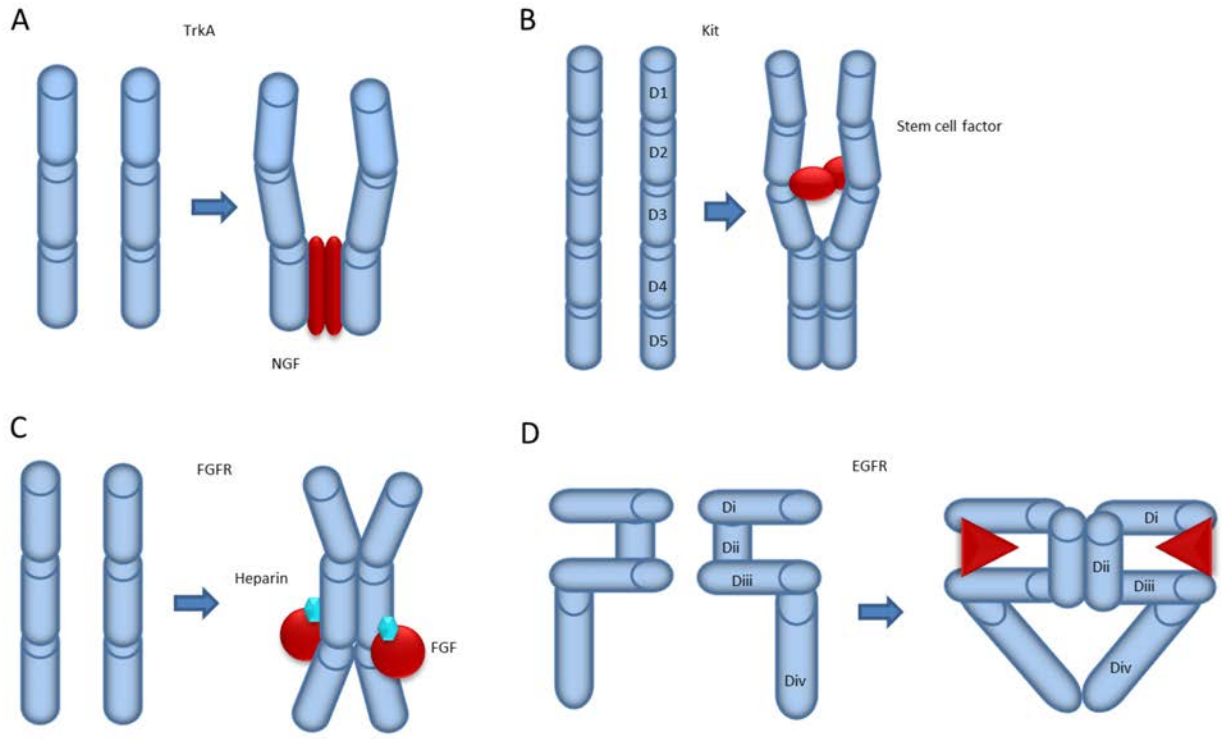

Figure 1.8 The four basic mechanisms of ligand interaction with the extracellular domain of the tyrosine kinase receptors (Modified from Lennon and Schlessinger[175]). A) TRK A is activated when ligand binds two receptors without the receptor contacting each other directly B) Binding of Stem cell factor induces KIT activation by inducing a conformational change in two domains not involved in the ligand binding C) Activation of FGFR requires FGF ligand and the co-activator heparin D) ligand binding to EGFR exposes a previously occluded site and activation of receptor without direct contact of the receptor with ligand.

i. The activation loop inhibition

In the activation loop of the insulin receptor a tyrosine residue projects into and blocks the active site. Binding of insulin causes phosphorylation of this residue and removes this blockade permitting the receptor to adopt an active configuration[182].

ii. C-terminal tail inhibition

In the case of the TIE-2 receptor the activation loop already exists in an active conformation in the absence of phosphorylation. Instead the autoinhibition of the receptor is co-ordinated by the unphosphorylated C-terminal tail which binds to the kinase domain, blocking substrate access. Tyrosine phosphorylation disrupts this interaction enabling activation and substrate binding[183]. Indeed, it has been shown that deletion of the C-terminal tail in TIE-2 increases kinase activity of the receptor[184].

iii. Juxtamembrane inhibition

Several RTKs are autoinhibited by the juxtamembrane region which contains several tyrosine phosphorylation sites which can negatively regulate catalytic activity. Sequences within the juxtamembrane are in contact with the kinase domain imposing biochemical and structural constraints. These autoinhibitory interactions differ amongst RTKs[185]. For example, in the juxtamembrane of the ephrin (Eph) receptors there is a highly conserved motif, containing two tyrosine residues, which functions as a clamp across the kinase domain in the inactive state. Following ligand stimulation the inhibitory conformation of the juxtamembrane is destabilised permitting trans-phosphorylation and receptor activation.

Similarly a tyrosine residue (Tyr553) is contained within the juxtamembrane of muscle-specific kinase (MUSK) which is essential for the activity of the receptor. Mutation of this

tyrosine residue results in loss of ligand induced phosphorylation of MUSK. However, unlike Eph receptors, crystal structure studies show that in the inactive state the juxtamembrane of MUSK is disordered and that Tyr553 does not directly interact with the kinase domain. Consistent with this, the soluble cytoplasmic domain harbouring a Phe substitution of Tyr553 can still undergo kinase activation *in vitro*, implying that additional constraints must be present *in vivo*[186;187].

1.4.4 RTK signalling networks

RTKs have multiple tyrosine phosphorylation sites, some of which regulate catalytic activity as explained above and others which are required for the recruitment of downstream signalling proteins. Upon activation, RTKs engage adaptor proteins, such as Grb2-associated binding protein 1 (GAB1) which can bind to multiple RTKs. For example, in neural cells both EGF and TRK receptors can recruit identical adaptor proteins producing different effects; proliferation and differentiation respectively [188]. Equally, different isoforms of the same RTK can recruit different adaptor proteins and produce different phenotypes[175]. The versatility of docking proteins enables RTKs to influence a large number of signalling pathways.

The expression of multiple isoforms of different RTKs have been described in cancer cells and is thought to contribute to tumour development. Since experimental work presented in this thesis explores the expression of the RTK discoidin domain receptor 1 (DDR1) and its different isoforms there now follows section outlining the basic principles of splicing.

1.4.5 Splicing

Alternative splicing is a major mechanism for the modulation of gene expression enabling a single gene to increase its coding capacity to synthesize structurally and functionally distinct

protein isoforms. An extreme example is the *Drosophila Dscam* gene, which can potentially generate 38016 different protein isoforms[189]. Genes are transcribed into pre-mRNAs which contain intronic and exonic sequences. Post-translational modifications include removal of intronic sequences and joining of exons. This process is highly regulated and executed by the spliceosome, a multi-component complex consisting of five small nuclear ribonucleoproteins; U1, U2, U4, U5 and U6 and over 100 other proteins. The splicesome recognises exon-intron boundries known as splice sites and catalyses the 'cut and paste' reaction. Identification of borders is facilitated by regulatory cis-sequences found at exon-intron boundaries. Splicing regulation also involves trans-elements, cellular proteins and RNAs, that respond to changes in cell status and environment to produce both constitutive splicing and alternative splice variants (ASV)[190]. ASV can be generated in five main ways (Figure 1.9)[191].

- **Exon skipping** An exon is spliced out of the primary transcript. This is the mechanism most often used to generate ASV.
- **Mutually exclusive exons** One of two exons but not both is retained in mRNAs after splicing.
- **Alternative donor site** An alternative 5' splice junction (donor site) is used, changing the 3' boundary of the upstream exon.
- **Alternative acceptor site** An alternative 3' splice junction (acceptor site) which changes the 5' boundary of the downstream exon.

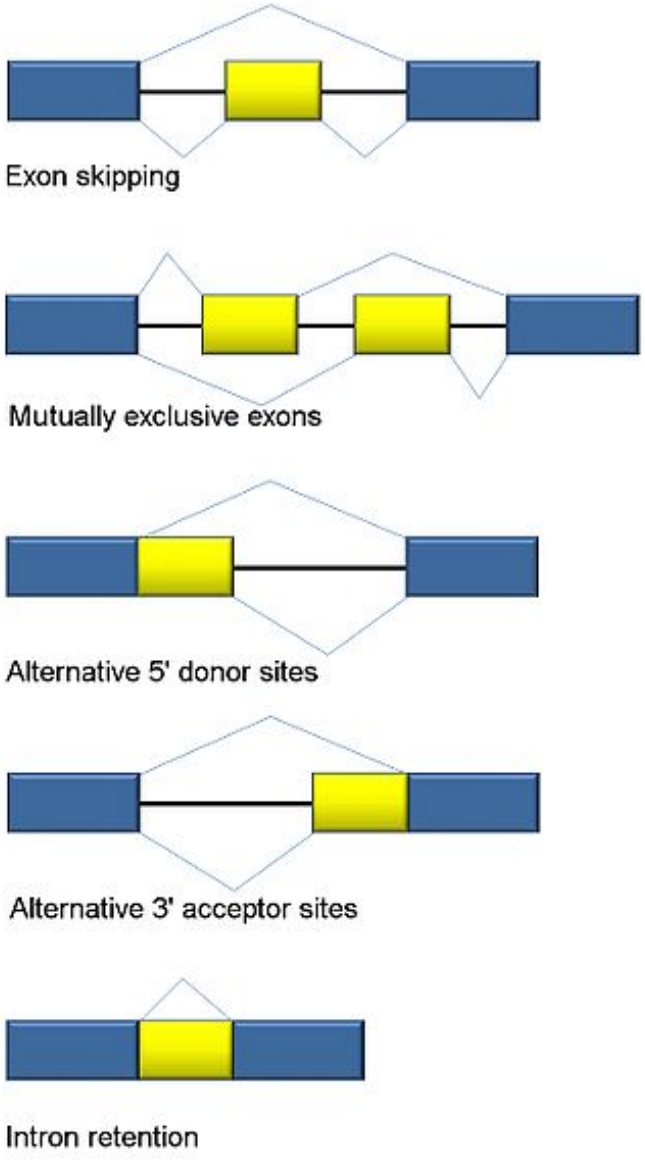

Figure 1.9 A schematic representation of the five mechanisms of alternative splicing. A) An exon is spliced out of the transcript B) One of two exons but not both are retained C) An alternative 5'donor site D) An alternative 3' acceptor site E) Intron retention (Reproduced from Black[191])

- **Intron retention** If the retained intron is in the coding region, the intron must encode amino acids in frame with the neighbouring exons. If not, a stop codon or a shift in the reading frame will cause the protein to be non-functional. This is the least common mechanism of ASV generation in normal cells but is found frequently in cancerous cells.

Most RTKs genes can express different isoforms which are generated by alternative splicing. For example alternative splicing of the *FGFR* genes results in the production of over 48 different isoforms of FGFR which vary in their ligand binding and kinase activity[192]. Although the function of many of these ASV is not fully understood, it is emerging that certain isoforms are expressed according to the cellular context. For instance, in chondrocytes, an alternative splice form of FGFR3 lacking the 'acid-box' (Figure 1.7) in the extracellular domain is expressed in the undifferentiated chondrocyte cell line ATDC5, while the full-length FGFR3 is not. Moreover, BaF3, a mouse pro-B cell line that expresses this splice variant has been shown to have a higher mitogenic response than cells expressing full-length FGFR3[193].

Soluble isoforms of RTKs lacking transmembrane and intracellular domain are also generated by normal cells and can interact with the ligand. They can be produced by one of two mechanisms, ectodomain shedding or ASV. Ectodomain shedding is a process in which expressed RTKs are cleaved by cell surface proteases, predominantly members of the matrix metalloproteinase (MMP) family [194]. Recently, Jin *et al.,* using a pool of cancerous and normal tissue identified 60 novel soluble ASV derived from 21 RTKs[195].

1.4.6 ASV RTKs and cancer

Abnormally spliced mRNAs are found in many different malignancies. Until recently, it was unclear whether such aberrant patterns of splicing were primary oncogenic mechanisms, or merely secondary to the process of tumour formation. Support for the former hypothesis comes from the observation that specific ASVs can contribute to tumour progression[196;197].

In a proportion of cancerous cells the aberrant ASV production has been attributed to genomic mutations affecting the cis-regulatory sequences. For instance, aberrant splicing of the *KIT* oncogene occur following 3' deletion of 1-14 base pairs in intron 10 resulting in loss of the splice site at the exon 11 boundary. The resulting protein remains in-frame but lacks exon 11 which is necessary for autoinhibition thus rendering the receptor constitutively active[198].

Changes in splicing pattern can also result from alterations of the trans-regulatory elements. For example, an ASV of recepteur d'origine nantais (RON), ΔRON lacking exon 11 has been identified in gastric carcinoma cell line and is capable of inducing an invasive phenotype[199]. ΔRON transcripts do not contain mutations. Instead, ΔRON production is controlled by a 'silencer and an enhancer of splicing' located in exon 12. The splicing factor SF2/ASF binds to this region in exon 12, regulating the inclusion or skipping of exon 11, controlling the production of ΔRON. The overexpression SF2/ASF was shown to increase ΔRON [200]. Furthermore, SF2/ASF has been shown to be an oncogene with the capacity to transform mouse fibroblasts[201].

1.4.7 Deregulation of RTKs in cancer

As RTKs are involved in regulating cell growth and survival their expression and activation must be tightly regulated in normal cells. Deregulation of these control mechanism can contribute to carcinogenesis. Indeed more than 30 RTKS have been implicated in cancer development. The constitutive activation of RTKs occurs through three possible mechanisms [(202)]:

- Ligand-receptor autocrine circuits freeing the cell from the need for paracrine growth factors.
- Receptor over-expression favouring local receptor oligomerization and reciprocal activation even in the absence of interacting ligand.
- Structural alterations that enable constitutive activation.

These mechanisms are not mutually exclusive, I will now describe three RTKs; erythroblastic leukemia viral oncogene homolog 2 (Erbb2/Her2), KIT and fms-related tyrosine kinase 3 (FLT3) to illustrate the basic principles of aberrant RTK activation in tumours.

1.4.7.1 Erbb2 (Her2)

The aberrant activation of EGFR family of receptors has been linked to the pathogenesis of many cancers which include breast cancer and lung cancer. The Erbb2/Her2 receptor belongs to this sub-family but does not contain an ectodomain to which ligand bind, instead forming homo- and hetero-dimers with other members of the EGFR family. Mutations of Erbb2/Her2 can cause the receptor to adopt an active conformation and favours homo-dimerization leading to uncontrolled growth. Receptor over-expression due to gene

amplification, seen in approximately 25% of breast cancers, also promotes spontaneous receptor dimerization and activation[203]. Although Her2 cannot directly bind ligand, ligand-induced activation of other EGFR results in hetero-dimerization between ligand-activated receptor and Her2. The EGFR/Her2 hetero-dimer produces an aggressive phenotype with poor prognosis[204].

1.4.7.2 KIT

Gain-of-function mutations of the KIT receptor are associated with several highly malignant tumours. These mutations cluster in either the sequence coding for the juxtamembrane region or the kinase domain. Mutations in exon 11 which codes for the juxtamembrane of KIT are found predominantly in gastrointestinal stromal tumours (GIST). These mutations relieve autoinhibition in turn permitting autophosphorylation of the kinase domain. The majority of GISTs are heterozygous for mutant KIT and cells from these tumours harbour heterodimers formed between mutant and wild-type KIT resulting in receptor activation in the absence of ligand[205].

Mutations of exon 17, affecting part of the coding region for the kinase domain, are more commonly seen in germ cell tumours. These mutations allow the receptor to adopt an active conformation and lead to constitutive activation. Exon 17 mutations in KIT often occur at Asp816 which is a highly conserved residue. Interestingly, mutations of the corresponding residue in MET and RET and are associated with renal and thyroid carcinomas, respectively[202;206;207].

1.4.7.3 FLT3

Mutations in the *FLT3* gene occur in approximately 5-15% of children and 25-35% of adults with acute myeloid leukaemia (AML)[208]. Internal Tandem Duplications (ITDs) and activation loop mutations are two common types of mutations which cause ligand-independent activation of FLT3. ITDs are insertions of repeated base pairs between 3-400 base pairs in length occurring in exon 14. Activating loop mutations mainly occur in exon 20 and are most commonly missense point mutations or insertions. Usually one or other type of mutation is found but occasionally both ITDs and activation loop mutations can be detected in the same malignancy [209;210].

1.4.8 Negative regulators of RTKs

The internalization and subsequent down-regulation of RTKs is controlled by two types inducible modifications, dephosphorylation and ubiquitination.

1.4.8.1 Deregulation of protein tyrosine phosphatases

Protein tyrosine phosphatases (PTP) can dephosphorylate RTKs and as such function as negative or positive mediators of signalling triggered by RTKs. Impaired tyrosine phosphatase activity due to loss-of-function mutations have been described and highlights their tumour suppressive role[211]. Other PTP such as, protein tyrosine phosphatase receptor kappa (PTPRk) has been shown to dephosphorylate EGFR and block EGFR-dependent signalling and inhibit the proliferation of human keratinocytes. In the same study the expression of PTPRk was shown to also decrease basal and EGF-stimulated EGFR tyrosine phosphorylation[212]. Flavell *et al.*, showed that over-expression of PTPRK in EBV-positive HL cell lines decreased their viability and proliferation while knockdown of PTPRk expression in

EBV-negative cell lines promoted proliferation, although they did not identify the cellular target of PTPRk [213].

1.4.8.2 Receptor ubiquitination

The c-Cbl proteins have a unique domain that binds phosphorylated tyrosine residues 'tagging' the RTK for receptor degradation and negatively regulates RTK function. c-Cbl achieves this by conjugating several ubiquitin molecules to the active RTK which serve as tags for lysosomal degradation. Alterations that uncouple c-Cbl from the RTK have been shown to contribute to carcinogenesis. For example, mutation of a C-terminal tyrosine in colony stimulating factor 1 receptor (CSF1R), which is the direct binding site for c-Cbl, enhances the transforming abilities of CSF1R in fibroblasts[214].

The leucine-rich repeats and immunoglobulin like (LRIG) proteins are a recently discovered family of negative regulators of RTKs. *LRIG1* is located at chromosome 3p14.3 and was first identified as a negative regulator of EGFR[215]. *In vitro* studies demonstrated a direct interaction between LRIG1 and EGFR which inhibited signalling by enhancing receptor ubiquitination and accelerating intracellular degradation. It has been proposed that in resting cells LRIG1 is only weakly expressed but upon RTK stimulation the *LRIG1* gene is transcriptionally activated and binds to all available receptors. Upon ligand induced activation of receptor, c-Cbl is activated and binds to the LRIG1-EGFR complex which then undergoes ubiquitination. The proposed function of LRIG1 is to mark EGFR for degradation [215;216].

The observation that LRIG1 is frequently deleted in lung and breast cancers lead to the hypothesis that LRIG1 functions as a tumour suppressor.[217] However, there is some

conflicting evidence with gene expression datasets suggesting in some tumours LRIG1 is over-expressed. Thomasson et al validated this finding in prostate tissue, showing that not only is LRIG1 over-expressed but is also associated with a poorer prognosis[218]. A second study found not only amplification of EGFR but also an increased copy number of 3p14.3 in a subset of breast cancers [219].

1.5 RTKs and HL

1.5.1 Protein tyrosine kinase expression in normal B cell development

Several protein tyrosine kinases (PTKs) such as syk, Bruton's tyrosine kinase (Btk) and src family kinases including lyn have been shown to be essential for normal B cell development[220] . Together these PTK are important transducers of signals originating from the pre-B cell receptor (pre-BCR) and the BCR. Syk participates in B cell fate decisions and antigen processing and is a critical component of the PI3K-Akt pathway. Btk is involved in pre-B cell maturation by regulating IL-7 responsiveness, cell surface phenotype changes, and the activation of lambda chain gene rearrangements[221]. In mature B cells, Btk is essential for BCR-mediated proliferation and survival. The importance of Btk is demonstrated in the primary immunodeficiency disease, X-linked agammaglobulinaemia (Bruton's agammaglobulinaemia), where patients with Btk mutations have normal pre-B cell populations in their bone marrow but these cells fail to mature and enter the circulation[222]. Mouse models have also demonstrated the contribution of several members of src family kinases to B cell development. For example, $lyn^{-/-}$ mice fail to produce mature B cells while mice lacking lyn, fyn and blk produce B cells arrested at an even earlier stage[223].

1.5.2 Receptor tyrosine kinase expression in normal B cell development

In contrast to PTKs, there is little information on the expression and activation of RTKs in normal B cells. Both KIT and FLT3 have been reported to be expressed during early B cell development [(224).] However, $KIT^{-/-}$ mice produce normal B cells while $FLT3^{-/-}$ mice show only a mild decrease in B cell populations[(225)]. Interestingly, a chimeric mouse model in which bone marrow harbours both wild type and $FLT3^{-/-}$ does demonstrate that B cells preferentially employs FLT3 dependent pathways to prime B cell progenitors[(226)]. These mouse models suggest that neither is essential for B cell development and that in their absence an alternative pathway is utilised.

The ablation of TRKA is lethal in the postnatal period. However, a mouse model has been developed in which TRKA can be restored to neuronal cells only which in turn produce a non-lethal phenotype. In this model, the immune system develops normally but there is deregulation of immunoglobulin production and the accumulation of B1 B cells; a subset of mature B cells which cannot differentiate into memory cells[(227)]. Although nerve growth factor (NGF), the ligand for TRKA, has been reported to be important in preventing memory B cell apoptosis, mice deficient in TRKA can still mount a humoral immune response.

B cell homing to the GC and interaction with FDC is critically dependent on integrin-mediated adhesion. The RTK, MET and its ligand hepatocyte growth factor (HGF) has been shown to have an important role in the regulation of this process. Van der Voort *et al.,* demonstrated that MET was up-regulated in centroblasts and can be induced in normal GC B cells by CD40 stimulation[(228)]. A subsequent study by Weimar *et al.,* found that MET is not expressed in B cells isolated from peripheral blood mononuclear cells (PBMCs) but can be induced by HGF or phorbol 12-myristate 13-acetate (PMA). They also found that GC B cells

stained positive for MET expression and that HGF induced adhesion of these cells to ECM, an effect that is mediated by integrins[229]. A more recent study found that in mature B cells, macrophage inhibitory factor (MIF) recruits MET to the CD74/CD44 complex which stimulates HGF secretion in turn promoting cell survival[230].

1.5.3 Contribution of RTKs to the pathogenesis of HL

To-date, a limited number of studies have examined the expression of RTKs in HL but from these it is clear that a number of RTKs are aberrantly expressed in this disease. For example it has been reported that primary HRS cells express both FGF ligands (FGF1 and 2) and 3 of 4 receptors (FGFR2, FGFR3 and FGFR4) and HL cell lines express FGFR3 but neither ligand[231]. The expression of multiple members of the FGFR family in HL is in contrast to other haematological malignancies such as multiple myeloma (MM) which only express FGFR3. In MM, FGFR3 is up-regulated as a consequence of the t(4;14) translocation. In the HL study, neither the t(4;14) translocation nor the *FGFR3* gene amplification could be detected in the 5 cases examined[231].

A global gene expression analysis of HL cell lines and subsequent analysis of biopsy samples revealed the over-expression in HRS cells of 6 RTKs: DDR2, RON, platelet derived growth factor α (PDGRFα), EPHB1, TRKA and TRKB[232]. Three of these RTKs; PDGFRa, TRKA and TRKB were also shown to be activated in primary HRS cells[232]. Although this study reported no significant association between subtype and RTK expression they did note that a greater number of RTKs are co-expressed in NSHL. When using a pan-tyrosine antibody, NSHL also showed a higher phosphorylated content suggesting activation. They further reported that a proportion of HRS cells express PDGF and EPH, the ligands for PDGFRa and EPHB1, respectively. Collagen and NGF (on granulocytes), which are the ligands for DDR2 and TRKA,

respectively were also observed to be present in the microenvironment in many cases of HL. These data suggest that these receptors are likely to be activated by ligand through both autocrine and paracrine mechanisms[232]. However, not all of the cases examined showed co-expression of both the receptor and its respective ligand. Sequence analysis of all six receptors showed no mutations which might account for constitutive activation. Interestingly, their study also identified several ASV, including the previously reported splicing of exon17 in TRKB and a splice variant of RON but also two novel ASVs of EPHB1[232].

A subsequent study by the same group also showed that another RTK, TIE-1 is overexpressed in primary HRS cells. This group also showed that the co-expression of 3 or more RTKs was associated with an EBV-negative status, suggesting that RTK signalling might functionally replace the virus in EBV-negative cases [233].

Another study by Renne *et al*., found that the overexpression of TRKA observed in HRS cells was not due to gene amplification. Furthermore, in a proportion of cases they found co-expression of its ligand, NGFβ, suggesting the constitutive activation of TRKA in HRS cells maybe a consequence of autocrine stimulation. In the same study, using an RTK inhibitor at concentrations known to be specific for TRKA, decreased HRS cell survival [234].

The expression of KIT in HL is controversial. It was first reported to be expressed in HRS cells in 11/21 HL cases[235]. This was supported by a subsequent study by the same group who found KIT but not its ligand, stem cell factor (SCF), to be expressed in HL cell lines. It was also shown that fibroblasts present in HL secrete SCF and that co-culture of HL cell lines with these fibroblasts increases HL cell survival[236]. This work has been disputed by three further studies that have not found KIT expression in primary HRS cells. In two of these studies mast

cells in HL biopsies were strongly positive for KIT[237;238]. The third study observed KIT expression in HL cell lines to be restricted to L1236 cells[239].

A recent study found HRS cells express both colony stimulating factor 1 (CSF-1) and its receptor CSF1R, neither of which are usually expressed in cells of B cell origin. They observed the constitutive expression and activation of CSF1R in both HL cell lines and primary HL tissue[240]. This study also identified a potential mechanism for the up-regulation of *CSF1R.* *CSF1R* transcripts found in HRS cells originate within a long terminal repeat (LTR) element. Transcriptional activation of the *CSF1R* LTR promoter was caused by a combination of epigenetic mechanisms and transcription factors such as NF-κB and AP-1[240].

The following sections are focused on two RTKs, MET and DDR1, in greater detail as these are the subject of the experimental work presented later in this thesis.

1.5.4 MET

HGF is the cognate ligand for MET and both ligand and receptor are distributed widely. HGF is produced by cells of mesenchymal origin and act on MET, expressed by epithelial cells in a paracrine manner[241]. Stimulation of MET by HGF causes autophosphorylation of two tyrosine residues 1234 and 1235 in the activation loop activating intrinsic kinase activity and in turn phosphorylating two further tyrosine residues 1349 and 1356 in the catalytic domain which enables binding of docking proteins[242-244]. In the absence of ligand the kinase activity of the receptor is inhibited by peptides in the C-terminal tail. The same peptides have been shown to be capable of inhibiting RON but no other RTKs[245]. The MET receptor triggers activation of a number of key signalling pathways (Figure 1.10) [246].

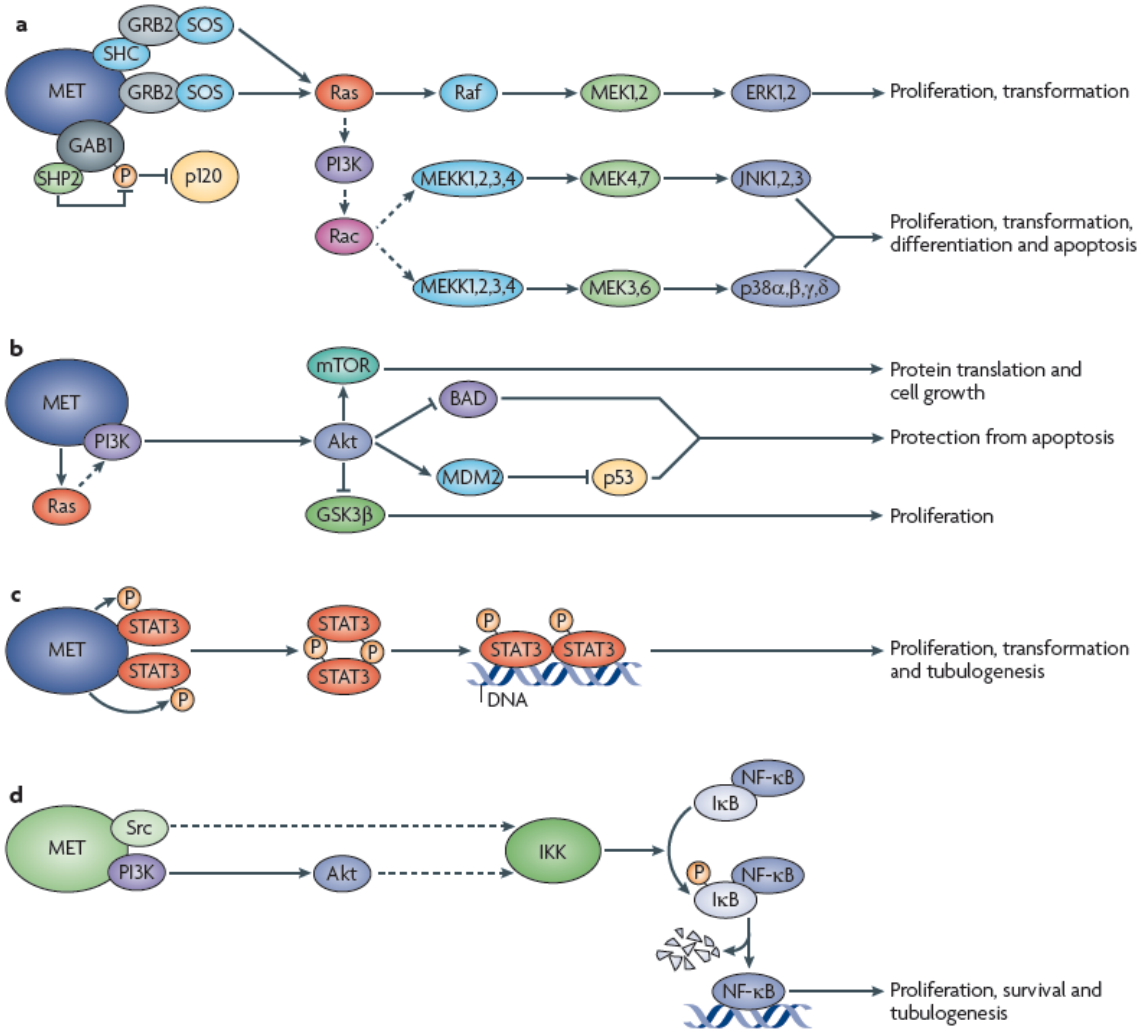

Figure 1.10 A diagrammatic representation of four key signalling pathways regulated by MET. Shown here is A) ERK, JNK and p38, B) Akt C) Stat3 D) NF-κB all of which can be activated by MET (Reproduced from Trusolino 2010 [246])

Under physiological conditions, several protein phosphatases such as PTPRJ, PTPRF, PTPN1 and PTPN2 have been shown to negatively regulate MET[246]. Receptor inactivation can also occur by c-Cbl mediated ubiquitination. Tyrosine phosphorylation of a residue at 1003 in the MET juxtamembrane results in the recruitment of ubiquitin ligase c-Cbl to MET, leading to receptor internalisation and lysosomal degradation[247].

Recently, LRIG1 has also been shown to bind to and negatively regulate MET. The mechanism of the negative regulation of MET by LRIG1 is unknown but Shattuck *et al.,* found that unlike EGFR, MET degradation occurred in an c-Cbl-independent manner[248-250].

The deregulation of MET has been linked to the invasive behaviour of several different malignancies including breast cancer, osteosarcomas, hepatocellular carcinoma and renal cell carcinoma[251]. The oncogenic capacity of MET has been validated in several animal models. For example, NIH 3T3 cells express HGF/SF and become tumourigenic in nude mice following the ectopic expression of MET[252].

The constitutive activation of MET occurs through several mechanisms, MET protein over-expression, *MET* gene amplification, germ-line and somatic mutations of *MET* and HGF over-expression. Mutations of MET broadly fall into two groups. The first group increases kinase activity of the MET receptor and promotes Ras-mediated signalling[253]. These mutations of *MET* have been shown to transform NIH3T3 fibroblasts but only in the presence of HGF [254]. The second group does not confer transforming capabilities but offers protection from apoptosis through activation of PI3K[253]. Other alterations of *MET* include splice mutations which delete the juxtamembrane domain essential for binding the c-Cbl E3-ligase. This uncoupling of c-Cbl mediated ubiquitination has been shown to be responsible for a proportion of lung adenocarcinomas[255].

The expression of MET in HL cell lines was first reported in 1990 and subsequently confirmed in two further studies[256-259]. A third study detected MET expression on activated centroblasts from lymph nodes of non-HL patients and in HL (positive cell type not specified). This study also reported the correlation between MET expression and EBV status in primary HL tissue and that MET can be induced by EBV in B cells isolated from PBMC. In contrast, Teofili *et al.,* found that MET is expressed in all primary HRS cells (45 lymph node and 12 bone marrow samples) but there was no association with EBV status. In addition, HGF was elevated in serum of patients with HL compared to normal controls [229;259]. Two further studies reported MET expression can be induced, in GC B cells, either by CD40 stimulation or by the co-operation of AP1 and NF-κB[228;260].

RON, the second member of the HGFR family, has been reported to be expressed by HRS cells (section 1.5.3). Expression of its ligand, macrophage stimulating protein (MSP), has not been investigated in HL [261]. Although RON is normally engaged by its ligand, MET and RON can form hetero-complexes leading to trans-phosphorylation of either receptor in the absence of respective ligand[262]. Reports from ovarian and bladder cancer suggest that the co-expression of MET and RON is associated with a more aggressive phenotype[263;264].

1.5.4 DDR1

The discoidin domain receptor (DDR) subfamily consists of two members, DDR1 and DDR2. They are unusual amongst RTKs for several reasons. First, their cognate ligands are triple helical activated collagens rather than soluble growth factors. Binding to collagen occurs through their discoidin domain and is integrin independent[147;265]. Second, while most RTKs exist as inactive monomers until ligand binding induces dimerization, this is not the case with DDR1 which exists in a pre-dimerized state[266]. Third, in contrast to all other RTKs, the

activation of DDR1 and DDR2 is slow with DDR1 taking up to 18 hours to reach maximal phosphorylation[267].

The structure of DDR1 is also not typical as it has an unusually long juxtamembrane region. Like other RTKs, alternative splicing around the juxtamembrane generates multiple isoforms. The DDR1c isoform is the longest, while DDR1b lacks 6 amino acids in the kinase region and exon 11 is absent in DDR1a. First described in colorectal carcinoma cell lines, DDR1d and DDR1e are truncated receptors missing the entire kinase domain, or parts of it, respectively. In Figure 1.11 these isoforms are depicted in diagrammatic form[268]. More recently, a further two soluble variants have been identified[195].

The relative expression of the isoforms differs between cell types. For example, DDR1b is the predominant form found during embryogenesis, whereas DDR1a is found in breast cancer cell lines and uniquely triggers leukocyte migration[269-272]. Phospho-peptide mapping has identified isoform-specific binding motifs which appears to be critical for differential downstream signalling[273]. For instance, a binding motif not found in DDR1a but present in DDR1b allows direct association with the adaptor protein ShcA. The functions of the kinase deficient isoforms are less clear. Recent the DDR1e isoform has been shown to be up-regulated in T cells upon stimulation with anti-CD3 monoclonal antibody and *in vitro* induce T cell migration through a 3D-collagen matrix[274].

The interaction between DDR1 and collagen is complex and maybe cell context dependent. One study showed that leukocytes express DDR1a which in response to collagen mediates cell migration[270]. In contrast, it has also been shown that over-expression of either DDR1a or DDR1b, in Madin-Darby Canine Kidney cells (MDCK) grown in 3D collagen matrix decreased collagen induced migration[275]. In addition to the phosphorylation and activation

of DDR1 in response to collagen, the shed kinase deficient isoforms interact with collagen to inhibit collagen fibrillogenesis and increase matrix mineralization[276].

DDR1 is induced by DNA damage and is a direct transcriptional target of the tumour suppressor gene p53[277]. Moreover, DDR1 is known to contribute to the invasive phenotype in numerous malignancies. For example in non-small cell lung cancer it is strongly associated with a more aggressive phenotype and lymph node metastases[278]. Similarly, in prostate cancer high expression of DDR1 was shown to contribute to invasive potential independent of hormonal status of the tumour[279].

A gene expression profiling study in B cell lineage ALL reported a high expression of DDR1 in cells without molecular rearrangement and those harbouring BCR-ABL[280]. A second study identified a somatic mutation of DDR1 (A803V) in AML corresponding to an amino acid in the kinase domain which potentially disrupts inhibition of the activation loop[281]. DDR1 expression has not been previously reported in HL but has already been described as an important inducer of several signalling pathways known to be associated with HL including JAK-STAT, NF-κB and PI3K[267;282]. A very recent study identified that DDR1 interacts with Notch 1 to promote pro-survival pathways and that collagen increases activated Notch 1 expression [283].

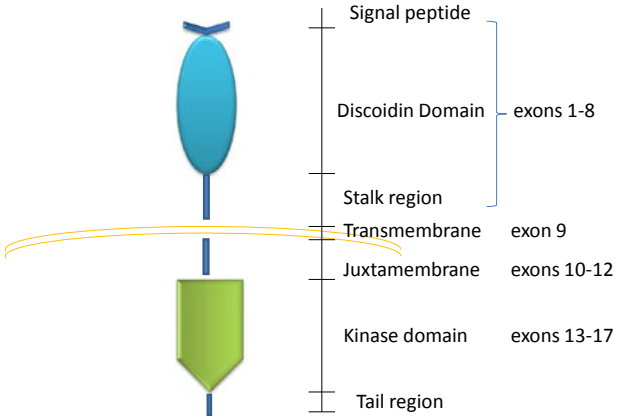

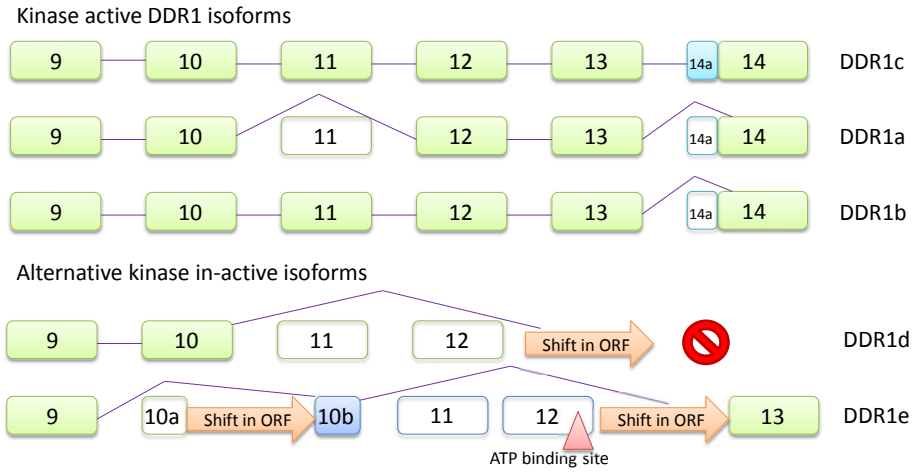

Figure 1.11 A) The domains of DDR1 in relation to exons B) A schematic representation of three kinase active isoforms and two ASV (numbering based on transcript variant 3 NM_013994.2)

1.6 Therapeutic targeting of RTKs

1.6.1 Oncogene addiction

Although cancer is a complex disease arising from the acquisition of multiple abnormalities, inhibition of a single oncogene can be sufficient to impair tumour cell survival and progression; a phenomenon termed oncogene addiction[284]. Evidence supporting this concept comes from cell lines, mouse models and clinical trials of targeted therapies. For example, in a transgenic mouse model, switching on the *C-MYC* oncogene in the hematopoietic cells led to the development of T-cell and myeloid leukaemia. However, when this gene was subsequently switched off, the leukaemic cells stopped dividing and displayed differentiation and apoptosis[285]. The earliest clinical evidence of oncogene addiction comes from the use of trastuzumab, a monoclonal antibody targeting Her2 in breast cancer[286]. The first targeted therapy in a haematological malignancy was imatinib used to treat chronic myeloid leukaemia (CML) [287].

CML is characterised by a balanced chromosomal translocation between the long arms of 9 and 22 (Philadelphia chromosome) giving rise to a novel constitutively activated kinase fusion protein formed between breakpoint cluster region and Abelson kinase (BCR-ABL). Imatinib was designed to target the kinase activity of BCR-ABL in CML. Clinical studies were impressive with >90% of patients with refractory CML achieving complete haematological remission with imatinib[288;289].

imatinib is now first line in the treatment of CML but resistance is observed in a proportion of patients which arises either de novo or during relapse after initial response. There are two main mechanisms of resistance. The first, is a more efficient cellular efflux which removes

the drug and prevents access to the target while the second is acquisition of new mutations which reactivate the kinase activity of BCR-ABL[290]. The re-activation of BCR-ABL highlights the dependence of CML on this specific oncogene. Cancer cells can also escape from oncogene addiction through the development of secondary mutations in a different oncogene. For instance, breast cancers induced in transgenic mice can acquire new mutations in p53 or Ras restoring proliferating properties to the tumour whilst inhibition of the primary pathway is still intact[284].

Oncogene switching is an alternative means by which cancer cells can escape oncogene addiction without *de novo* mutations and achieve chemo-resistance. For example, in glioblastoma both EGFR and MET can activate the PI3K pathway through recruitment of the adaptor protein GAB1. Ordinarily, GAB1 associates with EGFR but pharmacological inhibition of EGFR promotes GAB1 association with MET which can maintain PI3K signalling[291]. *In vitro* treatment of glioblastoma derived cell lines with EGFR inhibitor mono-therapy does not affect cell phenotype but a cocktail of EGFR, MET and PDGFR inhibitors did decrease cell viability[292]. From this a hierarchy model has been proposed in which inhibition of a dominant RTK results in the increased activity of other RTKs.

1.6.2 Secondary targets of small molecule inhibitors

Although imatinib was primarily designed to specifically inhibit the catalytic domain of abl kinase, it is also effective against other tyrosine kinases with structural similarity notably c-KIT and PDGF receptors[293]. Approximately 80% of GIST express KIT and 35% display PDGF receptors. Clinical trials in which imatinib were used to treat GIST showed that 75-90% of patients achieved a clinical response[294]. A study investigated the effect of imatinib in HRS cell survival, observed no effect on the only cell line shown to express KIT[239].

1.6.3 Second generation RTK inhibitors

Due to increasing resistance and intolerance to imatinib, efforts were made to develop new drugs that could also inhibit the BCR-ABL tyrosine kinase. While drug screening was used to develop imatinib, second generation inhibitors were developed with rational drug design approach due to increased knowledge of the structure of the BCR-ABL tyrosine kinase. Two drugs that have emerged are dasatinib and nilotinib and are already in clinical use. Both are more potent than imatinib. Furthermore, nilotinib has been shown to be effective against 32/33 mutations that are associated with imatinib resistance. The use of these newer generation drugs has not been studied in HL but a recent study identified DDR1 as a target of all three of these agents[295].

1.7 Study aims

Despite excellent overall cure rates, a proportion of HL patients will have disease which is either refractory to current treatments or which will recur. Moreover, in the paediatric age group, treatment is associated with significant long-term sequelae. In view of these limitations, new treatments are required which will not only improve cure rates but which will also reduce late-effects.

The use of RTK inhibitors is of proven benefit in the treatment of some cancers but to-date has not been explored in HL. This thesis investigates the aberrant expression and activation of RTKs in HL and considers RTKs as potential therapeutic targets in this disease. The specific aims of this thesis are to:

1. Provide a global analysis of the activation status of RTKs in HL cells. Following this, to explore the expression and activation in HL cell lines and primary HRS cells, of two RTKs, MET and RON.

2. To study the expression and regulation of DDR1 in HL, and to examine its activation by collagen, and how this contributes to the pathogenesis of HL.

3. Evaluate the effect of RTK inhibitors, including several next generation molecules, on the phenotype of HL cells.

CHAPTER 2

Materials and Methods

2.1 Primary HL samples

Paraffin embedded and frozen biopsy samples from primary paediatric HL were obtained through the Children's Cancer and Leukaemia Group (CCLG), study number 2007_BS_07. These samples were taken from patients recruited to one of three UK-wide HL paediatric clinical trials, HD1, HD2 or HD3. Samples were centrally reviewed and the histological subtypes were provided by the CCLG (Appendix I). Frozen samples were collected on dry ice from different CCLG centres and stored in the vapour phase of a -180^{o}C liquid nitrogen freezer.

2.2 Cell culture

2.2.1 Maintenance of cell lines

Suspension cell lines (Table 2.1) were maintained in RPMI 1640 medium (Gibco®, Invitrogen) supplemented with 10% v/v selected foetal calf serum (FCS; PAA the cell culture company) and 1% v/v penicillin/streptomycin (Gibco®, Invitrogen). All cells were incubated at 37^{o}C in a humidified atmosphere containing 5% CO_2 (Galaxy R CO_2 Incubator, RS Biotech). To replenish nutrients and remove waste, media was aspirated from flasks and cells pelleted by centrifugation (Eppendorf Centrifuge 5810R) at 150 rcf for 10 minutes. The supernatant was discarded and cell pellets were re-suspended in fresh pre-warmed media supplemented as above. Cells were counted and the appropriate number of cells transferred into sterile tissue culture vessels.

The adherent HCT116 cell line was maintained in (N-[2-Hydroxyethyl] piperazine-N'-[2-ethanesulphonic acid]) (HEPES)-buffered Dulbecco's Modified Eagle's Medium (DME/HEPES, Sigma) with supplements as above. Once cells were approximately 80% confluent, as

estimated by visual inspection under a microscope, they were sub-cultured to reduce cell density and prevent growth inhibition. Prior to passaging, HCTII6 cells were washed twice in phosphate-buffered saline (PBS: 1 PBS tablet dissolved in 100 ml of water, sterilised by autoclaving at 121^{o}C, 15 psi for 15 minutes). 1 ml of trypsin solution (Gibco®, Invitrogen) was then added to the cells and incubated at 37^{o}C for 5 minutes to allow detachment. Following gentle tapping of the flask to help dislodge cells, 15 ml of media was pipetted on to cells to neutralize the trypsin. The trypsinized cells were pelleted by centrifugation at 150 rcf for 10 minutes then re-suspended in fresh DME/HEPES media as above.

Table 2.1 Summary of cell lines and their origin.

Cell line	Growth Characteristics	Origin	Additional Information
L591	Suspension	Nodular Sclerosis HL	EBV-positive cell line originated from the pleural effusion of a female patient [296].
L1236	Suspension	Mixed Cellularity HL	EBV-negative cell line established from the peripheral blood of a male patient with advanced HL. The HRS cell origin of L1236 cells confirmed by identical immunoglobulin gene rearrangement sequences in L1236 cells and HRS cells of the same patient's bone marrow[88;297].
L540	Suspension	T–cell derived Nodular Sclerosis HL	EBV-negative HL cell line derived from bone marrow of a female patient with stage IV disease. Genomic analysis of the cell line revealed monoclonal rearrangements of T-cell receptor beta and gamma loci and germ line configuration of immunoglobulin genes[298;299].
L428	Suspension	Nodular Sclerosis HL	EBV-negative cell line established from the pleural effusion of a female patient with refractory disease[300].
KM-H2	Suspension	Mixed Cellularity HL progressing to Lymphocyte Depleted HL	EBV-negative cell line originally established from the pleural effusion of a male patient [301].
HDLM-2	Suspension	T-cell derived Nodular Sclerosis HL	EBV-negative cell line originally established from the pleural effusion of an elderly male patient. Genomic analysis revealed monoclonal rearrangements of T cell receptor beta and gamma loci and germ line configuration of immunoglobulin genes[298].
DG75	Suspension	BL	Established from the pleural effusion of a 10-year-old boy with BL[302].
BL41	Suspension	BL	Established from the tumour tissue of an 8-year-old Caucasian boy with BL; cells were described to be EBV-negative[303].
BL2	Suspension	BL	Established from the bone marrow of a relapsed 7-year-old Caucasian boy with non-endemic BL; cells are described to express to be EBV-negative and that somatic immunoglobulin gene hypermutation can be induced[304;305].
BJAB	Suspension	BL	EBV-negative, African-type BL [306]
K-562	Suspension	CML	Established from the pleural effusion of a female patient with chronic CML in blast crisis. Cells carry the Philadelphia chromosome with a BCR-ABL b3-a2 fusion gene[307].
HCT116	Adherent	Colon carcinoma	Established from the primary colon carcinoma of an adult male; cells were described to carry a RAS mutation[308].

2.2.2 Cryopreservation of cells

Aliquots of 5 x 10^6 cells were pelleted by centrifugation at 150 rcf for 10 minutes at 4^oC and re-suspended in 1 ml of chilled freezing solution (50% v/v supplemented RPMI medium, 40% v/v FCS and 10% v/v dimethyl sulphoxide (DMSO; Sigma)). Cells were transferred to cryopreservation tubes (Nunc®, Roskilde, Denmark) and cooled slowly overnight to -80^oC in a freezing box surrounded by sponge soaked in isopropanol. Cells were then transferred to either a -80^oC storage box for the short-term or moved to the vapour phase of a -180^oC liquid nitrogen freezer for long-term storage.

2.2.3 Recovery of frozen cells

Cells were thawed quickly at 37^oC to minimize exposure to DMSO. Pre-warmed RPMI with supplements was added gradually to the cells to dilute the DMSO and allow the cells to recover slowly. Cells were re-suspended in 5 ml of medium and grown in a 25 cm^3 flask at 37^oC in a humidified incubator with 5% CO_2.

2.2.4 Cell counting

Cell concentration was determined in non-adherent cell lines by removing a volume of cell suspension and mixing with an equal volume of trypan blue (typically 100 µl each). For adherent cell lines, cells were first harvested in the same manner as for sub-culture followed by the addition of 100 µl of trypan blue to 100 µl of cell suspension. 20 µl this solution was pipetted into disposable Glasstic® slide 10 (Hycor Biomedical Ltd., Edinburgh, UK). Using an inverted light microscope, all live (bright spherical) cells contained within five grids of the Glasstic® grid were counted. This number was then averaged and multiplied by 10^4 to obtain the number of cells per ml.

2.2.5 Mycoplasma testing

All cell lines were periodically tested using the MycoAlert® mycoplasma detection kit (Lonza) as per manufacturer's guidelines and were found to be consistently negative for mycoplasma.

2.3 RNA analysis

All procedures related to RNA work were carried out on ice with gloved hands to minimise RNase actions. Other measures to protect the samples from RNase degradation included the use of filtered tips (Rainin; Starlab), RNase free reagents and plasticware and cleaning of equipment and work surfaces with RNaseZap (Ambion,Inc).

2.3.1 RNA extraction from cultured cells

24 hours prior to harvesting, cells were counted and re-suspended in fresh pre-warmed supplemented media at a concentration of $3x10^5$cells/ml. Typically RNA was extracted from $3x10^6$ cells. The cell suspension was transferred to a 50 ml falcon tube and centrifuged at 150 rcf for 10 minutes at 4^oC to pellet the cells. The supernatant was aspirated and the cells were washed in cold 1xPBS to remove serum. The cells were then transferred to 1 ml microcentrifuge tubes (Eppendorf) and centrifuged at 800 rcf for 10 minutes at 4^oC. The cell pellet was kept on ice at all times to prevent RNA degradation. Total RNA was isolated from cells using the QIAGEN RNeasy® mini kit according to the manufacturer's protocol (Qiagen). RNA was eluted from the columns provided in the RNeasy™ kit with 30 µl of DEPC-treated water pipetted directly onto the membrane. The concentration of RNA was determined using a spectrophotometer (NanoDrop ND-1000).

2.3.2 Reverse transcription (RT) of RNA to cDNA

RNA was reverse transcribed to cDNA using SuperScript® III first-strand synthesis system (Invitrogen). Each reaction was performed in sterile 0.2 ml PCR tubes containing 1 µg RNA from each sample. First a mix consisting of 50 ng (500 µg/ml) random primers (Promega), 1 µl of 10 mM deoxyribonucleotide triphosphates (dNTP; Roche) was added to each sample. The volume made up to 13 µl using DNase/RNase-free water (Promega). This mixture was then incubated at 65°C for 5 minutes and then cooled on ice for 1 minute to denature RNA and prohibit re-annealing. A second master mix consisting of the following components was made up in a sterile microcentrifuge tube for each of the RNA samples: 4 µl of 5 X first strand buffer, 1 µl of 0.1 M dithiothreitol (DTT), 1 µl RNaseOUT™, 1 µl SuperScript® III RT (all Invitrogen). 7 µl of this master mix was added to each cDNA sample. Using an Eppendorf Thermal Cycler, cDNA was synthesised by incubating samples at 25^{o}C for 5 minutes followed by 50^{o}C for 1 hour. The reaction was terminated by heating the samples to 70^{o}C for 15 minutes and then held at 4^{o}C. The cDNA samples were stored at -20^{o}C until required.

2.3.3 Taqman® quantitative polymerase chain reaction (q-PCR)

2.3.3.1 PCR amplification of cDNA

A 20 µl reaction was set up in the wells of a 96-well optical reaction plate (Applied Biosystems). Each reaction contained 5 µl of diluted cDNA (typically 1:10 with RNAse/DNAse free water), 10 µl of 1x Taqman® Universal PCR MasterMix, 1 µl of 20x primers and probe (Table 2.2), 1 µl of endogenous control (typically GAPDH; all Taqman® Applied Biosystems) and 3 µl of RNAse/DNAse free PCR grade water. All samples were set up in triplicate and a negative control was included which contained water instead of cDNA. The plate was sealed

with an optically clear adhesive film (Applied Biosystems) and then placed in the ABI Prism 7700 Sequence Detection System (Applied Biosystems). Samples were subjected to enzyme activation at 50^{o}C for 2 minutes, a denaturation at 95°C for 10 minutes then by 40 cycles of denaturation at 95°C for 15 seconds and extension at 60°C for 1 minute.

2.3.3.2 The comparative Ct method (ΔΔCt) for relative quantification of gene expression

Livak and Schmittgen reported the delta-delta (ΔΔ) Ct method as an approach to quantify target genes transcripts normalised against the value of an endogenous control (e.g. GAPDH)[309]. Through the ΔΔCt method, variations in starting quantity or quality can be compensated. First, the difference between the Ct values of the target gene and the endogenous gene was calculated for each sample studied i.e. target Ct - endogenous Ct. A reference sample is selected as the 'baseline' sample for expression of the target gene. Then the difference between each of the samples ΔCt and the reference samples ΔCt was calculated, generating the ΔΔCt value for each sample (ΔΔCt = reference ΔCt - target ΔCt). The ΔΔCt for each sample was then converted to an absolute value using the following equation: fold change in expression level = $2^{-\Delta\Delta Ct}$ [309].

Table 2.2 List of Taqman® primers and probe

Target Gene	Applied Biosystem Assay number	Location
DDR1 (set 1)	Hs00233612_m1	Exon5-6 (NM_013994.2)
DDR1 (set2)	Hs01058424_g1	Exon16-17 (NM_013994.2)
MET	Hs01565584_m1	Exon 3
RON	Hs00899925_m1	Exon 20
LRIG1	Hs00394257_m1	Exon 6-7

2.4 Protein analysis

2.4.1 Protein extraction from cultured cells

For suspension cell lines, 24 hours prior to harvesting, cells were counted and resuspended in fresh pre-warmed supplemented media at a concentration of $3x10^5$cells/ml. To harvest cells, the cell suspension was transferred to a 50ml Falcon tube and centrifuged at 150 rcf for 10 minutes at 4^oC. The supernatant was aspirated and the cell pellet was washed in cold 1xPBS to remove serum. For samples which were subsequently analysed for phosphorylated proteins, 1 mM of activated sodium vanadate was added to 1xPBS. The cells were then transferred to 1 ml microcentrifuge tubes (Eppendorf) and centrifuged at 800 rcf for 10 minutes at 4^oC. The supernatant was aspirated and the cell pellet either kept on ice for immediate lysis or stored at -80^oC for use later.

Flasks of adherent cells were grown to 80% confluence and placed on ice. The medium was removed and 5 ml of chilled PBS was added directly to the flask and aspirated. 1 ml of chilled lysis buffer containing Radio-Immuno-Precipitation Assay (RIPA; 50 mM Tris-HCl pH 8, 150 mM NaCl, 1% Triton X-100, 0.5% sodium deoxycholate, 0.1% SDS), 1 mM of activated sodium vanadate and 1X protease inhibitor cocktail (Roche) was pipetted directly onto the cells and the flask left on ice for 30 minutes. Cell scrapers (Corning Inc,) were used to displace any adhering cells. The cells were then transferred to 1ml microcentrifuge tubes and lysed as described below.

2.4.2 Protein lysis

Suspension cells harvested for protein analysis were lysed by the addition of RIPA lysis buffer supplemented as above. Typically, 80 µl of lysis buffer was added to a pellet of $1x10^6$ cells.

Cells were thoroughly mixed with lysis buffer and left on ice for 30 minutes. Following this, the solution was centrifuged at 16000 rcf for 15 minutes at 4^{o}C to collect cell debris. The supernatant was transferred to a clean 0.5 ml tube and either used immediately or frozen at -20^{o}C.

2.4.3 Quantification of protein

Protein was quantified using the Bio-Rad Protein Assay (Bio-Rad Laboratories). 1 mg/ml stock bovine serum albumin (BSA; Sigma-Aldrich) was diluted to 0.1, 0.2, 0.3, 0.4 and 0.5 mg/ml concentrations with distilled water for protein standards. For each sample, 2 µl of whole cell protein lysate was diluted in 18 µl distilled water. 10 µl of diluted protein and standards was plated out in duplicate into each well of a 96 well plate (IWAKI). Bio-Rad Protein Assay Reagent was diluted 1:5 in distilled water and 200 µl pipetted into each well. Absorbance was read on a Bio-Rad 680 microplate reader at 595 nm. The standards were used to plot a calibration curve from which the protein content of the samples was determined.

2.4.4 Sodium dodecyl sulphate polyacrylamide gel electrophoresis

Sodium dodecyl sulphate polyacrylamide gel electrophoresis (SDS-PAGE) gels were made in two phases. An 8% resolving gel consisting of 30:1 acrylamide:bisacrylamide (Bio-rad), 390 mM TRIS-HCL pH 8.8, 0.1% w/v SDS, 0.06% w/v N,N,N',N'- tetramethylethylenediamine (TEMED, Sigma) and 0.1% w/v freshly prepared ammonium persulphate (APS; Sigma) was mixed and poured immediately into mini-Protean 3 Bio-rad apparatus. To give a uniform surface, 500 µl isopropanol was pipetted onto the surface of the gel. The gel was allowed to polymerise for 45 minutes before the isopropanol was rinsed off with water. A 5% stacking

gel consisting of 30:1 acrylamide:bisacrylamide, 125 mM TRIS-HCL pH 6.8, 0.1% w/v SDS 0.1% w/v TEMED and 0.1% w/v APS was pipetted on top of the resolving gel, a comb was inserted in the stacking gel and allowed to polymerise for 30 minutes. The gel combs were removed and wells washed out with 1x running buffer consisting of 30 g TRIS, 144 g glycine (Fisher Scientific), 10 g SDS in 10 litres distilled water.

Typically, 30 µg of protein was diluted 1:1 v/v 2X laemilli buffer (125mM TRIS-HCl pH6.8, 20% glycerol, 4% SDS, 10% β-mercaptoethanol, 0.004% bromophenol blue; Sigma). The protein was denatured by boiling at 95^{o}C for 10 minutes and sample contents were collected by brief centrifugation. Samples were loaded into each well alongside 10 µl of a protein marker (either Kaleidoscope marker; Bio-Rad or Spectra™ Multicolor Broad Range Protein ladder; Fermentas) Gels were run in 1X running buffer and the solubilised proteins were separated by electrophoresis at 125 V, (400 mA limit) for 2 hours.

2.4.5 Protein transfer

In a tank of transfer buffer (30 g TRIS, 144 g glycine, 2 litres methanol in 8 litres distilled water) six sponges, six pieces of Whatman® chromatography paper (Sigma-Aldrich) and one piece of nitrocellulose membrane (Amersham Hybond-C extra; GE Healthcare Life Science) were pre-soaked. These were then stacked in the following order: 3 sponges, 3 pieces of filter paper, gel, 1 nitrocellulose membrane, 3 pieces of filter paper, and 3 sponges, ensuring air bubbles were pushed out between each layer. The stack was set up, whilst submerged in transfer buffer, in an XCell II Blot Module (Invitrogen) which was then placed into the XCell *Surelock* Mini-Cell (Invitrogen). Transfer buffer was poured into the tank around the plates up to a depth of two thirds of the tank. Protein was allowed to transfer from the gel to the nitrocellulose membrane at 40 V, 400 mA for 2 hours while the tank was placed on ice.

2.4.6 Immunoblotting

Non-specific protein binding was blocked by incubating the membrane for 1 hour at room temperature in 5% non-fat dried milk dissolved in TRIS buffered saline-tween (TBS-T), consisting of 1.21 g TRIS and 8.77 g NaCl in 1 litre distilled water (pH adjusted to 7.6 using concentrated HCl) with 0.5 ml Tween20 (Fisher Scientific). For phospho-specific antibodies, membranes were blocked with filtered 5% BSA and 0.05% Tween20 in TBS. The membrane was sealed in a bag incubated in diluted primary antibody (Table 2.3) overnight on an orbital shaker at 4^{o}C.

After rinsing three times for 10 minutes in TBS-T the membrane was incubated for 1 hour in the corresponding HRP-conjugated secondary IgG (DakoCytomation). The membrane was again rinsed by three 10 minute washes in TBS-T.

Antibody-protein complexes were detected using the enhanced chemiluminescence (ECL) kit (Amersham Biosciences). 1 volume of each ECL reagent was mixed in a tube immediately prior to use. The membrane was incubated in the ECL mixture for 1 minute and then the excess liquid drained off. The membrane was transferred to an autoradiography cassette and in a dark room a sheet of Hyperfilm™ (Amersham Biosciences) was placed on top. The film was exposed to the membrane for between 30 seconds to 1 hour. The Hyperfilm™ was developed in a Kodak X-OMAT 1000 processor (Kodak Limited).

Following the detection of the protein of interest, membranes were stripped by incubation in 1x mild stripping solution (Chemicon) for 20 minutes on a shaker. The membrane was then re-blocked and re-probed as described above but using only 1 hour incubation in primary antibody to either MCM-7 or β-actin.

Table 2.3 List of primary antibodies used for immunoblotting.

Target protein	Clone	Company	Species	Dilution (Immunoblotting)
DDR1	C-20	Santa- Cruz	Rabbit	1:200
MET	C-12	Santa- Cruz	Rabbit	1:200
MET	25H2	Cell signalling	Mouse	1:1000
pMET Tyr1003	13D11	Cell signalling	Rabbit	1:1000
pMET Tyr1234/35	D26 XP™	Cell signalling	Rabbit	1:1000
pMET Tyr1349	130H2	Cell signalling	Rabbit	1:1000
pGab1 Tyr307	-	Cell signalling	Rabbit	1:1000
RON	C-20	Santa- Cruz	Rabbit	1:200
LRIG1	-	Agrisera	Rabbit	1:1000
PARP	-	Cell Signalling	Rabbit	1:1000
Phospho-Tyrosine	4G10	Millipore	Mouse	1:200
STAT3	124H6	Cell Signalling	Mouse	1:1000
pSTAT3 Tyr705	D3A7	Cell Signalling	Rabbit	1:1000
STAT5	-	Cell Signalling	Rabbit	1:1000
pSTAT5 Tyr694	C71E%	Cell Signalling	Rabbit	1:1000
Nck2	8.8	Sigma	Mouse	1:250

2.4.7 Immunoprecipitation

Immunoprecipitation (IP) reactions were performed on cells split 24 hours prior to harvesting to ensure they were in the log phase of growth as described in section 2.2.1. For each IP reaction, 100 µl of Protein G agarose bead slurry (Millipore) were transferred to 1.5 ml Eppendorf tubes and then washed with RIPA buffer. This was done three times by centrifugation at 2000 rcf for 1 min followed by aspiration of supernatant and re-suspension of beads in RIPA buffer. After the final spin, the beads were re-suspended in RIPA buffer as 50% slurry.

Typically for IP experiments, 500 µg of protein was harvested and sample volumes equalised with RIPA buffer to 500 µl. To reduce non-specific binding, lysates were pre-cleared by adding 50 µl of agarose bead-RIPA slurry and incubating on rotating wheel at 4^{o}C for 1 hour. The samples were centrifuged for 1 min at 2000 rcf to pellet the beads. The supernatant was transferred to fresh eppendorf micro-centrifuge tubes and bead pellet discarded. To each sample, 2 µg of primary DDR1 antibody was added. A duplicate positive control lysate was incubated with an irrelevant rabbit immunoglobulin (instead of DDR1 antibody) to serve as a negative control. The samples were incubated with the antibody overnight on a rotating wheel at 4^{o}C.

The following day, 100 µl of the pre-prepared 50% agarose bead slurry was added to each sample and incubated for 2 hours on the rotating wheel at 4^{o}C. This enabled the antibody-protein complexes to bind to the beads which were then subjected to centrifugation to pellet the bound immune-complexes. The supernatant was discarded and the beads washed three times with RIPA buffer as described above. After the final spin the beads were re-suspended in 100 µl of SDS buffer and boiled for 5 minutes at 95^{o}C to elute the immune

complexes from the beads. The sample was centrifuged for 1 min at 2000 rcf to pellet the bead. The supernatant was collected and subjected to SDS-PAGE and immunoblotting, as described in sections 2.4.4 and 2.4.5.

Protein detection was performed as described in section 2.4.6 but instead of a rabbit secondary, Cleanblot® was used to reduce non-specific binding to the immunoglobulin light and heavy chains. SuperSignal (Millipore) was used as an alternative chemi-luminescent agent to enhance signal intensity of the phosphorylated proteins.

To confirm equal IP efficiency the membrane was stripped as detailed in section 2.4.7 and re-probed with DDR1 antibody. Cleanblot® was again used as the secondary antibody.

2.4.8 The Human Phospho-Receptor tyrosine kinase array (phospho-array)

2.4.8.1 Principle of the phospho-array

The phosphorylation status of 42 RTKs was analysed using a commercially available array (Ary001, R&D system). The kit comprises nitrocellulose membranes containing capture and control antibodies which have been spotted in duplicate. Internal negative and positive controls are also included on the array. The respective RTK bind to these antibodies through their extracellular domain and unbound material is washed off. A pan phospho-tyrosine HRP-conjugated antibody is then applied to the membrane which forms immune complex with the bound phosphorylated RTKs (Figure 2.1). These complexes were then visualised by chemiluminesence.

2.4.8.2 Protocol for the phospho-array

To prepare cells for this array, the cell lines were maintained as described in section 2.2.1 and 24 hours prior to harvest, cells were counted and re-suspended at $3x10^5$/ml in either fresh media supplemented with 10% serum or fresh media without serum. Cells were lysed according to the method in section 2.4.2 using the following lysis buffer (1% Igepal, 20mM TRIS-HCL 137 mM sodium chloride, 10% glycerol, 2 mM EDTA, 2 mM sodium vanadate and 1x protease inhibitor). Protein concentration was determined as set out in section 2.4.3 and the 50 µg of whole cell lysate was applied to membrane and the array was performed according to the manufacturer's guidelines.

The membranes were visualised with ECL reagent and the signal strength from each spot measured by pixel densitometry. To account for variations in exposure, a blank area of the developed film immediately outside the region of the array was also measured. The average of the duplicate spots was calculated and the relative phosphorylation of individual RTK then determined relative to the background.

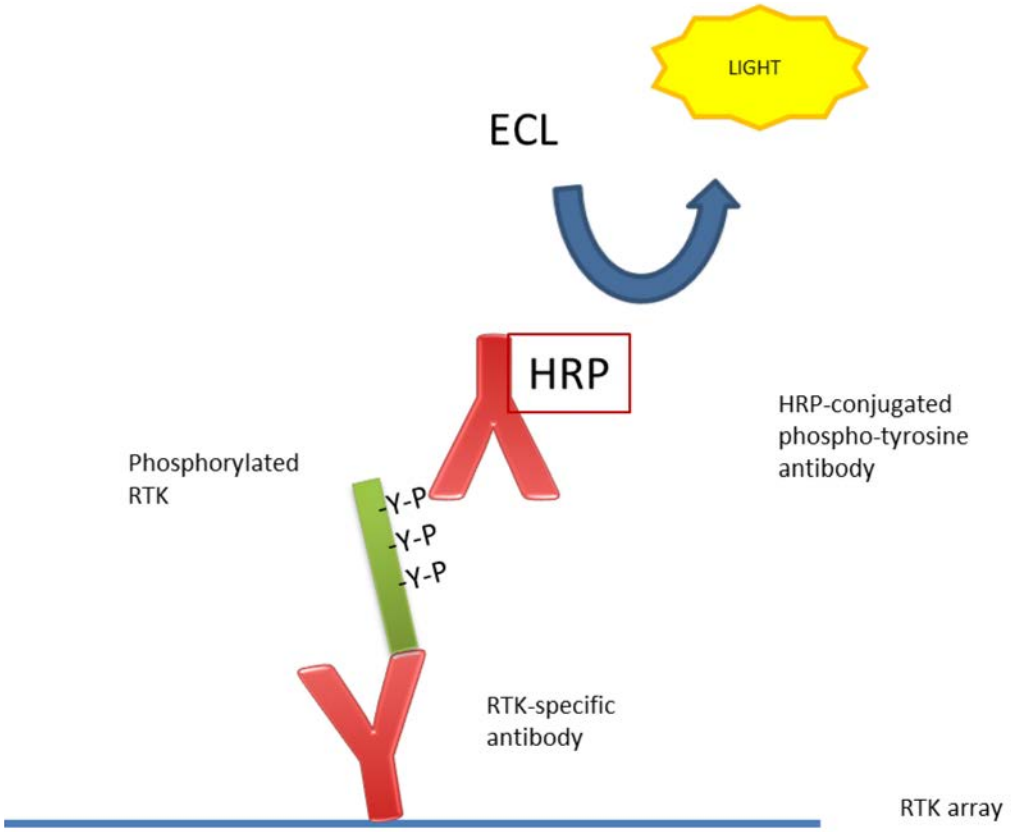

Figure 2.1 A schematic of the immune-complexes formed in the RTK array. (Reproduced from R&D systems product information)

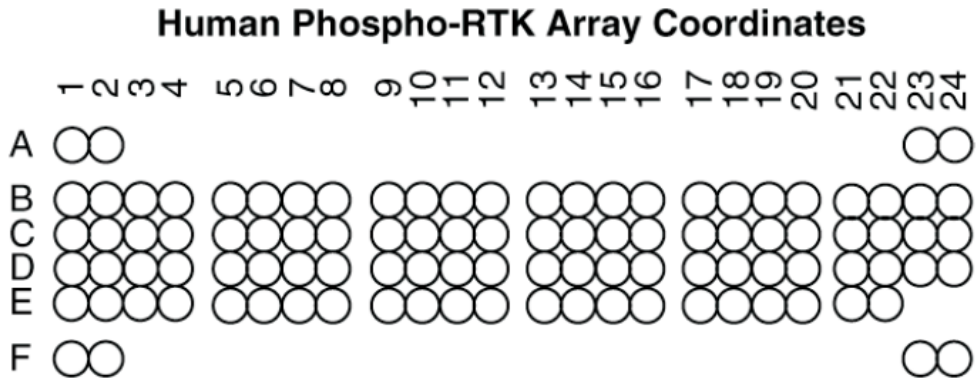

Coordinate	Receptor Family	RTK/Control		Coordinate	Receptor Family	RTK/Control
A1, A2	Control (+)	PY-Control*		D1, D2	Tie	Tie-2
A23, A24	Control (+)	PY-Control*		D3, D4	NGF R	TrkA
B1, B2	EGF R	EGF R		D5, D6	NGF R	TrkB
B3, B4	EGF R	ErbB2		D7, D8	NGF R	TrkC
B5, B6	EGF R	ErbB3		D9, D10	VEGF R	VEGF R1
B7, B8	EGF R	ErbB4		D11, D12	VEGF R	VEGF R2
B9, B10	FGF R	FGF R1		D13, D14	VEGF R	VEGF R3
B11, B12	FGF R	FGF R2α		D15, D16	MuSK	MuSK
B13, B14	FGF R	FGF R3		D17, D18	Eph R	EphA1
B15, B16	FGF R	FGF R4		D19, D20	Eph R	EphA2
B17, B18	Insulin R	Insulin R		D21, D22	Eph R	EphA3
B19, B20	Insulin R	IGF-I R		D23, D24	Eph R	EphA4
B21, B22	Axl	Axl		E1, E2	Eph R	EphA6
B23, B24	Axl	Dtk		E3, E4	Eph R	EphA7
C1, C2	Axl	Mer		E5, E6	Eph R	EphB1
C3, C4	HGF R	HGF R		E7, E8	Eph R	EphB2
C5, C6	HGF R	MSP R		E9, E10	Eph R	EphB4
C7, C8	PDGF R	PDGF Rα		E11, E12	Eph R	EphB6
C9, C10	PDGF R	PDGF Rβ		E13, E14	Control (-)	Mouse IgG_1
C11, C12	PDGF R	SCF R		E15, E16	Control (-)	Mouse IgG_{2A}
C13, C14	PDGF R	Flt-3		E17, E18	Control (-)	Mouse IgG_{2B}
C15, C16	PDGF R	M-CSF R		E19, E20	Control (-)	Goat IgG
C17, C18	RET	c-Ret		E21, E22	Control (-)	PBS
C19, C20	ROR	ROR1		F1, F2	Control (+)	PY-Control*
C21, C22	ROR	ROR2		F23, F24	Control (+)	PY-Control*
C23, C24	Tie	Tie-1				

Figure 2.2 Template and location coordinates of the RTKs found on the human phospho-array.

2.5 FACS detection of surface proteins

2.5.1 Principle of flow cytometry

In flow cytometry, a laser light source of single wavelength passes onto a fluorescent-labelled sample. A number of detectors are aimed at the point where the sample passes through the light beam: one in line with the light beam (Forward Scatter or FSC) and several perpendicular to it (Side Scatter (SSC) and fluorescent detectors). Each individual cell passing through the beam scatters the ray, and the fluorescent labels emit a light at a longer wavelength than the light source. This combination of scattered and fluorescent light is picked up by the detectors. From this it is possible to derive various types of information about the physical and chemical structure of each individual particle. FSC correlates with the cell volume and SSC depends on the inner complexity of the particle (i.e., shape of the nucleus, the amount and type of cytoplasmic granules or the membrane roughness). Each fluorescent label has its own wavelength at which light is excited and emitted. However, compensation is required to account for the overlap between the spectra generated by different fluorescent labels[(310)].

2.5.2 Detection of DDR1 protein expression (indirect method)

Flow cytometry was used to detect DDR1 cell surface proteins on primary GC B cells, extracted, purified and transfected as outlined in section 2.15. Samples were washed in 1x PBS and re-suspended in 50 µl of AutoMACS® buffer (Miltenyi Biotec). Except for the unstained control cells, 20 µl of appropriate dilute antibody was added to the cells. This was left to incubate in the dark at 4^{o}C for 15 minutes. 1 ml of AutoMACS® buffer was added to each of the samples and centrifuged at 800 rcf for 10 minutes. The supernatant was then

aspirated and the pellet re-suspended in 500 µl of AutoMACS®. The DDR1 antibody used in this experiment was unconjugated so the incubation process described above was repeated with a second fluorescein isothiocyanate (FITC)-conjugated rabbit antibody. Prior to analysis 5 µl of propidium iodide (PI) was added to the samples on FACS calibur (Becton Dickinson).

Live cells were gated by morphology and PI positive staining. This population was then used subsequent analysis and the following controls were used to set up compensation and quadrants:

- Unstained cells
- Cells positive for $CD10^{+}PE$
- Cells positive for NGFR-APC
- Cells stained with Rabbit-FITC alone
- Cells stained with DDR1 alone

Data was analysed using Flowjo software (Treestar Inc).

2.6 Quantification of HGF by enzyme linked immune-absorbant assay (ELISA)

The production of HGF by HL cell lines was measured using a commercially available ELISA kit (Quantikine R&D systems). For this assay, cells were maintained in normal growth conditions and split 24 hours prior to the start of the experiment. For each cell line, $3x10^6$ cells were counted and centrifuged at 800 rcf for 10 minutes to pellet the cells. The pellets were washed twice in serum free media and re-suspended in 10 ml of serum free media and transferred to 25 cm^3 flasks. At 24 hours and 48 hours the cell suspension was centrifuged as above and the supernatant retained for immediate analysis. The ELISA was performed in accordance with the manufacturer's protocol and absorbance read at 450 nm. A calibration

curve was calculated from the standards included in the kit and from this HGF concentration was determined.

2.7 Treatment of cells with collagen

Soluble type I collagen (extracted from rat tails; Sigma) was added to media at a concentration of 10 μg/ml.

2.8 Treatment of cell lines with RTK inhibitors

All RTK inhibitors were dissolved in DMSO to produce 10mM stock solutions which were stored as aliquots at -20^{o}C. Cells were split 24 hours before treatment with drugs and resuspended at a concentration of 3x10^{5}/ml in fresh media supplemented with 10% serum. Aliquots of the drug to be tested were thawed as required and serially diluted in media to produce the desired concentration and applied to the cells.

2.9 Cytotoxity and cell proliferation assays

2.9.1 Cell Proliferation

2.9.1.1 Principle of Celltiter 96®AQ$_{ueous}$ One Solution cell proliferation

The Celltiter 96®AQ$_{ueous}$ One Solution cell proliferation assay (Promega) is a colorimetric method for determining proliferation by metabolic activity. The reagent contains an electron coupling reagent (phenazine ethosulfate; PES) and a tetrazolium compound [3-(4,5-dimethylthiazol-2-yl)-5-(3-carboxymethoxyphenyl)-2-(4-sulfophenyl)-2H-tetrazolium; MTS].

The MTS tetrazolium compound is bio-reduced by metabolically active cells producing formazan and the quantity of formazan, measured by absorbance at 490 nm, is used to as marker of proliferating cells.

2.9.1.2 Protocol of Celltiter 96®AQ_{ueous} One Solution cell proliferation

100 µl of cell suspension were seeded per well at a concentration of $2x10^5$/ml, a concentration previously determined in optimisation experiments. This number of cells was sufficient to produce a signal on the linear range of the assay and ensured sufficient nutrients for the experimental period which was typically 3 days. For measurement of cell proliferation, cells were seeded in a 96 well plate at time zero. The plate containing cells were incubated at 37^oC in a humidified atmosphere containing 5% CO_2. 2 hours prior to reading the absorbance, 20µl of Celltiter 96®AQ_{ueous} One Solution was added and the plate returned to the incubator. The absorbance was read on a microplate reader at 490 nm. To prevent contamination of cells a separate plate was used for each time point measured.

2.9.1.3 Data Analysis

Background absorbance at 490nm was corrected by subtracting the mean of a triplicate set of wells with media alone and no cells from the experimental wells. Cells were typically seeded in quadruplicate and for drug inhibition studies wells containing cells treated with vehicle alone (DMSO) were included. Vehicle-only cells were assigned a value of 100 and metabolic activity of treated cells was calculated as a proportion of this to give relative percentage cell proliferation.

2.9.2 Measurement of apoptosis by FACS detection of Annexin V staining

2.9.2.1 Principle of Annexin V staining

Apoptosis is characterised by morphological changes including the loss of plasma membrane. In apoptotic cells, the membrane phospholipid phosphatidylserine (PS) is translocated from the inner to the outer leaflet of the plasma membrane, thereby exposing

PS to the external cellular environment. Annexin V is a 35kDa Ca^{2+}-dependent phospholipid-binding protein that has a high affinity for PS, and binds to cells with exposed PS[311]. Annexin V conjugated to a fluorochrome, such as FITC, can be detected by flow cytometric analysis which, in conjunction with PI, can distinguish viability, apoptosis and necrosis.

2.9.2.2 Protocol for Annexin V staining

Typically, $5x10^5$ cells were washed twice with cold PBS by centrifugation at 800 rcf for 10 minutes at 4^oC and then resuspended in 100 µl 1X Binding Buffer (0.1 M HEPES, pH 7.4; 1.4 M NaCl; 25 mM $CaCl_2$; BD Pharmigen). This solution was transferred to a 5 ml FACS tube and 5µl of Annexin V was added to each sample. The cells were gently mixed and incubated for 15 min at room temperature in the dark. 400 µl of 1X Binding Buffer was pipetted into each tube and the samples analyzed by flow cytometry as soon as possible (within 1 hour).

The following controls were used to set up compensation and quadrants:

- Unstained cells
- Cells stained with Annexin V-FITC alone (no PI)
- Cells stained with PI alone (no Annexin V-FITC)

2.10 Nucleofection

2.10.1 Knockdown of gene by siRNA

ON-TARGETplus SMARTpool siRNA from Dharmacon were used for the silencing of DDR1 (Table 2.4). Scrambled siRNA served as the corresponding control for all knockdown experiments.

24 hours prior to nucleofection, cells were counted and re-suspended at a concentration of $5x10^5$/ml in fresh supplemented media containing 10% serum. For L428 cells the number required for each experiment was calculated based on $3x10^6$ cells per reaction. On the day of nucleofection 3 ml of media per reaction was pre-warmed in an incubator at 37^oC. The required number of cells were counted and centrifuged at 100 rcf for 7 minutes at room temperature. Supernatant was aspirated and the cell pellet was re-suspended in 100 µl of the pre-prepared nucleofection solution. 3 µg per reaction of either DDR1 siRNA or scrambled siRNA was added and 100 µl transferred to sterile cuvette (Amaxa; Lonza) ensuring there were no bubbles. The cuvette was placed in the nucleofector device (Amaxa; Lonza) and program X-001 selected. The cuvette was taken out of the device but the sample left in, for 10 minutes at room temperature. Following this, 500 µl of pre-warmed media was pipetted into the cuvette and transfected solution transferred into the prepared media. 4 hours later a further 9 ml of warm media was added to each sample. Cells were incubated at 37^oC in a humidified atmosphere with 5% CO_2 until required for analysis.

Table 2.4 DDR1 ON-TARGET SMARTpool siRNA target sequence and location (NM_013994.2).

Target Sequence	Target location (EXON)
UGGUUACUCUUCAGCGAAA	3
GGAGCUACCGGCUGCGUUA	7
GCGUGUGUGUGCAGGACGA	14
ACGAGCAGGUCAUCGAGAA	16

2.10.2 LRIG1 expression plasmid

Cell lines were split 24 hours prior to nucleofection and resuspended in fresh supplemented media at a concentration of $3x10^5$/ml. 4 µg of the LRIG1pcDNA3.1-myc tagged overexpression plasmid (Gift from Dr Colleen Sweeny, UC Davis Cancer Centre, California) or 4 µg of pcDNA3.1 (empty vector; Invitrogen) were nucleofected using the Amaxa nucleofector and solutions as described above. The protocol was individualised based on the cell line to be transfected:

- L428 L solution program X-001
- L540 V solution program T-001
- KMH2 T solution program T-001

2.11 Immunohistochemistry

2.11.1 Preparation of tissue sections

Frozen sections of 5 µm thickness were cut using a standard cryostat and placed onto uncoated slides. Paraffin-embedded blocks were cut to 4 µm thickness and placed onto adhesive-coated slides (Vectabonded, Surgipath™). Where the tissue blocks were retained by the local CCLG centre, pre-cut 4 µm tissue sections were requested.

For immunohistochemical staining, sections of paraffin-embedded tissue biopsies were de-waxed and rehydrated. This was done by immersing the slides sequentially in each of the following solutions for 10 minutes: Histoclear (a xylene substitute), 100% ethanol and 70% ethanol.

Next, the endogenous peroxidase activity was blocked for 10 minutes in 3% hydrogen peroxide in methanol (Sigma-Aldrich). Slides were rinsed thoroughly in running tap water and subjected to different methods of antigen retrieval, optimised to individual antibodies (Table 2.5)

2.11.2 Antigen retrieval

Microwave antigen retrieval

Citrate buffer (1.26 g sodium citrate, 0.25 g citric acid, 800 ml distilled water; pH adjusted to pH 6.0 with 0.1 M sodium hydroxide) was made up to 1 litre and boiled in a glass beaker for 10 minutes at full power before immersing the slides pre-loaded on a rack into the buffer. Ensuring that the slides were submerged completely the beaker was covered with cling film which was pierced. The beaker was returned to the microwave and heated for 10 minutes at moderate power then 10 minutes at low power. The buffer was allowed to cool (approximately 30 minutes) before the slides were removed and rinsed in running water.

Agitated low temperature epitope retrieval (ALTER)

Slides were loaded in a rack and placed in a 1.5 litre glass beaker containing 1 litre of EDTA buffer pH8 with Tween20 (Binding site, Birmingham). The beaker was covered in foil and placed on a hotplate stirrer (Jenway) set at 600 rpm and 65^{o}C for 16 hours. The solution was then cooled by placing the beaker under running water for 5 minutes.

Wax Capture Buffer (WCap Buffer)

Slides were placed in plastic slide staining jar filled with 250mls of WCAP buffer pH8.0 (Bio-Optica Milano s.p.a.). This jar was incubated in a water bath set at 98°C for 20 minutes. The

slides were then transferred to a rack submerged in warm distilled water and allowed to cool for 10 minutes.

2.11.3 Detection of antigen

After antigen retrieval, slides were placed on a slide tray and the tissue section encircled using a PAP-PEN (Dako). Slides were incubated in TBS pH 7.6 for 5 minutes and then blocked using 2X casein blocking solution (Vector laboratories) to reduce non-specific background staining. The sections were incubated with diluted primary antibody overnight at 4^{o}C. Samples were washed in TBS for 5 minutes. Secondary detection was performed with DakoChemate envision secondary antibody (Dako) using 2 drops of biotinylated universal secondary antibody for each tissue section for 30 minutes. Sections were washed again in TBS for 5 minutes.

2.11.4 Visualization and counterstaining

Visualisation was carried out using diaminobenzidine (DAB) (Vector laboratories). Substrate solution was applied to each tissue section ensuring complete coverage (usually 100 µl) for between 30 seconds to 2 minutes. During this process the substrate was converted to an insoluble brown product by the antigen-bound peroxidases. Slides were rinsed with TBS, counterstained with Mayer's haematoxylin (Sigma) for 30 seconds, washed under running tap water for 5 minutes. The stained sections were then sequentially dehydrated through 70% ethanol, 100% ethanol and Histoclear for 10 minutes each, before being mounted with a coverslip using DPX mounting (Invitrogen).

Table 2.5 Antibodies and retrieval methods used for immunohistochemistry.

Target protein	Retrieval method	IHC Dilution
DDR1	ALTER	1:80
MET	CITRATE BUFFER	1:200
LRIG1	CITRATE BUFFER	1:800
RON	CITRATE BUFFER	1:400
p-RON	WCAP BUFFER	1:25
LMP1	ALTER	1:25
COLLAGEN I	ALTER	1:200
COLLAGEN II	ALTER	1:500

2.12 Van Gieson method

For Van Gieson's stain, tissue sections were first dewaxed and rehydrated as described in section 2.11.1. Slides were then placed on a slide tray and tissue sections encircled using a PAP-PEN. 100 µl of 4% iron alum was pipetted onto the slides ensuring the section was completely covered. After 5 minutes slides were rinsed in tap water and the nuclei counter-stained with Mayer's haematoxylin for 5 minutes. The sections were again washed in warm tap water and placed on a slide tray and 100 µl of Van Gieson's solution applied for 10 minutes. The slides were blot dried with filter paper ensuring no contact with water after this point. Following the Van Gieson method, stained sections were dehydration by rinsing in 100% ethanol for 30 seconds followed by Histoclear for 5 minutes.

2.13 cDNA sequencing

2.13.1 Primer design

Polymerase chain reaction (PCR) primers were designed using primer 3 software (www.primer3.com). Human genomic sequence for DDR1 was obtained from the NCBI genome browser (www.ncbi.nlm.nih.gov). Desirable characteristics of the primer sequences were a length of 18-25 bp, G+C content of 40-60% with an annealing temperature of 58 - 62^{O}C. For the amplification of cDNA, oligonucleotide primers were designed to bind specifically the gene of interest. Basic local alignment search tool (BLAST) searches (http://www.ncbi.nlm.nih.gov/BLAST/) were performed in all cases to ensure that primers were not complimentary to other regions of the genome and bound specifically to the target sequences. Primers were synthesised by Alta-Biosciences (University of Birmingham) and supplied as lyophilized pellets (Table 2.6). Primers were reconstituted in DEPC treated water (Applied Biosystems) to a concentration of 100 µM and stocks stored at -20^{o}C in aliquots.

2.13.2 RT-PCR of cDNA

A PCR-reaction master mix consisting of the following components was made up in a sterile eppendorf tube for each of the cDNA plus a water control: 12.5 µl 2X PCR MasterMix (Promega), 2.5 µl 3' primer, 2.5 µl 5' primer (2µM) 17.5 µl of this master mix was pipetted into sterile 0.2 ml PCR tubes, 2 µl of synthesized cDNA was added to the master mix and the total volume made up to 25 µl with RNase/DNase free water. PCR amplification in an Eppendorf Thermal Cycler included an initial 5 minute denaturation at 94°C, followed by 30 cycles of denaturation for 30 seconds at 94°C, an annealing step for 1 minute at a temperature specific for primers, and an extension for 1 minute at 72°C. A final extension step of 72°C for 10 minutes ensured all single stranded molecules have been replicated and was followed by storage at 4^{O}C.

2.13.3 Agarose gel electrophoresis of PCR products

The amplification of PCR products was confirmed by electrophoresis using agarose gels. 5 µl of each sample, alongside the water control which had gone through the PCR cycles, was loaded. 5 µl of 100 bp Ready-Load™ DNA ladder (Invitrogen) was added to the first lane of the submerged gel in the gel electrophoresis tank. The gel was run for 1 hour at 120 V, 95 mA. Photographs were taken under UV light and documented using a GeneFlash Syngene Bio Imaging Analyzer.

Table 2.6 DDR1 primers for sequencing cDNA

PRIMER	FORWARD	REVERSE
Pair 1	5’ ccttaggcccgagggatc 3’	5’ tgcctgagatcacctcctga 3’
Pair 2	5’ agctaccggctgcgttactc 3’	5’ acgccggaagcgacattcca 3’
Pair 3	5’ ccaggctatgcaggtccact 3’	5’ agcacctgggcggttgttga 3’
Pair 4	5’ acggagggtgttggaagagg 3’	5’ gatcttgagggctgtcgacc 3’
Pair 5	5’ ctcgactccgcttcaaggag 3’	5’ caactaggcagttccgcgtg 3’
Pair 6	5’ caatgctgctgcatgatgtggcag 3’	5’ tggcttcccctggatcgctc 3’
Spanning exon10-15	5’ gagctgacggttcacctctc 3’	5’ agcagcattgggtagctgat 3’

2.13.4 Gel extraction and Purification

Amplified PCR products were purified for sequencing using one of two methods. In the first method PCR samples were directly purified after confirmation of a single PCR product on gel electrophoresis. For this, the QIAquick PCR purification kit was used in accordance with the manufacturer's guidelines.

In the second method, PCR products were first separated by gel electrophoresis, stained with ethidium bromide and visualised by UV light on a transilluminator. Individual bands were excised from the gel using a sterile scalpel blade and transferred to sterile 1.5 microcentrifuge tubes. Extraction of the PCR product from the gel slice was carried out using a Qiagen Gel extraction kit according to the manufacturer's guidelines. cDNA was eluted from the column in 50µl deionised water and stored at -20^{o}C until required.

2.13.5 Sequencing PCR

cDNA was sequenced using Big Dye sequencing kit (Applied Biosystems). 10 ng of either directly purified or gel extracted PCR was added to the sequencing mix which consisted of 1 µl of Big Dye, 3.5 µl of 5X buffer, 1 µl of either forward or reverse sequencing primer (10 pmol/µl). The final volume was made up to a 20 µl volume with DEPC-treated water. Samples and reagents were kept on ice at all times. An Eppendorf Thermocycler was used to denature the samples at 96^{o}C for 1 min followed by 25 cycles of rapid thermal ramp to 96^{o}C for 10 seconds, 50^{o}C for 5 seconds and 60^{o}C for 4 minutes.

After PCR amplification, the cDNA was precipitated by the addition of 64 µl of 96% ethanol and 2 µl of EDTA (0.25M) and incubated at room temperature for 15 minutes. The cDNA was pelleted by centrifugation at 16000 rcf for 20 minutes then washed twice with 70% ethanol. Ensuring all ethanol was aspirated, the samples were air-dried for 15 minutes and re-

suspended in 10 µl HiDi-formamide. The samples were then subjected to automated sequence analysis.

2.14 Microarray

The GeneChip® Human Genome U133 Plus 2.0 microarray (HG-U133 Plus 2.0; Affymetrix) allows the simultaneous analysis of expression levels of more than 47,000 transcripts and variants. Total RNA was extracted from L428 cells transfected with either DDR1 siRNA or scrambled siRNA according to methods in sections 2.3 and 2.10. Three independent biological replicates were prepared for microarray analysis which was performed by Dr John Arrand. Outputs from microarray chips were analysed Dr Wenbin Wei using GCOS software (Affymetrix).

2.15 Purification and transfection of GC B cells

All investigations using GC B cells referred to in this thesis were extracted from tonsils of paediatric patients under ethical approval (06/q2702/50). Subsequent purification and transfection of GC B cells were conducted by Dr Martina Vockerodt. Briefly, $CD10^+$ GC B cells were isolated by magnetic separation using anti-CD10-phycoerthrin (PE) (Becton Dickinson, BD) and anti-PE microbeads with LS columns (Miltenyi Biotec). For transfections, purified $CD10^+$ GC B cells were nucleofected with either pSG5-LMP1 or pSG5 in addition to the expression vector pMACSLNFGR.

2.16 Purification of human tonsillar B cell subsets

This experiment was performed by Dr Jennifer Anderton. In brief; $CD77^+$ centroblasts were enriched by magnetic separation with anti-CD77 antibody (Becton Dickinson, BD) and anti-IgM microbeads using LS columns (Miltenyi Biotec). The flow-through of the magnetic

separation, containing $CD77^-$ depleted mononuclear cells, was incubated with anti-CD10-PE (Becton Dickinson, BD) and anti-PE microbeads followed by magnetic enrichment on LS columns. The elute contained $CD10^+/CD77^-$ centrocytes. Naïve B cells were isolated indirectly by depletion of all non-naïve cells using a cocktail of antibodies to CD10, CD2, CD16, CD27, CD36, CD43 and CD235a (Miltenyi Biotec). Memory B cells were purified by first negative depletion using antibodies against CD2, CD14, CD16, CD36, CD43 and CD235a, finally by positive selection with CD27 microbeads (Miltenyi Biotec).

2.17 Statistical analysis

The significance of RTK expression per case was evaluated with respect to EBV status and histological subtype using two sample *t*-test. A value of $p < 0.05$ was considered to be highly significant.

CHAPTER 3

The activation of receptor tyrosine kinases in HL cells with emphasis on MET and its potential regulation by LRIG1

3.1 Introduction

RTKs are key regulators of important cellular processes and their deregulation is critical to the pathogenesis of many diseases, including cancer [175]. However, our understanding of the contribution of RTKs to the pathogenesis of HL remains limited. Previous studies have shown that while RTK expression is restricted in normal B cells [226-228;230;312], multiple RTKs are over-expressed in HRS cells. Moreover, the activation status of many of the RTKs previously shown to be over-expressed in HRS cells has not yet been established (Table 3.1). The objectives of this study are to:

- Provide a global analysis of the activation status of RTKs in HL cells using a phosphorylation specific antibody array.
- Explore the expression and activation in HL cell lines and primary HRS cells, of two RTKs, MET and RON, which were detected by this array analysis.
- Investigate the expression of LRIG1 and its contribution to the activation of MET in HL cells.

Table 3.1 Summary of published work that have studied the expression and activation of RTKs, and expression of their ligands, in HL derived cell lines and primary HRS cells.

RTK	EXPRESSION		ACTIVATION		LIGAND		REF
	CELL LINE	PRIMARY	CELL LINE	PRIMARY	CELL LINE	PRIMARY	
PDGFRα	-	✓	-	-	-	-	(232;313)
	✓	✓	-	✓	-	✓	
DDR2	✓	✓	-	-	-	stroma	(232)
EPHB1	✓	✓	-	-	-	✓	
RON	✓	✓	-	-	-	-	
TRKB	×	✓	-	✓	-	-	
TYRO3	× Detected on gene array	-	-	-	-	-	
MER	× Detected on gene array	-	-	-	-	-	
TRKA	✓	✓	-	✓	-	granulocytes	
	✓	✓	✓	✓	✓	-	(234)
TIE1	-	✓	-	-	-	-	(233)
MET	-	✓	-	-	-	serum	(259)
	✓	-	-	-	weak	-	(258)
	-	✓	-	-	-	-	(229)
							(256;257)
KIT	✓	✓	-	-	✓(L1236)	fibroblasts	(122;235)
	×	×	-	-	-	-	(238)
	✓(L1236)	×	-	-	✓(L1236)	-	(239)
	×	× +ve mast cells	-	-	-	-	(237)
CSF1R	✓	✓	✓	✓	✓	-	(240)
	-	-	-	-	-	✓	(314)
FGFR1	×	×	-	-	×	✓	(231)
FGFR2	×	✓	-	-	×	✓	
FGFR3	✓	✓	-	-	×	✓	
FGFR4	×	✓	-	-	×	✓	
VEGFR family	-	-	-	-	✓ (hypoxic)	serum	(315)

✓ Detection of the RTK irrespective of the number of cases or lines which are positive.

× RTK expression or activation was studied but not found

- RTK expression or activation not studied or reported in the paper

3.2 Results

3.2.1 Expression and activation of RTKs in HL cell lines

I first studied the phosphorylation status of 42 known RTKs in three HL cell lines (L591, L428 and L1236) and in purified $CD10^+$ human GC B cells, using a commercially available antibody array. This array contains capture and control antibodies which have been spotted in duplicate on nitrocellulose membranes. The immobilised antibodies capture both phosphorylated and non-phosphorylated RTKs, but only the phosphorylated forms are detected following the binding of a pan-tyrosine antibody. (See methods section 2.4.8, page 78). Figure 3.1a shows an example of such an array after visualisation with chemiluminescence.

The array analysis was performed twice on each HL cell line; once in medium containing 10% serum and once in medium without serum. Figure 3.1b shows that all HL cell lines displayed a marked activation of multiple RTKs. Table 3.2 lists those RTKs which were activated in 2 or more HL cell lines (either in serum free medium or in serum containing medium, or both). From this analysis, it was apparent that RTKs from at least three major RTK subfamilies, HGFR, AXL and FGFR were consistently activated in the HL cell lines. I also observed that some RTKs were activated only in HL cell lines grown in serum-containing media (e.g. Insulin receptor family members). In contrast, I noted that the activation of other RTKs, for example VEGFR3, was more pronounced in serum free medium. A further group of RTK displayed activation in both serum-containing and in serum-free media; these included MET and RON which are discussed in detail below.

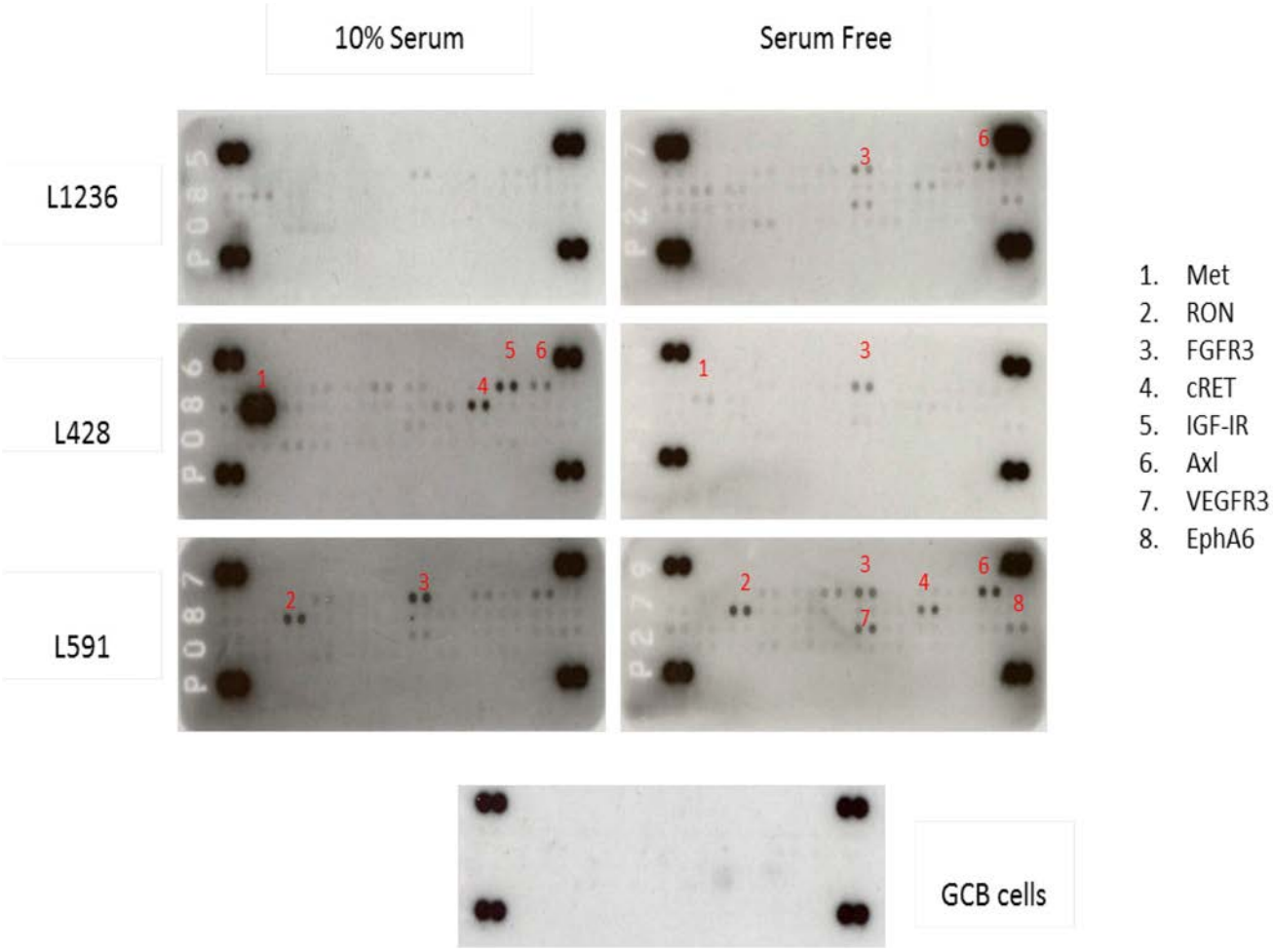

Figure 3.1A Multiple RTKs are activated in HL cell lines. Each array has antibodies to 42 RTKs spotted in duplicate and includes negative controls and positive controls (in each corner to aid alignment). RTKs were identified using a template supplied with the array (see methods section 2.4.8); spots for several RTKs are highlighted (numbered 1-8). L1236, L428 and L591 HL cell lines grown either in medium supplemented with 10% serum or in medium without serum were analysed and compared to $CD10^{+}$ GC B cells freshly isolated from a human tonsil (one replicate; sample provided by Dr Vockerodt).

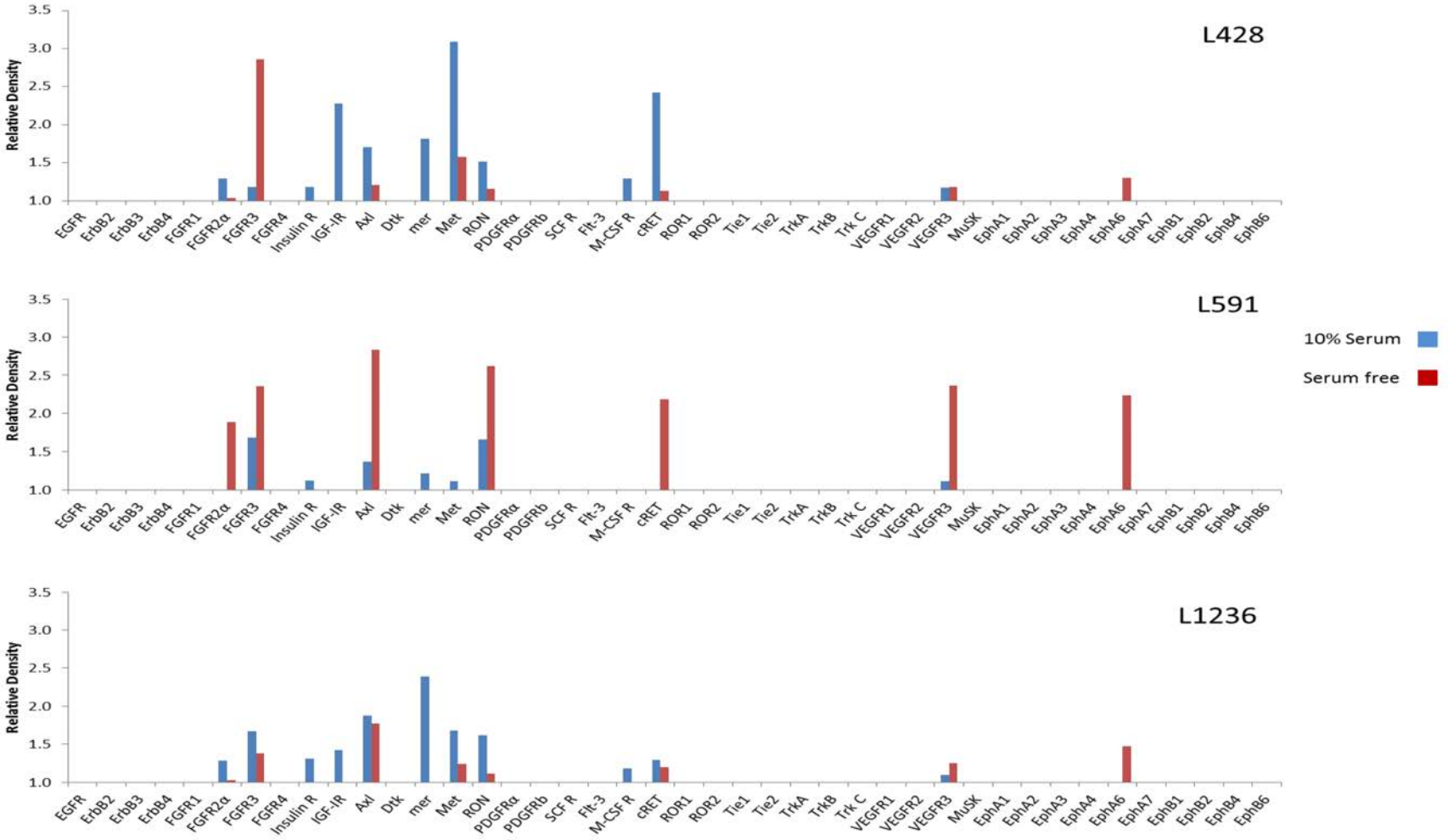

Figure 3.1B Summary of results from antibody array. Signal strength of each dot was measured by densitometry. A background measurement taken of a blank area of the film immediately next to the array was set as a baseline to account for differences in exposure between blots. The phosphorylation of each RTK was calculated relative to this baseline.

Table 3.2 Activation of various RTK, in HL cell lines, grouped according to sub-family.

RTK SUB-FAMILY	10% SERUM	SERUM FREE
EGFR	×	×
FGFR		
FGFR1	×	×
FGFR2α	✓✓	✓✓✓
FGFR3	✓✓✓	✓✓✓
FGFR4	×	×
INSULIN RECEPTORS		
Insulin R	✓✓✓	×
IGF-IR	✓✓	×
AXL		
AXL	✓✓✓	✓✓✓
DTK (Tyro3)	×	×
Mer	✓✓✓	×
HGFR		
MET	✓✓✓	✓✓
RON	✓✓✓	✓✓✓
PDGFR		
PDGFRα	×	×
PDGFRβ	×	×
KIT	×	×
FLT3	×	×
CSF1R	✓✓	×
RET	✓✓	✓✓✓
ROR	×	×
TIE	×	×
TRK	×	×
VEGFR		
VEGFR1	×	×
VEGFR2	×	×
VEGFR3	✓✓✓	✓✓✓
EPHRINS		
EphA6	×	✓✓ ✓

✓ per activated cell line × not activated in any cell line

3.2.2 MET is over-expressed in HL cell lines and in primary tissue

Having observed the robust phosphorylation of MET in all HL cell lines, I chose to focus on this RTK in more detail. I first compared the expression of MET mRNA in 6 HL derived cell lines and in 3 BL derived cell lines with that in $CD10^+$ GC B cells isolated from three donors (provided by Dr Vockerodt). Figure 3.2a shows that compared to GC B cells, MET mRNA levels were higher only in L428, L540 and L1236 HL cell lines. I next used a polyclonal antibody to measure MET protein levels in these cell lines. This antibody detects both pro-MET, the 170kDa glycosylated precursor and MET; the 145kDa functional protein. Consistent with the results of the q-PCR analysis, I observed that MET protein levels were highest in L428, L540 and L1236 HL cell lines (Figure 3.2b). The high levels of MET expression in L428 and L1236 cells is consistent with the activation of this receptor in these cell lines shown by antibody array.

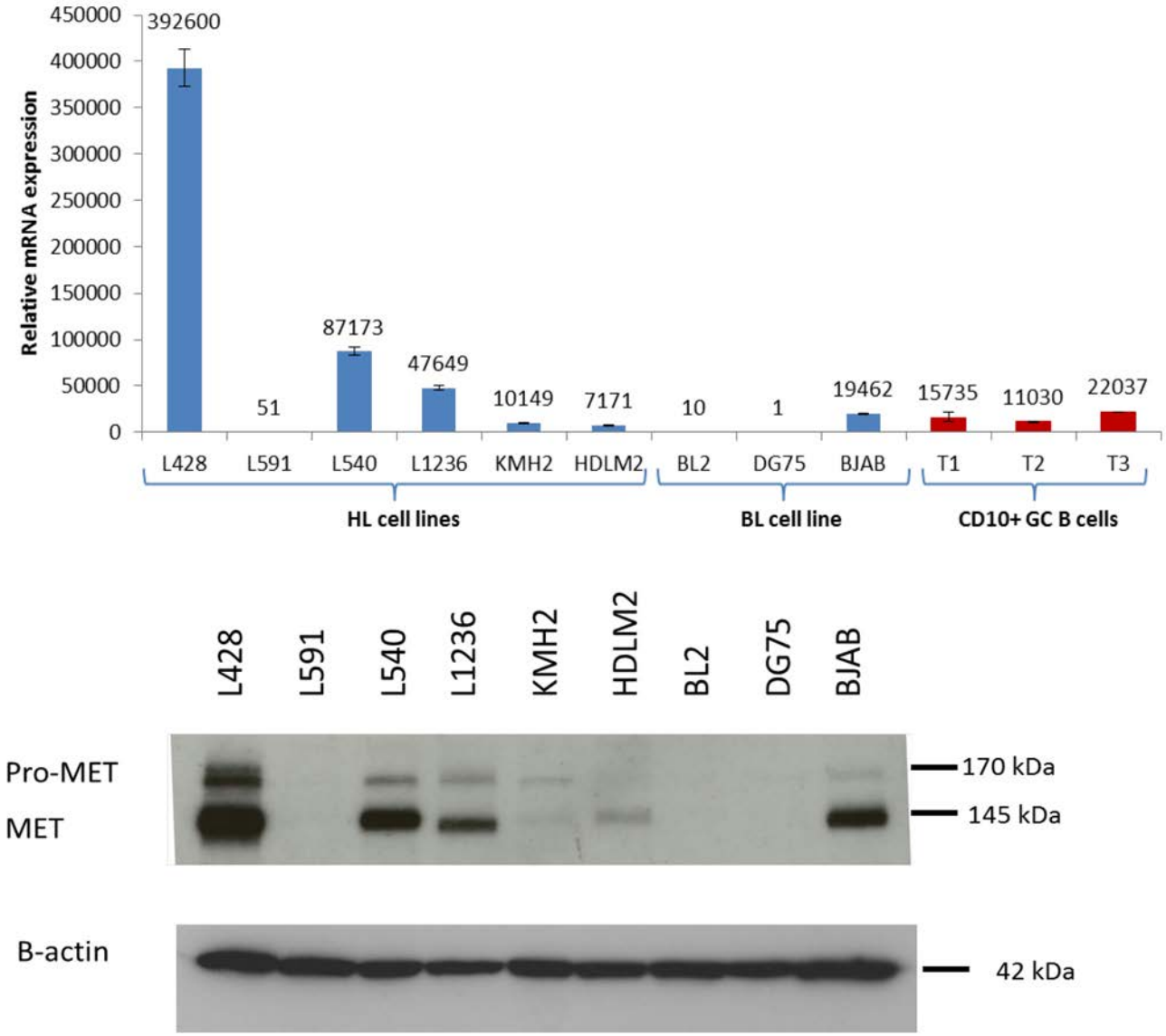

Figure 3.2 A) Expression of MET in HL and BL cell lines compared to that in CD10$^+$ GC B cells. Relative expression of MET mRNA in cell lines was determined by q-PCR analysis. All samples were analysed in triplicate using the ΔΔ CT method. The unsorted CD10$^+$ GC B cells included in the comparison were from three different donors. The results show one representative example of three independent experiments.

Figure 3.2 B) Expression of MET protein in a panel of HL and BL cell lines. 30µg of total protein from whole cell lysate was loaded. The results show one representative example of three independent experiments.

Having shown that MET is over-expressed in some HL-derived cell lines, I next studied the expression of this receptor in biopsies from children with HL. These samples were obtained from the Children's Cancer and Leukaemia Group (CCLG) and are described in detail in appendix I. To detect MET protein, immunohistochemistry (IHC) was performed on 44 cases which were available for analysis using the same polyclonal antibody described above. However, I excluded 18 cases on the basis that no staining could be observed in blood vessels which was used as an internal positive control. Of the remaining 26 cases, I observed strong expression of MET in primary HRS cells in 17 cases, weak expression in 7 cases, and no staining in 2 cases (Figure 3.3). There was no association between MET expression and histological subtype (Table 3.3).

Following the detection of MET expression by HRS cells in almost all HL cases, I next investigated if there was an association between EBV status and MET expression in primary HRS cells. I performed IHC on 54 cases and observed LMP1 expression in 27/54 (50%) of cases. Figure 3.4 shows three cases, the first is representative of the staining seen in an LMP1 negative sample and the others of LMP1 positive cases. There was no association between MET expression and EBV status (Table 3.4).

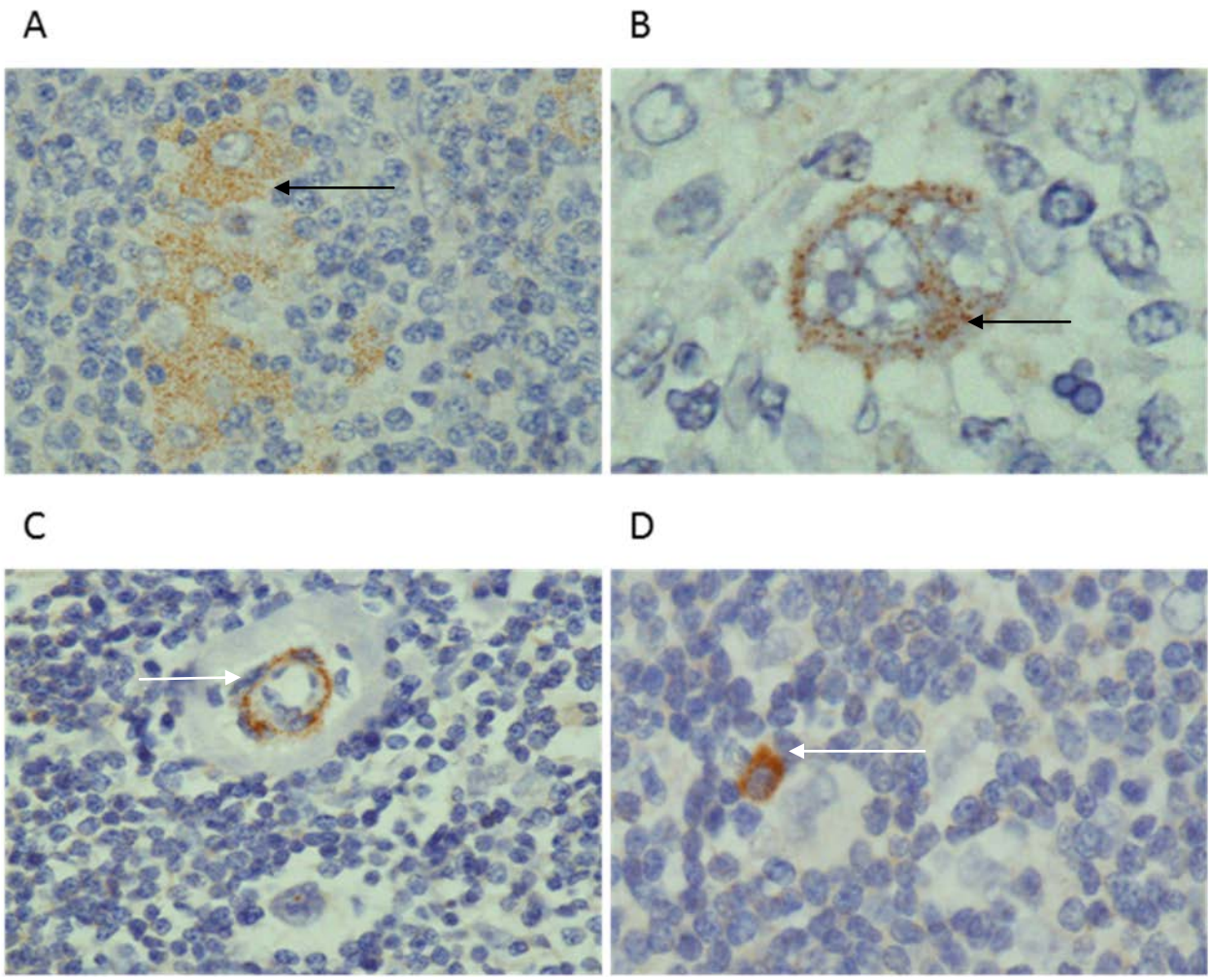

Figure 3.3 MET expression in primary HL. Representative photomicrographs of HRS cells showing immune-reactivity to MET (A and B; black arrows) and no staining of HRS cells for MET is seen (lower panels) but show a positively stained blood vessel (left; white arrow) and plasma cell (right, white arrow).

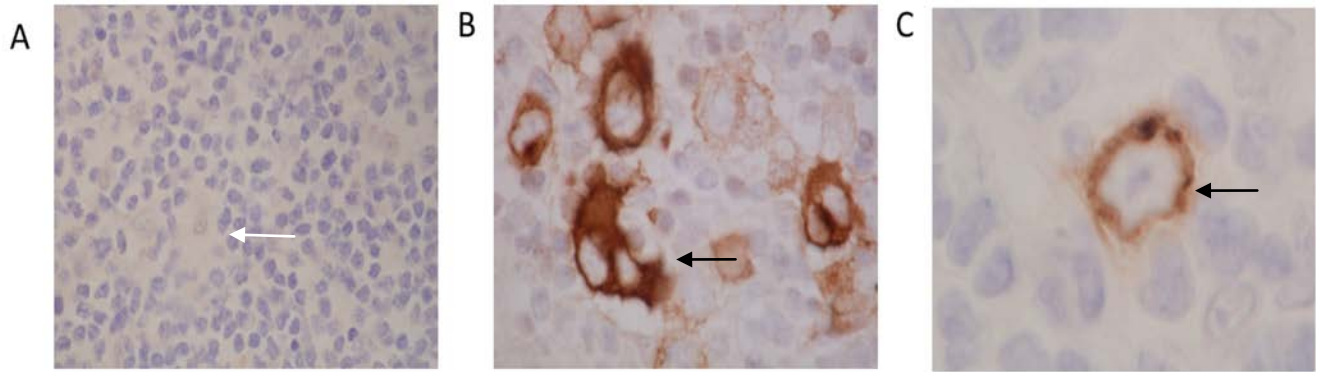

Figure 3.4 LMP1 expression by immunohistochemistry. A) Case 14-193, a nodular lymphocyte predominant HL case which was negative for LMP1 B) Case 14-172, a nodular sclerosis case of HL which was strongly positive for LMP1 C) Case 14-219, a mixed cellularity case of HL which was positive for LMP1.

Table 3.3 MET expression in primary HL stratified by histological subtype. There was no significant association (p>0.05)

	MET positive	MET negative
Nodular Sclerosis	18	1
Mixed cellularity	3	0
Lymphocyte predominant	2	1
Hodgkin's disease (unspecified)	1	0

Table 3.4 MET expression in primary HL stratified by EBV status. There is no significant association (p>0.05)

	EBV positive	EBV negative
MET positive	13	11
MET negative	1	1

3.2.3 Ectopic expression of LMP1 induces MET expression

I also considered the possibility that MET expression might be induced by the EBV-encoded LMP1, when this viral oncogene is expressed in GC B cells, the presumed progenitors of HRS cells. This seemed a reasonable proposition given that this viral gene has been shown to induce MET expression in NPC cells [316]. To do this, I examined the expression of MET following the transfection of purified $CD10^+$ GC B cells with either LMP1-expressing or control vector. These transfections were performed previously and LMP1 status has been reported before[172]. Figure 3.5 shows that relative to vector-only transfected GC B cells, the levels of MET mRNA were up-regulated in GC B cells expressing LMP1.

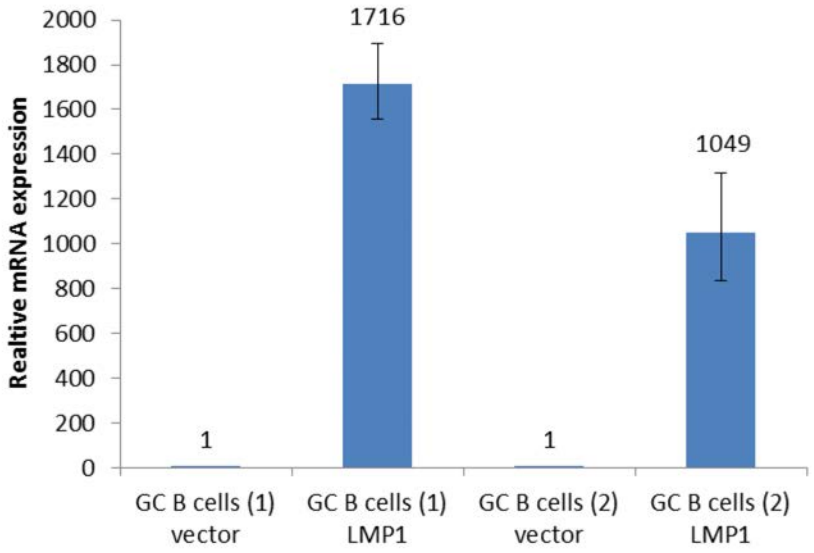

Figure 3.5 Expression of MET mRNA in CD10$^+$ GC B cells transfected with LMP1 or empty vector. q-PCR analysis for MET was performed on two separately isolated and transfected CD10$^+$ populations. The expression of MET mRNA in vector control was set at a value of 1 and relative expression of GC B cells expressing-LMP1 was determined by q-PCR analysis Samples were analysed in triplicate and are presented as ΔΔ CT values in comparison to corresponding vector control.

3.2.4 Intrinsic kinase activity of MET is constitutive in HL cell lines

Although the antibody array had suggested that MET was activated in at least two of the HL cell lines, it was unable to reveal which of the tyrosine residues present in MET were phosphorylated in these cells. This is important because the phosphorylation of Tyr1234 and Tyr1235, which are often used to measure MET activation, alone are not sufficient for MET-induced transformation, which also requires ligand (HGF) binding [(254)]. Ligation of MET by HGF leads to the phosphorylation of Tyr1349 in the catalytic domain which is required for binding of adaptor proteins such as GAB1 [(317)]. A third phosphorylation site, Tyr1003 is essential for the ubiquitination and degradation of MET[(246)]. Therefore, I performed a more detailed study of the phosphorylation status of MET. For this experiment, the HL cell lines were grown in serum-free conditions overnight and immunoblotted using antibodies directed against these three phosphorylation sites. The results of these experiments are shown in Figure 3.6. Phosphorylation of Tyr1234/1235 and Tyr1003 was clearly observed in L428 cells and to a lesser extent in L540, L1236 and KMH2 cells. Phosphorylation of Tyr1349 was detected only in KMH2 cells and consistent with this I observed the phosphorylation of GAB1 only in this cell line. These results show that while most HL cell lines display constitutive activation of the intrinsic kinase domain (Tyr1234/1235), only one cell line (KMH2) shows activation of the catalytic domain.

I stained primary HL cases with these antibodies, but no immuno-reactivity was observed either on paraffin-embedded samples or on frozen sections.

I next used ELISA to measure HGF in the supernatant of these cell lines. I observed that only KMH2 cells produced significant amounts of HGF (Figure 3.7). This is consistent with the observation that GAB1 and Tyr1349 are phosphorylated only in KMH2 cells.

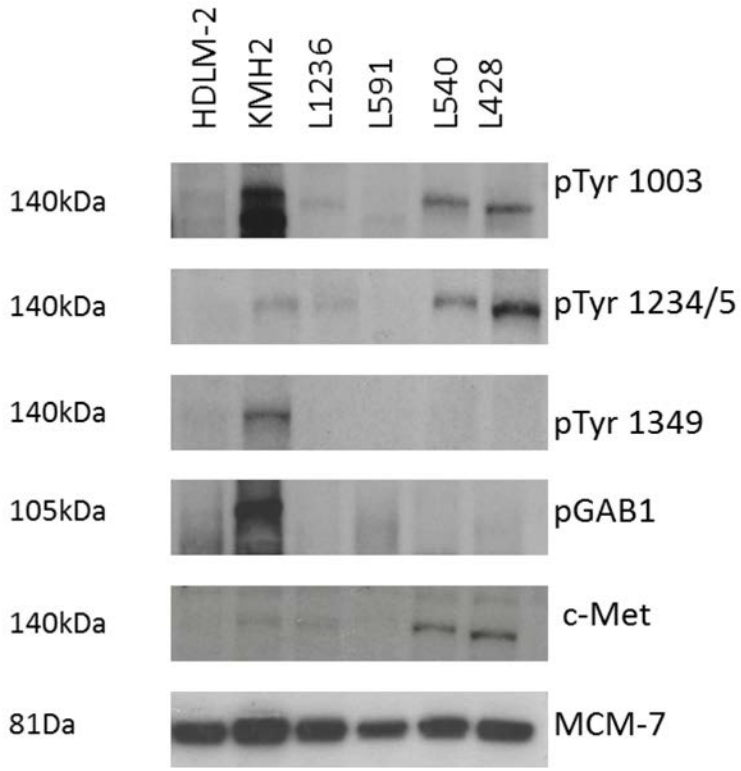

Figure 3.6 MET and GAB1 phosphorylation in a panel of HL cell lines. Cells were maintained in normal growth conditions and 24hours prior to harvesting washed twice and re-suspended in serum-free media. 30µg of whole cell lysate was loaded for immunoblotting. Each phospho-specific antibody was run on different membranes which were each stripped and then immunoblotted for total MET protein levels. Equal protein loading was also confirmed on each membrane using an antibody to MCM-7 (shown here are representative blots).

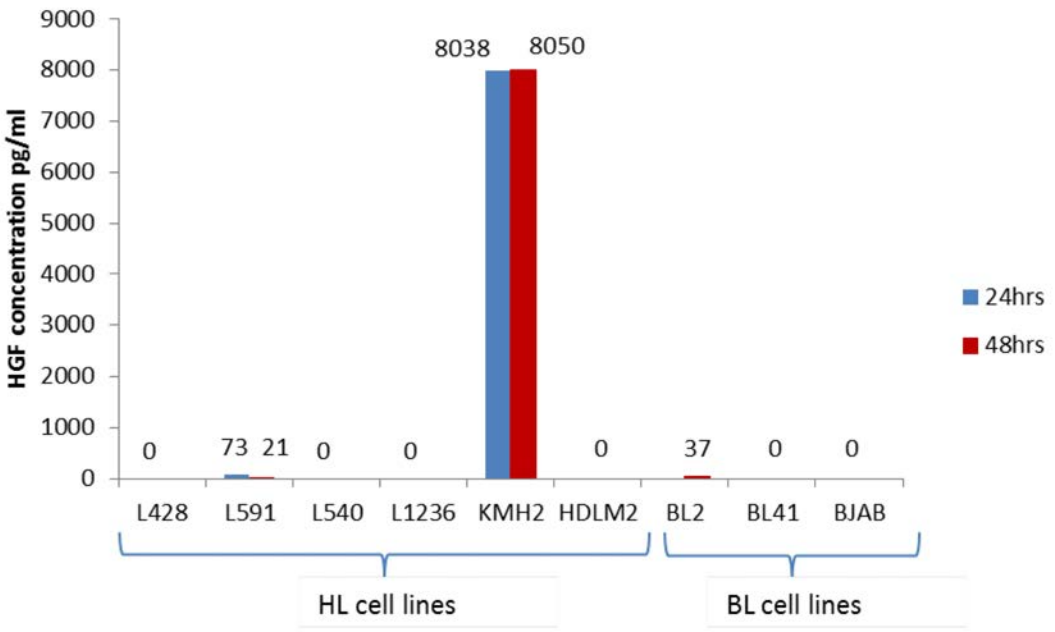

Figure 3.7 Production of HGF by HL cell lines. An ELISA was used to measure the levels of HGF in the supernatant of BL and HL cell lines cultured in serum free media for 24 and 48 hours.

3.2.5 RON is over-expressed in HL cell lines and in primary HRS cells

The antibody array analysis had shown that another member of the HGF family, RON, was activated in the HL cell lines. I first used q-PCR to show that RON was highly expressed in L428, L591 and L1236 cells, but not in the other HL cell lines nor in the BL cell lines (Figure 3.8a). Furthermore, immunoblotting revealed the presence of full length RON and pro-RON protein in these same three cell lines (Figure 3.8b). However, several other HL cell lines, including L540, appeared to express bands at approximately 100kDa, 80kDa and 75kDa. Although this could be consistent with the expression of previously described splice variants of RON, I did not investigate this further [318].

IHC was then performed to study RON expression in primary HL. I initially used the same polyclonal antibody employed in the immunoblotting experiment described above to detect total RON. I observed the strong cytoplasmic and granular expression of RON in HRS cells in 35/44 cases of primary HL, a further 5 cases were weakly positive and 4 showed no expression of RON (Figure 3.9). There was no association between RON expression and either histological subtype or MET status (Tables 3.5 and 3.6). I then studied the activation of RON in selected HL cases using an antibody that detects the phosphorylation of RON (Tyr 1238/1239) in the intrinsic kinase domain. I observed that in all cases (n=10) phosphorylated RON was detectable in HRS cells (Figure 3.10).

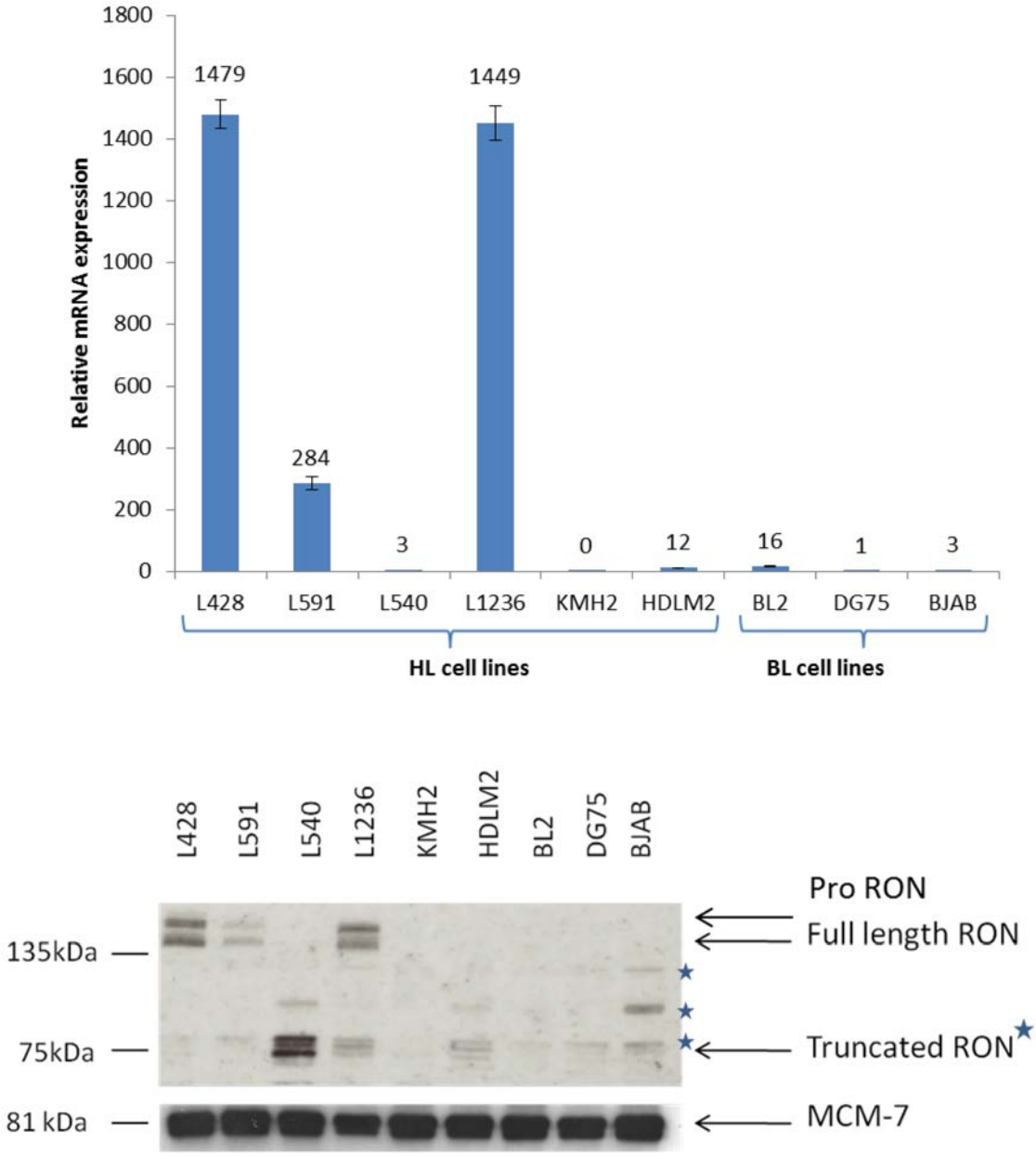

Figure 3.8 A) Expression of RON in HL and BL cell lines. A panel of HL and BL cell lines were maintained under normal growth conditions then re-suspended in fresh media at $3x10^5$/ml 24hrs prior to RNA and protein extraction. Expression of RON mRNA was determined by q-PCR analysis. All samples were analysed in triplicate using the ΔΔ CT method.

Figure 3.8 B) Expression of RON protein in a panel of HL and BL cell lines. 30µg of total protein from whole cell lysate was loaded. Equal loading was confirmed using an antibody against MCM-7

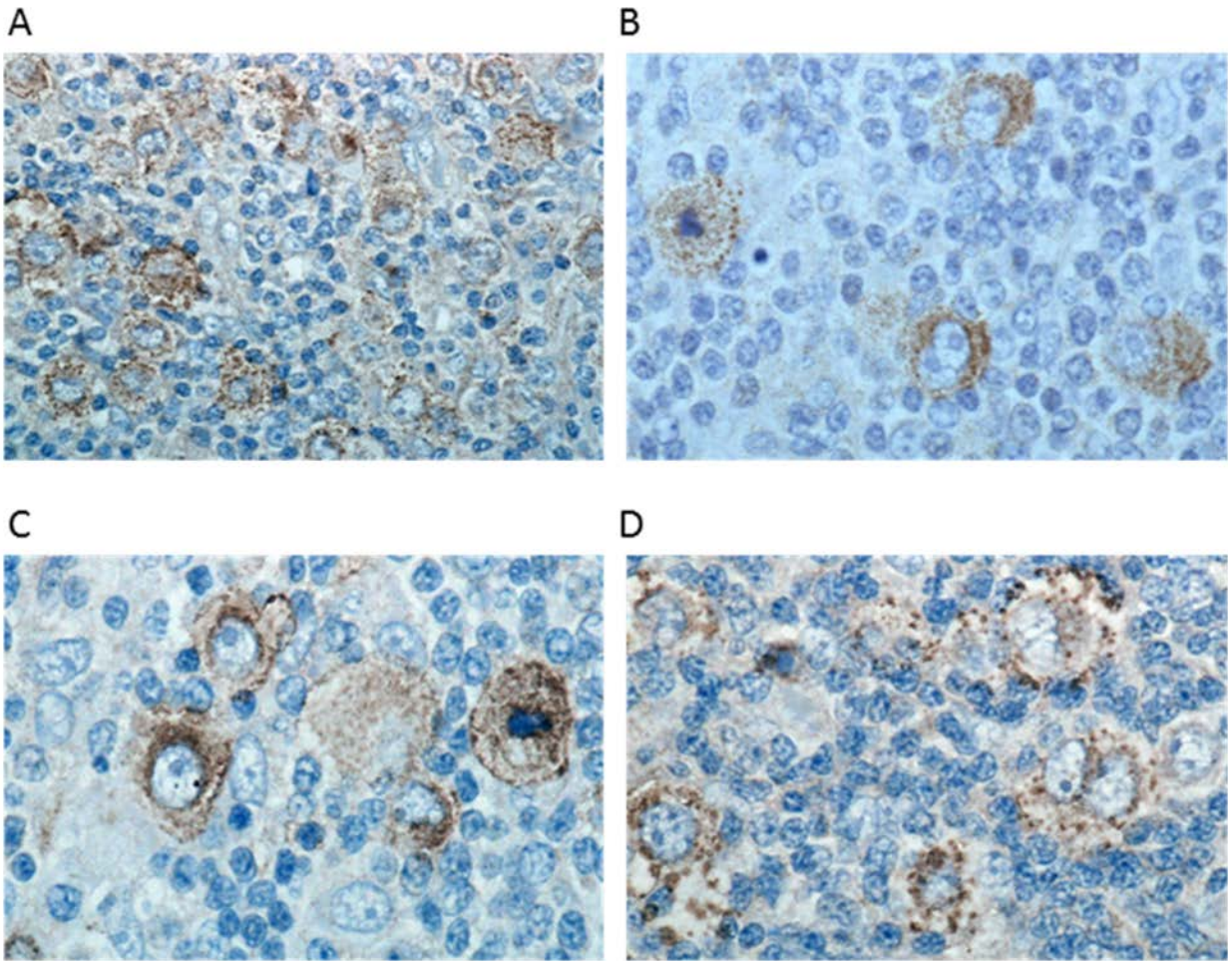

Figure 3.9 RON expression in primary HL. Representative photomicrographs of HRS cells positive for RON in four different cases of primary paediatric HL.

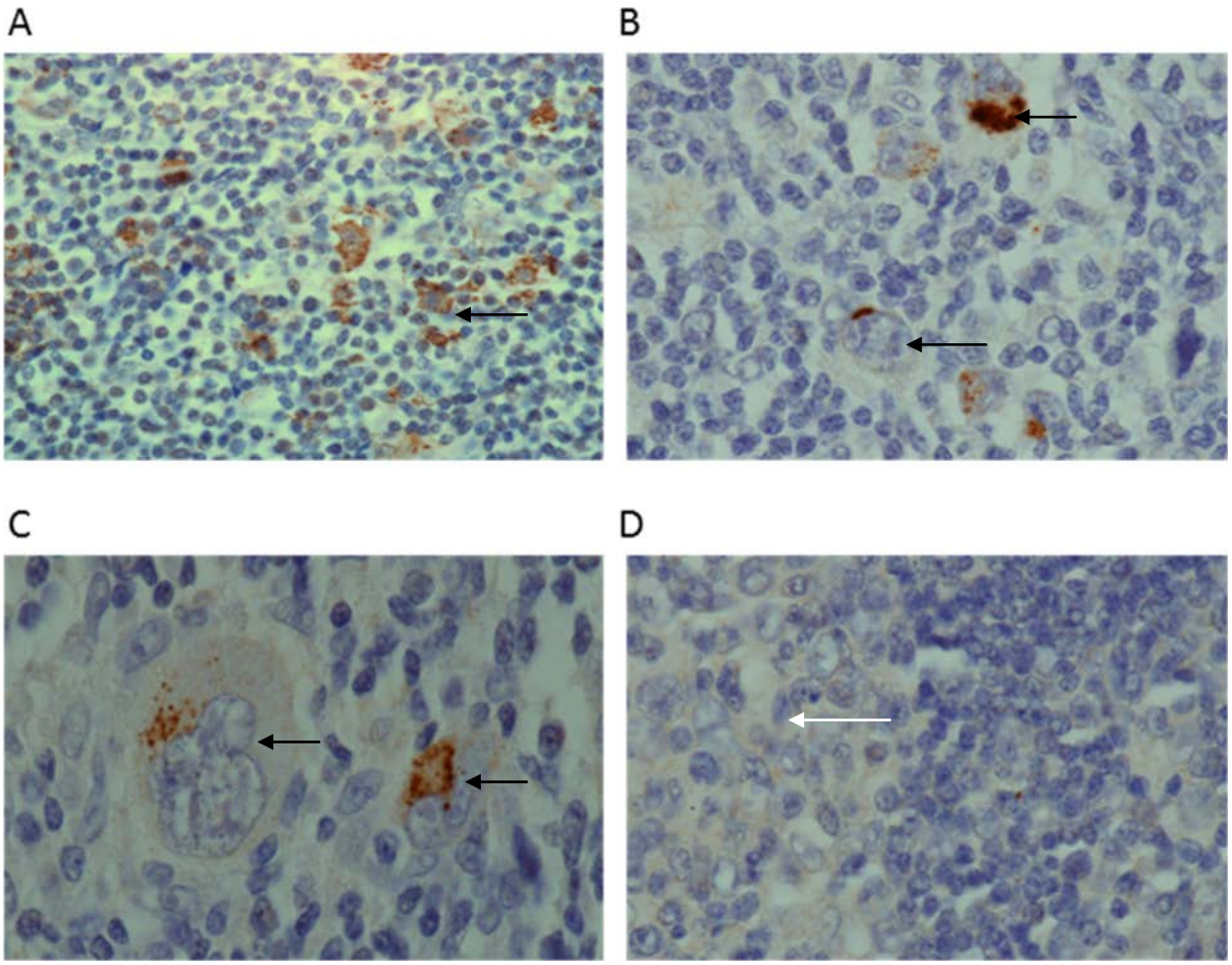

Figure 3.10 Phospho-RON expression in primary HL. Representative photomicrographs of primary tissue showing HRS cells positive for p-RON (A, B and C; black arrows), and low level p-RON in GC B cells (D; white arrows)**.**

Table 3.5 RON expression in primary HL stratified by histological subtype. There was no significant association (p>0.05)

	RON positive	RON negative
Nodular Sclerosis	28	1
Mixed cellularity	7	0
Lymphocyte predominant	3	3
Hodgkin's disease (unspecified)	2	0

Table 3.6 RON expression in primary HL stratified by MET status. There was no significant association (p>0.05)

	RON positive	RON negative
MET positive	24	0
MET negative	2	0

3.2.6 LRIG1 is down-regulated in HL cell lines and in primary HRS cells in some cases

In the preceding experiments I showed that MET is expressed and activated in HL derived cell lines. Because the LRIG1 protein has recently been shown to bind to MET and induce its degradation, I next explored if the loss of LRIG1 might account for the high levels of expression and activation of MET observed in HL cells. I first compared the expression of LRIG1 mRNA in a panel of HL and BL cell lines with that in $CD10^{+}$ GC B cells. Figure 3.11a shows that LRIG1 was down-regulated in all HL cell lines. In contrast, the three BL cell lines examined expressed levels of LRIG1 comparable to those found in GC B cells. Immunoblotting revealed that LRIG1 was also down-regulated at the protein level in all six HL cell lines (Figure 3.11b).

I next analysed by IHC the expression of LRIG1 in primary HL. Of the 44 cases available for this analysis, 20 were excluded because no staining for LRIG1 was observed in blood vessels which were used as an internal positive control. Of the remaining 24 cases, LRIG1 expression was absent in HRS cells in 11 cases. Loss of LRIG1 expression in HRS cells was supported by the re-analysis of a dataset in which gene expression in micro-dissected HRS cells was compared to that in GC B cells (Figure 3.13)[319]. In positive cases, LRIG1 expression was particularly prominent in so called 'mummified' HRS cells. Furthermore, the staining of LRIG1 in these 'mummified' cells appeared as dense granules within the cytoplasm while in the 'conventional' HRS cells that expressed LRIG1 the stain appeared more diffuse smaller granules (Figure 3.12). In one case, HRS cells were negative for LRIG1 but surrounding macrophages were positive. Low level expression of LRIG1 was also detected in the germinal centres of normal tonsil tissue. There was no association between LRIG1 expression and either histological subtype or MET expression (Tables 3.7 and 3.8).

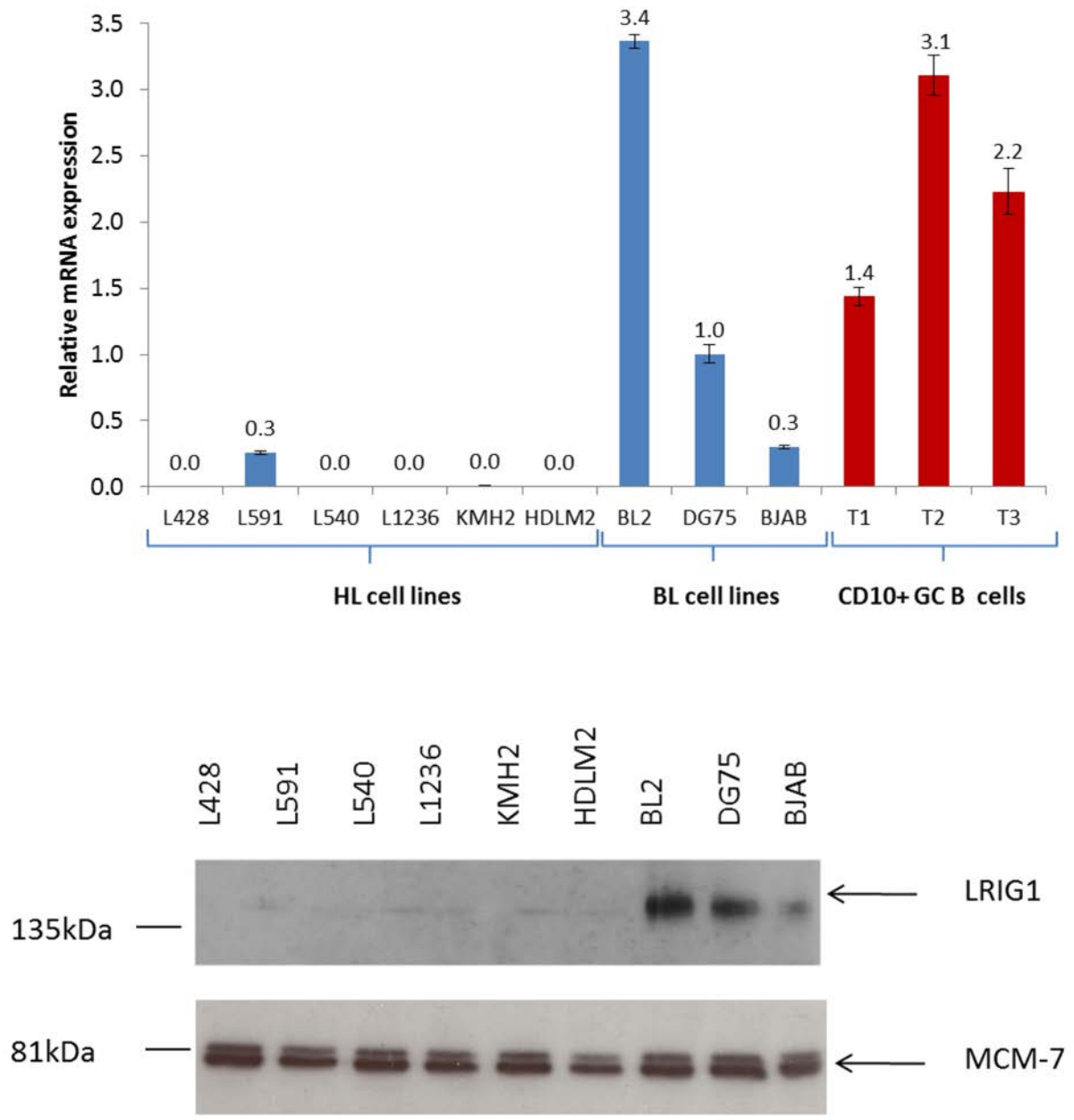

Figure 3.11 A) Expression of LRIG1 mRNA in HL cells, BL cells and GC B cells. The expression of LRIG1 mRNA was determined by q-PCR analysis with all sample analysed in triplicate using the ΔΔCT method. **B) Expression of LRIG1 protein in a panel of HL and BL cell lines.** 30µg of total protein from whole cell lysate was loaded. Equal loading was confirmed using an antibody to MCM-7. Data for both q-PCR and immunoblots are representative of three independent experiments.

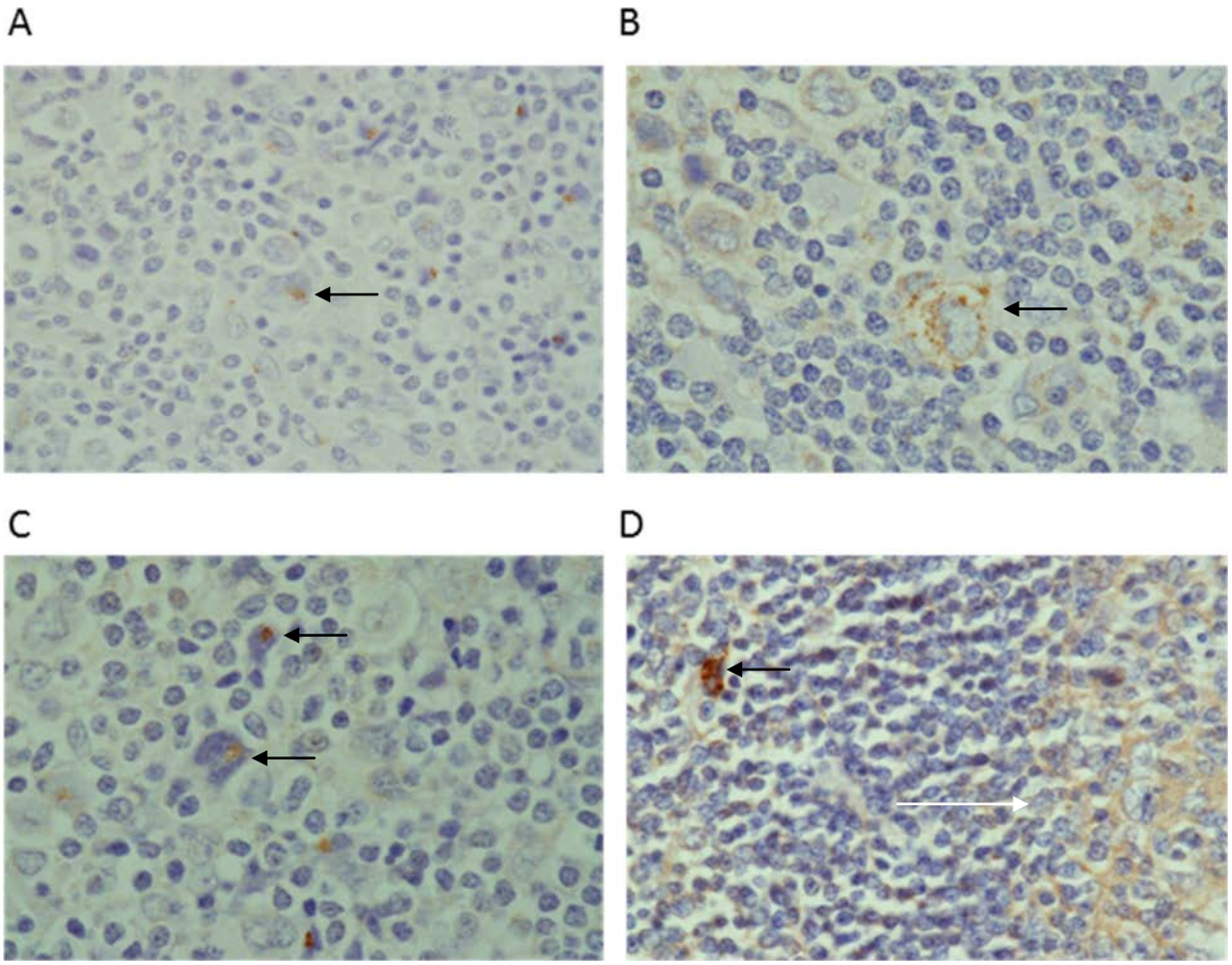

Figure 3.12 LRIG1 expression in primary HRS cases. Photomicrographs show LRIG1 immuno-reactivity in primary HRS cells, seen as cytoplasmic granules (A and B; black arrows). LRIG1 immune-reactivity seen in 'mummified' cells and occasional non-malignant cells (C; black arrows). Intense staining in a non-malignant cell (D; black arrow) and low level expression in residual GC (D; white arrow).

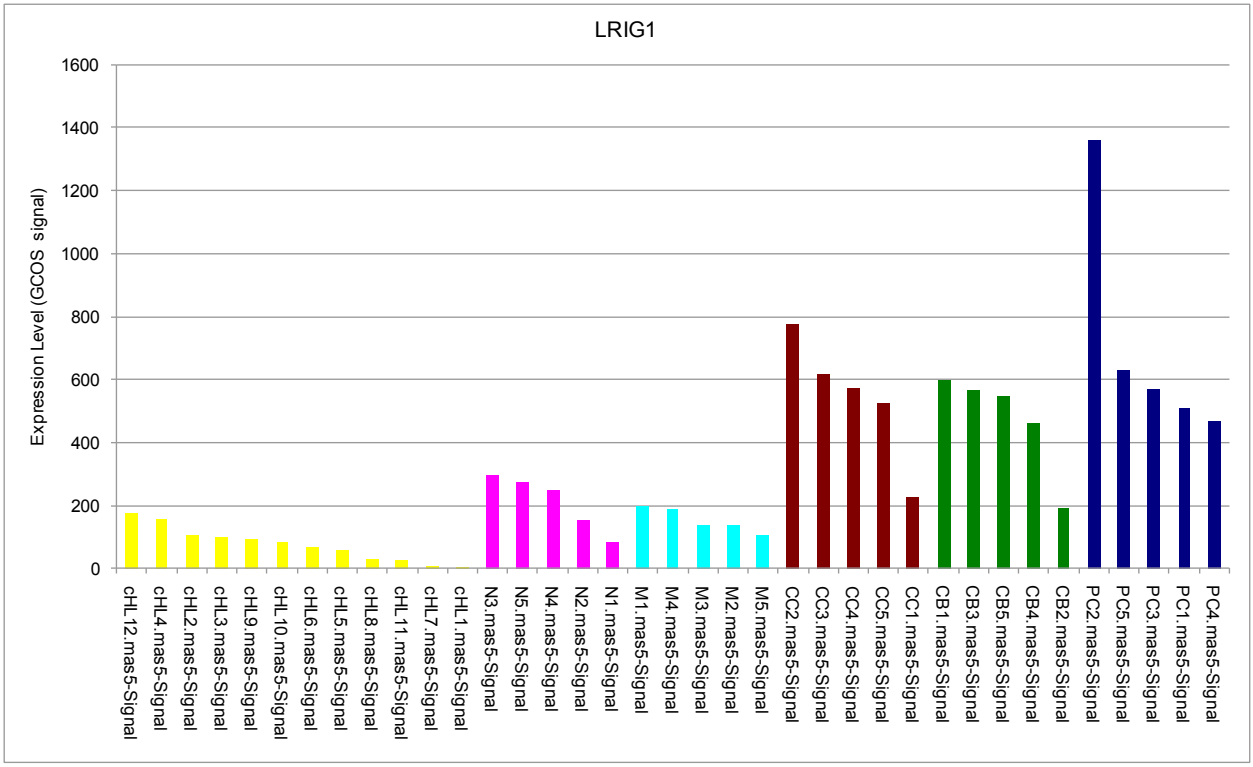

Figure 3.13 LRIG1 expression in a published gene expression dataset. GCOS outputs for LRIG1 obtained from a study in which gene expression in micro-dissected HRS cells was compared to that in different B cell subsets. Compared to centrocytes and centroblasts (GC B cells), LRIG was down-regulated in HL cells[319].

Table 3.7 LRIG1 expression in primary HL stratified by histological subtype. There was no significant association (p>0.05)

	LRIG1 positive	LRIG1 negative
Nodular Sclerosis	12	6
Mixed cellularity	1	1
Lymphocyte predominant	0	3
Hodgkin's disease (unspecified)	0	1

Table 3.8 LRIG1 expression in primary HL stratified by MET status. There was no significant association (p>0.05)

	LRIG1 positive	LRIG1 negative
MET positive	7	8
MET negative	1	1

3.2.7 Effect of ectopic expression of LRIG1 on MET expression and activation in HL cell lines

Based on my observations that LRIG1 is down regulated in the cell lines and in a proportion of primary HL cases, I next explored the influence of LRIG1 expression on the expression and phosphorylation of MET in HL cell lines. To do this, I transfected L428, L540 and KMH2 cell lines using either an LRIG1pcDNA3.1-myc tagged expression vector (a gift from Dr Colleen Sweeney, UC Davis Cancer Centre) or a corresponding control vector and harvested the cells after 48hrs. I first confirmed the expression of LRIG1 in transfected cells and subsequently showed that the ectopic expression of LRIG1 decreased the levels of MET and activated MET in L540 and KMH2 cells, but not in L428 cells (Figure 3.14).

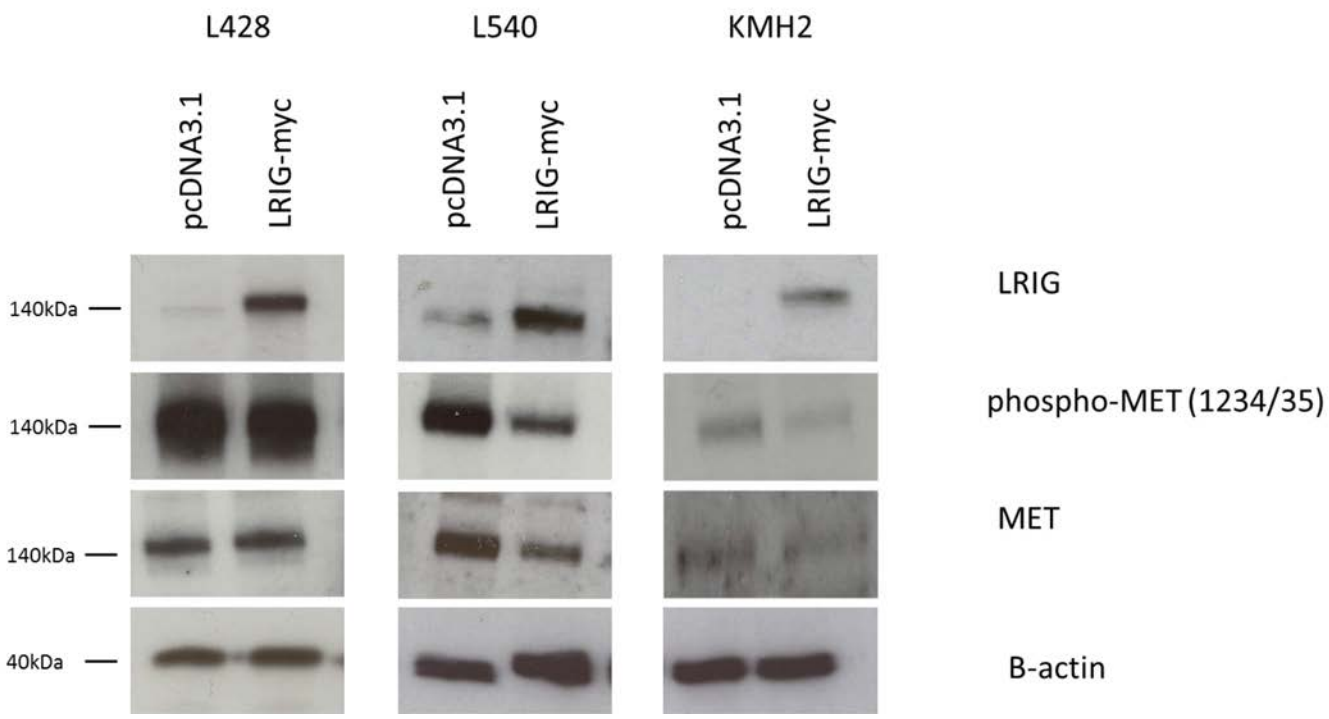

Figure 3.14 Effect of LRIG1 over-expression on MET expression and activation in three HL derived cell lines, L428, L540 and KMH2. Cells were maintained under normal growth conditions then re-suspended in fresh media at $5x10^5$/ml 24hrs prior to transfection with LRIG1pcDNA3.1-myc plasmid or pcDNA3.1 vector. Pellets harvested at 48hrs and 30μg of total protein from whole cell lysate was loaded. LRIG1 over expression was confirmed and phospho-MET and total MET was analysed by immunoblotting. Equal loading control was confirmed by blotting for β-actin.

3.3 Discussion

In this study I have used an array approach to show that HL cell lines display activation of multiple RTKs. Previous studies have reported that a number of RTKs are overexpressed either in HL cell lines, primary HRS cells, or both. However, many of these studies have not explored the activation status of these RTKs (Table 3.1). The work presented here provides the first unbiased survey of RTK activation in HL cells.

The concurrent activation of numerous RTKs has been reported in other cancers such as glioblastoma[292]. There is emerging evidence that RTKs co-operate to form signalling networks with one another as well as with other membrane bound signalling proteins under both physiological and pathological conditions[320]. Within this network a single RTK may dominate and drive critical pathways. Additional activated RTKs which do not necessarily drive the malignant phenotype have the capacity to replace the dominant RTK and could account for the development of resistance to RTK inhibitors. Alternatively, multiple RTKs may feed into a single pathway to maintain robust signalling[175].

An important observation made here was that HL cells are characterised by the consistent activation of members of three major RTK subfamilies: HGFR, AXL and FGFR. However, I showed that within individual HL cell lines, not all members of the same RTK family were activated. This observation is consistent with previous studies which show that members of the same RTK subfamily have overlapping functions. For example, the aberrant activation of different members of the Ephrin subfamily is observed in different tumours but all lead to the same invasive phenotype [321].

Comparison of the RTK shown to be activated in my study with those previously reported to be activated either in HL cell lines, primary HRS cells, or both, revealed only one RTK in common (CSF1R)[240]. Furthermore, I did not detect the activation in HL cell lines, of PDGFRα, TRKA or TRKB which were previously reported to be activated in primary HRS cells [232;233]. The failure to detect activation of these RTK in cell lines could be because either the cell lines are no longer dependent upon RTK activation for their growth, or that these RTK requires signals present in the microenvironment of HL for their activation. Notwithstanding the potential pitfalls associated with the analysis of cell lines, I was able to show for the first time the activation of several RTKs previously reported to be overexpressed in HL (FGFR2, FGFR3, MET and RON) [231-233;259], two of which (RON and MET) were studied in more detail and whose activation status was confirmed in primary HRS cells. Furthermore, I showed the activation in HL cells, of a number of RTKs not previously reported in these cells (Insulin R, IGF-IR, AXL, MER, RET and VEGFR3). However, it is important to be wary of drawing too many conclusions from cell lines that have been grown in culture for many years and generated from patients with advanced, refractory or relapsed disease. Therefore, further studies will be required to determine if these additional RTK are also activated in primary HRS cells.

I observed that some RTK were only activated in HL cells grown in serum-containing medium (e.g. Insulin receptor family members), suggesting that this group of RTK are activated by ligands present in serum. In contrast, I observed that the activation of other RTKs, for example VEGFR3, was more pronounced in serum-free medium suggesting that these RTK might be part of a response to serum withdrawal. A further group of RTK displayed

activation in both serum-containing and in serum-free medium; these included MET and RON.

Previous studies have shown that MET is highly expressed by HRS cells, a result which I confirmed in my cases series[229;259]. Furthermore, I showed using q-PCR analysis that MET mRNA levels were higher in HL cell lines compared to GC B cells, a finding that corroborates the results of a previous study in which germinal centres displayed only weak positivity for MET by immunohistochemistry[228]. The over-expression of MET could alone be sufficient to promote HRS cells growth as it can induce receptor dimerization in the absence of ligand. The possibility that MET is not only over-expressed in HRS cells, but also aberrantly activated in these cells is supported by the observation, made in my study, that activated MET is detectable in HL cell lines.

Mutation studies suggest that the constitutive phosphorylation of Tyr 1234 and Tyr 1235 alone is not sufficient for transformation but also requires ligand (HGF) binding which activates the receptor leading to phosphorylation of Tyr1349 in the catalytic domain [254;317]. Phosphorylation of Tyr1349 is required for the binding of adaptor proteins, including GAB1 [322]. For this reason I performed a more detailed study of the phosphorylation status of MET in the HL cell lines. I observed that only KMH2 cells displayed phosphorylation of both Tyr1349 and GAB1. The possibility that the phosphorylation of Tyr1349 is mediated by an autocrine pathway in KMH2 cells was supported by the observation that only this cell line secreted HGF. However, the detection in most cases of HL, of HGF expression by surrounding non-malignant cells [259], and my finding that HGF is not expressed by most HL cell lines, suggests that the activation of Tyr1349 in HRS cells might normally require signals from the tumour microenvironment.

I also studied the phosphorylation of MET at Tyr1003. The phosphorylation of this residue has been shown to be required for the degradation of MET[249]. For example, mutation of this residue enhances the stability of MET and its loss leads to cellular transformation. In keeping with the reported ability of HGF to activate Tyr1003, phosphorylation of this residue was found to be particularly prominent in KMH2 cells. However, an unexpected finding was that this residue was phosphorylated, albeit less strongly, in the three remaining MET-expressing HL cell lines. This could simply reflect phosphorylation in response to the constitutive activation of MET in these cells. Although phosphorylation of Tyr1003 might be expected to result in the degradation of MET, phosphorylation of this residue has also been shown to prevent binding of caspases to a caspase cleavage site, which includes this tyrosine residue, thereby potentially protecting cells from apoptosis [323;324]. The influence of Tyr1003 phosphorylation on the activity of MET in HRS cells requires further investigation.

One possible mechanism to account for the high level expression of MET in HL cells, at least in a proportion of cases, may involve EBV. I showed that LMP1 expression in GC B cells, the presumed progenitors of HL, up-regulated MET. This is consistent with a previous study that has shown that LMP1 can up-regulate MET in NPC cells[316]. It has also been shown that CD40L and EBV infection can up-regulate MET in B cells [228]. Although others have shown that MET is more frequently expressed by HRS cells in EBV-positive cases of HL, I found no such association [229]. The overexpression of MET in EBV-negative cases suggests that in the absence of virus other mechanism may up-regulate MET. For example, it has been shown that the aberrant activation of AP-1 in HL can up-regulate MET expression[260].

Consistent with a previous study I observed that the other member of the HGFR family, RON was highly expressed in both HL cell lines and in primary HRS cells[232;233]. I was also able to

show that RON was activated in these cells. The detection of RON and Met expression in HRS cells of the same case suggest they may be co-expressed by the same cells. This could be important because it has been previously shown that the co-expression Met and RON permits the reciprocal phosphorylation of these receptors in the absence of their cognate ligands [(325)]. Furthermore, it has also been shown that MET can be activated following the ligation of RON with its ligand, MSP and that the transforming ability of a constitutively activated Met is reduced when it hetero-dimerizes with an inactive RON receptor [(326)].

LRIG1 has been shown to negatively regulate the expression and activation of MET [(250)]. I observed that LRIG1 was significantly down-regulated in a re-analysis of a microarray study in which gene expression in primary HRS cells was compared with that in centrocytes[(319)]. I also showed that LRIG1 protein expression was down-regulated in all HL cell lines and that its re-expression in two cell lines reduced MET expression and activation. Although analysis of primary tissues revealed the down-regulation of LRIG1 in less than half of cases, which was in contrast to the micro-array analysis described above which showed that LRIG1 was down-regulated in all cases. In the cases I examined the loss of LRIG1 was not associated with expression of MET and I was unable to determine if there was any correlation with the activation of MET in these samples.

In conclusion I have shown that HL cells are characterised by the activation of multiple RTK, many of which have not previously been shown to be activated in these cells. I have confirmed the over-expression and activation in HRS cells of two of these RTK, MET and RON. Finally, I have presented preliminary evidence suggesting that LRIG1 is down-regulated in HRS cells in a proportion of cases, and that it can regulate MET expression and activation in HL cell lines.

CHAPTER 4

The receptor tyrosine kinase, Discoidin domain receptor 1, is an LMP1 target gene which is aberrantly expressed and activated in Hodgkin's lymphoma cells

4.1 Introduction

The importance of the tumour microenvironment in the pathogenesis of HL is highlighted by the existence of numerous interactions between HRS cells and stromal cells which promote the proliferation and survival of HRS cells. These interactions are facilitated by various receptor-ligand pairs which include CD40-CD40L, CD30-CD30L and RANK-RANKL[89;141]. However, little is known about the contribution of the non-cellular components of the microenvironment to the pathogenesis of HL. The abundance of collagen in the HL microenvironment is well described but it is not known if it enhances HRS cell growth or survival[3].

Collagen can serve as a ligand for several different types of receptor which include the discoidin domain receptors, DDR1 and DDR2[148]. Although DDR2 has been shown to be expressed in HL[232;233], DDR1 has not been described in this malignancy, but is frequently over-expressed in other cancers including hepatocellular carcinoma, breast cancer and non-small cell lung carcinomas[278;327;328]. Furthermore, the activation of DDR1 by collagen has been shown to induce many of the hallmarks of cancer, including increased invasiveness and protection from apoptosis[270;329;330]. Many of the signalling molecules activated by DDR1 include several that are known to be aberrantly activated in HL e.g. STAT5[331] and NF-κB[282]

The objectives of this chapter are to:

- Determine if DDR1 is expressed in HRS cells and if its activation could be induced by collagen.
- Investigate if DDR1 is regulated by the EBV oncogene, LMP1.
- Study the effects of DDR1 knockdown on the phenotype of HL cell lines.

4.2 Results

4.2.1 DDR1 is over-expressed in HL cell lines

I first compared the expression of DDR1 in a panel of HL and BL cell lines with that in $CD10^+$ GC B cells, the presumed progenitors of these two lymphomas. Three different tonsil samples were used in this analysis (samples provided by Dr Vockerodt). Initially, I used Taqman® q-PCR primers and probe (set 1) to amplify a sequence within the discoidin domain of DDR1 (Figure 4.1). This assay should detect all known isoforms of DDR1. I found that, compared to GC B cells, DDR1 expression was higher in 5/6 HL cell lines and in 1/3 BL cell lines (Figure 4.2a). I repeated the q-PCR with a different set of primers (set 2) which amplified a sequence within the C-terminus (Figure 4.1). Figure 4.2b shows that q-PCR analysis with this second set of primers and probe produced essentially similar results to those obtained with the first set.

I next studied the expression of DDR1 in the same cell lines using a polyclonal antibody which was raised against the C-terminus of DDR1. Figure 4.3 shows the results of immunoblotting with this antibody. I observed a band at 126kDa which corresponds to one or both full length DDR1 proteins, DDR1a and DDR1b. I noted two further bands at 86kDa and 63kDa. The 63kDa band might be the membrane bound β-subunit. The identity of the 86kDa band is unknown but it is strongly expressed in 5/6 HL cell lines and is only weakly expressed or absent in BL lines. It is not likely to be DDR1e which has a predicted weight of 95kDa, nor is it DDR1d, a truncated isoform which cannot be detected with this antibody. L540 cells do not appear to express full length DDR1 but do have these additional bands.

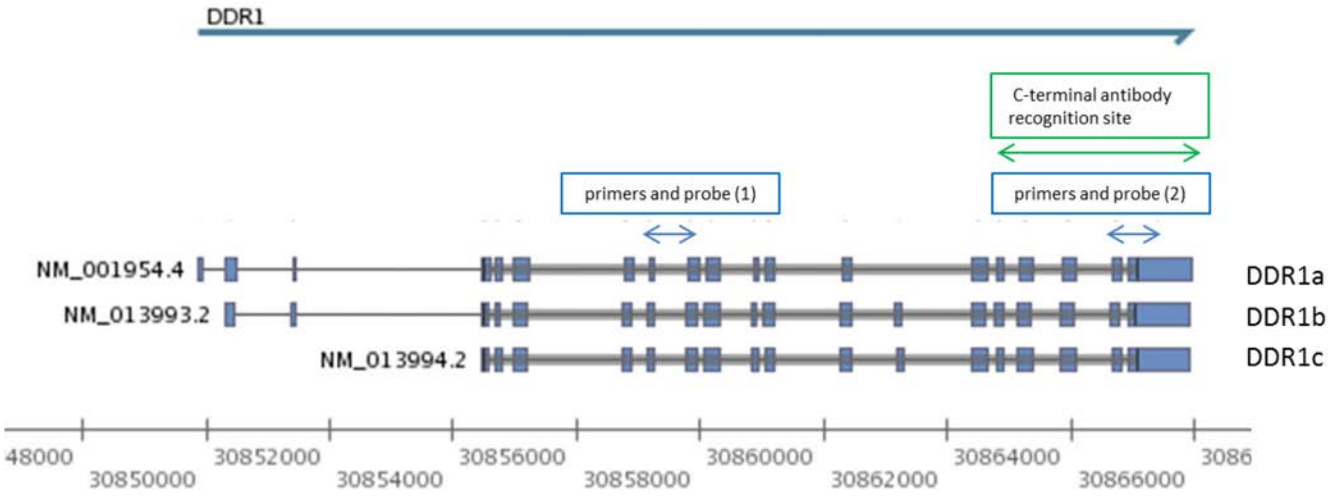

Figure 4.1 Schematic of the position of q-PCR primer amplification sites and the DDR1 antibody recognition region against three DDR1 isoforms. Two different primers and probes were used to analyse DDR1 mRNA expression, the first amplifies a part of the discoidin domain and the second, a part of the C-terminus. The antibody used for detection of protein is a polyclonal antibody raised against the C-terminus.

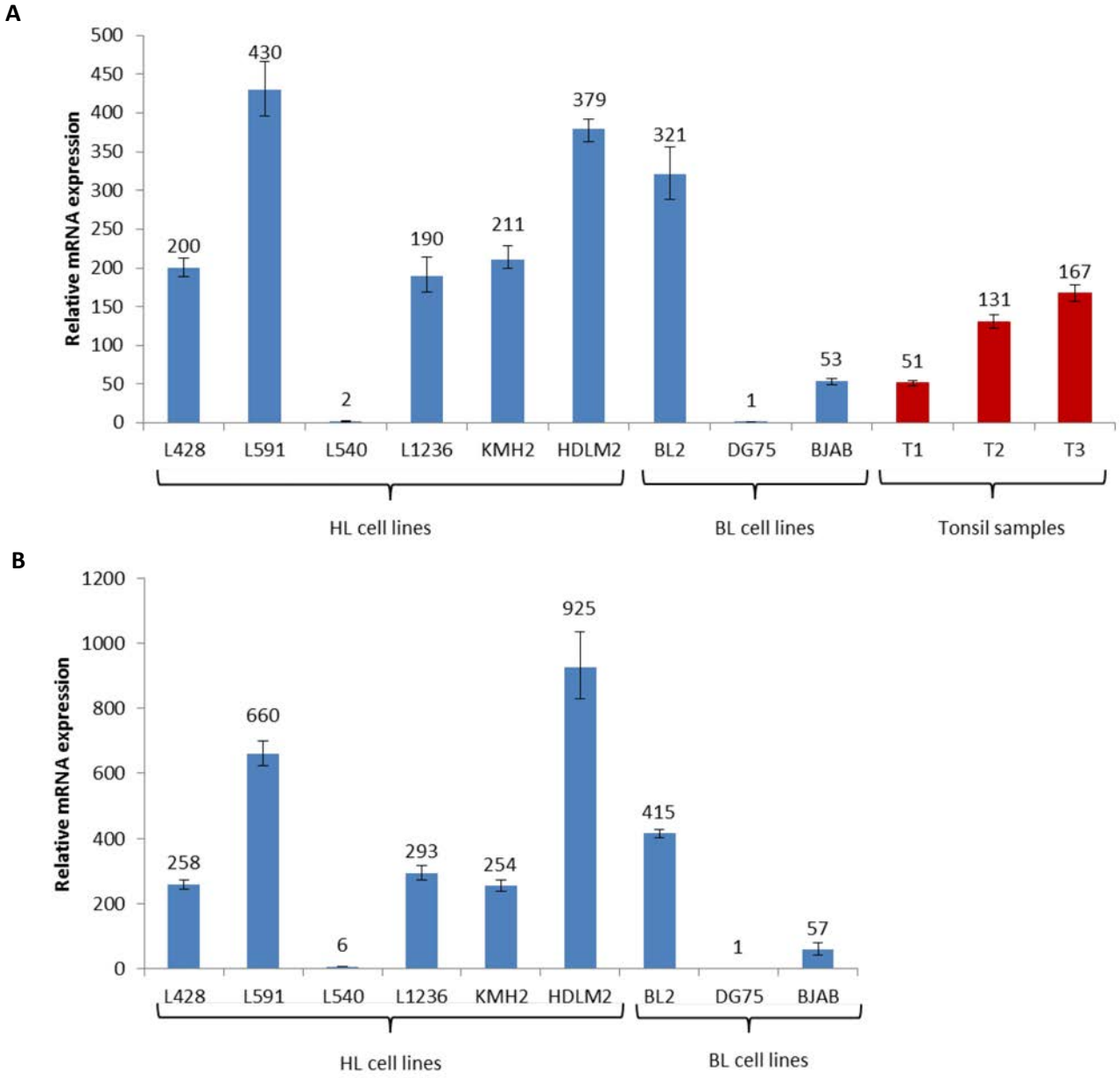

Figure 4.2 Expression of DDR1 mRNA in a panel of HL and BL cells. The relative expression of DDR1 mRNA as determined by q-PCR analysis using two sets of Taqman® primers and probes specific for DDR1 (A = set 1 and B = set 2, see figure 4.1 for primer locations). All samples were analysed in triplicate using the ΔΔ CT method, the unsorted $CD10^{+}$ GC B cells included in the comparison were from three different tonsils (set 1 only). The results shown are representative of three independent experiments.

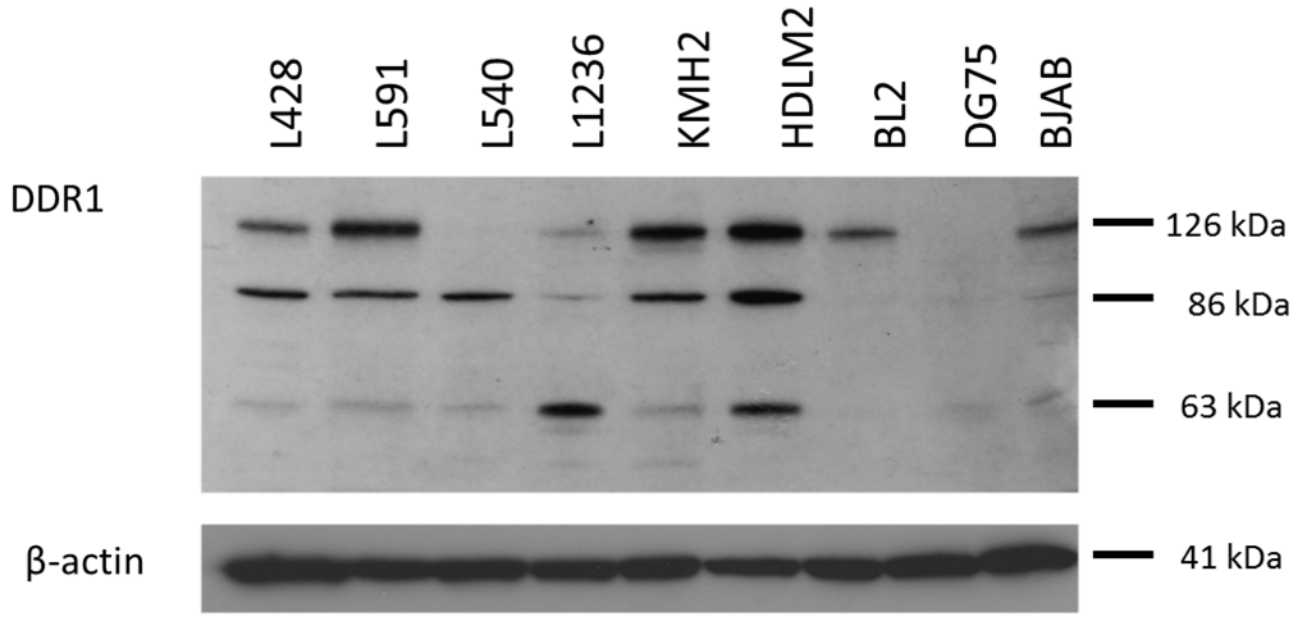

Figure 4.3 Expression of DDR1 protein in a panel of HL and BL cell lines. Immunoblot of whole cell lysates using a polyclonal DDR1 antibody. A band is seen at the expected size of 126kDa corresponding to DDR1a/b. Two further bands were identified at 86kDa and 63kDa. Equal loading was confirmed using an antibody against β-actin (41kDa).

4.2.2 DDR1 is expressed in primary paediatric HRS cells

Having established that DDR1 is over-expressed in HL cell lines, I then studied the expression of DDR1 in primary HL. Paraffin embedded biopsies of paediatric HL were obtained from the CCLG. 54 cases were available for this analysis. Immunohistochemistry using the DDR1 polyclonal antibody described above revealed strong expression of DDR1 in primary HRS cells in 69% (37/54) of cases. DDR1 expression was localised mainly to the cell membrane and as aggregates in the cytoplasm. I also noted DDR1 was expressed by a proportion of plasma cells. There was no significant association between DDR1 expression and histological subtype ($p>0.05$) (Table 4.1). No expression of DDR1 was detectable in the germinal centres of non-malignant tonsils (Figure 4.4).

4.2.3 HRS cells are intimately associated with collagen in HL

Following the observation that primary HRS cells over-express DDR1, I next explored the distribution of its ligand, collagen, in primary HL. First, I used a Van Gieson's stain which is a method for the specific detection of collagen in tissue sections but which does not differentiate individual collagen types (Figure 4.5). I also performed immunohistochemistry for type I and type IV collagen on selected cases. I observed that in some cases type IV was more strongly associated with HRS cells whereas in other cases both collagen types were present (Figure 4.6).

I observed two main patterns of collagen distribution. In the first pattern (pattern 1), there was prominent collagen deposition which was intimately associated with the HRS cells. In the second pattern (pattern 2) there was less collagen present in the immediate vicinity of the HRS cells and only a few tumour cells were in direct contact with collagen. I sub-divided

HL cases into one of two groups using an arbitrary cut off of greater than or less than 50% of HRS cells in contact with collagen. Tables 4.2 and 4.3 shows the numbers of HL cases in each group (n=38) stratified by DDR1 status and by subtype. Cases showing the pattern I localisation of collagen were significantly more likely to be of the NS subtype (p=0.0041). However, there was no significant association between the distribution of collagen and DDR1 expression.

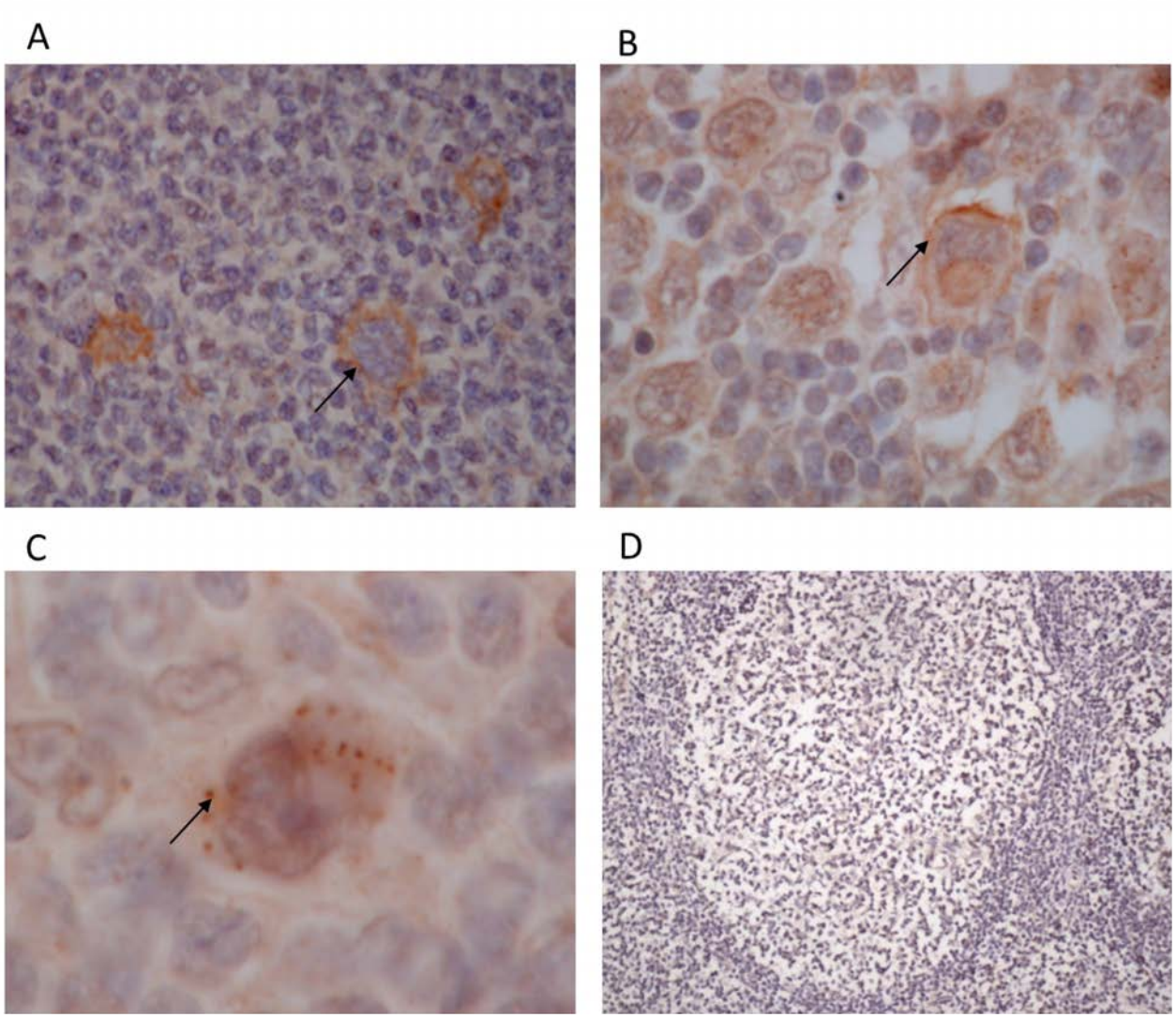

Figure 4.4 Immunohistochemistry for DDR1. Representative photomicrographs of primary HRS cells in paediatric HL showing immuno-reactivity to a polyclonal DDR1 antibody A) Membrane staining in case 14-193, Nodular lymphocyte predominant HL B) Membrane staining in case 14-172, nodular sclerosis C) Case 14-219,mixed cellularity showing aggregates of DDR1 in the cytoplasm D) No staining was observed in GC B cells of normal tonsil tissue.

Table 4.1 DDR1 expression stratified by subtype. There was no significant association between subtype and DDR1 positivity (n=54 p>0.05).

	DDR1 positive	DDR1 negative
Nodular sclerosis	25	9
Mixed cellularity	7	2
Lymphocyte predominant	3	3
Hodgkin's disease (unspecified)	2	3

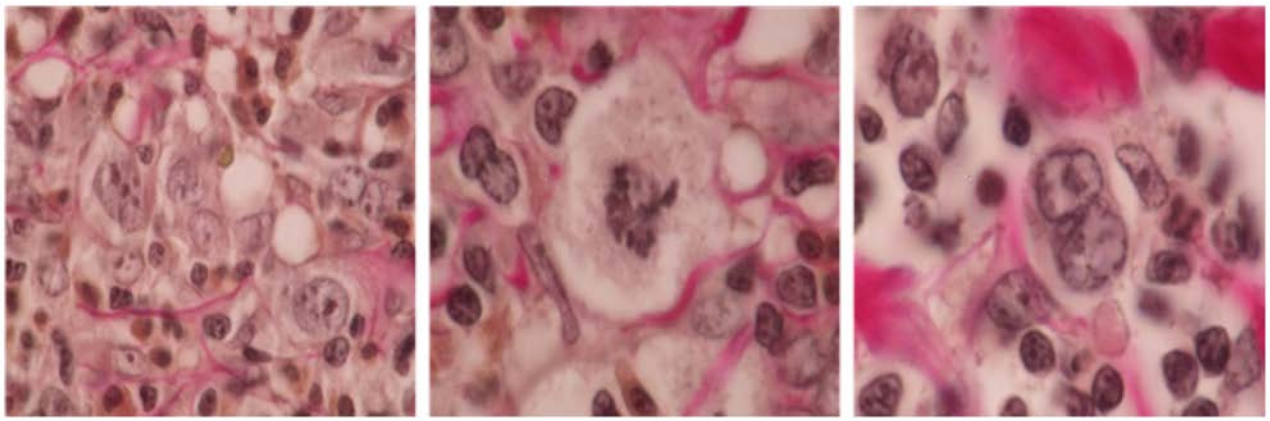

Figure 4.5 Detection of collagen in paediatric HL. A Van Gieson's stain to detect all collagen types in paediatric HL, visualised as a bright pink stain. In many cases the collagen 'wraps' around and associates intimately with individual HRS cells.

Table 4.2 Numbers of cases of HL classified on the basis of the distribution of collagen immediately adjacent to HRS cells, stratified by DDR1 status. There was no significant association between DDR1 expression and the distribution of collagen (n=38 p>0.05)

	Collagen in direct contact >50% (Pattern 1)	Collagen in direct contact <50% (Pattern 2)
DDR1 positive	17	10
DDR1 negative	6	5

Table 4.3 Numbers of cases of HL classified on the basis of the distribution of collagen immediately adjacent to HRS cells, stratified by histological subtype. There was a significant association between histological subtype and the distribution of collagen (n=38 p=0.0041)

	Collagen in direct contact >50% (Pattern 1)	Collagen in direct contact <50% (Pattern 2)
Nodular sclerosis	20	6
Mixed cellularity	3	3
Lymphocyte predominant	0	4
Hodgkin's disease (unspecified)	0	2

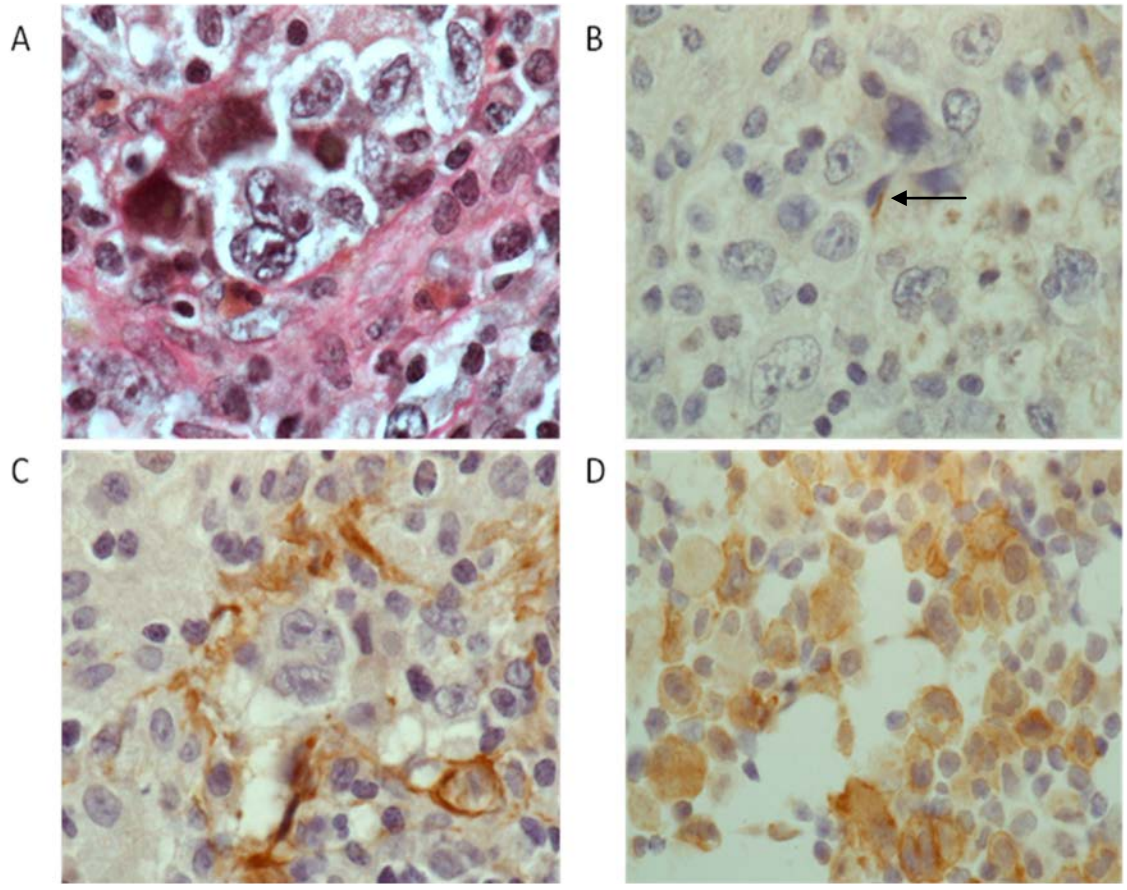

Figure 4.6 (i) Collagen and DDR1 expression in paediatric HL Case 4-409 (EBV negative NS HL subtype) A) A Van Gieson's stain showing a thick band of collagen enveloping tumour cells B) Immunohistochemistry for collagen type I (black arrow indicates a strongly positive fibroblast) C) Immunohistochemistry for collagen type IV D) Immunohistochemistry for DDR1

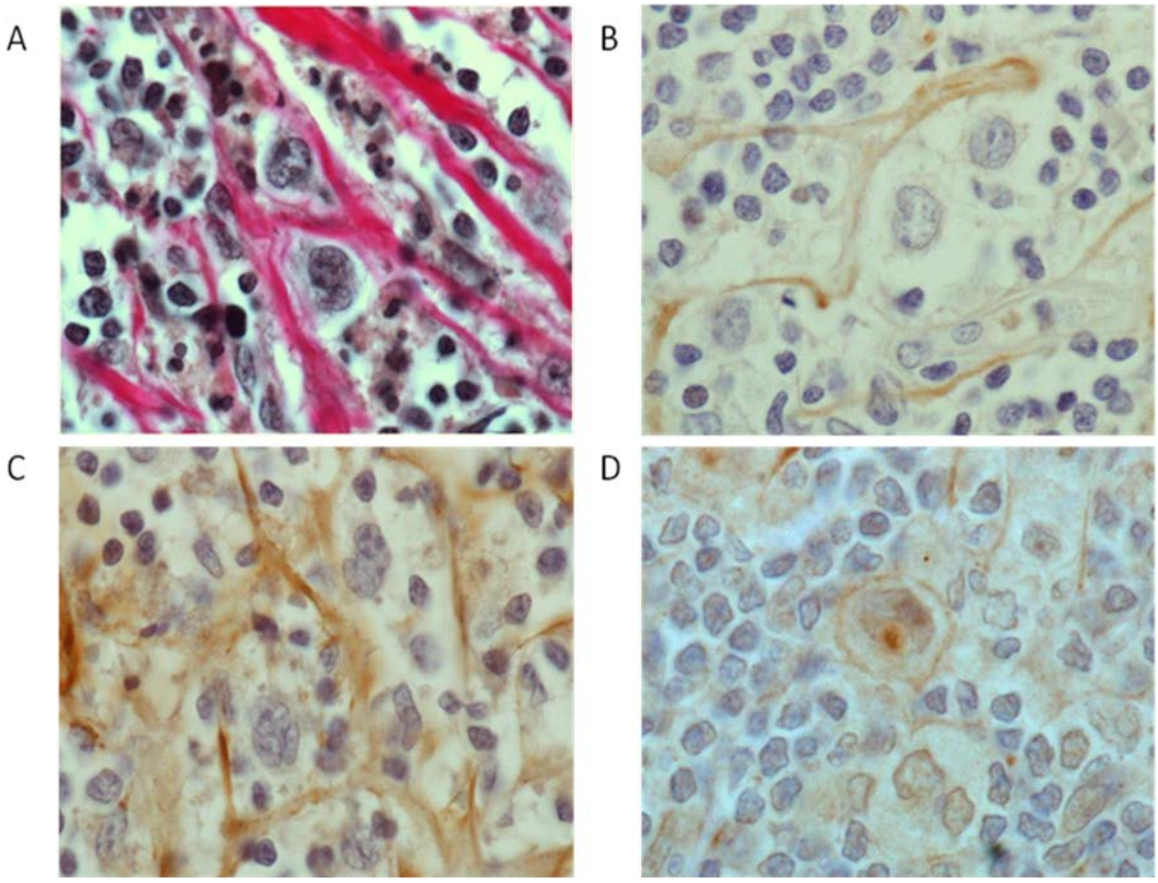

Figure 4.6 (ii) Collagen and DDR1 expression in paediatric HL Case 4-499 (EBV negative NS HL subtype) A) A Van Gieson's stain detecting collagen in contact with HRS cells B) Immunohistochemistry for collagen type I C) Immunohistochemistry for collagen type IV D) Immunohistochemistry for DDR1 expression

4.2.4 Ectopic expression of LMP1 induces DDR1 in GC B cells

Interrogation of an earlier microarray analysis performed following the ectopic expression of LMP1 in GC B cells had suggested that DDR1 was up-regulated by this viral gene[172]. Using RNA from this same experiment, I performed q-PCR on two LMP1 transfected samples and two empty vector controls seeking independent validation of this array result. Figure 4.7 shows that in both samples there was a striking up-regulation of DDR1 following LMP1 expression. I next used flow cytometry to measure DDR1 protein expression. For this experiment $CD10^+$ GC B cells were isolated from a fresh tonsil and co-transfected with either LMP1 or empty vector together with NGFR which was subsequently used to enrich transfected cells (transfection performed by Dr Vockerodt). Following this, I harvested and incubated the cells with primary DDR1 antibody followed by a rabbit-FITC conjugated secondary antibody. Gating was performed so that only live and transfected cells were included in the comparison of DDR1 expression in LMP1-transfected and empty vector-transfected control cells. A live transfected population of 13% is consistent with previous transfection experiments in GC B cells[172]. Figure 4.8 shows that when compared to control cells, a 20% increase in the number of cells expressing DDR1 was observed in LMP1-transfected GC B cells.

To address the possibility that the up-regulation of DDR1 by LMP1 could simply reflect the ability of this viral gene to drive GC B cell differentiation. I, therefore, investigated the expression of DDR1 among different B cell subsets. The isolation of naïve B cells, centrocytes, centroblasts and memory B cells was performed by Dr Anderton as previously described[332]. I performed q-PCR analysis on mRNA extracted from these four subsets and found that DDR1 expression was lowest in both centrocytes and centroblasts but higher in

naïve B cells and in memory B cells (Figure 4.9). These results are consistent with the re-analysis of a published global gene expression microarray [319] which showed that DDR1 expression was higher in memory and plasma cells compared to GC B cells (Figure 4.10).

Finally, using the same patient cohort described in section 4.3.2 I investigated if there was an association between DDR1 and LMP1 expression in primary tumours. A chi-squared test showed that there was no significant correlation between LMP1 status and DDR1 expression ($p>0.05$; Table 4.4).

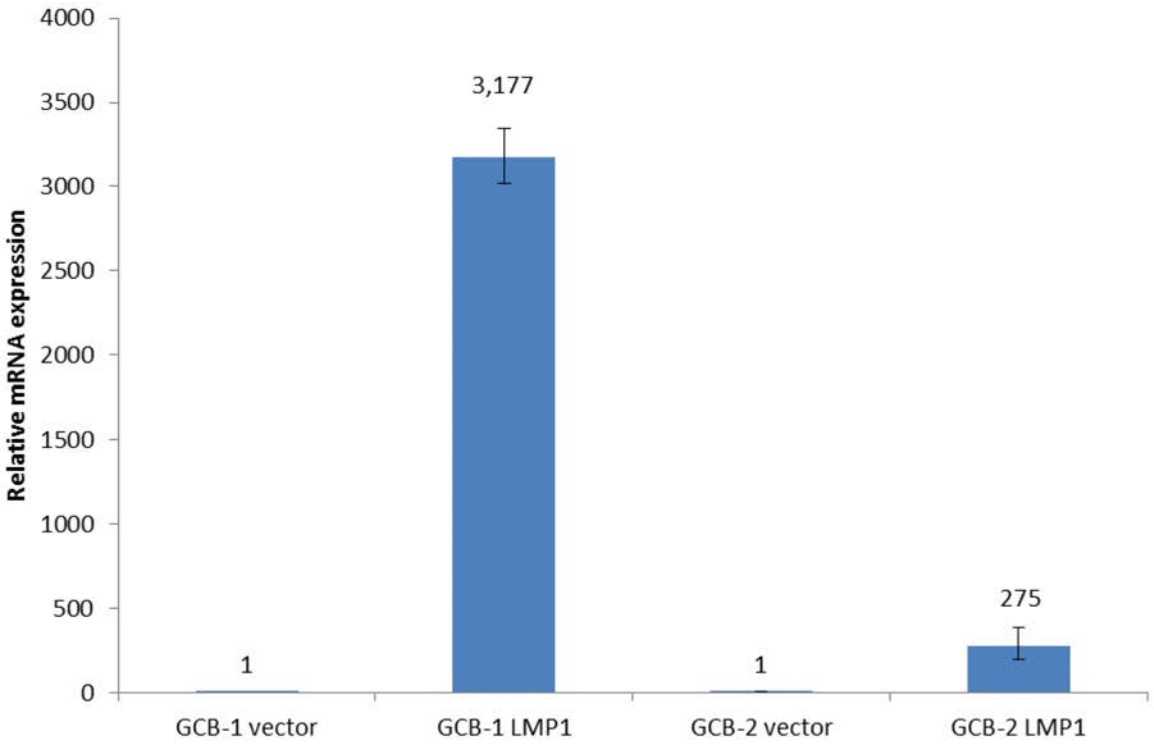

Figure 4.7 Relative expression of DDR1 mRNA in CD10+ GC B cells transfected with either LMP1 or with empty vector. A q-PCR analysis using Taqman primers and probe (set 1) for DDR1 was performed on two separately isolated and transfected $CD10^{+}$ populations. Results are shown as fold change in LMP1 expressing cells relative their corresponding vector only control which was set to a value of 1. Samples were analysed in triplicate and are presented as ΔΔ CT values in comparison to corresponding vector control.

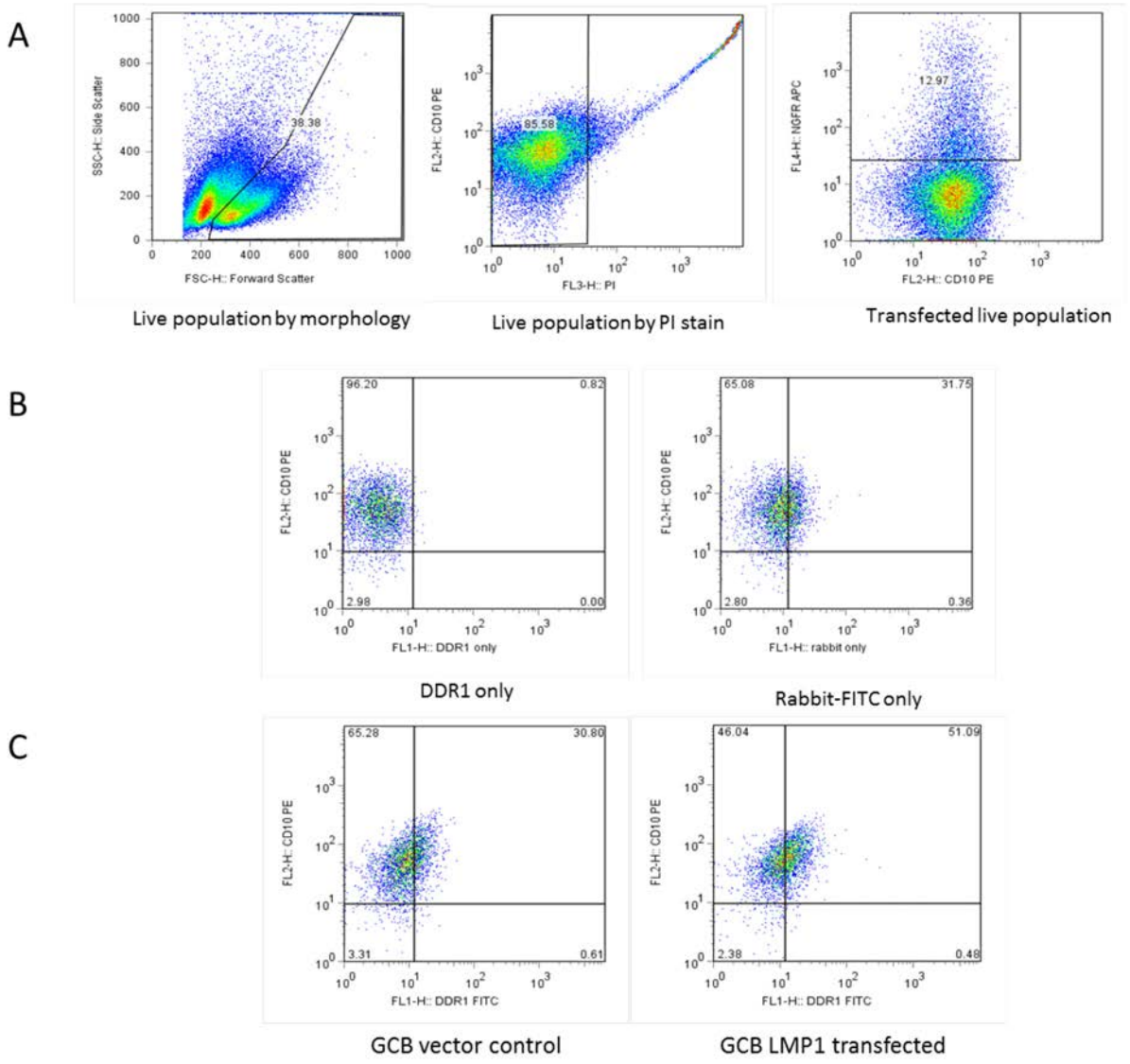

Figure 4.8 DDR1 protein expression in CD10+ GC B cells transfected with either LMP1 or empty vector. Samples were incubated with DDR1 primary antibody followed by a FITC-conjugated rabbit secondary antibody. A) The population to be analysed were first gated by morphology and propidium iodide stain to identify live cells, then selected by NGFR expression. B) Further gates were applied to account for fluorescence from DDR1 unconjugated antibody and rabbit-FITC antibody. C) The vector control population showed a similar fluorescence to rabbit-FITC only sample while an increase in DDR1-FITC positive cells is seen when LMP1 is ectopically expressed consistent with an up-regulation of DDR1 in LMP1 expressing cells.

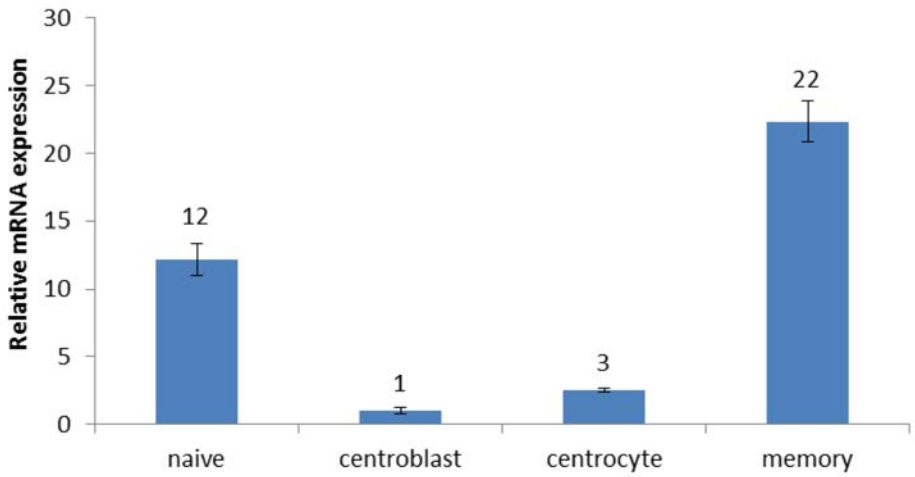

Figure 4.9 Expression of DDR1 mRNA across different B cell subsets. B cell subsets were separated as described in Materials and Methods (section 2.16 page 96). mRNA from naïve B cells, centroblasts, centrocytes and memory B cells were analysed in triplicate by q-PCR using Taqman primers and probe (set 1) for DDR1. Results are shown as fold change relative to centroblasts which was set to a value of 1 as determined by q-PCR analysis using a ΔΔCT method.

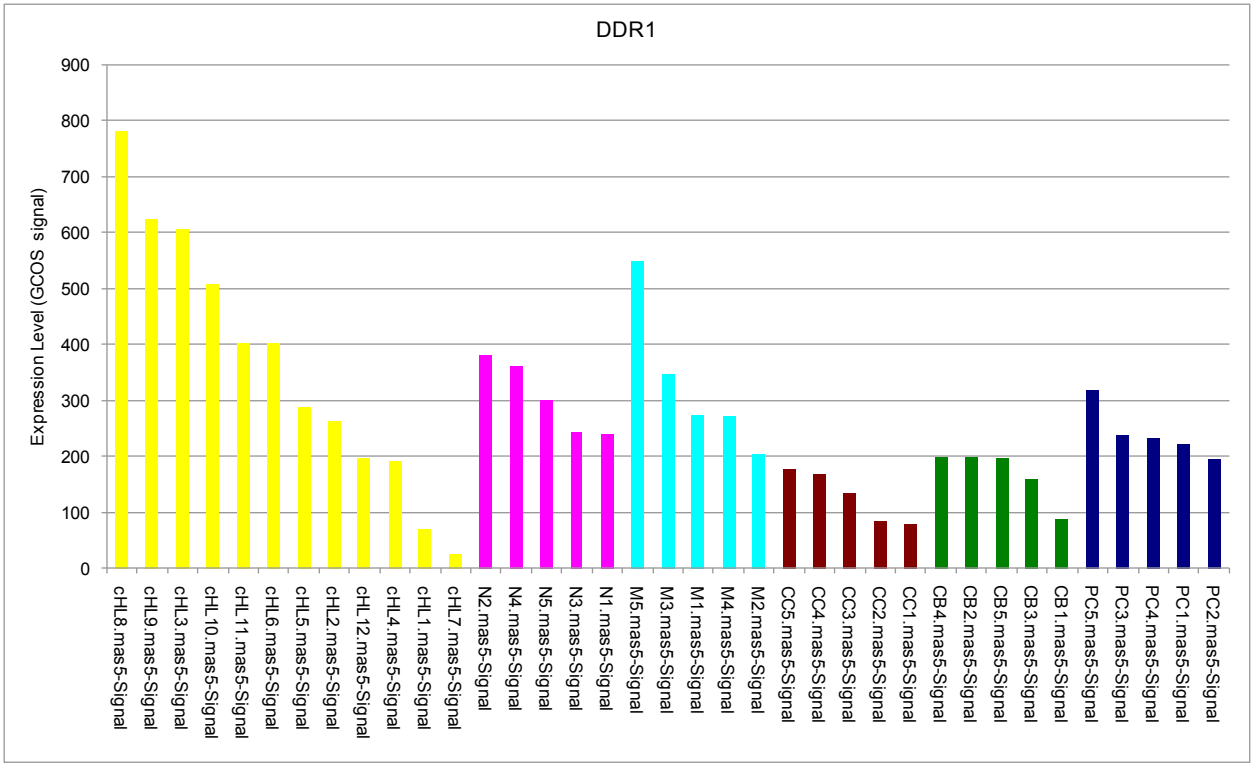

Figure 4.10 DDR1 expression in a published gene expression dataset. GCOS outputs for DDR1 obtained from a study in which gene expression in micro-dissected HRS cells was compared to that in different B cell subsets. Compared to centrocytes and centroblasts (GC B cells), DDR1 was over-expressed in HL cells in a proportion of cases. These data are consistent with the over-expression of DDR1 observed in my study.

Table 4.4 DDR1 expression in primary HL stratified by EBV status There was no statistically significant association between DDR1 expression and EBV status (Chi-squared test, p>0.05)

	DDR1 positive	DDR1 negative
LMP1 positive	20	9
LMP1 negative	17	10

4.2.5 Regulation of DDR1 phosphorylation by collagen in HL cells

I next investigated the activation of DDR1 in HL cell lines. Soluble type I collagen has been shown to activate DDR1 in range of cell types. Therefore, I used media supplemented with soluble type I collagen to study the activation of DDR1 in HL cell lines. Cells were stimulated with collagen for defined periods of time then harvested and DDR1 phosphorylation measured using a method adapted from L'hote and colleagues[267]. This method is based on the immunoprecipitation (IP) of DDR1 from whole cell lysates followed by immunoblotting for the detection of phosphorylated tyrosine residues. Equal IP efficiency was confirmed by stripping the blot and re-probing for DDR1. The IP technique was optimised on a colon cancer cell, HCT116, reported to show DDR1 phosphorylation upon stimulation with collagen type I[267]. I confirmed that in HCT116, the phosphorylation of DDR1 peaked at 12 hours following the addition of collagen (Figure 4.11).

Once established, I used this method to analyse the phosphorylation of DDR1 in L428 cells. L428 cells were grown in serum free conditions overnight and harvested 2 hours after the addition of soluble collagen type I or media alone as a control. Figure 4.12 shows that in L428 cells, DDR1 phosphorylation was higher in control cells compared to those cells treated with collagen despite comparable levels of total DDR1. HCT116 stimulated with type I collagen for 12 hours was included as a positive control.

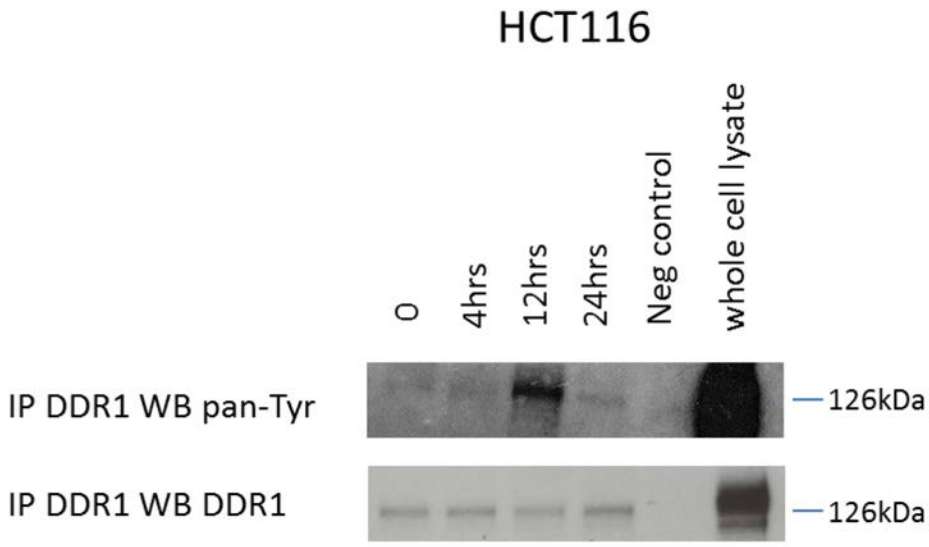

Figure 4.11 Detection of phosphorylated DDR1 in HCT116 cells following stimulation with collagen type I. Immunoblot for pan-phosphorylated tyrosine proteins following immunoprecipitation with DDR1 antibody; a strong band corresponding to DDR1a/b at 126kDa is detected 12 hrs after the addition of collagen. 500 µg of whole cell lysate was required for IP experiments. IP efficiency was confirmed using the same antibody to DDR1 to that used to perform the IP.

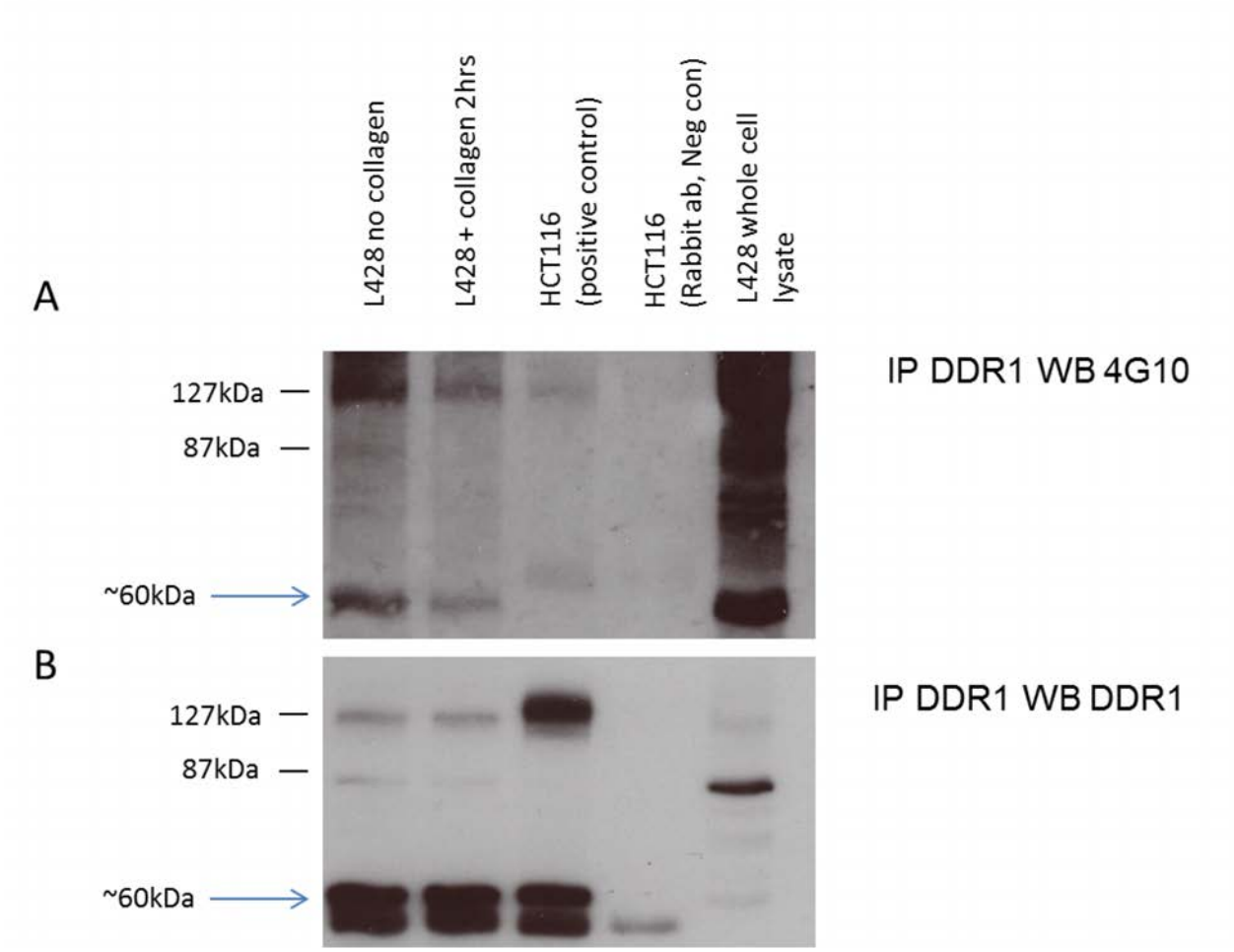

Figure 4.12 Detection of phosphorylated DDR1 in L428 cells following stimulation with collagen type I for 2hrs. A) Immunoblot for pan-phosphorylated tyrosine proteins following immunoprecipitation with DDR1 antibody. A strong band corresponding to DDR1a/b at 126kDa is detected. In addition, there is a band in the L428 cell line around 60kDa and a slightly higher band in the HCT116 cell line at the expected weight for the β subunit. B) The blot was stripped and re-probed with DDR1 antibody to confirm equal IP efficiency.

I further considered the effect of the addition of type I collagen on the activation of DDR1 in L428 cells grown in either serum-containing or in serum free media over a time course. I observed that the DDR1 present in L428 cells was phosphorylated in the absence of collagen in both 10% serum and in serum free conditions. I repeated this experiment with the L591 HL cell line. In contrast to L428 cells, L591 cells showed no detectable DDR1 phosphorylation in the absence of collagen but phosphorylation was induced after collagen treatment in cells grown in 10% serum but not in serum free media. These data suggest that the phosphorylation of DDR1 by collagen in L591 cells requires a co-factor present in the serum (Figure 4.13).

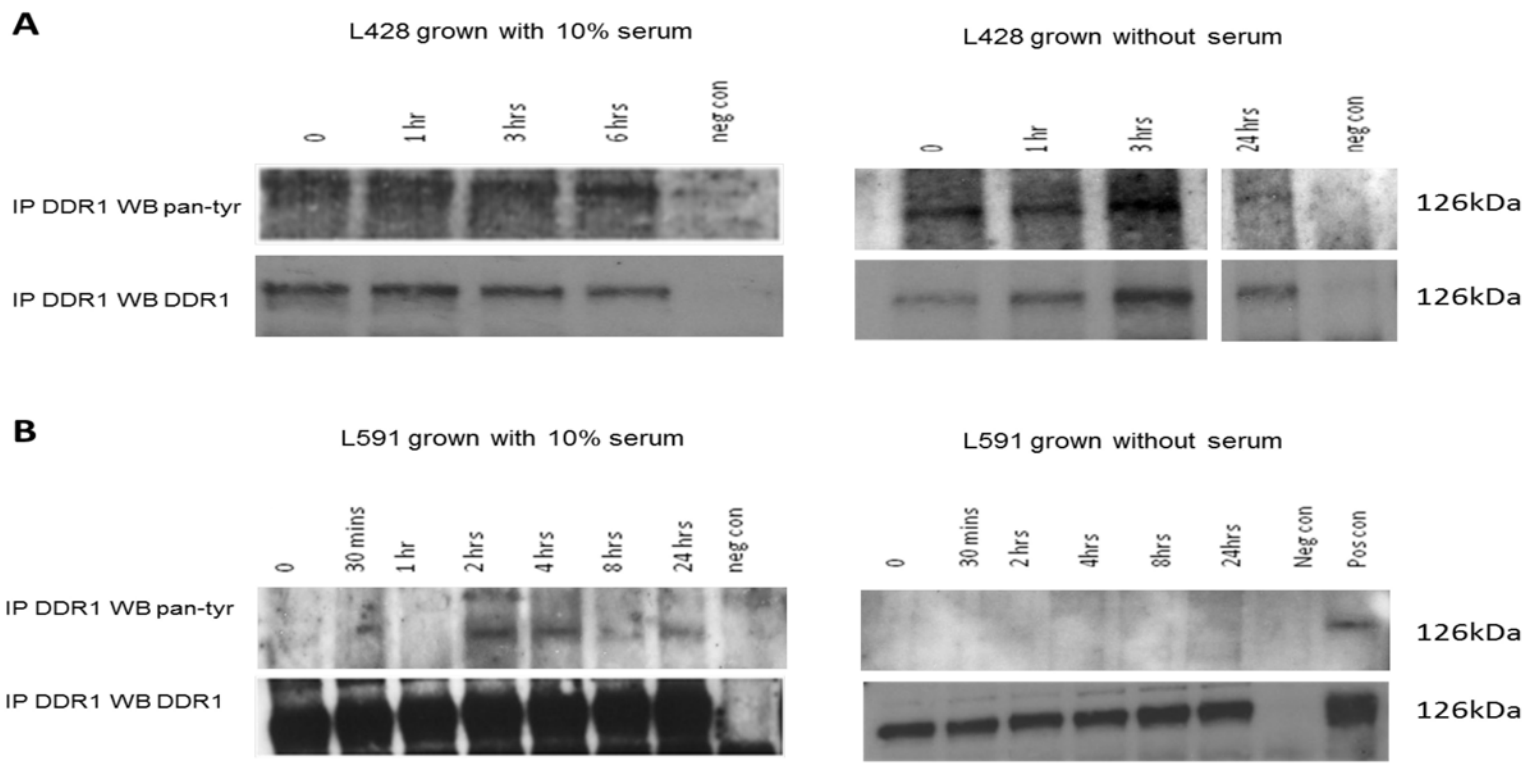

Figure 4.13 Activation of DDR1 in two HL cell lines A) L428 and B) L591 following stimulation with collagen type I 24hrs prior to treatment the cells were washed and re-suspended in either 10% serum or serum free media. 10µg/ml of soluble type I collagen was added to the cells (T=0). The cells were harvested at the time points indicated. Immunoblotting was performed for pan-phosphorylated tyrosine proteins following immunoprecipitation with DDR1 antibody. The positive control was HCT116 cells stimulated with collagen for 12hrs and the negative control was HCT116 cells stimulated in the same manner but the IP was performed with total rabbit immunoglobulins A) Phosphorylation of L428 cells was observed in the absence collagen treatment

4.2.6 Knockdown of DDR1 expression in HL cell lines

Having shown that DDR1 is constitutively activated in L428 cells, I used this cell line to investigate the impact of DDR1 on the phenotype of HL cells. I nucleofected L428 cells with either smart pool DDR1 siRNA or scrambled siRNA as a control and harvested the transfected cells at 24, 48 and 72 hours post-transfection. Figure 4.14 shows regions within the full length DDR1 sequence that are targeted by individual siRNAs contained with this pool. When compared to control cells, the treatment of L428 cells with the pooled siRNA efficiently reduced both DDR1 mRNA and protein expression (Figure 4.15). The knockdown showed loss of the 126kDa protein whereas other bands reacting with the DDR1 antibody were unaffected.

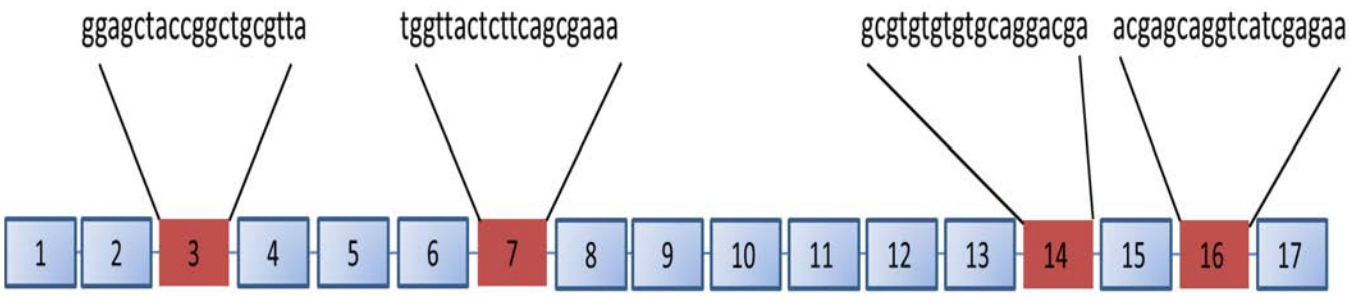

Figure 4.14 Schematic of the exon structure of full length DDR1 (NM_013994.2) illustrating the coding sequence targeted by individual corresponding siRNA contained within the Dharmacon SMARTpool.

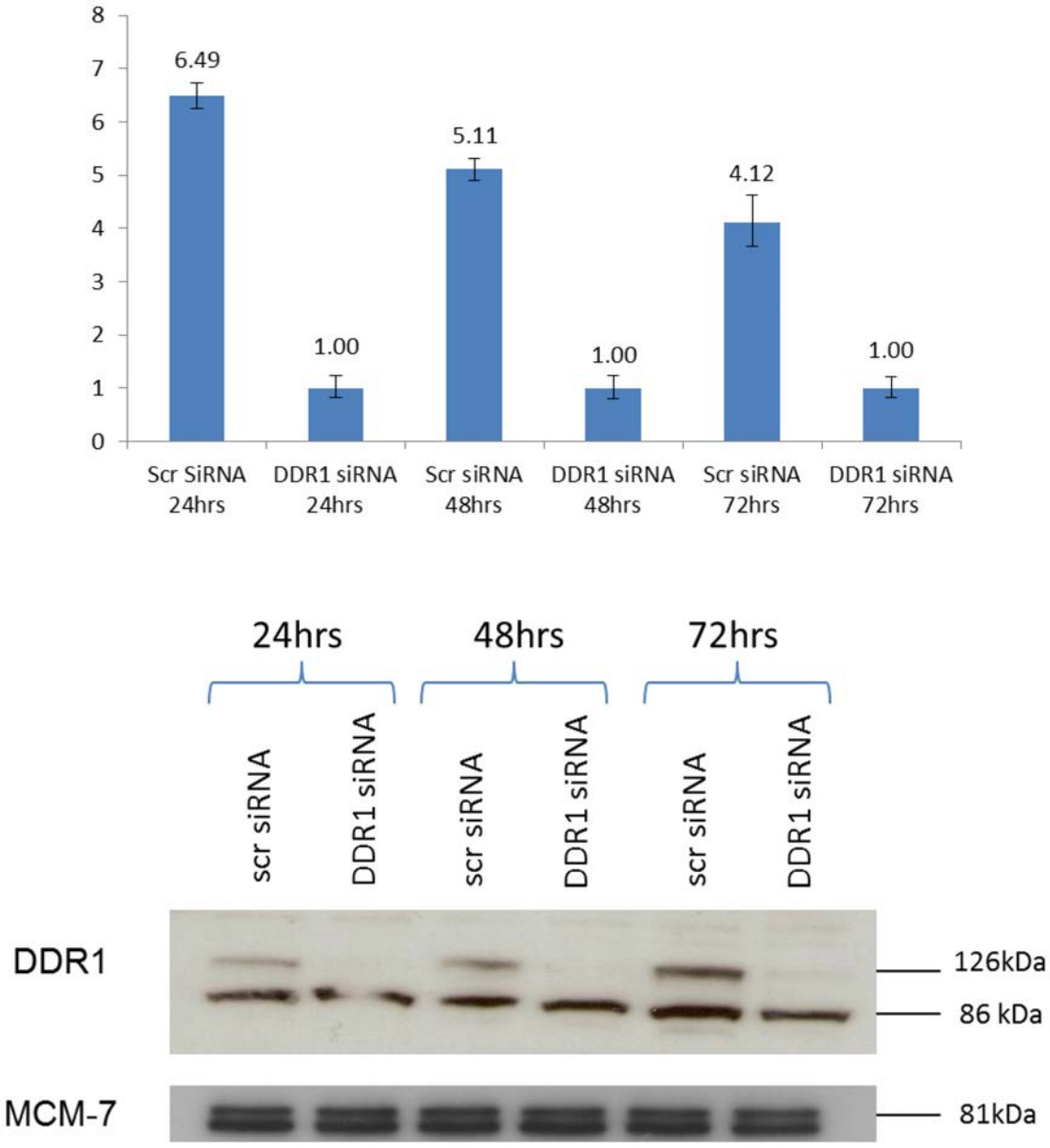

Figure 4.15 Transient silencing of DDR1 expression in L428 cells The L428 cell line was nucleofected using smart pool DDR1 siRNA or corresponding control and cells were harvested at 24, 48 and 72hrs post transfection for confirmation of knockdown A) mRNA expression of DDR1 following knockdown. The RNA analysis was performed in triplicate and relative DDR1 mRNA levels were calculated using ΔΔ CT. B) 30µg of total protein from whole cell lysate was loaded and immunoblotted for DDR1 using polyclonal C-terminal DDR1 antibody. Equal loading was confirmed using an antibody to MCM7.

I investigated the effect of the knockdown of DDR1 expression in L428 cells on two key phenotypes, proliferation and apoptosis. For all the following experiments described here I confirmed the knockdown of DDR1 to levels comparable to those shown in Figure 4.15. I used a 'proliferation assay' (Promega see section 2.9.1 page 84) which measures metabolic activity as an indicator of proliferation. I observed that the knockdown of DDR1 had no effect on the proliferation of L428 cells (Figures 4.16). I used two assays to study the effects of DDR1 on apoptosis; flow cytometric detection of Annexin V-FITC and immunoblotting for PARP cleavage. Staurosporine treated L428 cells were used as a positive control in the Annexin V experiment. Figures 4.17 and 4.18 which are representative of three experimental replicates show that the knockdown of DDR1 had no effect on the number of L428 cells undergoing apoptosis.

Next I explored in L428 cells the influence of DDR1 knockdown on three of its downstream molecules, STAT3, STAT5 and the adaptor protein NCK2, which have been reported in other cell types[277;331;333]. Immunoblotting of transfected L428 cells showed no difference either in the protein levels or in the phosphorylation status of STAT3 and STAT5 following DDR1 knockdown. Immunoblotting also revealed no change in the levels of NCK2 after DDR1 knockdown (Figure 4.19).

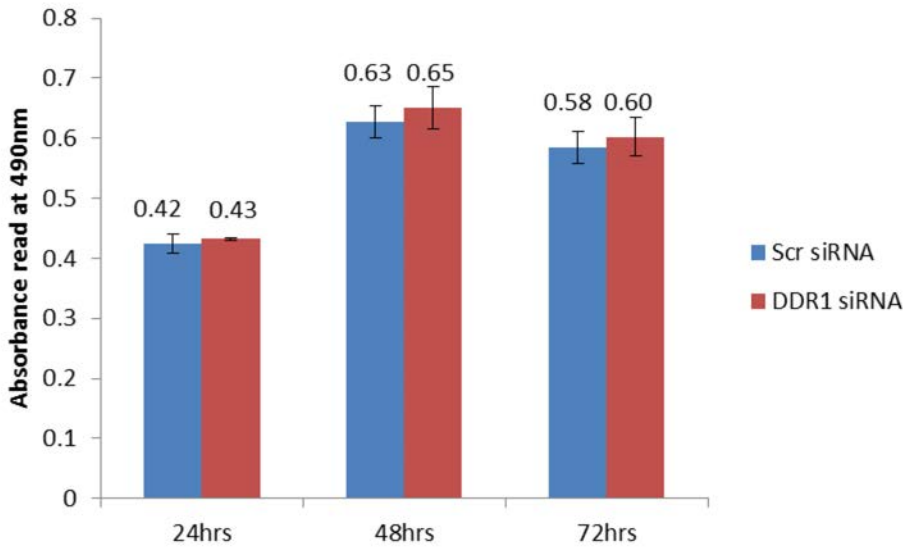

Figure 4.16 Proliferation in L428 cells following the knockdown of DDR1 L428 cells were nucleofected with DDR1 siRNA or scrambled siRNA as a corresponding control. At 22, 46 and 70hrs post transfection the Promega proliferation reagent was added and the absorbance at 490 nm was read 2 hours later. This assay measures metabolically active cells.

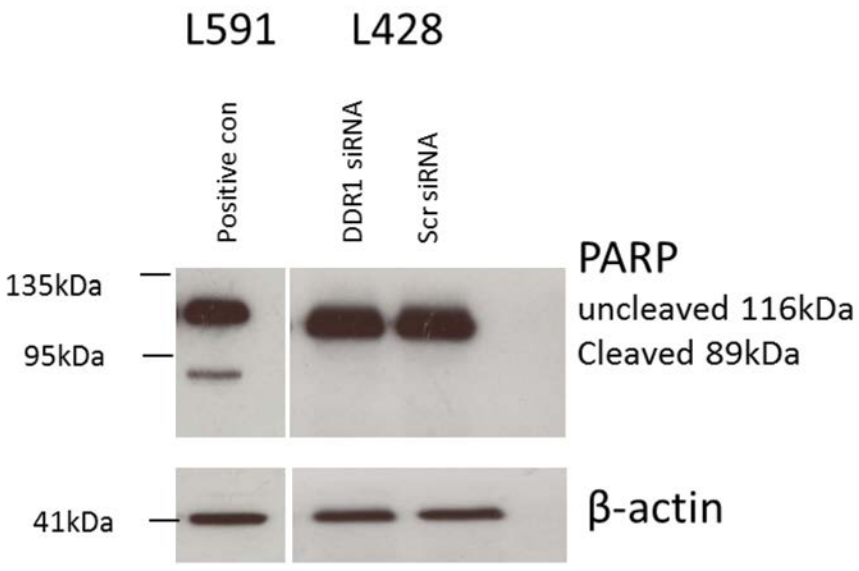

Figure 4.17 PARP cleavage in L428 cells following DDR1 knockdown 30µg of protein from whole cell lysate from L428 cells in which DDR1 knockdown was confirmed were immunoblotted for PARP. L591 was used as a positive control for PARP cleavage and equal loading was confirmed using an antibody against β-actin.

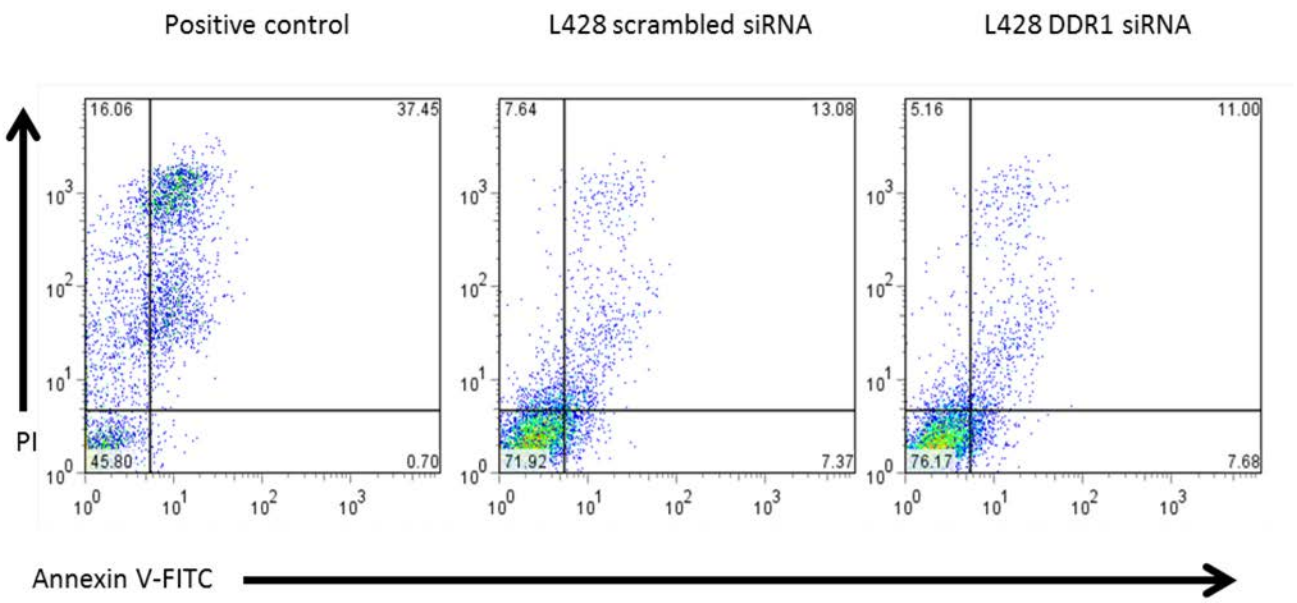

Figure 4.18 Apoptosis in L428 cells using Annexin V staining measured by flow cytometry 48hrs post nucleofection. L428 cells were transfected with either DDR1 siRNA or scrambled siRNA as a control and harvested at 48 hrs for Annexin V analysis. Cells that are positive for FITC and negative for PI are undergoing apoptosis (LR quadrant). Cells positive for both FITC and PI are dead, necrosed or at end stage apoptosis (UR quadrant) while cells negative for both are alive (LL quadrant). L428 cells treated with 1 µM of staurosporine served as a positive control for the assay.

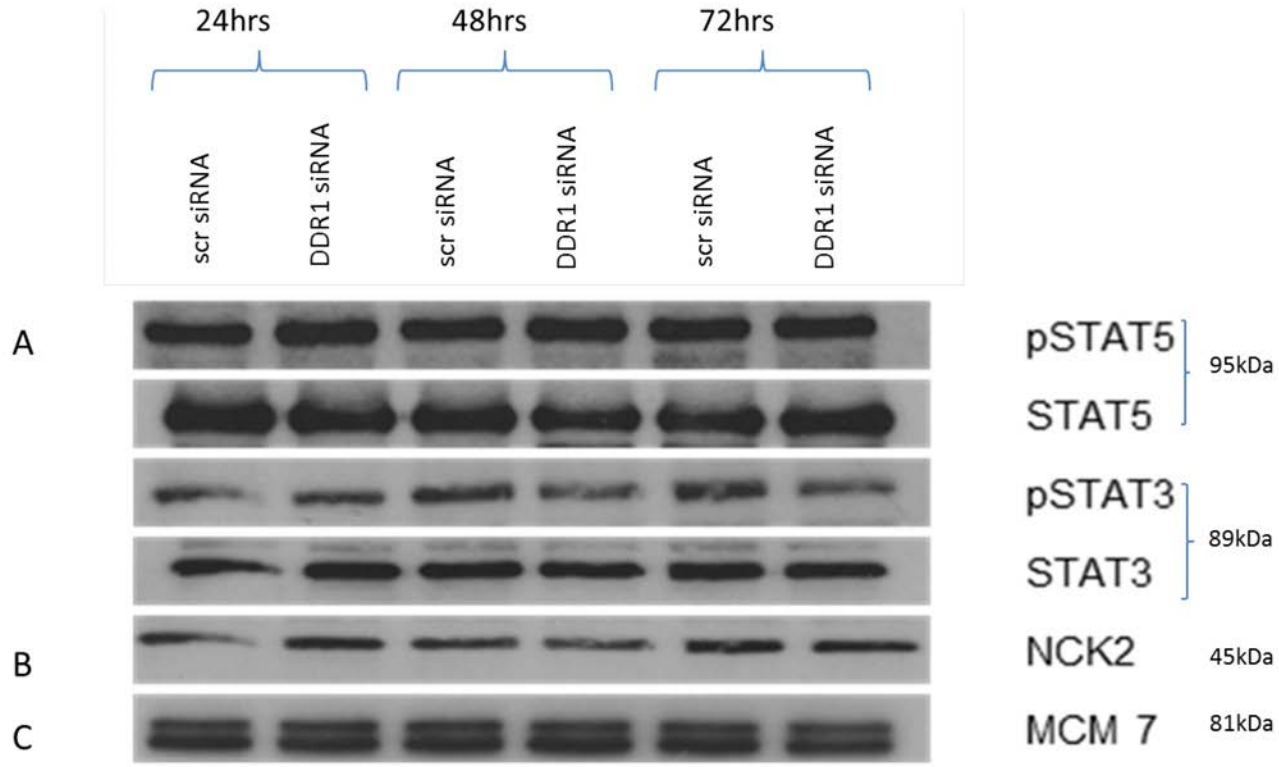

Figure 4.19 Immunoblot for downstream targets of DDR1 following its knockdown in L428 cells. L428 cells were nucleofected with DDR1 siRNA or scrambled siRNA as a control and pellets were harvested at 24, 48 and 72hrs post transfection. Immunoblotting for pSTAT5 and pSTAT3 was performed first then the membrane was stripped and immunoblotted for total STAT5 and STAT3 respectively. Equal loading was confirmed using an antibody against MCM-7.

4.2.7 Gene expression profiling in L428 cells treated with DDR1 siRNA

Gene expression profiling was used to investigate the influence of DDR1 loss on the global transcriptional programme of L428 cells. To do this, I repeated the knockdown of DDR1 in the L428 cell line; RNA was isolated from three independent experiments in which L428 cells were transfected with either DDR1 siRNA or with scrambled siRNA as a control. RNA was harvested 48 hours post transfection.

RNA was biotin-labelled with an IVT labelling kit (Affymetrix, Santa Clara, CA, USA), then randomly fragmentation and hybridized to Affymetrix HG-U133 Plus2 microarrays. Scanned images of microarray chips were analyzed using Affymetrix GeneChip Operating Software (GCOS).

Ratios for GAPDH and beta-actin (3'/5') were within acceptable limits (0.92- 0.97 for GAPDH and 1.20- 1.47 for beta-actin). BioB spike controls were present in all 6 chips, with BioC, BioD, and CreX also present in increasing intensity. Scaling factors for all arrays ranged from 1.45 to 2.63. Average background were within acceptable limits from 31 to 36, as well as raw Q values (0.89 – 1.02). The percentage of genes called present was comparable across arrays from 37.1% to 40.5%. The gene expression signal was calculated using the MAS5 algorithm of Affymetrix Expression Console with the default settings except the target signal was set to 100.

Gene expression profiles of L428 cells transfected with DDR1 siRNA were compared with those of L428 cells transfected with scrambled siRNA. Differentially expressed genes with p values < 0.01 and fold change > 1.3 were identified using limma[334]. The knockdown of DDR1 in L428 cells was followed by the up-regulation of 18 genes and the down-regulation of 43

genes. Although the down-regulated genes included DDR1 the fold change observed (-1.83) was substantially less than that detected by q-PCR analysis on the same RNA. It was also notable that the fold changes in expression for those genes recorded as significant were very modest (only 3 genes had a fold change > 1.5). When the 60 probe sets differentially expressed following knockdown of DDR1 were compared with the top 60 probe sets differentially expressed in L428 cells compared with GC B cells, and with the top 60 probe sets differentially expressed in L428 cells following transfection with LMP1, no overlapping probe sets were found in either comparison. However, it should be noted that the LMP1-L428 experiment was performed on the 'Focus array' which list substantially few probe sets (Affymetrix).

Table 4.5 List of genes differentially expressed following DDR1 knockdown in L428 cells

Gene	NCBI Gene Symbol	Fold Change
discoidin domain receptor tyrosine kinase 1	DDR1	-1.83
solute carrier family 2 (facilitated glucose transporter), member 3	SLC2A3	-1.52
ectonucleoside triphosphate diphosphohydrolase 1	ENTPD1	-1.49
ATPase, class VI, type 11B	ATP11B	-1.49
LAG1 homolog, ceramide synthase 6	LASS6	-1.48
sortilin 1	SORT1	-1.45
myelin protein zero-like 1	MPZL1	-1.44
ankyrin repeat and FYVE domain containing 1	ANKFY1	-1.42
small nucleolar RNA host gene 4 (non-protein coding)	SNHG4	-1.40
RAP1, GTP-GDP dissociation stimulator 1	RAP1GDS1	-1.40
acyl-CoA binding domain containing 5	ACBD5	-1.39
Coiled-coil domain containing 124	CCDC124	-1.38
muscleblind-like 2 (Drosophila)	MBNL2	-1.38
GrpE-like 2, mitochondrial (E. coli)	GRPEL2	-1.38
CTD (carboxy-terminal domain, RNA polymerase II, polypeptide A) small phosphatase like 2	CTDSPL2	-1.38
Mix1 homeobox-like 1 (Xenopus laevis)	MIXL1	-1.38
bone morphogenetic protein 1	BMP1	-1.36
mbt domain containing 1	MBTD1	-1.36
secretory carrier membrane protein 1	SCAMP1	-1.35
MORN repeat containing 1	MORN1	-1.35
bicaudal D homolog 2 (Drosophila)	BICD2	-1.35
family with sequence similarity 177, member A1	FAM177A1	-1.35
chromosome 9 open reading frame 41	C9orf41	-1.34
transmembrane emp24 protein transport domain containing 8	TMED8	-1.34
vesicle transport through interaction with t-SNAREs homolog 1B (yeast)	VTI1B	-1.34
Mdm2, transformed 3T3 cell double minute 2, p53 binding protein (mouse) binding protein, 104kDa	MTBP	-1.33
mannosidase, endo-alpha	MANEA	-1.33
WD repeat domain 64	WDR64	-1.33
RAD9 homolog B (S. pombe)	RAD9B	-1.33
NMDA receptor regulated 2	NARG2	-1.33
sorting nexin 13	SNX13	-1.33
Hypothetical protein LOC100289294	LOC100289294	-1.32
Scm-like with four mbt domains 2	SFMBT2	-1.32
TAF4b RNA polymerase II, TATA box binding protein (TBP)-associated factor, 105kDa	TAF4B	-1.32
transmembrane protein 67	TMEM67	-1.31
zinc finger protein 567	ZNF567	-1.31
bone morphogenetic protein receptor, type IB	BMPR1B	-1.31
hypothetical protein LOC100128788	LOC100128788	-1.31
AT hook containing transcription factor 1	AHCTF1	-1.31

Continued overleaf

EFR3 homolog B (S. cerevisiae)	EFR3B	-1.31
solute carrier family 39 (zinc transporter), member 14	SLC39A14	-1.31
REX1, RNA exonuclease 1 homolog (S. cerevisiae)-like 1	REXO1L1	-1.30
post-GPI attachment to proteins 3	PGAP3	-1.30
chromosome 14 open reading frame 79	C14orf79	1.31
alkaline ceramidase 1	ACER1	1.31
epidermal growth factor receptor (erythroblastic leukemia viral (v-erb-b) oncogene homolog, avian)	EGFR	1.31
G protein-coupled receptor 44	GPR44	1.31
cementum protein 1	CEMP1	1.31
phosphodiesterase 5A, cGMP-specific	PDE5A	1.31
glutamate decarboxylase 2 (pancreatic islets and brain, 65kDa)	GAD2	1.31
protein phosphatase 2, regulatory subunit B, gamma	PPP2R2C	1.32
Similar to hCG1997308	LOC100287627	1.32
RAB40B, member RAS oncogene family	RAB40B	1.32
phosphodiesterase 6B, cGMP-specific, rod, beta	PDE6B	1.33
NK6 homeobox 1	NKX6-1	1.34
Erythropoietin	EPO	1.34
adenylosuccinate synthase like 1	ADSSL1	1.38
hypothetical LOC388796 /// small nucleolar RNA, H/ACA box 71B	LOC388796	1.40
hypothetical LOC388796 /// small nucleolar RNA, H/ACA box 71B	SNORA71B	1.40
pleckstrin homology domain containing, family G (with RhoGef domain) member 4B	PLEKHG4B	1.42
histone cluster 1, H2bg	HIST1H2BG	1.50

4.2.8 Sequence analysis of DDR1 cDNA in HL cell lines

In the preceding experiments I had consistently observed several bands on immunoblotting, which were unchanged following DDR1 knockdown. I next explored the possibility that these bands might represent mutated forms or alternative splice variants of DDR1. An initial rapid screen of the coding region of DDR1 was performed using 6 overlapping primer pairs spanning the entire coding sequence of the DDR1 receptor (Figure 4.20). Sequencing was performed on the L428 and L591 cell lines. In both cell lines 5 out of 6 primer pairs gave clean PCR products. However, the primer pair spanning the juxtamembrane region gave multiple bands (Figure 4.21). Manual inspection and NCBI BLAST analysis showed that neither L591 nor L428 cells harboured point mutations, insertions or deletions in the exon sequence. The sequencing of genomic DNA was not performed so any mutations in the intron sequence or mutations of the intron-exon boundaries will not have been detected.

4.2.9 Detection of multiple DDR1 transcripts in HL cells

The sequence generated from the primer pair spanning the juxtamembrane region had a region of overlapping sequence with a similar pattern in both L428 and L591 cells (Figure 4.22). On closer inspection the sequence is a single clean sequence for exon 10 but two overlapping sequences begin where exon 11 should be. A more detailed examination using NCBI BLAST software showed two mRNA transcripts were present. In summary, the sequence analysis of L428 and L591 cells suggests that there are two predominant isoforms of DDR1 that co-exist in HL cell lines. In the first, only exon 11 is absent and is consistent with the presence of DDR1a while in the second, both exon 11 and 12 were spliced out. ExPASy translation of this second sequence shows a shift in the open reading frame to the amino acid sequence GAPV followed by a stop codon, the same as that found in DDR1d.

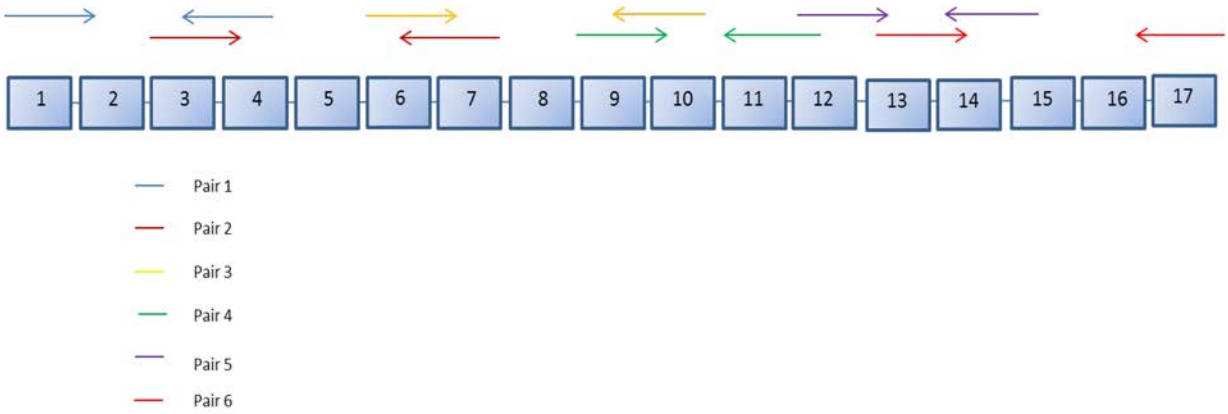

Figure 4.20 Schematic of primer pair location in relation to DDR1 exon sequence. (Table 2.6 page 94)

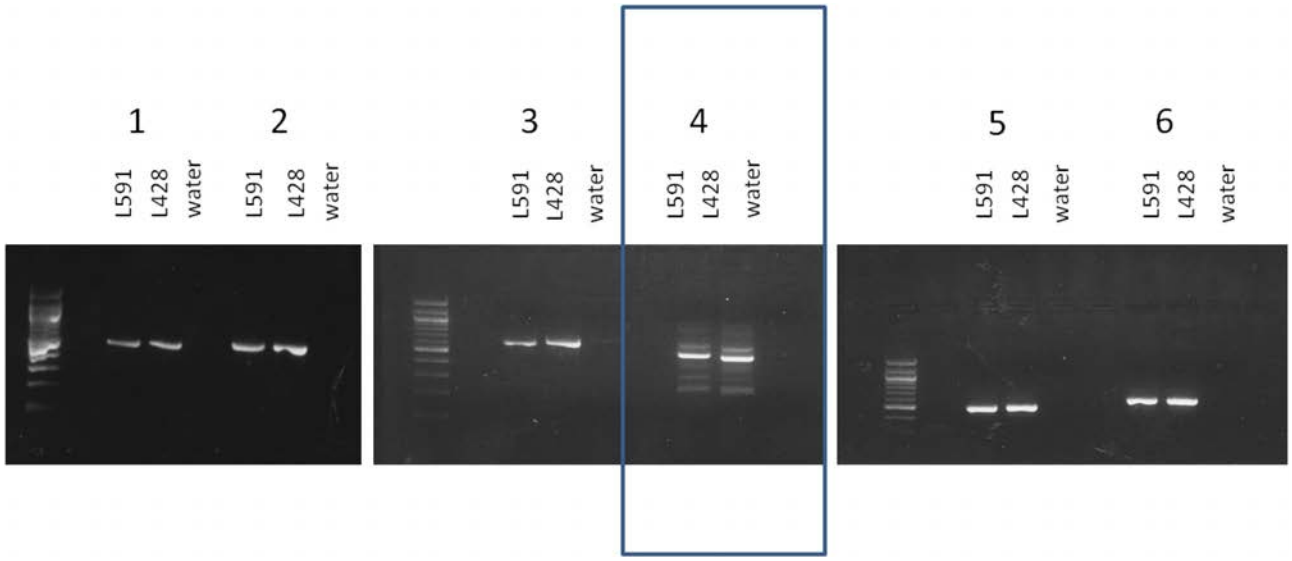

Figure 4.21 Reverse transcriptase PCR of 6 primer pairs spanning DDR1. cDNA was synthesised and amplified from L428 and L591 cell lines **A)** A single PCR product was detected for primer pairs 1, 2, 3, 5 and 6. Multiple products were detected after amplification with primer pair 4 which spans exon 10 and exon 13. No bands were seen in the water control.

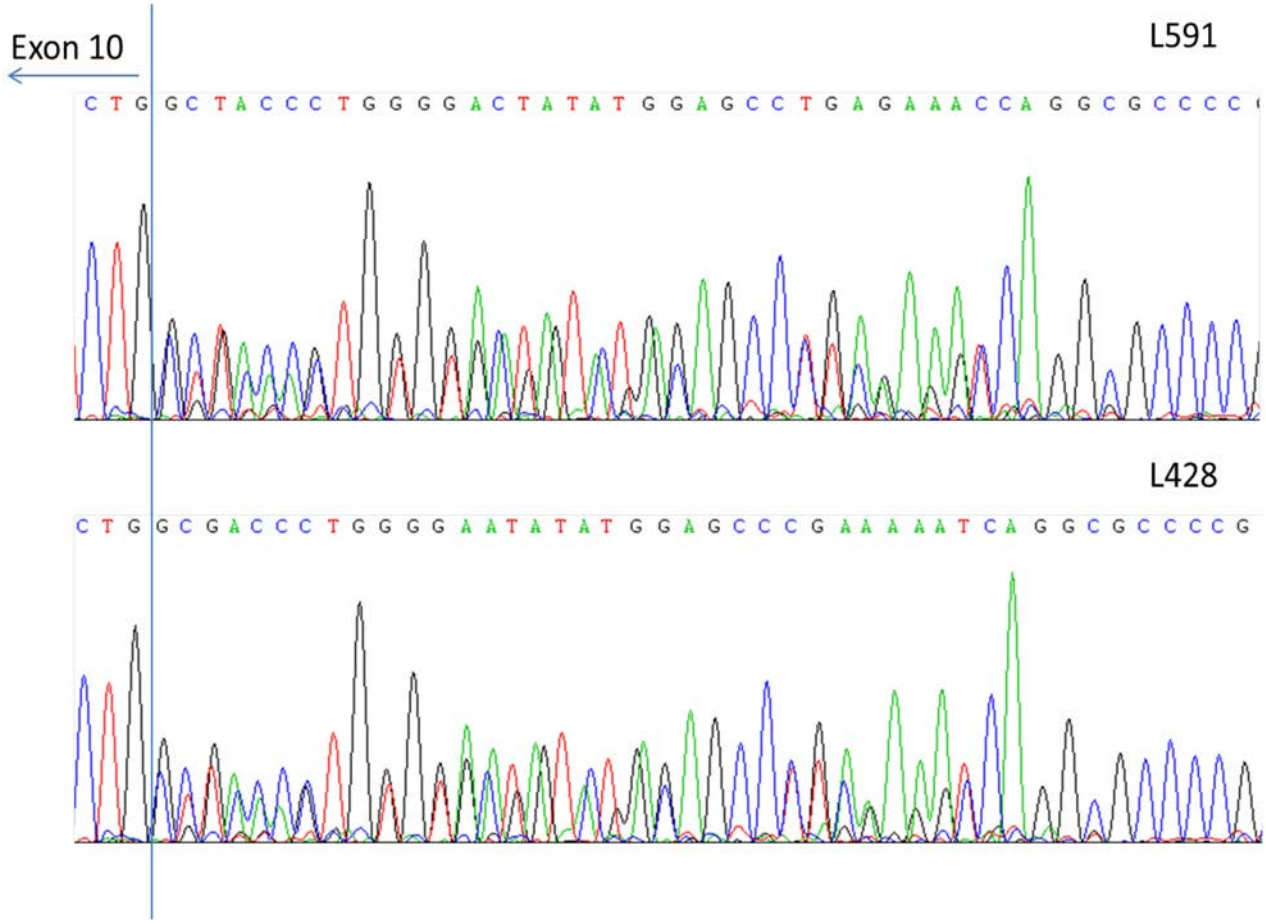

Figure 4.22 Sequence analysis of a part of the juxatamembrane region of DDR1 in L591 and L428 cells. There are no mutations in the exon sequence but there is an overlapping sequence after exon 10. BLAST analysis shows that in this region, exon 11 is absent and the overlapping sequence consists of exon10 followed by exon 12. This is consistent with the presence of DDR1a which has exon 11 spliced out. In the second sequence exons 11 and 12 have been spliced out which might represent DDR1d.

The existence of DDR1a is supported by the detection of the 126kDa protein by immunoblotting. However, because DDR1d lacks the C-terminus it cannot be recognised by the antibody used in immunoblotting. DDR1e retains the C-terminus and has exons 11 and 12 spliced out but has an additional deletion of the first part of exon 10. I did not observe this deletion in either cell line. The absence of DDR1e in HL cell lines is further supported by the failure to detect a protein at the predicted weight of 95kDa.

Sequencing of the PCR products obtained after amplification with primer pair 4 yielded two sequences consistent with the presence of DDR1a and DDR1d. However, it is clear from Figure 4.21 that there are multiple minor products which may have been masked by these more abundant isoforms. Therefore, to identify potentially novel alternative splice variants encompassing the entire juxtamembrane, I designed a new pair of primers which amplified this region. I performed PCR using these primers on both L428 and L591 cells. Bands were extracted, purified and sequenced. The strongest band generated a sequence corresponding to DDR1a. A weaker band gave a sequence consistent with DDR1b and a third band a sequence consistent with DDR1d (the sequence data is not shown here as they represent well established isoforms). Sequence analysis of four additional bands identified novel transcripts. These sequences were subjected to ExPASy translate software to determine if they might be translated to produce functional proteins. Figure 4.23 shows the predicted amino acid sequence of these four novel transcripts which are aligned to the amino acid sequence of DDR1c, the longest isoform. Transcript 1 has similarities to DDR1d because it lacks exon 11 and is truncated at the same position in exon 13 but unlike DDR1d it retains a part of exon 12. The three other transcripts shown in Figure 4.23 are characterised by a shift

in the open reading frame resulting in a different amino acid sequence to that of DDR1c. Furthermore, they display variable losses between exon 11 and exon 14.

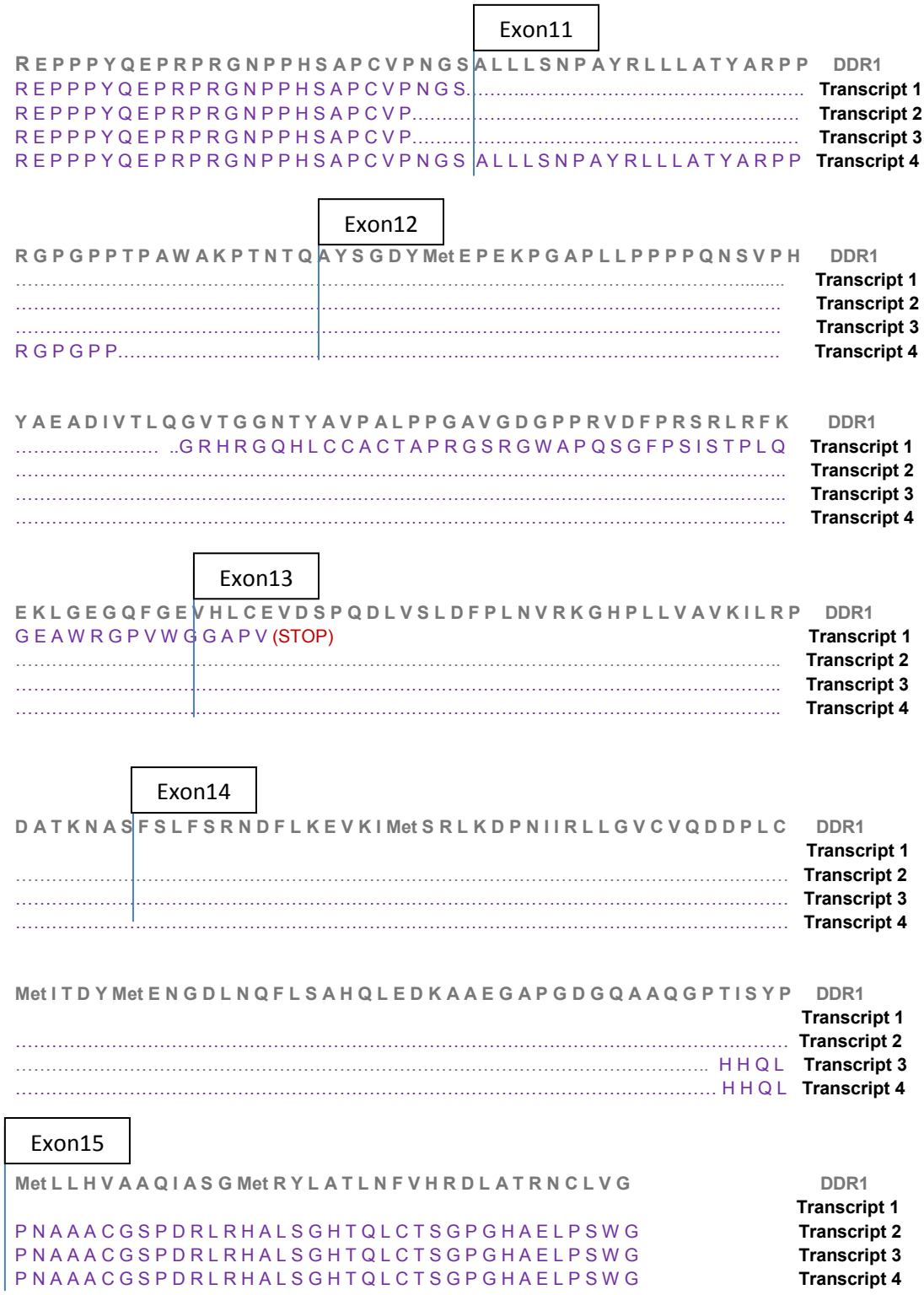

Figure 4.23 Amino acid sequences of DDR1 isoforms. The amino acid sequence of DDR1c (the longest transcript) is shown in the top row followed by 4 novel transcripts. Transcript 1 has a deletion of exon 11 and part of exon 12 resulting in a shift in the reading frame and a stop codon. Transcripts 2-4 have variable segments spliced out and a shift in reading frame.

4.3 Discussion

In this chapter I have shown for the first time that DDR1 is over-expressed in primary HRS cells. Furthermore, I have shown that in many cases, DDR1-expressing HRS cells are intimately associated with collagen, the ligand for DDR1.

Although these observations suggest that DDR1 is likely to be activated in primary HRS cells, this could not be confirmed because antibodies capable of detecting the phosphorylated forms of DDR1 are not available. However, I was able to study the activation of DDR1 in HL cell lines following the addition of soluble type I collagen. To do this I used a method in which DDR1 is immunoprecipitated and then immunoblotted using a pan-phosphorylated tyrosine antibody. Using this assay I observed that the phosphorylation of DDR1 in the L428 HL cell line was independent of collagen and of serum, suggesting that DDR1 is constitutively activated in these cells. In contrast, the phosphorylation of DDR1 in L591 cells required both the addition of collagen and of serum. This latter observation is consistent with a previous study which showed that in some cell lines, the addition of collagen is not sufficient to induce DDR1 phosphorylation in the absence of serum[(267)]. The failure to induce DDR1 phosphorylation in the absence of serum suggests that an additional co-factor is required. The identity of this co-factor in L591 cells is not known. However, it has been shown that the activation of DDR1 by collagen in MCF7 breast cancer cells requires Wnt5a [(335)]. The requirement of additional co-factors for the activation of RTKs is not unique to DDR1. For example, the activation of the FGFR family requires the binding of heparin to both ligand and receptor. Alternatively, the activation of DDR1 might require the phosphorylation of an associated molecule, for instance src phosphorylation has been shown to be essential for DDR2 activation[(336)].

Very little is known about the mechanisms which contribute to the over-expression of DDR1 in cancer cells. I considered the possibility that DDR1 expression might be influenced by the presence of EBV in HRS cells. I showed that DDR1 is up-regulated following the ectopic expression of LMP1 in GC B cells, suggesting that this viral oncogene contributes to the over-expression of DDR1 in EBV-positive cases. Although I did not find an association between DDR1 expression and the presence of EBV in the cases I examined, this could be explained by the existence of an alternative mechanism which can up-regulate DDR1 in EBV-negative cases.

The expression of LMP1 in primary human GC B cells has previously been reported to recapitulate up-to one-quarter of the transcriptional changes characteristic of HRS cells[172]. For this reason, this model would be appear to be a useful system for the detection of LMP1 induced transcriptional changes relevant to the pathogenesis of HL. Indeed, the up-regulation of DDR1 by LMP1 in GC B cells might constitute a pathogenic event. However, an alternative explanation is that the up-regulation of DDR1 merely reflects the ability of LMP1 to drive post GC B cell differentiation. This latter possibility was suggested by my observation that DDR1 expression is higher in memory B cells compared to centrocytes, and by the re-analysis of the published micro-array dataset referred to above which showed that when compared to centrocytes, DDR1 expression was higher in both memory cells and plasma cells[319].

Despite the complete silencing of a 126kDa DDR1 protein following the treatment of L428 cells with DDR1 specific siRNA, I failed to identify any significant changes in cell proliferation (metabolic activity) or apoptosis following this treatment. Furthermore, the knockdown of DDR1 in L428 cells did not change the expression or the activation of several known

downstream targets of DDR1, including STAT5 and STAT3[331;333]. Finally, a micro-array analysis of global gene expression following DRR1 knockdown in L428 cells revealed surprisingly few significantly changed genes. Although the array analysis provided confirmation of the successful knockdown of DDR1 in these experiments, it only revealed a modest decrease in DDR1 expression (less than two-fold) which was in the contrast to the ~5-fold down-regulation of DDR1 observed in the siRNA-treated cells by q-PCR analysis. Furthermore, comparison of DDR1 target genes with genes previously shown to be differentially expressed in the L428 cell line (compared to GC B cells), in LMP1-transfected GC B cells and in micro-dissected HRS cells, revealed no significant overlap[172].

DDR1a has been reported to be over-expressed in various cancers and to contribute to malignancy[278;337]. Therefore it was surprising that the knockdown of DDR1a in L428 cells did not result in an obvious phenotype. I now discuss potential explanations for this observation.

Redundancy of DDR1 expression

As individual RTK have been shown to converge on the same signalling pathways, it follows that the knockdown of a single RTK might alone be insufficient to disrupt a cell signalling pathway and reveal a change in cellular phenotype. Therefore, one possible explanation for my results is that the functions of DDR1 can be replaced by other molecules. While I considered the possibility that DDR1 might activate STAT5 in HL cells, other mechanisms have been shown to contribute to the aberrant activation of STAT5 in these cells. For instance amplification of *JAK2* gene or mutation in SOCS1 leads to an accumulation of STAT5 in a proportion of HL cases[126;338].

Loss of dependency on DDR1 in HL cell lines

The use of cell lines as models to explore the function of a receptor that may require complex signals from the microenvironment for its activation is open to question. This is particularly relevant in the case of HL cell lines which by their very nature no longer require signals from the microenvironment for their survival. It follows that such cells are likely to have acquired additional aberrations which enable cell growth in the absence of growth promoting stimuli from the microenvironment.

Phosphorylation of DDR1 is alone insufficient for receptor activation

The decision to use L428 cells to investigate the phenotypic consequences of DDR1 activation was based upon the observation that DDR1 was constitutively phosphorylated in this cell line. However, it is not known if the constitutive phosphorylation of DDR1 I observed in this cell line was sufficient for its activation. This was further compounded by the inability of the IP methodology to localise the phosphorylation to specific residues in DDR1, some, but not all, of which have been shown to be important for the activation of downstream signals.

Presence of alternative DDR1 isoforms not targeted by the siRNA

Immunoblotting showed that only a protein at 126kDa corresponding predominantly to DDR1a was abolished following siRNA treatment. Two major bands, one at ~86kDa and the other at 63kDa, were unaffected by siRNA treatment. Although I have not confirmed their identity, these bands were also detectable following immunoprecipitation and blotting with DDR1 antibody. Furthermore, both bands were detectable following the blotting of these immunoprecipitates with a pan-tyrosine antibody, suggesting these proteins are

phosphorylated. Therefore one explanation for the lack of a phenotype in siRNA treated cells is the existence of additional isoforms which might substitute for the functions of DDR1a.

To investigate the existence of additional isoforms I sequenced DDR1 cDNA. I showed that the predominant isoform present in both L428 and L591 cells is DDR1a. I also found DDR1d and substantially lower levels of DDR1b in HL cells but I did not detect DDR1c or DDR1e. However, the expression of DDR1d cannot account for the additional bands observed on immunoblotting since the region detected by the antibody is not present in this isoform. I also identified numerous novel transcripts of DDR1 several of which are predicted to produce truncated proteins one of which shared similarities to DDR1d. The functional significance of the expression of the known and novel isoforms of DDR1 in HL cells is currently unknown.

CHAPTER 5

RTKs as therapeutic targets in Hodgkin's lymphoma

5.1 Introduction

Many RTKs are targets of new generation small molecule RTK inhibitors, several of which are already in clinical use[339]. Some of these agents are highly effective forms of therapy for patients with tumours with activated RTKs, for example imatinib for BCR-ABL-positive chronic myeloid leukaemia and FLT3 inhibitors (e.g. PKC412) for acute myeloid leukaemia[339;340]. To-date, RTKs have not been used to treat paediatric HL because a detailed knowledge of the expression and activation status of RTKs in HL is lacking. However, in the preceding chapters I have shown that several RTKs are constitutively activated in HL, these included DDR1 which has recently been described as a major additional target of the RTK inhibitors, imatinib, dasatinib and nilotinib[295;341].

The objectives of this study are to:

- Evaluate the effect of imatinib, dasatinib and nilotinib on the proliferation of HL derived cell lines.
- Investigate the influence of next generation TK inhibitors lestaurtinib, dovitinib and vargatef on the proliferation of HL derived cell lines.

5.2 Results

5.2.1 Optimisation of cytotoxicity assays

To screen for potential cytotoxic effects of RTK inhibitors in HL cells I used a commercially available 'proliferation assay' (Promega), which measures the metabolic activity of cells (methods section 2.9.1 page 84). I first optimised this assay on K562 cells, a myeloid cell line, the proliferation of which has been shown to be inhibited by dasatinib at nanomolar concentrations[342]. Figure 5.1 shows that as little as 62nM of dasatinib reduced the proliferation of K562 cells to the same degree as the positive control, staurosporine.

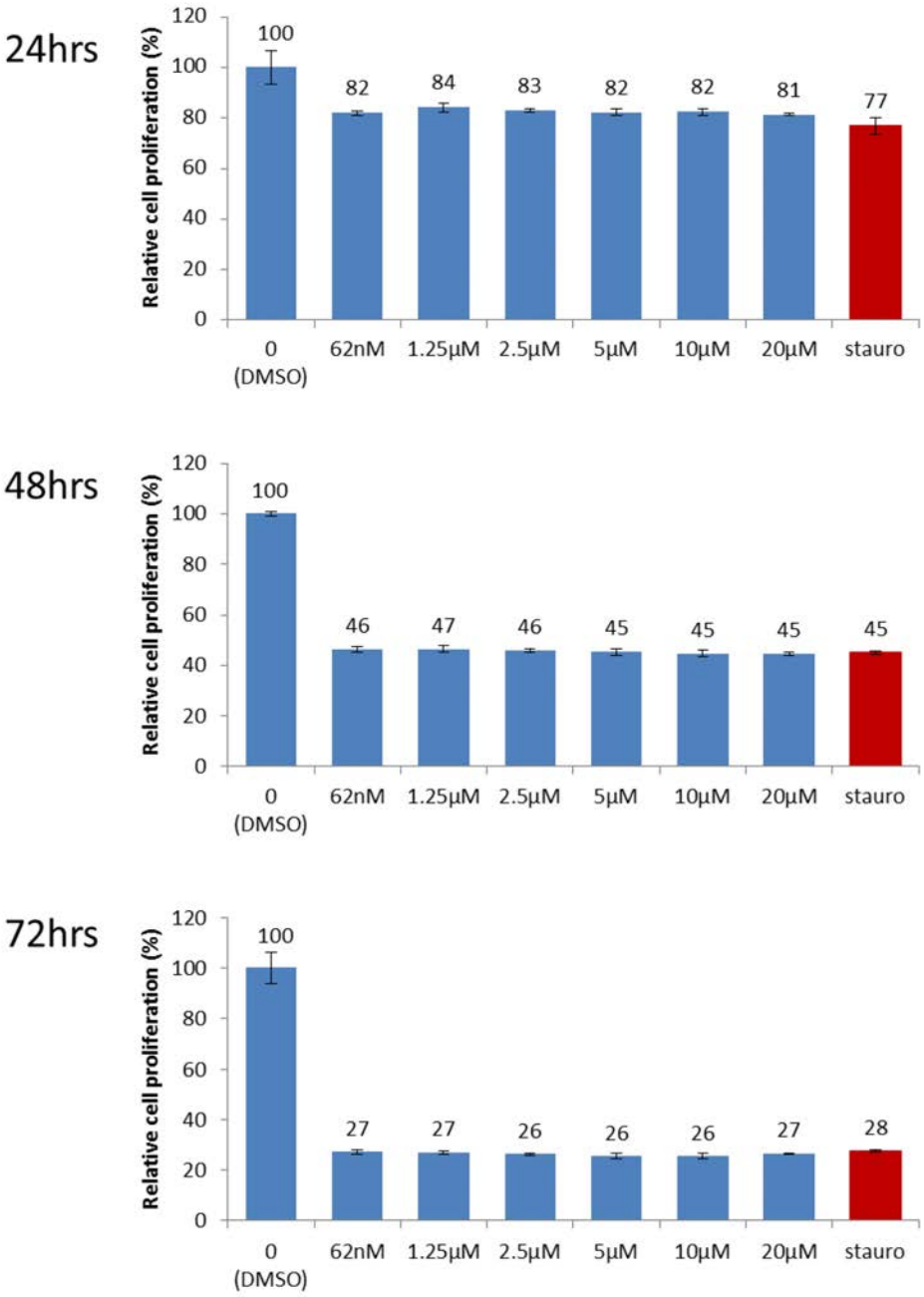

Figure 5.1 Proliferation of K562 cells treated with increasing concentration of dasatinib. K562 cells were maintained in normal growth conditions then re-suspended in fresh media containing 10% serum 24hrs prior to drug treatment. Cells were treated with increasing concentrations of dasatinib for the times indicated. Promega proliferation reagent was added at 22, 46 and 70hrs respectively and 2hrs later absorbance at 490nm was read to measure metabolic activity. Cell proliferation was calculated relative to vehicle (DMSO) only control cells. K562 cells treated with staurosporine served as a positive control. Shown are data from one of two independent experiments.

5.2.2 Effect of imatinib, dasatinib and nilotinib on the proliferation of HL cell lines

Having optimized the cytotoxicity assays, I tested the influence of imatinib, dasatinib and nilotinib on five HL cell lines; L428, L591, L1236, L540 and KMH2. I chose two drug concentrations, 5µM and 10µM.

Figure 5.2 shows representative results of cell proliferation assays on the HL cell lines following treatment with RTK inhibitors. All experiments were performed in triplicate in normal growth conditions with 10% serum. The error bars indicate analysis of quadruplicate wells for a single experiment. With the exception of a modest effect in L540 cells (Figure 5.2d), I found little or no inhibition of proliferation following the treatment of a panel of HL cell lines with imatinib. Similarly, the treatment of HL cells with nilotinib induced modest or inhibition of the proliferation of these cell lines. In contrast, all five cell lines showed a decrease in cell proliferation following treatment with dasatinib, with a maximum inhibition at 72hours in L428, L1236 and L540 cells treated with 10µM dasatinib.

I also performed immunoblotting for PARP cleavage as a measure of apoptosis following the treatment of L428 and L591 cells with these drugs. Figure 5.3 shows that compared to controls, 10µM of dasatinib increased PARP cleavage in both L428 and L591 cells. Cells treated with imatinib also showed a marginal increase in PARP cleavage, whilst treatment of cells with nilotinib resulted in PARP cleavage comparable to vehicle only control.

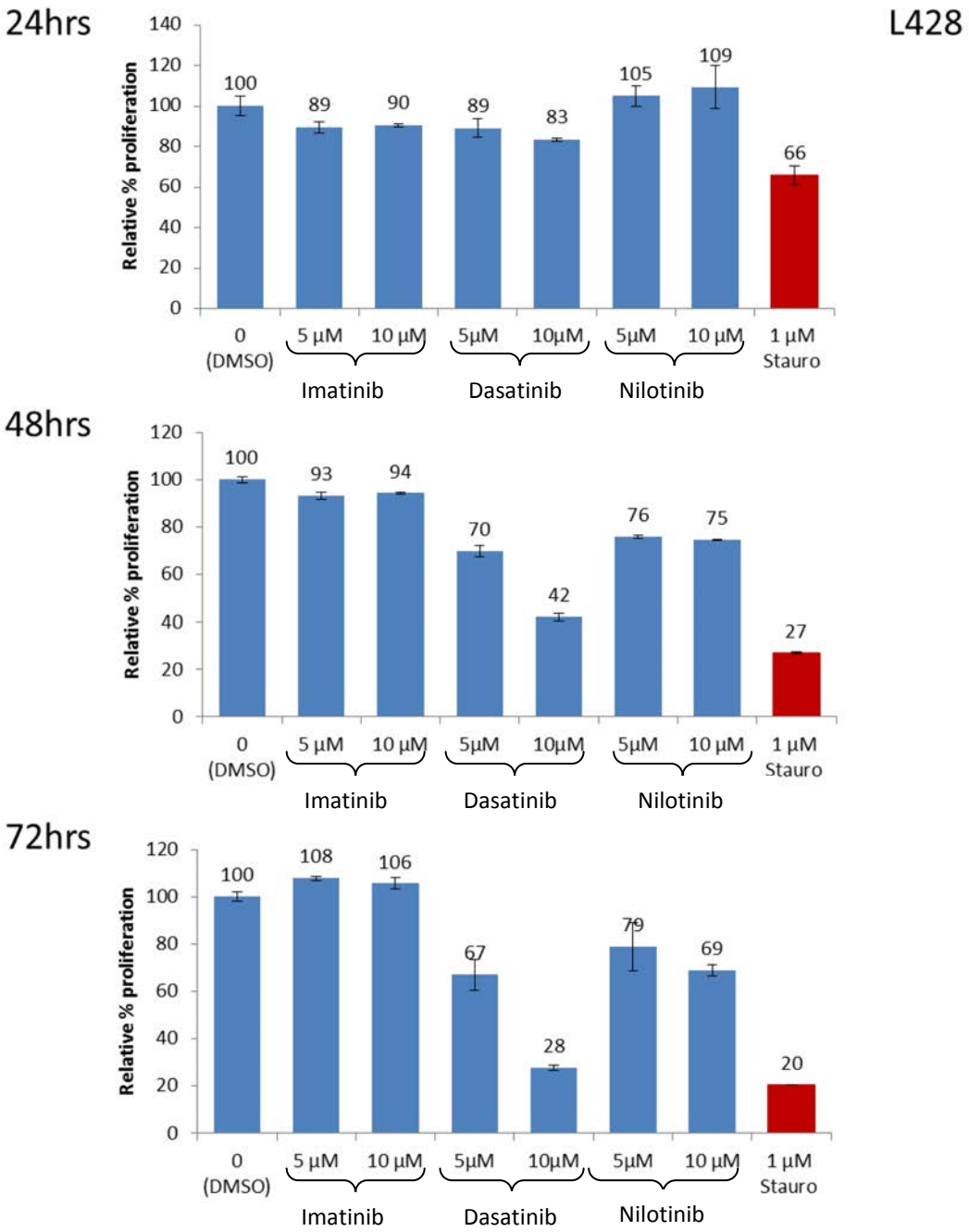

Figure 5.2 Cell proliferation in HL cell lines treated with RTK inhibitors. Cells were maintained in normal growth conditions then re-suspended in fresh media containing 10% serum 24hrs prior to drug treatment. Cells were treated with RTK inhibitors at the concentration and times indicated. Promega proliferation reagent was added at 22, 46 and 70hrs respectively and 2hrs later absorbance at 490nm was read to measure metabolic activity. Cell proliferation was calculated relative to DMSO only control cells. Each cell line was also treated with staurosporine which served as a positive control.

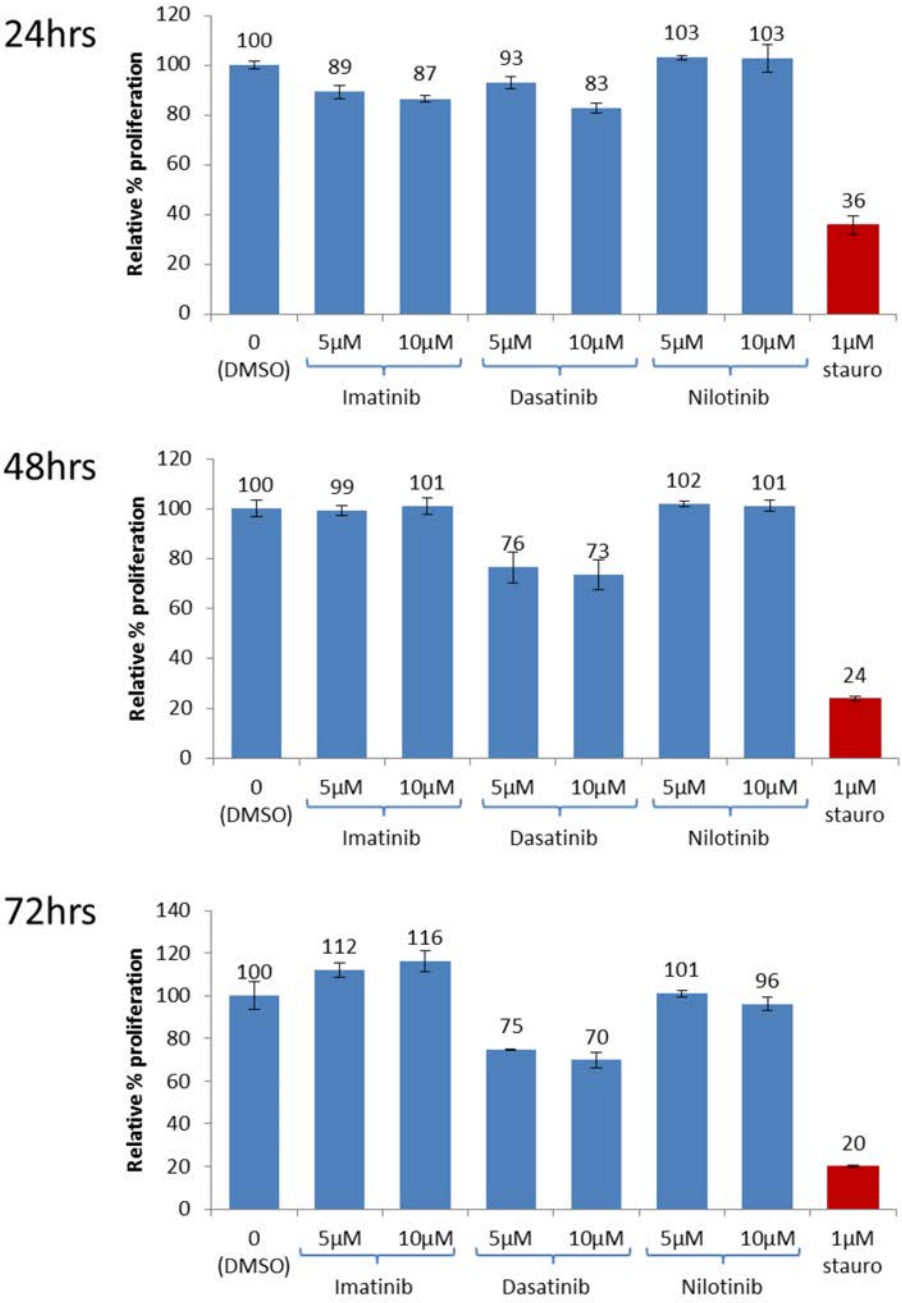
24hrs
L591
Relative % proliferation
120
100
80
60
40
20
0
100
89
87
93
83
103
103
36
0 (DMSO)
5μM
10μM
5μM
10μM
5μM
10μM
1μM stauro
Imatinib
Dasatinib
Nilotinib
48hrs
Relative % proliferation
100
99
101
76
73
102
101
24
0 (DMSO)
5μM
10μM
5μM
10μM
5μM
10μM
1μM stauro
Imatinib
Dasatinib
Nilotinib
72hrs
Relative % proliferation
140
120
100
80
60
40
20
0
100
112
116
75
70
101
96
20
0 (DMSO)
5μM
10μM
5μM
10μM
5μM
10μM
1μM stauro
Imatinib
Dasatinib
Nilotinib

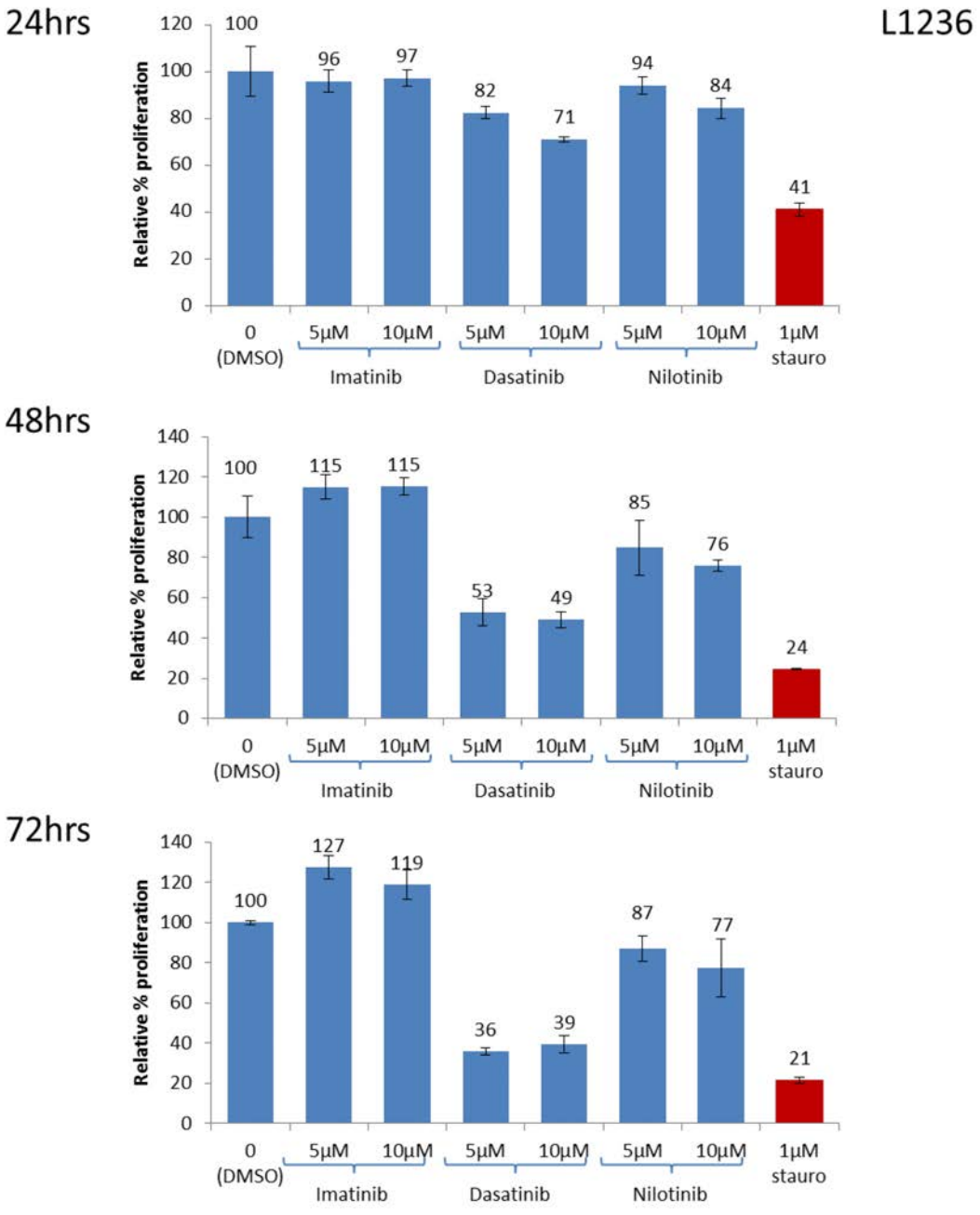
24hrs
L1236
Relative % proliferation
120
100
80
60
40
20
0
100
96
97
82
71
94
84
41
0 (DMSO)
5µM
10µM
5µM
10µM
5µM
10µM
1µM stauro
Imatinib
Dasatinib
Nilotinib
48hrs
Relative % proliferation
140
120
100
80
60
40
20
0
100
115
115
53
49
85
76
24
0 (DMSO)
5µM
10µM
5µM
10µM
5µM
10µM
1µM stauro
Imatinib
Dasatinib
Nilotinib
72hrs
Relative % proliferation
140
120
100
80
60
40
20
0
100
127
119
36
39
87
77
21
0 (DMSO)
5µM
10µM
5µM
10µM
5µM
10µM
1µM stauro
Imatinib
Dasatinib
Nilotinib

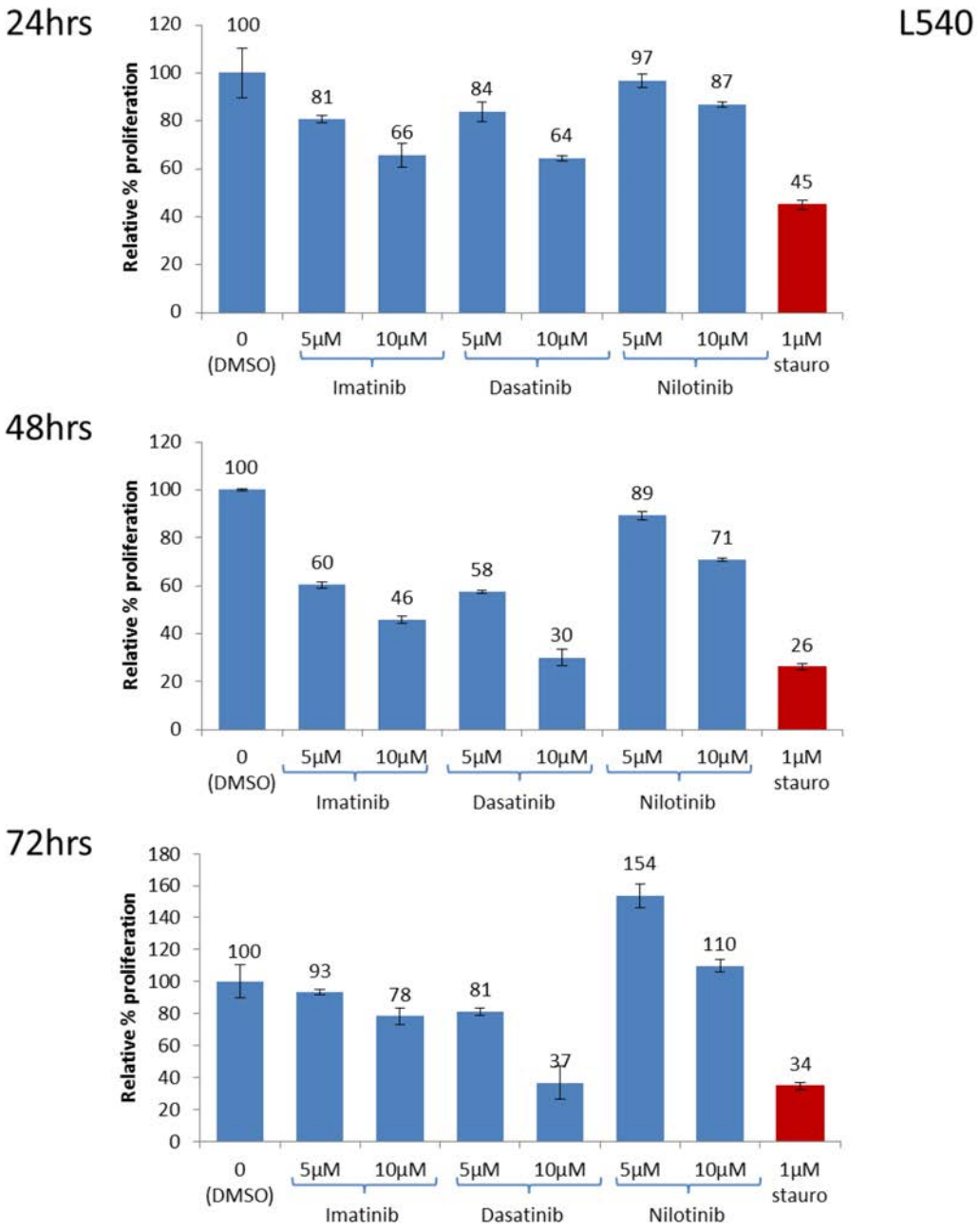
24hrs
L540
Relative % proliferation
120
100
80
60
40
20
0
100
81
66
84
64
97
87
45
0 (DMSO)
5μM
10μM
5μM
10μM
5μM
10μM
1μM stauro
Imatinib
Dasatinib
Nilotinib
48hrs
Relative % proliferation
120
100
80
60
40
20
0
100
60
46
58
30
89
71
26
0 (DMSO)
5μM
10μM
5μM
10μM
5μM
10μM
1μM stauro
Imatinib
Dasatinib
Nilotinib
72hrs
Relative % proliferation
180
160
140
120
100
80
60
40
20
0
100
93
78
81
37
154
110
34
0 (DMSO)
5μM
10μM
5μM
10μM
5μM
10μM
1μM stauro
Imatinib
Dasatinib
Nilotinib

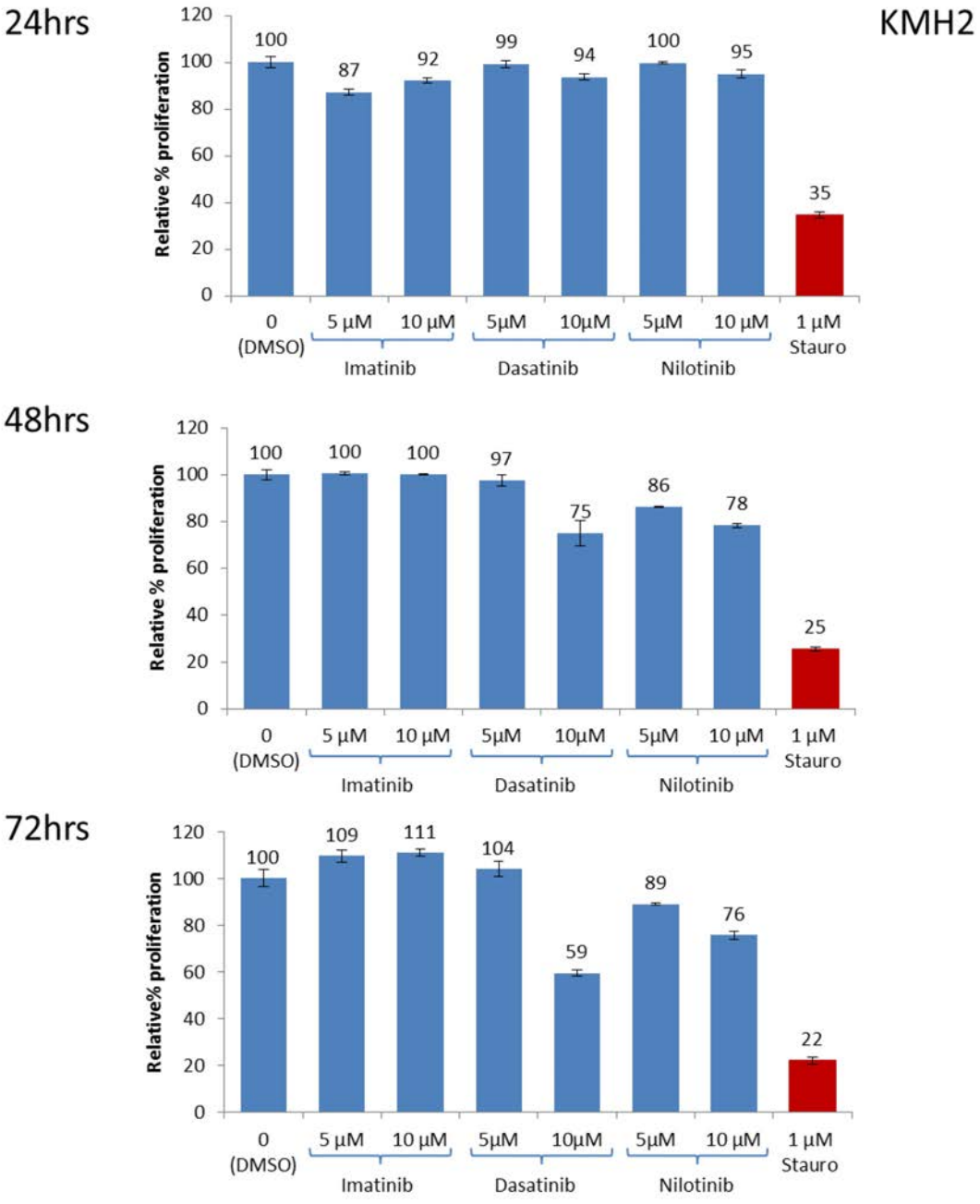
24hrs
KMH2
Relative % proliferation
120
100
80
60
40
20
0
100
87
92
99
94
100
95
35
0 (DMSO)
5 µM
10 µM
5µM
10µM
5µM
10 µM
1 µM Stauro
Imatinib
Dasatinib
Nilotinib
48hrs
Relative % proliferation
100
100
100
97
75
86
78
25
0 (DMSO)
5 µM
10 µM
5µM
10µM
5µM
10 µM
1 µM Stauro
Imatinib
Dasatinib
Nilotinib
72hrs
Relative% proliferation
100
109
111
104
59
89
76
22
0 (DMSO)
5 µM
10 µM
5µM
10µM
5µM
10 µM
1 µM Stauro
Imatinib
Dasatinib
Nilotinib

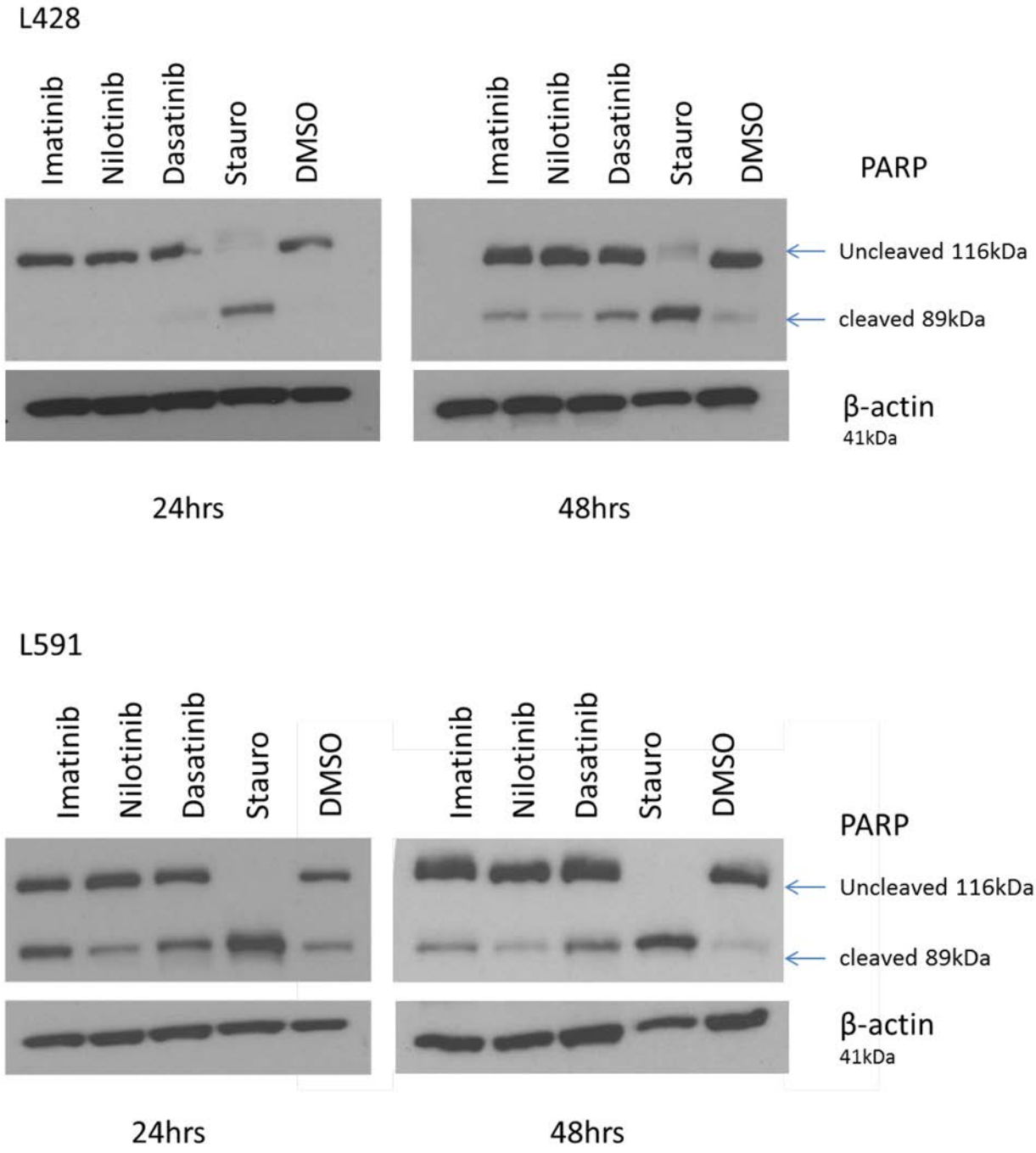

Figure 5.3 Detection of cleaved PARP following treatment with RTK inhibitors. Cells were maintained in media containing 10% serum and re-suspended in fresh media 24hrs prior to drug treatment. Cells were treated with 10µM imatinib, 10µm nilotinib or 10µM dasatinib and harvested at the time points indicated. 30µg of protein from whole cell lysate was loaded and immunoblotted for PARP cleavage. Equal loading was confirmed using an antibody to β-actin.

5.2.3 Effect of next generation RTK inhibitors on cell proliferation in HL cell lines

In the preceding experiments, I observed that HL cell lines were more sensitive to dasatinib than to either imatininb or nilotinib. This is of interest because although dasatinib was originally designed to target BCR-ABL it has since been shown to have a broader range of activity against RTKs[295]. Given that I have shown that HRS cells display aberrant activation of multiple RTKs, I investigated the effect of a further three RTK inhibitors, lestaurtinib (CEP-701), dovitinib (CHIR-258) and vargatef (BIBF-1120), which were developed to target multiple RTKs[343-345].

I treated the same five HL derived cell lines: L428, L591, L1236, L540 and KMH2 with each of the three drugs at two different concentrations (1 µM and 10 µM). I measured cell proliferation of drug treated cells relative to control cells at 24 hours and 48 hours. All experiments were repeated twice and the error bars indicate variation between triplicate wells of a single experiment. Vargatef appeared to be inactive against these cell lines at the concentration and time points tested. I observed a dose-dependent reduction in cell proliferation relative to control cells in all five HL cell lines tested with two of the RTK inhibitors, lestaurtinib and dovitinib. For both drugs the level of inhibition at 10 µM, which increased over two days, ranged from a 50% reduction to a 75% reduction in cell proliferation compared to control (Figure 5.4).

To explore the dose-response further, I repeated the cell proliferation assays, using a wider range of drug concentrations. I focused on three cell lines; L428, L591 and L1236 and extended the drug treatment to three days. Figures 5.5 and 5.6 shows confirmation of my previous observation, that both drugs were potent inhibitors of the proliferation of HL cell

lines. However, I observed while lestaurtinib remained active at much lower concentrations, the effect of dovitinib was less effective below a concentration of 10µM.

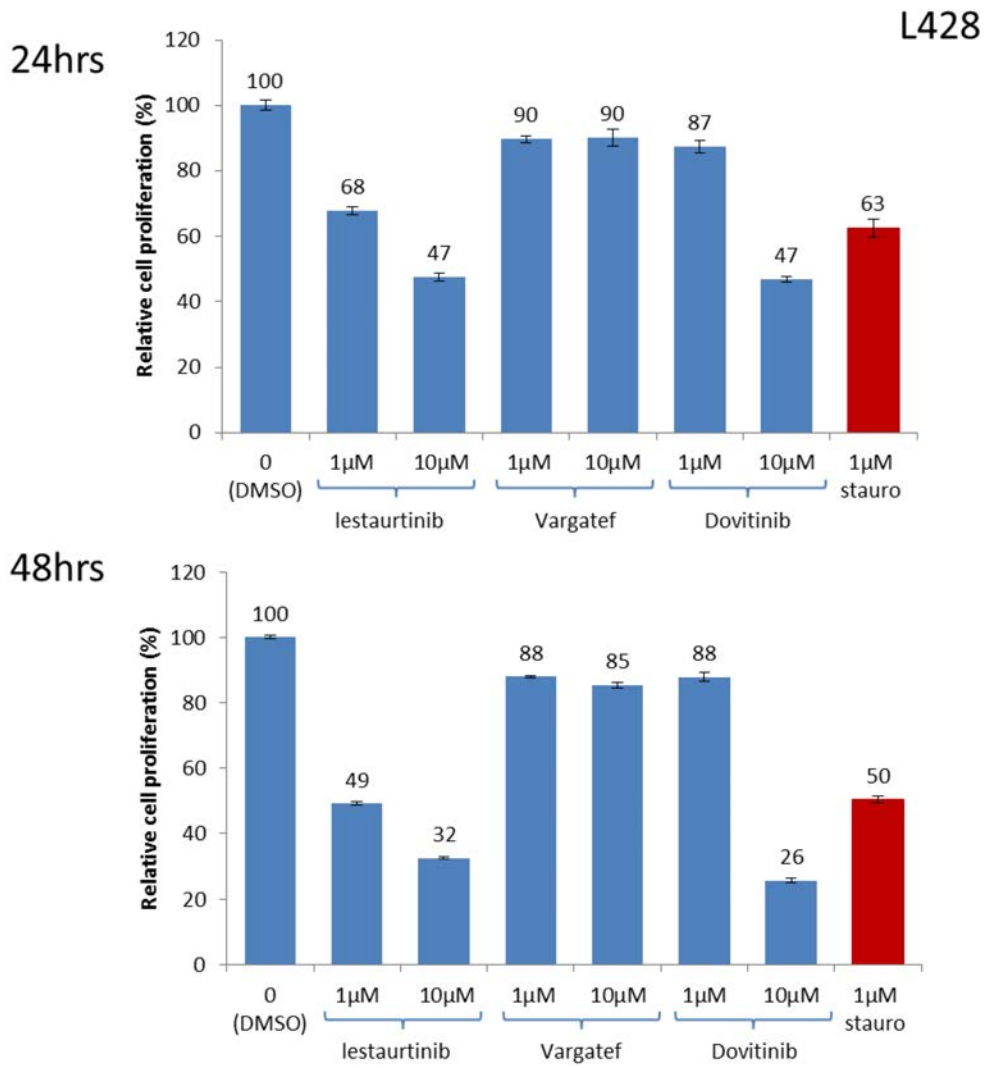

Figure 5.4 Cell proliferation in HL cell lines treated with RTK inhibitors. Cells were maintained in normal growth conditions then re-suspended in fresh media containing 10% serum 24hrs prior to drug treatment. Cells were treated with RTK inhibitors at the concentration and times indicated. Promega proliferation reagent was added at 22 and 46hrs respectively and 2hrs later absorbance at 490nm was read to measure metabolic activity. Cell proliferation was calculated relative to DMSO only control cells. Each cell line was also treated with staurosporine which served as a positive control for that respective experiment.

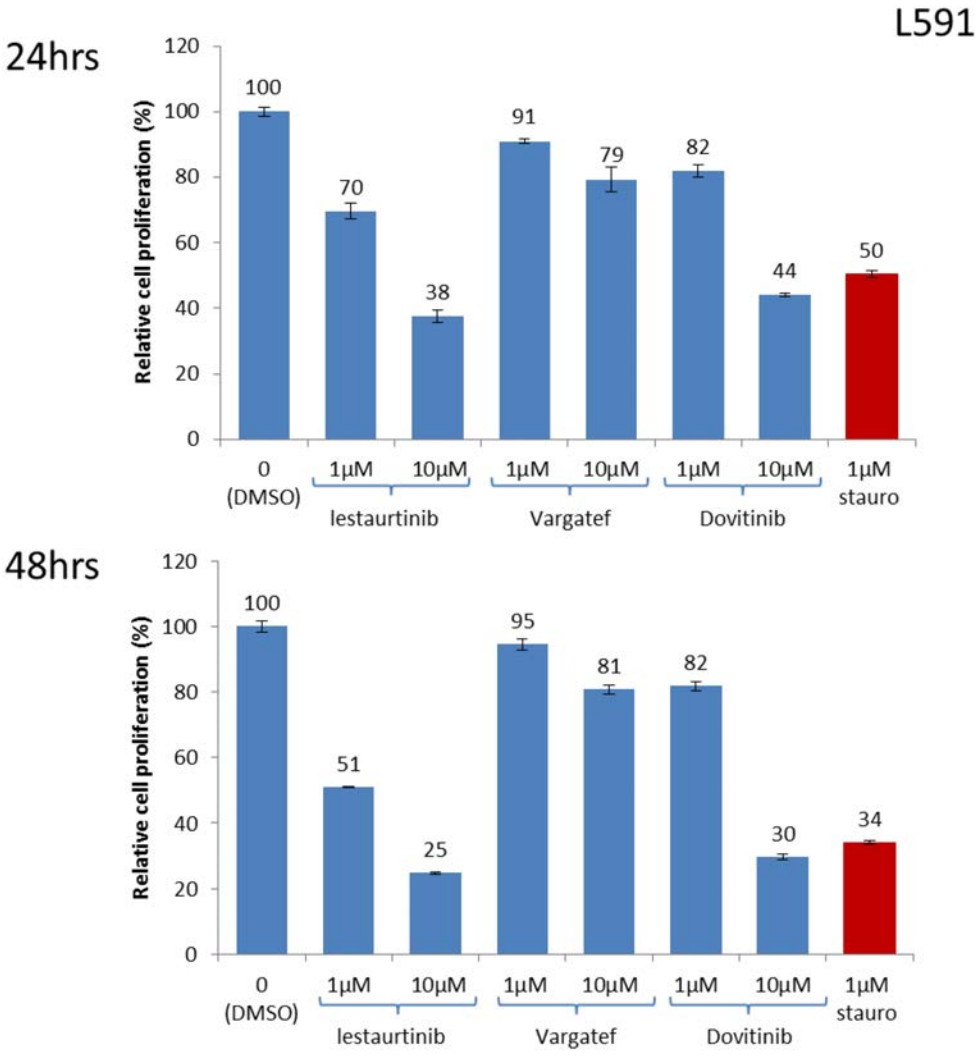
L591
24hrs
Relative cell proliferation (%)
120
100
80
60
40
20
0
100
70
38
91
79
82
44
50
0 (DMSO)
1µM
10µM
1µM
10µM
1µM
10µM
1µM stauro
lestaurtinib
Vargatef
Dovitinib
48hrs
Relative cell proliferation (%)
120
100
80
60
40
20
0
100
51
25
95
81
82
30
34
0 (DMSO)
1µM
10µM
1µM
10µM
1µM
10µM
1µM stauro
lestaurtinib
Vargatef
Dovitinib

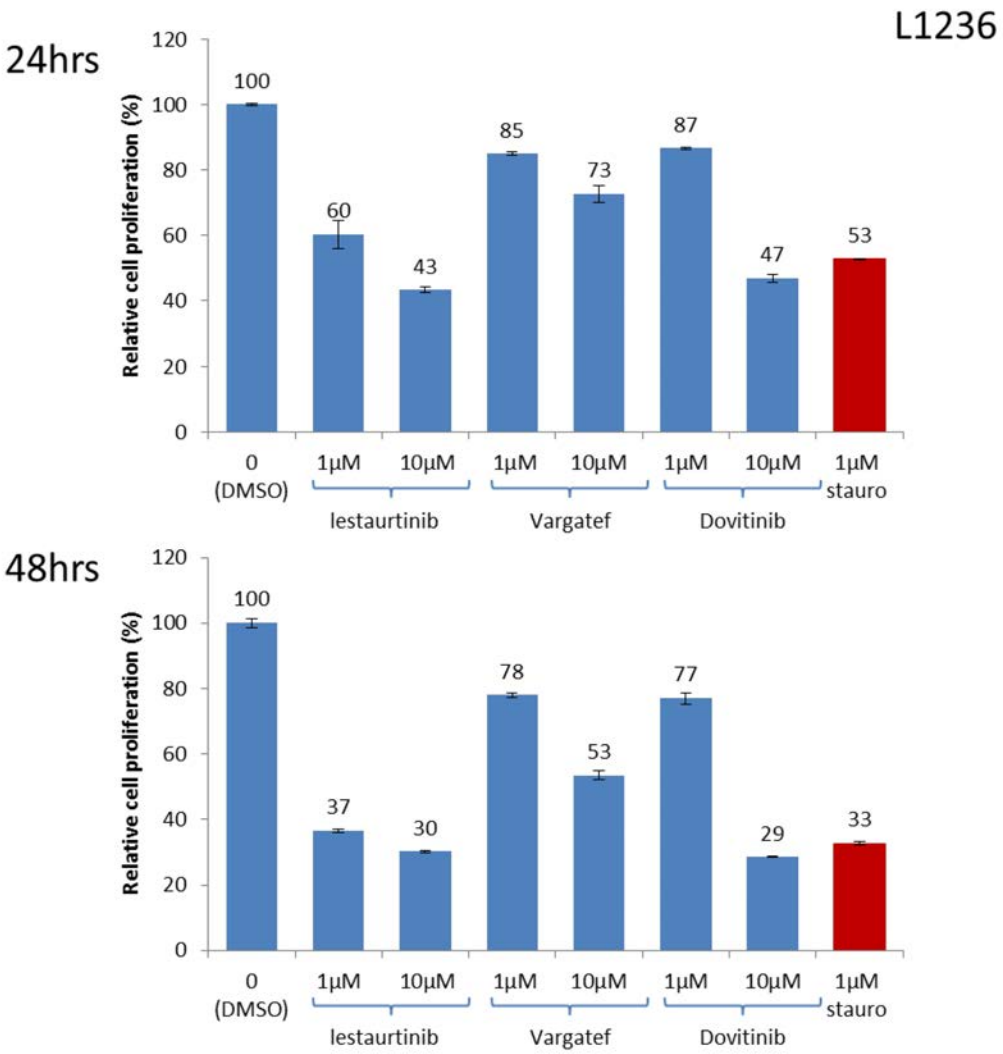
L1236
24hrs
Relative cell proliferation (%)
120
100
80
60
40
20
0
100
60
43
85
73
87
47
53
0 (DMSO)
1µM
10µM
1µM
10µM
1µM
10µM
1µM stauro
lestaurtinib
Vargatef
Dovitinib
48hrs
Relative cell proliferation (%)
120
100
80
60
40
20
0
100
37
30
78
53
77
29
33
0 (DMSO)
1µM
10µM
1µM
10µM
1µM
10µM
1µM stauro
lestaurtinib
Vargatef
Dovitinib

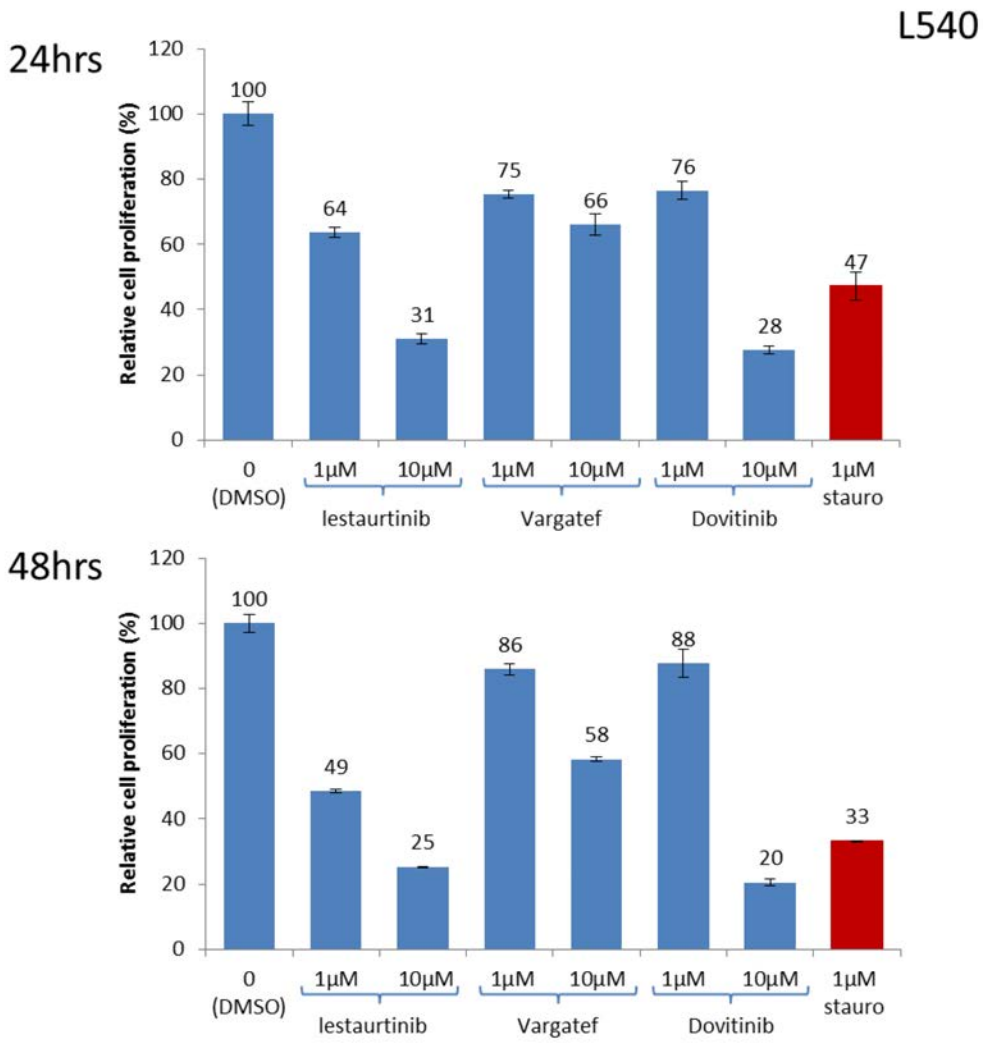
L540
24hrs
Relative cell proliferation (%)
120
100
80
60
40
20
0
100
64
31
75
66
76
28
47
0 (DMSO)
1μM
10μM
1μM
10μM
1μM
10μM
1μM stauro
lestaurtinib
Vargatef
Dovitinib
48hrs
Relative cell proliferation (%)
120
100
80
60
40
20
0
100
49
25
86
58
88
20
33
0 (DMSO)
1μM
10μM
1μM
10μM
1μM
10μM
1μM stauro
lestaurtinib
Vargatef
Dovitinib

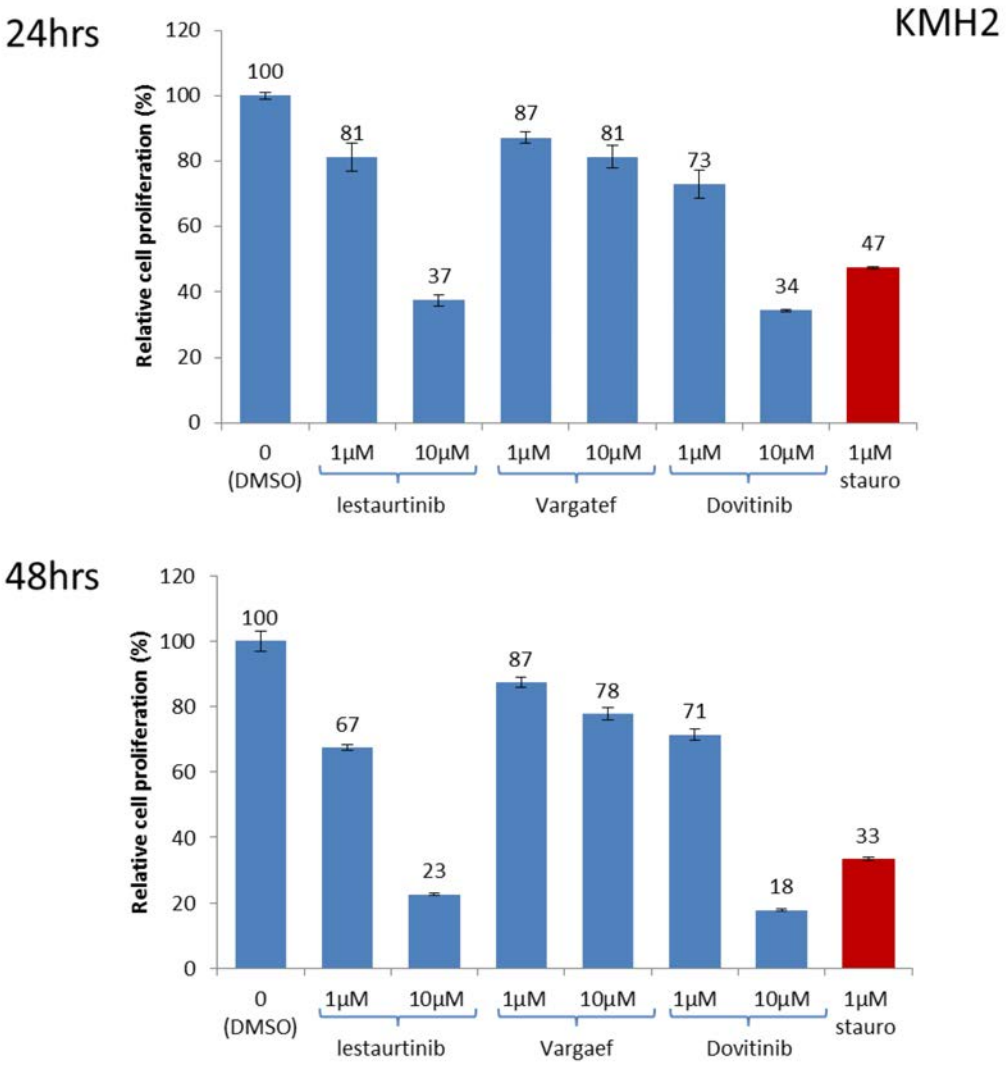
24hrs
KMH2
Relative cell proliferation (%)
120
100
80
60
40
20
0
100
81
37
87
81
73
34
47
0 (DMSO)
1µM
10µM
lestaurtinib
1µM
10µM
Vargatef
1µM
10µM
Dovitinib
1µM stauro
48hrs
Relative cell proliferation (%)
120
100
80
60
40
20
0
100
67
23
87
78
71
18
33
0 (DMSO)
1µM
10µM
lestaurtinib
1µM
10µM
Vargaef
1µM
10µM
Dovitinib
1µM stauro

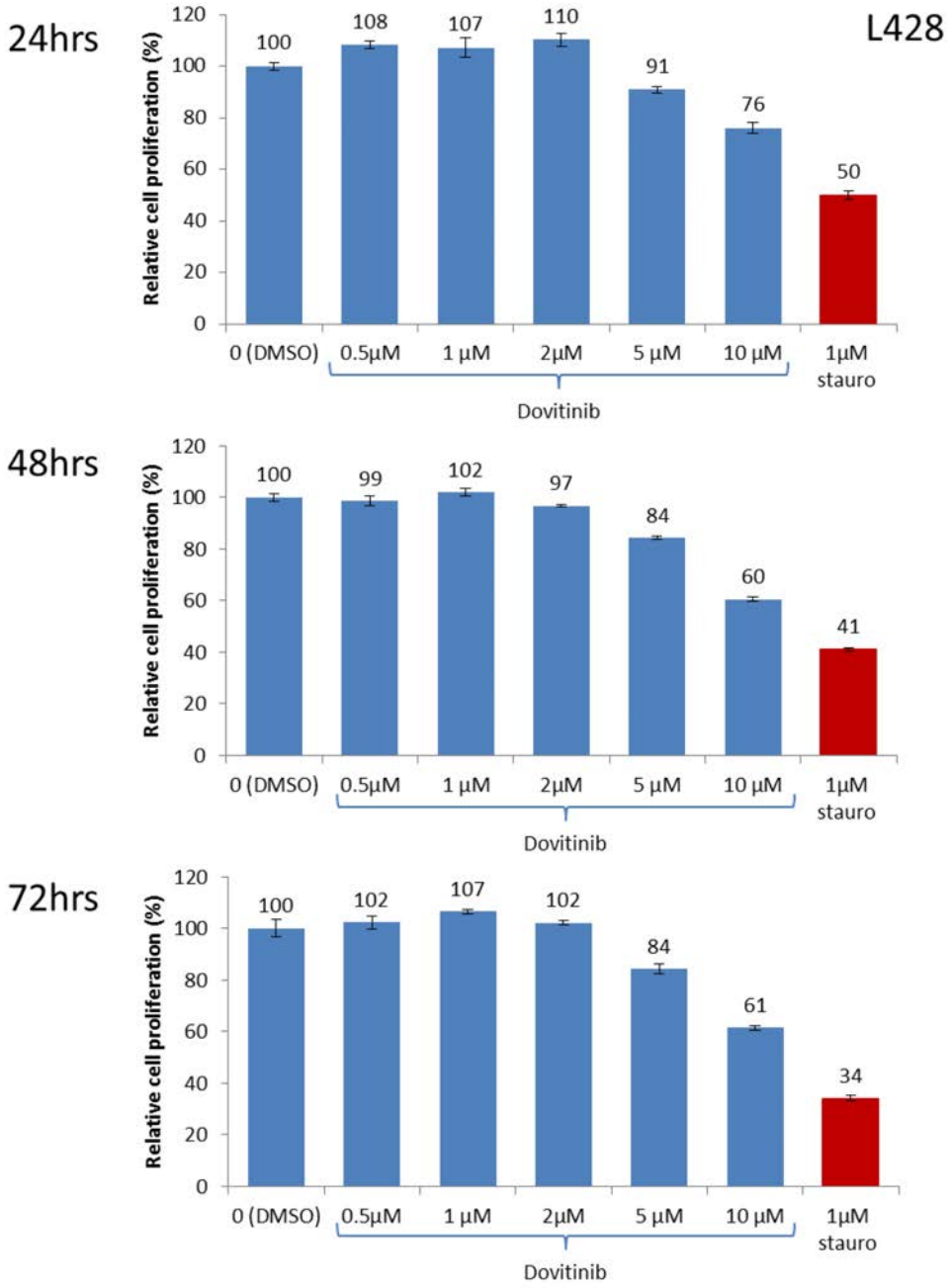

Figure 5.5 Cell proliferation in HL cell lines treated with dovitinib. Cells were maintained in normal growth conditions then re-suspended in fresh media containing 10% serum 24hrs prior to drug treatment. Cells were treated with dovitinib at the concentration and times indicated. Promega proliferation reagent was added at 22, 46 and 70hrs respectively and 2hrs later absorbance at 490nm was read to measure metabolic activity. Cell proliferation was calculated relative to DMSO only control cells. Each cell line was also treated with staurosporine which served as a positive control.

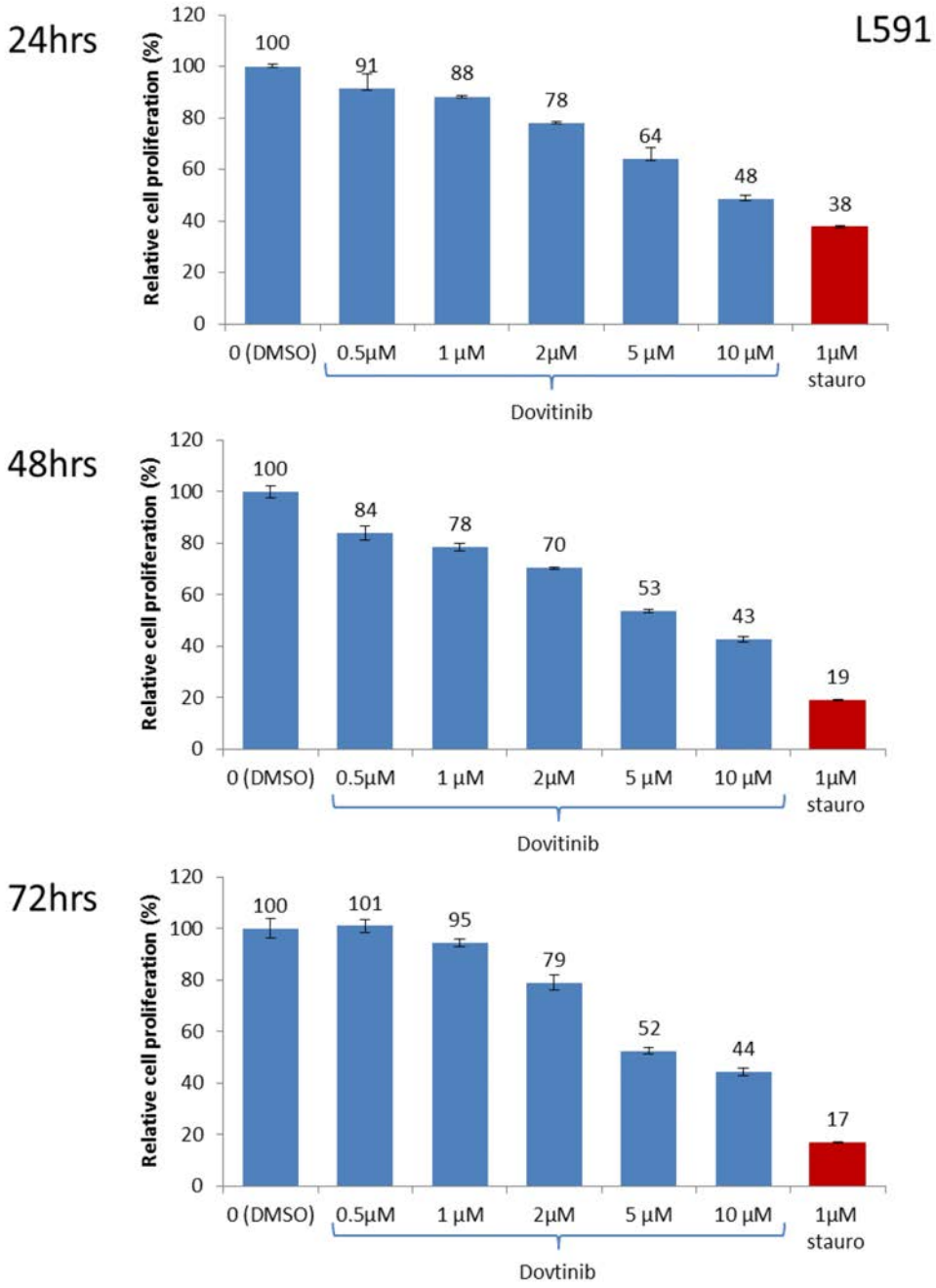
24hrs
L591
Relative cell proliferation (%)
120
100
80
60
40
20
0
100
91
88
78
64
48
38
0 (DMSO)
0.5µM
1 µM
2µM
5 µM
10 µM
1µM stauro
Dovitinib
48hrs
Relative cell proliferation (%)
100
84
78
70
53
43
19
0 (DMSO)
0.5µM
1 µM
2µM
5 µM
10 µM
1µM stauro
Dovitinib
72hrs
Relative cell proliferation (%)
100
101
95
79
52
44
17
0 (DMSO)
0.5µM
1 µM
2µM
5 µM
10 µM
1µM stauro
Dovtinib

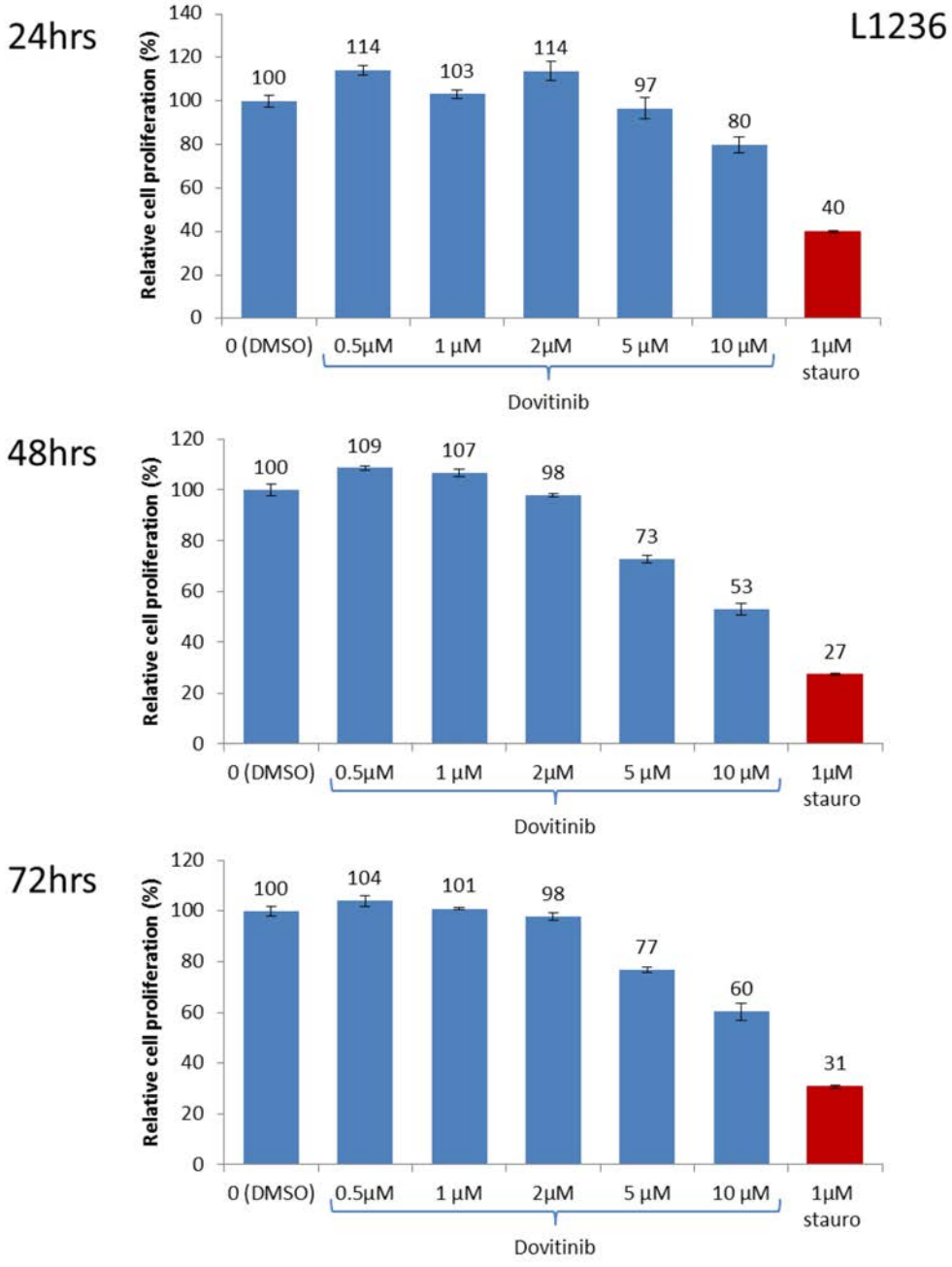
24hrs
L1236
Relative cell proliferation (%)
140
120
100
80
60
40
20
0
100
114
103
114
97
80
40
0 (DMSO)
0.5µM
1 µM
2µM
5 µM
10 µM
1µM stauro
Dovitinib
48hrs
Relative cell proliferation (%)
120
100
80
60
40
20
0
100
109
107
98
73
53
27
0 (DMSO)
0.5µM
1 µM
2µM
5 µM
10 µM
1µM stauro
Dovitinib
72hrs
Relative cell proliferation (%)
120
100
80
60
40
20
0
100
104
101
98
77
60
31
0 (DMSO)
0.5µM
1 µM
2µM
5 µM
10 µM
1µM stauro
Dovitinib

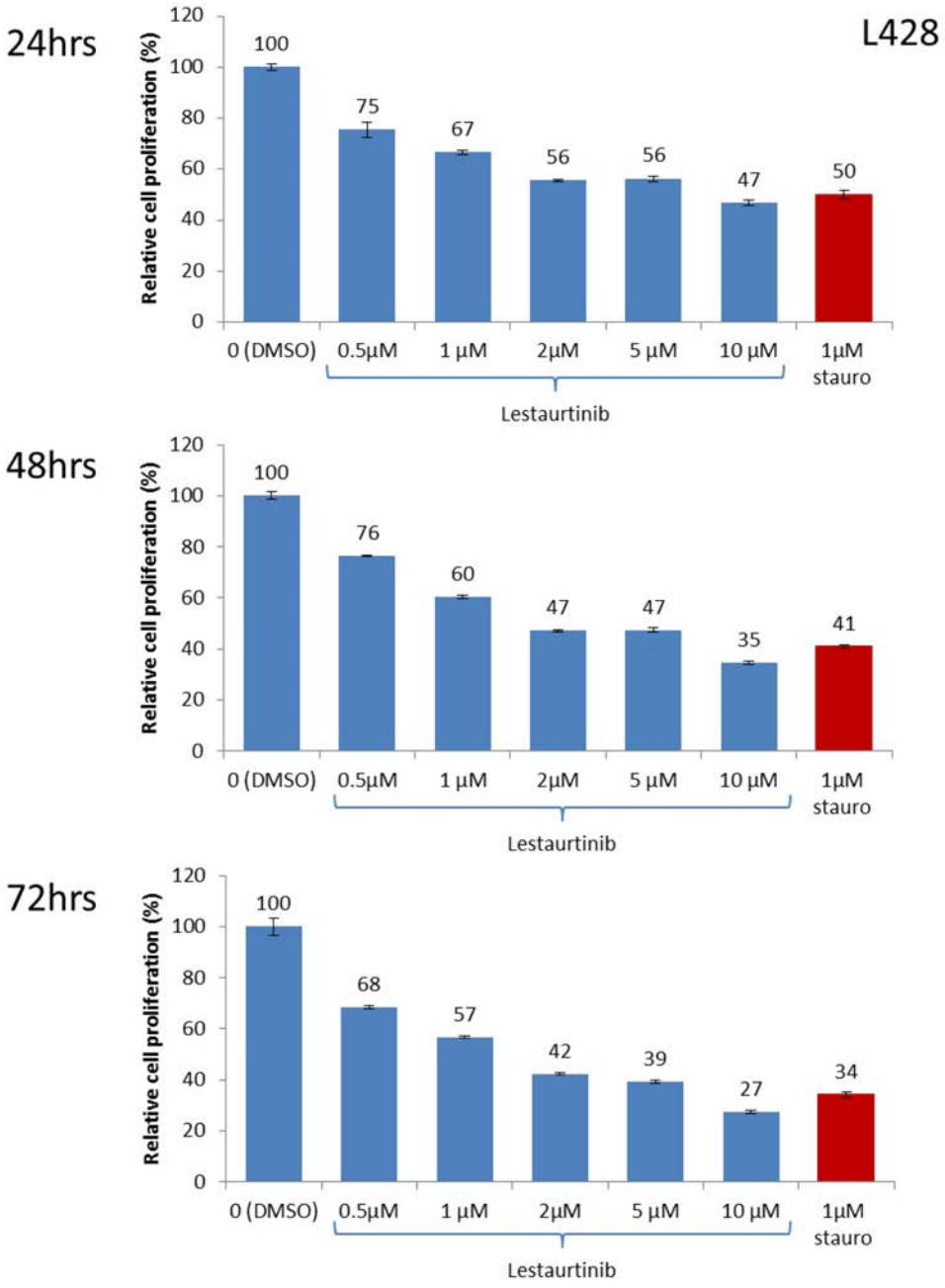

Figure 5.6 Cell proliferation in HL cell lines treated with lestaurtinib. Cells were maintained in normal growth conditions then re-suspended in fresh media containing 10% serum 24hrs prior to drug treatment. Cells were treated with lestaurtinib at the concentration and times indicated. Promega proliferation reagent was added at 22, 46 and 70hrs respectively and 2hrs later absorbance at 490nm was read to measure metabolic activity. Cell proliferation was calculated relative to DMSO only control cells. Each cell line was also treated with staurosporine which served as a positive control.

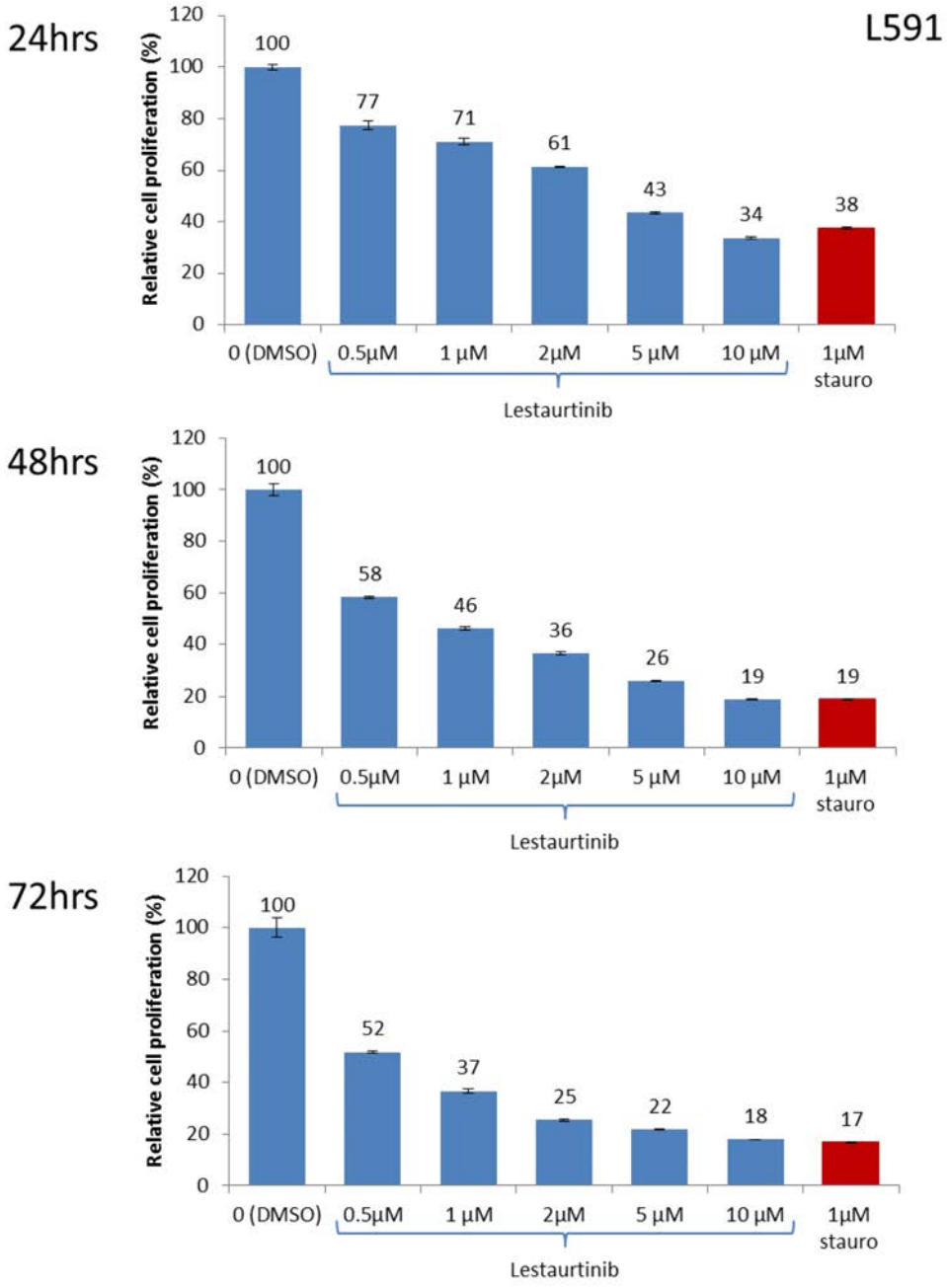
24hrs
L591
Relative cell proliferation (%)
120
100
80
60
40
20
0
100
77
71
61
43
34
38
0 (DMSO)
0.5µM
1 µM
2µM
5 µM
10 µM
1µM stauro
Lestaurtinib
48hrs
Relative cell proliferation (%)
100
58
46
36
26
19
19
0 (DMSO)
0.5µM
1 µM
2µM
5 µM
10 µM
1µM stauro
Lestaurtinib
72hrs
Relative cell proliferation (%)
100
52
37
25
22
18
17
0 (DMSO)
0.5µM
1 µM
2µM
5 µM
10 µM
1µM stauro
Lestaurtinib

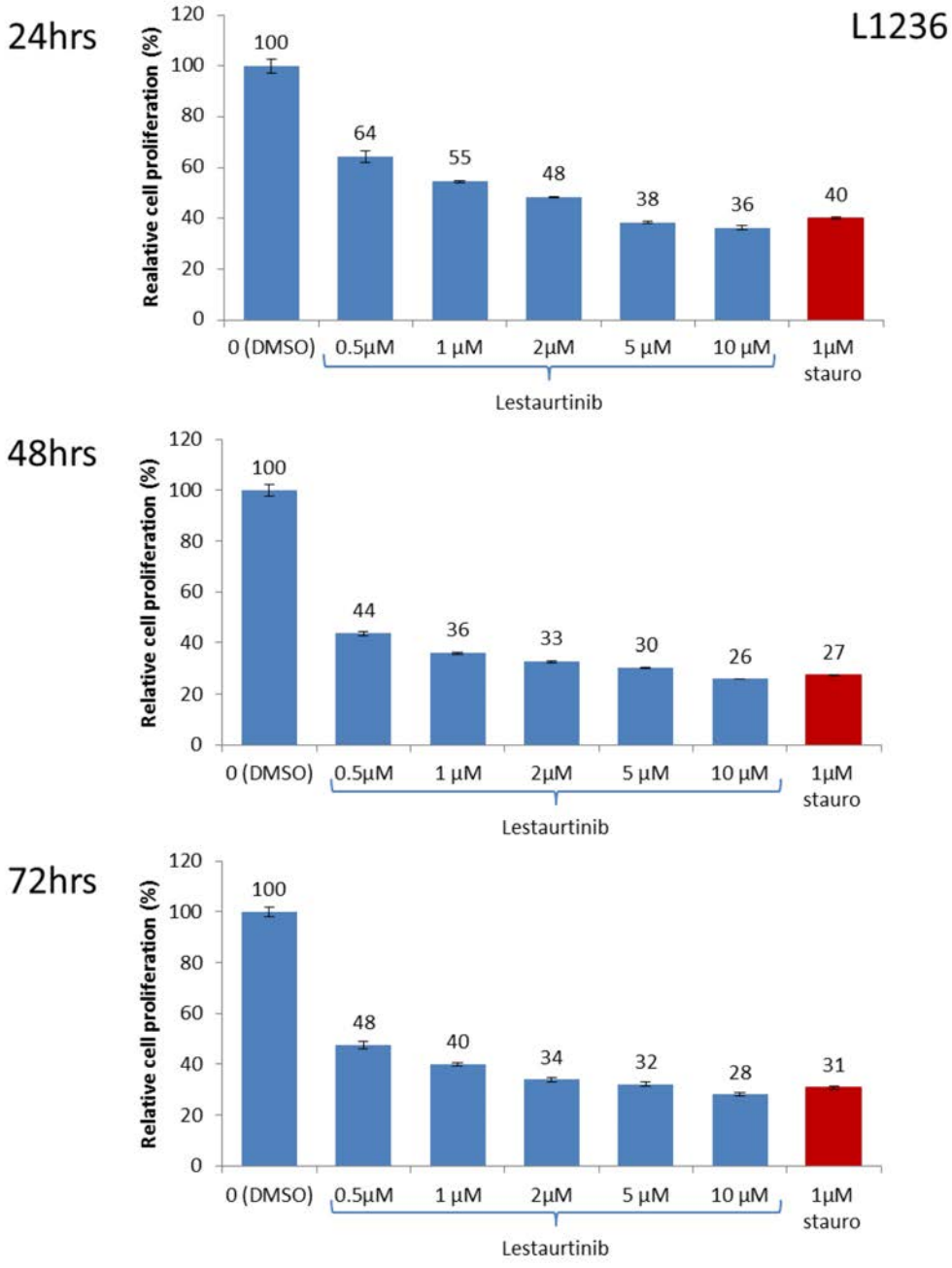
24hrs
L1236
Realative cell proliferation (%)
120
100
80
60
40
20
0
100
64
55
48
38
36
40
0 (DMSO)
0.5µM
1 µM
2µM
5 µM
10 µM
1µM stauro
Lestaurtinib
48hrs
Relative cell proliferation (%)
100
44
36
33
30
26
27
0 (DMSO)
0.5µM
1 µM
2µM
5 µM
10 µM
1µM stauro
Lestaurtinib
72hrs
Relative cell proliferation (%)
100
48
40
34
32
28
31
0 (DMSO)
0.5µM
1 µM
2µM
5 µM
10 µM
1µM stauro
Lestaurtinib

5.3 Discussion

In this chapter I have shown that HL cell lines are sensitive to new generation RTK inhibitors. I observed that HL cell lines were particularly sensitive to lestaurtinib. This drug otherwise known as CEP-701 is a tyrosine kinase inhibitor structurally related to staurosporine. lestaurtinib has been shown to inhibit FLT3, JAK2, TRKA, TRKB and TRKC[345-347]. I also observed that HL lines were sensitive to dovitinib, an RTK inhibitor which has been shown to inhibit VEGFR, PDGFR and FGFRs. Interestingly, vargatef, which is thought to target the same RTK as dovitinib, had little effect on the proliferation of HL cells.

Of the group of RTK inhibitors developed to target BCR-ABL only dasatinib showed any efficacy against HL cell lines. This could reflect the broader spectrum of activity of dasatinib compared to either imatinib or nilotinib. My results are also consistent with two previous studies which found that imatinib did not significantly reduce the proliferation of HL cells when used at concentrations below 10μM[232;239].

Although I have shown that several of the RTK inhibitors used in this study were effective against the proliferation of HL cell lines, the assay I used measures only metabolic activity which can be affected by both changes in cell cycle and cell death. Therefore, it will be important to properly define whether these drugs act predominantly to reduce cell proliferation or to promote apoptosis, or both.

Preclinical studies of lestaurtinib have characterised this orally available compound as a potent FLT3 inhibitor with an in vitro IC_{50} of 2 to 3 nM. Lestautinib also displays low nanomolar inhibition of TRKA and VEGFR, but it is not a potent inhibitor of other receptor tyrosine kinases related to FLT3 (IC_{50} is greater than 500 nM against KIT, and PDGFRβ)[347;348].

A widened screen of the kinase activity of lestaurtinib found it to be a potent JAK2 inhibitor (IC_{50} of 1 nM)[346]. Given the constitutive activation of JAK-STAT signalling in HL, the targeting of JAK2 may be an effective therapeutic approach. A recent phase II trial of relapsed/refractory myelofibrosis with JAK2 mutations reported an overall response rate of 27 %[346]. Consistent with my observations, recently the *in vitro* susceptibility of HL cell lines to lestaurtinib has been shown. Furthermore, the mechanism of action appeared to be through JAK2 inhibition[349]. Pharmacokinetic studies after single doses of oral lestaurtinib suggest that a plasma concentration, in excess of that required for the inhibition of HL cells observed in my study, can be achieved without dose limiting toxicities[350].

Dovitinib is also a multi-target tyrosine kinase inhibitor and has nanomolar potency against FLT3 but also demonstrated inhibition of VEGFR, CSF-1R and FGFRs[351]. It is already in phase II development in renal cell carcinoma, advanced breast cancer, and relapsed multiple myeloma (www.clinicaltrialsfeed.org) There is currently no data on the use of dovitinib in children but xenograft models to determine the pharmacokinetics of this drug suggest that a plasma concentration of 5µM might be achieved[352].

The multifactorial pathogenesis of HL means that any single-molecule targeted agent is unlikely to be curative if used alone. This hypothesis is supported by the results of clinical trials of FLT3 inhibitors in AML where mono-therapy has been disappointing[353]. Simultaneous inhibition of multiple targets is likely to be necessary in most patients, and this may be achievable in the future not only through the use of multi-target agents but also by combination molecular therapy.

In conclusion, in this chapter I have provided preliminary evidence suggesting that HL cell lines are sensitive to several next generation RTK inhibitors. The results of this study suggest that lestaurtinib and possibly dovitinib should be evaluated further in the treatment of HL.

CHAPTER 6

Future work

This thesis has identified a number of areas which could be pursued in the future. I outline these below:

6.1 Further study of the contribution of DDR1 to the pathogenesis of HL

Although I have shown that DDR1 is over-expressed in HRS cells, the knockdown of DDR1 in a HL cell line did not result in a detectable phenotypic change. As outlined previously the knockdown of a single RTK might alone be insufficient to disrupt a cell signalling pathway. Furthermore, the use of cell lines as models to explore the function of DDR1, that may require complex signals from the microenvironment for its activation, is questionable. Therefore, investigation of the phenotypic consequences of aberrant RTK activation may require the use of more appropriate model systems. One such approach might be to ectopically express DDR1 in GC B cells. This model is limited by the range of phenotypic assays that are technically feasible on transfected GC B cells. However, several assays, for example micro-array analysis, are possible on these cells and may reveal the signalling pathways activated by DDR1. In a complimentary approach it will also be possible to measure transcription factor activity in transfected GC B cells using a system recently established in our laboratory (PathDetect Trans-reporting system, Agilent Technologies). A more detailed investigation of the effects of DDR1 on cellular signalling might be conducted on more tractable systems such as BL cell lines. The BL system could also be used to study the activation of DDR1 following exposure to different collagen types or following cultivation in complex extracellular environments such as Matrigel™.

6.2 An investigation of the contribution of RON to the pathogenesis of HL

In addition to DDR1, I identified that numerous other RTKs were aberrantly activated in HL cell lines. Of these MET and RON were selected for further investigation. Owing to the lack of suitable antibody reagents, I was unable to confirm the activation of MET in paraffin embedded tissues of HL. However, I did detect the consistent activation of RON in primary HRS cells. These observations suggest that the contribution of RON to the pathogenesis of HL is worthy of further investigation. It seems probable that the same limitations identified above in respect of DDR1 may also apply to the future study of RON in HL cell lines. Therefore, I will consider adopting a similar approach to investigate the contribution of RON to the pathogenesis of HL as I have described above for DDR1.

6.3 Further study of RTK isoforms in HL

Investigating the contribution of the aberrant activation of DDR1 and RON to the pathogenesis of HL is further complicated by the potential existence of multiple isoforms of these receptors. For example, in HL cells I detected the presence of numerous DDR1 transcripts, including several novel forms. Likewise, RON is known to have several oncogenic isoforms some of which I may have detected by immunoblotting. Before proceeding to any functional investigation of these isoforms it will be necessary to determine if these transcripts are: 1) present in micro-dissected primary tumour cells, and 2) capable of generating protein following cDNA cloning and expression. I will also use genomic sequencing on micro-dissected primary HRS cells to investigate if the presence of these transcripts is a consequence of mutations in splice acceptor or donor sites.

6.4 The potential therapeutic use of RTK inhibitors in HL

Although my preliminary observations suggest that several of the RTK inhibitors I have investigated are effective against HL cell lines, there are several important issues which need to be resolved before these agents can be considered for the treatment of HL. First, the molecular target(s) of these RTKs inhibitors in HL cells need to be identified. This could be done using phosphorylation specific antibody arrays following the treatment of HL cells with these inhibitors. Second, it will be necessary to determine if the relevant target(s) can be inhibited at a clinical achievable plasma concentration. Third, it will be important to elucidate the mechanism of action and whether it involves cell cycle arrest, cell death or both.

Improved animal models could be used to study the effects of these inhibitors on the in vivo growth of HL cells. For example, the recently developed NOD/Shi-scid IL2rγnull (NOG) mouse has been shown not only to support more efficiently the growth of HL cell lines, but also to allow the stable reconstitution of normal human haematopoietic cell subsets[354]. Such a system offers the possibility of establishing an *in vivo* system in which tumour cell-microenvironment interactions are maintained, while at the same time permitting the testing of these therapeutic agents.

Reference List

(1) Hodgkin. On some Morbid Appearances of the Absorbent Glands and Spleen. Med Chir Trans 1832;17:68-114.

(2) Reed D. On the pathological changes in Hodgkin's disease, with special reference to its relationship to tuberculosis. J Hopkins Hosp Rep 1902;133-96.

(3) Swerdlow SH, Campo E, Harris NL, Jaffe ES, Pileri SA, Stein H, et al. WHO Classification of Tumours of Haematopoietic and Lymphoid Tissues. 4th. 2008. International Agency for Research on Cancer.

(4) Diehl V, Thomas RK, Re D. Part II: Hodgkin's lymphoma--diagnosis and treatment. Lancet Oncol 2004 Jan;5(1):19-26.

(5) Anagnostopoulos I, Hansmann ML, Franssila K, Harris M, Harris NL, Jaffe ES, et al. European Task Force on Lymphoma project on lymphocyte predominance Hodgkin disease: histologic and immunohistologic analysis of submitted cases reveals 2 types of Hodgkin disease with a nodular growth pattern and abundant lymphocytes. Blood 2000 Sep 1;96(5):1889-99.

(6) Diehl V, Sextro M, Franklin J, Hansmann ML, Harris N, Jaffe E, et al. Clinical presentation, course, and prognostic factors in lymphocyte-predominant Hodgkin's disease and lymphocyte-rich classical Hodgkin's disease: report from the European Task Force on Lymphoma Project on Lymphocyte-Predominant Hodgkin's Disease. J Clin Oncol 1999 Mar;17(3):776-83.

(7) Mason DY, Banks PM, Chan J, Cleary ML, Delsol G, de Wolf PC, et al. Nodular lymphocyte predominance Hodgkin's disease. A distinct clinicopathological entity. Am J Surg Pathol 1994 May;18(5):526-30.

(8) Nogova L, Reineke T, Brillant C, Sieniawski M, Rudiger T, Josting A, et al. Lymphocyte-predominant and classical Hodgkin's lymphoma: a comprehensive analysis from the German Hodgkin Study Group. J Clin Oncol 2008 Jan 20;26(3):434-9.

(9) Weiss LM, Chan JKC, Maclennan K, Warnke RA. In Hodgkin's Disease. Mauch PM, Armitage JO, Diehl V, Hoppe R, Weiss LM, editors. 101-120. 1999. Philadelphia, Lippencott Williams and wilkins.

(10) Shimabukuro-Vornhagen A, Haverkamp H, Engert A, Balleisen L, Majunke P, Heil G, et al. Lymphocyte-rich classical Hodgkin's lymphoma: clinical presentation and treatment outcome in 100 patients treated within German Hodgkin's Study Group trials. J Clin Oncol 2005 Aug 20;23(24):5739-45.

(11) Neiman RS, Rosen PJ, Lukes RJ. Lymphocyte-depletion Hodgkin's disease. A clinicopathological entity. N Engl J Med 1973 Apr 12;288(15):751-5.

(12) Pinkus GS, Said JW. Hodgkin's disease, lymphocyte predominance type, nodular--a distinct entity? Unique staining profile for L&H variants of Reed-Sternberg cells defined by monoclonal antibodies to leukocyte common antigen, granulocyte-specific antigen, and B-cell-specific antigen. Am J Pathol 1985 Jan;118(1):1-6.

(13) Paediatric oncology. 5-3-2011.

(14) Parkin DM, Stiller CA, Draper GJ, Bieber CA, Terracini B, Young JL. International incidence of childhood cancer. [Scientific publications 87]. 1988. International Agency for Research on Cancer.

(15) MacMahon B. Epidemiology of Hodgkin's disease. Cancer Res 1966 Jun;26(6):1189-201.

(16) Correa P, O'Conor GT. Epidemiologic patterns of Hodgkin's disease. Int J Cancer 1971 Sep 15;8(2):192-201.

(17) Cridland MD. Seasonal incidence of clinical onset of Hodgkin's disease. Br Med J 1961 Sep 2;2(5252):621-3.

(18) Douglas S, Cortina-Borja M, Cartwright R. Seasonal variation in the incidence of Hodgkin's disease. Br J Haematol 1998 Dec;103(3):653-62.

(19) Newell GR, Lynch HK, Gibeau JM, Spitz MR. Seasonal diagnosis of Hodgkin's disease among young adults. J Natl Cancer Inst 1985 Jan;74(1):53-6.

(20) Gilman EA, McNally RJ, Cartwright RA. Space-time clustering of Hodgkin's Disease in parts of the UK, 1984-1993. Leuk Lymphoma 1999 Dec;36(1-2):85-100.

(21) Mangoud A, Hillier VF, Leck I, Thomas RW. Space-time interaction in Hodgkin's disease in Greater Manchester. J Epidemiol Community Health 1985 Mar;39(1):58-62.

(22) Gutensohn N, Cole P. Childhood social environment and Hodgkin's disease. N Engl J Med 1981 Jan 15;304(3):135-40.

(23) Goldin LR, Pfeiffer RM, Gridley G, Gail MH, Li X, Mellemkjaer L, et al. Familial aggregation of Hodgkin lymphoma and related tumors. Cancer 2004 May 1;100(9):1902-8.

(24) Mack TM, Cozen W, Shibata DK, Weiss LM, Nathwani BN, Hernandez AM, et al. Concordance for Hodgkin's disease in identical twins suggesting genetic susceptibility to the young-adult form of the disease. N Engl J Med 1995 Feb 16;332(7):413-8.

(25) Harty LC, Lin AY, Goldstein AM, Jaffe ES, Carrington M, Tucker MA, et al. HLA-DR, HLA-DQ, and TAP genes in familial Hodgkin disease. Blood 2002 Jan 15;99(2):690-3.

(26) Niens M, Jarrett RF, Hepkema B, Nolte IM, Diepstra A, Platteel M, et al. HLA-A*02 is associated with a reduced risk and HLA-A*01 with an increased risk of developing EBV+ Hodgkin lymphoma. Blood 2007 Nov 1;110(9):3310-5.

(27) Klitz W, Aldrich CL, Fildes N, Horning SJ, Begovich AB. Localization of predisposition to Hodgkin disease in the HLA class II region. Am J Hum Genet 1994 Mar;54(3):497-505.

(28) Marshall WH, Barnard JM, Buehler SK, Crumley J, Larsen B. HLA in familial Hodgkin's disease. Results and a new hypothesis. Int J Cancer 1977 Apr 15;19(4):450-5.

(29) Oza AM, Tonks S, Lim J, Fleetwood MA, Lister TA, Bodmer JG. A clinical and epidemiological study of human leukocyte antigen-DPB alleles in Hodgkin's disease. Cancer Res 1994 Oct 1;54(19):5101-5.

(30) Svejgaard A, Platz P, Ryder LP, Nielsen LS, Thomsen M. HL-A and disease associations--a survey. Transplant Rev 1975;22:3-43.

(31) Enciso-Mora V, Broderick P, Ma Y, Jarrett RF, Hjalgrim H, Hemminki K, et al. A genome-wide association study of Hodgkin's lymphoma identifies new susceptibility loci at 2p16.1 (REL), 8q24.21 and 10p14 (GATA3). Nat Genet 2010 Dec;42(12):1126-30.

(32) Beck-Engeser GB, Lum AM, Huppi K, Caplen NJ, Wang BB, Wabl M. Pvt1-encoded microRNAs in oncogenesis. Retrovirology 2008;5:4.

(33) Pinkerton R, Plowman PN, Pieters R. Paediatric Oncology. 3, 267-286. 2004. London, Arnold.

(34) Carbone PP, Kaplan HS, Musshoff K, Smithers DW, Tubiana M. Report of the Committee on Hodgkin's Disease Staging Classification. Cancer Res 1971 Nov;31(11):1860-1.

(35) Lister TA, Crowther D, Sutcliffe SB, Glatstein E, Canellos GP, Young RC, et al. Report of a committee convened to discuss the evaluation and staging of patients with Hodgkin's disease: Cotswolds meeting. J Clin Oncol 1989 Nov;7(11):1630-6.

(36) Marcus R, Sweetenham JW, Williams ME. Lymphoma; Pathology, Diagnosis and Treatment. 1. 2007. Cambridge university press.

(37) Donaldson SS, Link MP. Combined modality treatment with low-dose radiation and MOPP chemotherapy for children with Hodgkin's disease. J Clin Oncol 1987 May;5(5):742-9.

(38) Hunger SP, Link MP, Donaldson SS. ABVD/MOPP and low-dose involved-field radiotherapy in pediatric Hodgkin's disease: the Stanford experience. J Clin Oncol 1994 Oct;12(10):2160-6.

(39) Landman-Parker J, Pacquement H, Leblanc T, Habrand JL, Terrier-Lacombe MJ, Bertrand Y, et al. Localized childhood Hodgkin's disease: response-adapted chemotherapy with etoposide, bleomycin, vinblastine, and prednisone before low-dose radiation therapy-results of the French Society of Pediatric Oncology Study MDH90. J Clin Oncol 2000 Apr;18(7):1500-7.

(40) Schellong G. Treatment of children and adolescents with Hodgkin's disease: the experience of the German-Austrian Paediatric Study Group. Baillieres Clin Haematol 1996 Sep;9(3):619-34.

(41) Schellong G, Potter R, Bramswig J, Wagner W, Prott FJ, Dorffel W, et al. High cure rates and reduced long-term toxicity in pediatric Hodgkin's disease: the German-Austrian multicenter trial DAL-HD-90. The German-Austrian Pediatric Hodgkin's Disease Study Group. J Clin Oncol 1999 Dec;17(12):3736-44.

(42) Schellong G, Bramswig JH, Schwarze EW, Wannenmacher M. An approach to reduce treatment and invasive staging in childhood Hodgkin's disease: the sequence of the German DAL multicenter studies. Bull Cancer 1988;75(1):41-51.

(43) Smith RS, Chen Q, Hudson MM, Link MP, Kun L, Weinstein H, et al. Prognostic factors for children with Hodgkin's disease treated with combined-modality therapy. J Clin Oncol 2003 May 15;21(10):2026-33.

(44) Kaplan HS. On the natural history, treatment, and prognosis of Hodgkin's disease. Harvey Lect 1968;64:215-59.

(45) Bhatia S, Robison LL, Oberlin O, Greenberg M, Bunin G, Fossati-Bellani F, et al. Breast cancer and other second neoplasms after childhood Hodgkin's disease. N Engl J Med 1996 Mar 21;334(12):745-51.

(46) Metayer C, Lynch CF, Clarke EA, Glimelius B, Storm H, Pukkala E, et al. Second cancers among long-term survivors of Hodgkin's disease diagnosed in childhood and adolescence. J Clin Oncol 2000 Jun;18(12):2435-43.

(47) Sklar C, Whitton J, Mertens A, Stovall M, Green D, Marina N, et al. Abnormalities of the thyroid in survivors of Hodgkin's disease: data from the Childhood Cancer Survivor Study. J Clin Endocrinol Metab 2000 Sep;85(9):3227-32.

(48) Carbone PP. The role of chemotherapy in the management of patients with Hodgkin's disease. Ann Intern Med 1967;67:433-7.

(49) van den Berg H, Stuve W, Behrendt H. Treatment of Hodgkin's disease in children with alternating mechlorethamine, vincristine, procarbazine, and prednisone (MOPP) and adriamycin, bleomycin, vinblastine, and dacarbazine (ABVD) courses without radiotherapy. Med Pediatr Oncol 1997 Jul;29(1):23-7.

(50) Viviani S, Bonadonna G, Santoro A, Bonfante V, Zanini M, Devizzi L, et al. Alternating versus hybrid MOPP and ABVD combinations in advanced Hodgkin's disease: ten-year results. J Clin Oncol 1996 May;14(5):1421-30.

(51) El-Badawy S, Aboulnaga S, Abou GA, Mokhless A, Zamzam M, Sidhom I, et al. Risk adapted combined modality treatment in children with Hodgkin's disease: NCI, Cairo. J Egypt Natl Canc Inst 2008 Jun;20(2):99-110.

(52) Schwartz CL, Constine LS, Villaluna D, London WB, Hutchison RE, Sposto R, et al. A risk-adapted, response-based approach using ABVE-PC for children and adolescents with intermediate- and high-risk Hodgkin lymphoma: the results of P9425. Blood 2009 Sep 3;114(10):2051-9.

(53) Wiedmann E, Baican B, Hertel A, Baum RP, Chow KU, Knupp B, et al. Positron emission tomography (PET) for staging and evaluation of response to treatment in patients with Hodgkin's disease. Leuk Lymphoma 1999 Aug;34(5-6):545-51.

(54) Euronet PHL-C1. 2011.

(55) Daw S, Wynn R, Wallace H. Management of relapsed and refractory classical Hodgkin lymphoma in children and adolescents. Br J Haematol 2011 Feb;152(3):249-60.

(56) Schellong G, Dorffel W, Claviez A, Korholz D, Mann G, Scheel-Walter HG, et al. Salvage therapy of progressive and recurrent Hodgkin's disease: results from a multicenter study of the pediatric DAL/GPOH-HD study group. J Clin Oncol 2005 Sep 1;23(25):6181-9.

(57) Akhtar S, El WA, Rahal M, Abdelsalam M, Al HH, Maghfoor I. High-dose chemotherapy and autologous stem cell transplant in adolescent patients with relapsed or refractory Hodgkin's lymphoma. Bone Marrow Transplant 2010 Mar;45(3):476-82.

(58) Baker KS, Gordon BG, Gross TG, Abromowitch MA, Lyden ER, Lynch JC, et al. Autologous hematopoietic stem-cell transplantation for relapsed or refractory Hodgkin's disease in children and adolescents. J Clin Oncol 1999 Mar;17(3):825-31.

(59) Brice P. Managing relapsed and refractory Hodgkin lymphoma. Br J Haematol 2008 Apr;141(1):3-13.

(60) Dores GM, Metayer C, Curtis RE, Lynch CF, Clarke EA, Glimelius B, et al. Second malignant neoplasms among long-term survivors of Hodgkin's disease: a population-based evaluation over 25 years. J Clin Oncol 2002 Aug 15;20(16):3484-94.

(61) Bath LE, Wallace WH, Critchley HO. Late effects of the treatment of childhood cancer on the female reproductive system and the potential for fertility preservation. BJOG 2002 Feb;109(2):107-14.

(62) Busia A, Laffranchi A, Viviani S, Bonfante V, Villani F. Cardiopulmonary toxicity of different chemoradiotherapy combined regimens for Hodgkin's disease. Anticancer Res 2010 Oct;30(10):4381-7.

(63) Villani F, Busia A, Villani M, Laffranchi A, Viviani S, Bonfante V. Cardiopulmonary response to exercise in patients with different degrees of lung toxicity after radio-chemotherapy for Hodgkin's disease. Anticancer Res 2009 Feb;29(2):777-83.

(64) Dudley DD, Chaudhuri J, Bassing CH, Alt FW. Mechanism and control of V(D)J recombination versus class switch recombination: similarities and differences. Adv Immunol 2005;86:43-112.

(65) Klein U, Dalla-Favera R. Germinal centres: role in B-cell physiology and malignancy. Nat Rev Immunol 2008 Jan;8(1):22-33.

(66) Teng G, Papavasiliou FN. Immunoglobulin somatic hypermutation. Annu Rev Genet 2007;41:107-20.

(67) Allen CD, Okada T, Cyster JG. Germinal-center organization and cellular dynamics. Immunity 2007 Aug;27(2):190-202.

(68) DeKoter RP, Singh H. Regulation of B lymphocyte and macrophage development by graded expression of PU.1. Science 2000 May 26;288(5470):1439-41.

(69) Dias S, Mansson R, Gurbuxani S, Sigvardsson M, Kee BL. E2A proteins promote development of lymphoid-primed multipotent progenitors. Immunity 2008 Aug 15;29(2):217-27.

(70) Lin YC, Jhunjhunwala S, Benner C, Heinz S, Welinder E, Mansson R, et al. A global network of transcription factors, involving E2A, EBF1 and Foxo1, that orchestrates B cell fate. Nat Immunol 2010 Jul;11(7):635-43.

(71) Nutt SL, Heavey B, Rolink AG, Busslinger M. Commitment to the B-lymphoid lineage depends on the transcription factor Pax5. Nature 1999 Oct 7;401(6753):556-62.

(72) Yang Q, Kardava L, St LA, Martincic K, Varnum-Finney B, Bernstein ID, et al. E47 controls the developmental integrity and cell cycle quiescence of multipotential hematopoietic progenitors. J Immunol 2008 Nov 1;181(9):5885-94.

(73) Kuppers R. B cells under influence: transformation of B cells by Epstein-Barr virus. Nat Rev Immunol 2003 Oct;3(10):801-12.

(74) Beck K, Peak MM, Ota T, Nemazee D, Murre C. Distinct roles for E12 and E47 in B cell specification and the sequential rearrangement of immunoglobulin light chain loci. J Exp Med 2009 Sep 28;206(10):2271-84.

(75) Cobaleda C, Jochum W, Busslinger M. Conversion of mature B cells into T cells by dedifferentiation to uncommitted progenitors. Nature 2007 Sep 27;449(7161):473-7.

(76) Thal MA, Carvalho TL, He T, Kim HG, Gao H, Hagman J, et al. Ebf1-mediated down-regulation of Id2 and Id3 is essential for specification of the B cell lineage. Proc Natl Acad Sci U S A 2009 Jan 13;106(2):552-7.

(77) Gonda H, Sugai M, Nambu Y, Katakai T, Agata Y, Mori KJ, et al. The balance between Pax5 and Id2 activities is the key to AID gene expression. J Exp Med 2003 Nov 3;198(9):1427-37.

(78) Corcoran LM, Karvelas M, Nossal GJ, Ye ZS, Jacks T, Baltimore D. Oct-2, although not required for early B-cell development, is critical for later B-cell maturation and for postnatal survival. Genes Dev 1993 Apr;7(4):570-82.

(79) Schubart DB, Rolink A, Kosco-Vilbois MH, Botteri F, Matthias P. B-cell-specific coactivator OBF-1/OCA-B/Bob1 required for immune response and germinal centre formation. Nature 1996 Oct 10;383(6600):538-42.

(80) Basso K, Dalla-Favera R. BCL6: master regulator of the germinal center reaction and key oncogene in B cell lymphomagenesis. Adv Immunol 2010;105:193-210.

(81) Crotty S, Johnston RJ, Schoenberger SP. Effectors and memories: Bcl-6 and Blimp-1 in T and B lymphocyte differentiation. Nat Immunol 2010 Feb;11(2):114-20.

(82) Wei F, Zaprazna K, Wang J, Atchison ML. PU.1 can recruit BCL6 to DNA to repress gene expression in germinal center B cells. Mol Cell Biol 2009 Sep;29(17):4612-22.

(83) Henderson A, Calame K. Transcriptional regulation during B cell development. Annu Rev Immunol 1998;16:163-200.

(84) Hummel M, Ziemann K, Lammert H, Pileri S, Sabattini E, Stein H. Hodgkin's disease with monoclonal and polyclonal populations of Reed-Sternberg cells. N Engl J Med 1995 Oct 5;333(14):901-6.

(85) Kuppers R, Rajewsky K, Zhao M, Simons G, Laumann R, Fischer R, et al. Hodgkin's disease: clonal Ig gene rearrangements in Hodgkin and Reed-Sternberg cells picked from histological sections. Ann N Y Acad Sci 1995 Sep 29;764:523-4.

(86) Kuppers R, Hansmann ML, Rajewsky K. Clonality and germinal centre B-cell derivation of Hodgkin/Reed-Sternberg cells in Hodgkin's disease. Ann Oncol 1998;9 Suppl 5:S17-S20.

(87) Marafioti T, Hummel M, Foss HD, Laumen H, Korbjuhn P, Anagnostopoulos I, et al. Hodgkin and reed-sternberg cells represent an expansion of a single clone originating from a germinal center B-cell with functional immunoglobulin gene rearrangements but defective immunoglobulin transcription. Blood 2000 Feb 15;95(4):1443-50.

(88) Kanzler H, Kuppers R, Hansmann ML, Rajewsky K. Hodgkin and Reed-Sternberg cells in Hodgkin's disease represent the outgrowth of a dominant tumor clone derived from (crippled) germinal center B cells. J Exp Med 1996 Oct 1;184(4):1495-505.

(89) Kuppers R. The biology of Hodgkin's lymphoma. Nat Rev Cancer 2009 Jan;9(1):15-27.

(90) Muschen M, Rajewsky K, Brauninger A, Baur AS, Oudejans JJ, Roers A, et al. Rare occurrence of classical Hodgkin's disease as a T cell lymphoma. J Exp Med 2000 Jan 17;191(2):387-94.

(91) Barry TS, Jaffe ES, Sorbara L, Raffeld M, Pittaluga S. Peripheral T-cell lymphomas expressing CD30 and CD15. Am J Surg Pathol 2003 Dec;27(12):1513-22.

(92) Chittal SM, Brousset P, Voigt JJ, Delsol G. Large B-cell lymphoma rich in T-cells and simulating Hodgkin's disease. Histopathology 1991 Sep;19(3):211-20.

(93) Seitz V, Hummel M, Marafioti T, Anagnostopoulos I, Assaf C, Stein H. Detection of clonal T-cell receptor gamma-chain gene rearrangements in Reed-Sternberg cells of classic Hodgkin disease. Blood 2000 May 15;95(10):3020-4.

(94) Kuppers R, Klein U, Schwering I, Distler V, Brauninger A, Cattoretti G, et al. Identification of Hodgkin and Reed-Sternberg cell-specific genes by gene expression profiling. J Clin Invest 2003 Feb;111(4):529-37.

(95) Rolink AG, Melchers F. Precursor B cells from Pax-5-deficient mice--stem cells for macrophages, granulocytes, osteoclasts, dendritic cells, natural killer cells, thymocytes and T cells. Curr Top Microbiol Immunol 2000;251:21-6.

(96) Schwering I, Brauninger A, Klein U, Jungnickel B, Tinguely M, Diehl V, et al. Loss of the B-lineage-specific gene expression program in Hodgkin and Reed-Sternberg cells of Hodgkin lymphoma. Blood 2003 Feb 15;101(4):1505-12.

(97) Torlakovic E, Tierens A, Dang HD, Delabie J. The transcription factor PU.1, necessary for B-cell development is expressed in lymphocyte predominance, but not classical Hodgkin's disease. Am J Pathol 2001 Nov;159(5):1807-14.

(98) Mathas S, Janz M, Hummel F, Hummel M, Wollert-Wulf B, Lusatis S, et al. Intrinsic inhibition of transcription factor E2A by HLH proteins ABF-1 and Id2 mediates reprogramming of neoplastic B cells in Hodgkin lymphoma. Nat Immunol 2006 Feb;7(2):207-15.

(99) Renne C, Martin-Subero JI, Eickernjager M, Hansmann ML, Kuppers R, Siebert R, et al. Aberrant expression of ID2, a suppressor of B-cell-specific gene expression, in Hodgkin's lymphoma. Am J Pathol 2006 Aug;169(2):655-64.

(100) Jundt F, Probsting KS, Anagnostopoulos I, Muehlinghaus G, Chatterjee M, Mathas S, et al. Jagged1-induced Notch signaling drives proliferation of multiple myeloma cells. Blood 2004 May 1;103(9):3511-5.

(101) Jundt F, Acikgoz O, Kwon SH, Schwarzer R, Anagnostopoulos I, Wiesner B, et al. Aberrant expression of Notch1 interferes with the B-lymphoid phenotype of neoplastic B cells in classical Hodgkin lymphoma. Leukemia 2008 Aug;22(8):1587-94.

(102) Stanelle J, Doring C, Hansmann ML, Kuppers R. Mechanisms of aberrant GATA3 expression in classical Hodgkin lymphoma and its consequences for the cytokine profile of Hodgkin and Reed/Sternberg cells. Blood 2010 Nov 18;116(20):4202-11.

(103) Yoon SO, Zhang X, Berner P, Blom B, Choi YS. Notch ligands expressed by follicular dendritic cells protect germinal center B cells from apoptosis. J Immunol 2009 Jul 1;183(1):352-8.

(104) Zweidler-McKay PA, He Y, Xu L, Rodriguez CG, Karnell FG, Carpenter AC, et al. Notch signaling is a potent inducer of growth arrest and apoptosis in a wide range of B-cell malignancies. Blood 2005 Dec 1;106(12):3898-906.

(105) Jundt F, Kley K, Anagnostopoulos I, Schulze PK, Greiner A, Mathas S, et al. Loss of PU.1 expression is associated with defective immunoglobulin transcription in Hodgkin and Reed-Sternberg cells of classical Hodgkin disease. Blood 2002 Apr 15;99(8):3060-2.

(106) Re D, Muschen M, Ahmadi T, Wickenhauser C, Staratschek-Jox A, Holtick U, et al. Oct-2 and Bob-1 deficiency in Hodgkin and Reed Sternberg cells. Cancer Res 2001 Mar 1;61(5):2080-4.

(107) Stein H, Marafioti T, Foss HD, Laumen H, Hummel M, Anagnostopoulos I, et al. Down-regulation of BOB.1/OBF.1 and Oct2 in classical Hodgkin disease but not in lymphocyte predominant Hodgkin disease correlates with immunoglobulin transcription. Blood 2001 Jan 15;97(2):496-501.

(108) Ushmorov A, Ritz O, Hummel M, Leithauser F, Moller P, Stein H, et al. Epigenetic silencing of the immunoglobulin heavy-chain gene in classical Hodgkin lymphoma-derived cell lines contributes to the loss of immunoglobulin expression. Blood 2004 Nov 15;104(10):3326-34.

(109) Ushmorov A, Leithauser F, Sakk O, Weinhausel A, Popov SW, Moller P, et al. Epigenetic processes play a major role in B-cell-specific gene silencing in classical Hodgkin lymphoma. Blood 2006 Mar 15;107(6):2493-500.

(110) Bargou RC, Emmerich F, Krappmann D, Bommert K, Mapara MY, Arnold W, et al. Constitutive nuclear factor-kappaB-RelA activation is required for proliferation and survival of Hodgkin's disease tumor cells. J Clin Invest 1997 Dec 15;100(12):2961-9.

(111) Hinz M, Loser P, Mathas S, Krappmann D, Dorken B, Scheidereit C. Constitutive NF-kappaB maintains high expression of a characteristic gene network, including CD40, CD86, and a set of antiapoptotic genes in Hodgkin/Reed-Sternberg cells. Blood 2001 May 1;97(9):2798-807.

(112) Hinz M, Lemke P, Anagnostopoulos I, Hacker C, Krappmann D, Mathas S, et al. Nuclear factor kappaB-dependent gene expression profiling of Hodgkin's disease tumor cells, pathogenetic significance, and link to constitutive signal transducer and activator of transcription 5a activity. J Exp Med 2002 Sep 2;196(5):605-17.

(113) Krappmann D, Emmerich F, Kordes U, Scharschmidt E, Dorken B, Scheidereit C. Molecular mechanisms of constitutive NF-kappaB/Rel activation in Hodgkin/Reed-Sternberg cells. Oncogene 1999 Jan 28;18(4):943-53.

(114) Cabannes E, Khan G, Aillet F, Jarrett RF, Hay RT. Mutations in the IkBa gene in Hodgkin's disease suggest a tumour suppressor role for IkappaBalpha. Oncogene 1999 May 20;18(20):3063-70.

(115) Emmerich F, Meiser M, Hummel M, Demel G, Foss HD, Jundt F, et al. Overexpression of I kappa B alpha without inhibition of NF-kappaB activity and mutations in the I kappa B alpha gene in Reed-Sternberg cells. Blood 1999 Nov 1;94(9):3129-34.

(116) Jungnickel B, Staratschek-Jox A, Brauninger A, Spieker T, Wolf J, Diehl V, et al. Clonal deleterious mutations in the IkappaBalpha gene in the malignant cells in Hodgkin's lymphoma. J Exp Med 2000 Jan 17;191(2):395-402.

(117) Schmitz R, Hansmann ML, Bohle V, Martin-Subero JI, Hartmann S, Mechtersheimer G, et al. TNFAIP3 (A20) is a tumor suppressor gene in Hodgkin lymphoma and primary mediastinal B cell lymphoma. J Exp Med 2009 May 11;206(5):981-9.

(118) Carbone A, Gloghini A, Gruss HJ, Pinto A. CD40 ligand is constitutively expressed in a subset of T cell lymphomas and on the microenvironmental reactive T cells of follicular lymphomas and Hodgkin's disease. Am J Pathol 1995 Oct;147(4):912-22.

(119) Carbone A, Gloghini A, Gattei V, Aldinucci D, Degan M, De PP, et al. Expression of functional CD40 antigen on Reed-Sternberg cells and Hodgkin's disease cell lines. Blood 1995 Feb 1;85(3):780-9.

(120) Hirsch B, Hummel M, Bentink S, Fouladi F, Spang R, Zollinger R, et al. CD30-induced signaling is absent in Hodgkin's cells but present in anaplastic large cell lymphoma cells. Am J Pathol 2008 Feb;172(2):510-20.

(121) Horie R, Watanabe T, Morishita Y, Ito K, Ishida T, Kanegae Y, et al. Ligand-independent signaling by overexpressed CD30 drives NF-kappaB activation in Hodgkin-Reed-Sternberg cells. Oncogene 2002 Apr 11;21(16):2493-503.

(122) Pinto A, Aldinucci D, Gloghini A, Zagonel V, Degan M, Improta S, et al. Human eosinophils express functional CD30 ligand and stimulate proliferation of a Hodgkin's disease cell line. Blood 1996 Nov 1;88(9):3299-305.

(123) Zheng B, Fiumara P, Li YV, Georgakis G, Snell V, Younes M, et al. MEK/ERK pathway is aberrantly active in Hodgkin disease: a signaling pathway shared by CD30, CD40, and RANK that regulates cell proliferation and survival. Blood 2003 Aug 1;102(3):1019-27.

(124) Baus D, Pfitzner E. Specific function of STAT3, SOCS1, and SOCS3 in the regulation of proliferation and survival of classical Hodgkin lymphoma cells. Int J Cancer 2006 Mar 15;118(6):1404-13.

(125) Mottok A, Renne C, Willenbrock K, Hansmann ML, Brauninger A. Somatic hypermutation of SOCS1 in lymphocyte-predominant Hodgkin lymphoma is accompanied by high JAK2 expression and activation of STAT6. Blood 2007 Nov 1;110(9):3387-90.

(126) Weniger MA, Melzner I, Menz CK, Wegener S, Bucur AJ, Dorsch K, et al. Mutations of the tumor suppressor gene SOCS-1 in classical Hodgkin lymphoma are frequent and associated with nuclear phospho-STAT5 accumulation. Oncogene 2006 Apr 27;25(18):2679-84.

(127) Kube D, Holtick U, Vockerodt M, Ahmadi T, Haier B, Behrmann I, et al. STAT3 is constitutively activated in Hodgkin cell lines. Blood 2001 Aug 1;98(3):762-70.

(128) Skinnider BF, Elia AJ, Gascoyne RD, Patterson B, Trumper L, Kapp U, et al. Signal transducer and activator of transcription 6 is frequently activated in Hodgkin and Reed-Sternberg cells of Hodgkin lymphoma. Blood 2002 Jan 15;99(2):618-26.

(129) Lamprecht B, Kreher S, Anagnostopoulos I, Johrens K, Monteleone G, Jundt F, et al. Aberrant expression of the Th2 cytokine IL-21 in Hodgkin lymphoma cells regulates STAT3

signaling and attracts Treg cells via regulation of MIP-3alpha. Blood 2008 Oct 15;112(8):3339-47.

(130) Scheeren FA, Diehl SA, Smit LA, Beaumont T, Naspetti M, Bende RJ, et al. IL-21 is expressed in Hodgkin lymphoma and activates STAT5: evidence that activated STAT5 is required for Hodgkin lymphomagenesis. Blood 2008 May 1;111(9):4706-15.

(131) Skinnider BF, Kapp U, Mak TW. The role of interleukin 13 in classical Hodgkin lymphoma. Leuk Lymphoma 2002 Jun;43(6):1203-10.

(132) Dutton A, Reynolds GM, Dawson CW, Young LS, Murray PG. Constitutive activation of phosphatidyl-inositide 3 kinase contributes to the survival of Hodgkin's lymphoma cells through a mechanism involving Akt kinase and mTOR. J Pathol 2005 Mar;205(4):498-506.

(133) Stambolic V, Suzuki A, de la Pompa JL, Brothers GM, Mirtsos C, Sasaki T, et al. Negative regulation of PKB/Akt-dependent cell survival by the tumor suppressor PTEN. Cell 1998 Oct 2;95(1):29-39.

(134) Kapp U, Dux A, Schell-Frederick E, Banik N, Hummel M, Mucke S, et al. Disseminated growth of Hodgkin's-derived cell lines L540 and L540cy in immune-deficient SCID mice. Ann Oncol 1994;5 Suppl 1:121-6.

(135) Aldinucci D, Lorenzon D, Cattaruzza L, Pinto A, Gloghini A, Carbone A, et al. Expression of CCR5 receptors on Reed-Sternberg cells and Hodgkin lymphoma cell lines: involvement of CCL5/Rantes in tumor cell growth and microenvironmental interactions. Int J Cancer 2008 Feb 15;122(4):769-76.

(136) Fischer M, Juremalm M, Olsson N, Backlin C, Sundstrom C, Nilsson K, et al. Expression of CCL5/RANTES by Hodgkin and Reed-Sternberg cells and its possible role in the recruitment of mast cells into lymphomatous tissue. Int J Cancer 2003 Nov 1;107(2):197-201.

(137) Jundt F, Anagnostopoulos I, Bommert K, Emmerich F, Muller G, Foss HD, et al. Hodgkin/Reed-Sternberg cells induce fibroblasts to secrete eotaxin, a potent chemoattractant for T cells and eosinophils. Blood 1999 Sep 15;94(6):2065-71.

(138) Marshall NA, Christie LE, Munro LR, Culligan DJ, Johnston PW, Barker RN, et al. Immunosuppressive regulatory T cells are abundant in the reactive lymphocytes of Hodgkin lymphoma. Blood 2004 Mar 1;103(5):1755-62.

(139) Cattaruzza L, Gloghini A, Olivo K, Di FR, Lorenzon D, De FR, et al. Functional coexpression of Interleukin (IL)-7 and its receptor (IL-7R) on Hodgkin and Reed-Sternberg cells: Involvement of IL-7 in tumor cell growth and microenvironmental interactions of Hodgkin's lymphoma. Int J Cancer 2009 Sep 1;125(5):1092-101.

(140) Schreck S, Friebel D, Buettner M, Distel L, Grabenbauer G, Young LS, et al. Prognostic impact of tumour-infiltrating Th2 and regulatory T cells in classical Hodgkin lymphoma. Hematol Oncol 2009 Mar;27(1):31-9.

(141) Aldinucci D, Gloghini A, Pinto A, De FR, Carbone A. The classical Hodgkin's lymphoma microenvironment and its role in promoting tumour growth and immune escape. J Pathol 2010 Jul;221(3):248-63.

(142) Barber DL, Wherry EJ, Masopust D, Zhu B, Allison JP, Sharpe AH, et al. Restoring function in exhausted CD8 T cells during chronic viral infection. Nature 2006 Feb 9;439(7077):682-7.

(143) Yamamoto R, Nishikori M, Kitawaki T, Sakai T, Hishizawa M, Tashima M, et al. PD-1-PD-1 ligand interaction contributes to immunosuppressive microenvironment of Hodgkin lymphoma. Blood 2008 Mar 15;111(6):3220-4.

(144) Trimboli AJ, Cantemir-Stone CZ, Li F, Wallace JA, Merchant A, Creasap N, et al. Pten in stromal fibroblasts suppresses mammary epithelial tumours. Nature 2009 Oct 22;461(7267):1084-91.

(145) Birgersdotter A, Baumforth KR, Porwit A, Sjoberg J, Wei W, Bjorkholm M, et al. Inflammation and tissue repair markers distinguish the nodular sclerosis and mixed cellularity subtypes of classical Hodgkin's lymphoma. Br J Cancer 2009 Oct 20;101(8):1393-401.

(146) Crocker J, Overton SP, Smith PJ. Type IV collagen in Hodgkin's disease. An immunohistochemical study. Am J Clin Pathol 1988 Jan;89(1):57-62.

(147) Vogel WF, Abdulhussein R, Ford CE. Sensing extracellular matrix: an update on discoidin domain receptor function. Cell Signal 2006 Aug;18(8):1108-16.

(148) Vogel WF. Collagen-receptor signaling in health and disease. Eur J Dermatol 2001 Nov;11(6):506-14.

(149) Cader FZ, Kearns P, Young L, Murray P, Vockerodt M. The contribution of the Epstein-Barr virus to the pathogenesis of childhood lymphomas. Cancer Treat Rev 2010 Jun;36(4):348-53.

(150) Woodman CB, Collins SI, Vavrusova N, Rao A, Middeldorp JM, Kolar Z, et al. Role of sexual behavior in the acquisition of asymptomatic Epstein-Barr virus infection: a longitudinal study. Pediatr Infect Dis J 2005 Jun;24(6):498-502.

(151) Carbone A, Gloghini A, Dotti G. EBV-associated lymphoproliferative disorders: classification and treatment. Oncologist 2008 May;13(5):577-85.

(152) Timms JM, Bell A, Flavell JR, Murray PG, Rickinson AB, Traverse-Glehen A, et al. Target cells of Epstein-Barr-virus (EBV)-positive post-transplant lymphoproliferative disease: similarities to EBV-positive Hodgkin's lymphoma. Lancet 2003 Jan 18;361(9353):217-23.

(153) Dolcetti R, Boiocchi M, Gloghini A, Carbone A. Pathogenetic and histogenetic features of HIV-associated Hodgkin's disease. Eur J Cancer 2001 Jul;37(10):1276-87.

(154) Young LS, Murray PG. Epstein-Barr virus and oncogenesis: from latent genes to tumours. Oncogene 2003 Aug 11;22(33):5108-21.

(155) Anagnostopoulos I, Herbst H, Niedobitek G, Stein H. Demonstration of monoclonal EBV genomes in Hodgkin's disease and Ki-1-positive anaplastic large cell lymphoma by combined Southern blot and in situ hybridization. Blood 1989 Aug 1;74(2):810-6.

(156) Weiss LM, Movahed LA, Warnke RA, Sklar J. Detection of Epstein-Barr viral genomes in Reed-Sternberg cells of Hodgkin's disease. N Engl J Med 1989 Feb 23;320(8):502-6.

(157) Ehlin-Henriksson B, Gordon J, Klein G. B-lymphocyte subpopulations are equally susceptible to Epstein-Barr virus infection, irrespective of immunoglobulin isotype expression. Immunology 2003 Apr;108(4):427-30.

(158) Thorley-Lawson DA. Epstein-Barr virus: exploiting the immune system. Nat Rev Immunol 2001 Oct;1(1):75-82.

(159) Amoroso R, Fitzsimmons L, Thomas WA, Kelly GL, Rowe M, Bell AI. Quantitative studies of Epstein-Barr virus-encoded microRNAs provide novel insights into their regulation. J Virol 2011 Jan;85(2):996-1010.

(160) Young LS, Rickinson AB. Epstein-Barr virus: 40 years on. Nat Rev Cancer 2004 Oct;4(10):757-68.

(161) Humme S, Reisbach G, Feederle R, Delecluse HJ, Bousset K, Hammerschmidt W, et al. The EBV nuclear antigen 1 (EBNA1) enhances B cell immortalization several thousandfold. Proc Natl Acad Sci U S A 2003 Sep 16;100(19):10989-94.

(162) Mancao C, Altmann M, Jungnickel B, Hammerschmidt W. Rescue of "crippled" germinal center B cells from apoptosis by Epstein-Barr virus. Blood 2005 Dec 15;106(13):4339-44.

(163) Bechtel D, Kurth J, Unkel C, Kuppers R. Transformation of BCR-deficient germinal-center B cells by EBV supports a major role of the virus in the pathogenesis of Hodgkin and posttransplantation lymphomas. Blood 2005 Dec 15;106(13):4345-50.

(164) Chaganti S, Bell AI, Pastor NB, Milner AE, Drayson M, Gordon J, et al. Epstein-Barr virus infection in vitro can rescue germinal center B cells with inactivated immunoglobulin genes. Blood 2005 Dec 15;106(13):4249-52.

(165) Mancao C, Hammerschmidt W. Epstein-Barr virus latent membrane protein 2A is a B-cell receptor mimic and essential for B-cell survival. Blood 2007 Nov 15;110(10):3715-21.

(166) Caldwell RG, Wilson JB, Anderson SJ, Longnecker R. Epstein-Barr virus LMP2A drives B cell development and survival in the absence of normal B cell receptor signals. Immunity 1998 Sep;9(3):405-11.

(167) Kilger E, Kieser A, Baumann M, Hammerschmidt W. Epstein-Barr virus-mediated B-cell proliferation is dependent upon latent membrane protein 1, which simulates an activated CD40 receptor. EMBO J 1998 Mar 16;17(6):1700-9.

(168) Kulwichit W, Edwards RH, Davenport EM, Baskar JF, Godfrey V, Raab-Traub N. Expression of the Epstein-Barr virus latent membrane protein 1 induces B cell lymphoma in transgenic mice. Proc Natl Acad Sci U S A 1998 Sep 29;95(20):11963-8.

(169) Miller CL, Lee JH, Kieff E, Burkhardt AL, Bolen JB, Longnecker R. Epstein-Barr virus protein LMP2A regulates reactivation from latency by negatively regulating tyrosine kinases involved in sIg-mediated signal transduction. Infect Agents Dis 1994 Apr;3(2-3):128-36.

(170) Miller CL, Lee JH, Kieff E, Longnecker R. An integral membrane protein (LMP2) blocks reactivation of Epstein-Barr virus from latency following surface immunoglobulin crosslinking. Proc Natl Acad Sci U S A 1994 Jan 18;91(2):772-6.

(171) Portis T, Dyck P, Longnecker R. Epstein-Barr Virus (EBV) LMP2A induces alterations in gene transcription similar to those observed in Reed-Sternberg cells of Hodgkin lymphoma. Blood 2003 Dec 1;102(12):4166-78.

(172) Vockerodt M, Morgan SL, Kuo M, Wei W, Chukwuma MB, Arrand JR, et al. The Epstein-Barr virus oncoprotein, latent membrane protein-1, reprograms germinal centre B cells towards a Hodgkin's Reed-Sternberg-like phenotype. J Pathol 2008 Sep;216(1):83-92.

(173) Herbst H, Foss HD, Samol J, Araujo I, Klotzbach H, Krause H, et al. Frequent expression of interleukin-10 by Epstein-Barr virus-harboring tumor cells of Hodgkin's disease. Blood 1996 Apr 1;87(7):2918-29.

(174) Baumforth KR, Birgersdotter A, Reynolds GM, Wei W, Kapatai G, Flavell JR, et al. Expression of the Epstein-Barr virus-encoded Epstein-Barr virus nuclear antigen 1 in Hodgkin's lymphoma cells mediates Up-regulation of CCL20 and the migration of regulatory T cells. Am J Pathol 2008 Jul;173(1):195-204.

(175) Lemmon MA, Schlessinger J. Cell signaling by receptor tyrosine kinases. Cell 2010 Jun 25;141(7):1117-34.

(176) Wehrman T, He X, Raab B, Dukipatti A, Blau H, Garcia KC. Structural and mechanistic insights into nerve growth factor interactions with the TrkA and p75 receptors. Neuron 2007 Jan 4;53(1):25-38.

(177) Liu H, Chen X, Focia PJ, He X. Structural basis for stem cell factor-KIT signaling and activation of class III receptor tyrosine kinases. EMBO J 2007 Feb 7;26(3):891-901.

(178) Yuzawa S, Opatowsky Y, Zhang Z, Mandiyan V, Lax I, Schlessinger J. Structural basis for activation of the receptor tyrosine kinase KIT by stem cell factor. Cell 2007 Jul 27;130(2):323-34.

(179) Spivak-Kroizman T, Lemmon MA, Dikic I, Ladbury JE, Pinchasi D, Huang J, et al. Heparin-induced oligomerization of FGF molecules is responsible for FGF receptor dimerization, activation, and cell proliferation. Cell 1994 Dec 16;79(6):1015-24.

(180) Ogiso H, Ishitani R, Nureki O, Fukai S, Yamanaka M, Kim JH, et al. Crystal structure of the complex of human epidermal growth factor and receptor extracellular domains. Cell 2002 Sep 20;110(6):775-87.

(181) Nolen B, Taylor S, Ghosh G. Regulation of protein kinases; controlling activity through activation segment conformation. Mol Cell 2004 Sep 10;15(5):661-75.

(182) Ward C, Lawrence M, Streltsov V, Garrett T, McKern N, Lou MZ, et al. Structural insights into ligand-induced activation of the insulin receptor. Acta Physiol (Oxf) 2008 Jan;192(1):3-9.

(183) Shewchuk LM, Hassell AM, Ellis B, Holmes WD, Davis R, Horne EL, et al. Structure of the Tie2 RTK domain: self-inhibition by the nucleotide binding loop, activation loop, and C-terminal tail. Structure 2000 Nov 15;8(11):1105-13.

(184) Niu XL, Peters KG, Kontos CD. Deletion of the carboxyl terminus of Tie2 enhances kinase activity, signaling, and function. Evidence for an autoinhibitory mechanism. J Biol Chem 2002 Aug 30;277(35):31768-73.

(185) Wybenga-Groot LE, Baskin B, Ong SH, Tong J, Pawson T, Sicheri F. Structural basis for autoinhibition of the Ephb2 receptor tyrosine kinase by the unphosphorylated juxtamembrane region. Cell 2001 Sep 21;106(6):745-57.

(186) Herbst R, Burden SJ. The juxtamembrane region of MuSK has a critical role in agrin-mediated signaling. EMBO J 2000 Jan 4;19(1):67-77.

(187) Till JH, Becerra M, Watty A, Lu Y, Ma Y, Neubert TA, et al. Crystal structure of the MuSK tyrosine kinase: insights into receptor autoregulation. Structure 2002 Sep;10(9):1187-96.

(188) Nakamura T, Sanokawa R, Sasaki Y, Ayusawa D, Oishi M, Mori N. N-Shc: a neural-specific adapter molecule that mediates signaling from neurotrophin/Trk to Ras/MAPK pathway. Oncogene 1996 Sep 19;13(6):1111-21.

(189) Schmucker D, Clemens JC, Shu H, Worby CA, Xiao J, Muda M, et al. Drosophila Dscam is an axon guidance receptor exhibiting extraordinary molecular diversity. Cell 2000 Jun 9;101(6):671-84.

(190) Pajares MJ, Ezponda T, Catena R, Calvo A, Pio R, Montuenga LM. Alternative splicing: an emerging topic in molecular and clinical oncology. Lancet Oncol 2007 Apr;8(4):349-57.

(191) Black DL. Mechanisms of alternative pre-messenger RNA splicing. Annu Rev Biochem 2003;72:291-336.

(192) Itoh N, Ornitz DM. Evolution of the Fgf and Fgfr gene families. Trends Genet 2004 Nov;20(11):563-9.

(193) L'hote CG, Knowles MA. Cell responses to FGFR3 signalling: growth, differentiation and apoptosis. Exp Cell Res 2005 Apr 1;304(2):417-31.

(194) Diaz-Rodriguez E, Cabrera N, Esparis-Ogando A, Montero JC, Pandiella A. Cleavage of the TrkA neurotrophin receptor by multiple metalloproteases generates signalling-competent truncated forms. Eur J Neurosci 1999 Apr;11(4):1421-30.

(195) Jin P, Zhang J, Sumariwalla PF, Ni I, Jorgensen B, Crawford D, et al. Novel splice variants derived from the receptor tyrosine kinase superfamily are potential therapeutics for rheumatoid arthritis. Arthritis Res Ther 2008;10(4):R73.

(196) Cartegni L, Chew SL, Krainer AR. Listening to silence and understanding nonsense: exonic mutations that affect splicing. Nat Rev Genet 2002 Apr;3(4):285-98.

(197) Faustino NA, Cooper TA. Pre-mRNA splicing and human disease. Genes Dev 2003 Feb 15;17(4):419-37.

(198) Chen LL, Sabripour M, Wu EF, Prieto VG, Fuller GN, Frazier ML. A mutation-created novel intra-exonic pre-mRNA splice site causes constitutive activation of KIT in human gastrointestinal stromal tumors. Oncogene 2005 Jun 16;24(26):4271-80.

(199) Collesi C, Santoro MM, Gaudino G, Comoglio PM. A splicing variant of the RON transcript induces constitutive tyrosine kinase activity and an invasive phenotype. Mol Cell Biol 1996 Oct;16(10):5518-26.

(200) Ghigna C, Giordano S, Shen H, Benvenuto F, Castiglioni F, Comoglio PM, et al. Cell motility is controlled by SF2/ASF through alternative splicing of the Ron protooncogene. Mol Cell 2005 Dec 22;20(6):881-90.

(201) Karni R, de SE, Lowe SW, Sinha R, Mu D, Krainer AR. The gene encoding the splicing factor SF2/ASF is a proto-oncogene. Nat Struct Mol Biol 2007 Mar;14(3):185-93.

(202) Blume-Jensen P, Hunter T. Oncogenic kinase signalling. Nature 2001 May 17;411(6835):355-65.

(203) Barros FF, Powe DG, Ellis IO, Green AR. Understanding the HER family in breast cancer: interaction with ligands, dimerization and treatments. Histopathology 2010 Apr;56(5):560-72.

(204) Suo Z, Risberg B, Kalsson MG, Willman K, Tierens A, Skovlund E, et al. EGFR family expression in breast carcinomas. c-erbB-2 and c-erbB-4 receptors have different effects on survival. J Pathol 2002 Jan;196(1):17-25.

(205) Joensuu H. Gastrointestinal stromal tumor (GIST). Ann Oncol 2006 Sep;17 Suppl 10:x280-x286.

(206) Piao X, Paulson R, van der Geer P, Pawson T, Bernstein A. Oncogenic mutation in the Kit receptor tyrosine kinase alters substrate specificity and induces degradation of the protein tyrosine phosphatase SHP-1. Proc Natl Acad Sci U S A 1996 Dec 10;93(25):14665-9.

(207) Taniguchi M, Nishida T, Hirota S, Isozaki K, Ito T, Nomura T, et al. Effect of c-kit mutation on prognosis of gastrointestinal stromal tumors. Cancer Res 1999 Sep 1;59(17):4297-300.

(208) Stirewalt DL, Radich JP. The role of FLT3 in haematopoietic malignancies. Nat Rev Cancer 2003 Sep;3(9):650-65.

(209) Kiyoi H, Towatari M, Yokota S, Hamaguchi M, Ohno R, Saito H, et al. Internal tandem duplication of the FLT3 gene is a novel modality of elongation mutation which causes constitutive activation of the product. Leukemia 1998 Sep;12(9):1333-7.

(210) Schnittger S, Schoch C, Dugas M, Kern W, Staib P, Wuchter C, et al. Analysis of FLT3 length mutations in 1003 patients with acute myeloid leukemia: correlation to cytogenetics, FAB subtype, and prognosis in the AMLCG study and usefulness as a marker for the detection of minimal residual disease. Blood 2002 Jul 1;100(1):59-66.

(211) Veeriah S, Brennan C, Meng S, Singh B, Fagin JA, Solit DB, et al. The tyrosine phosphatase PTPRD is a tumor suppressor that is frequently inactivated and mutated in glioblastoma and other human cancers. Proc Natl Acad Sci U S A 2009 Jun 9;106(23):9435-40.

(212) Xu Y, Baker D, Quan T, Baldassare JJ, Voorhees JJ, Fisher GJ. Receptor type protein tyrosine phosphatase-kappa mediates cross-talk between transforming growth factor-beta and epidermal growth factor receptor signaling pathways in human keratinocytes. Mol Biol Cell 2010 Jan 1;21(1):29-35.

(213) Flavell JR, Baumforth KR, Wood VH, Davies GL, Wei W, Reynolds GM, et al. Down-regulation of the TGF-beta target gene, PTPRK, by the Epstein-Barr virus encoded EBNA1 contributes to the growth and survival of Hodgkin lymphoma cells. Blood 2008 Jan 1;111(1):292-301.

(214) Bache KG, Slagsvold T, Stenmark H. Defective downregulation of receptor tyrosine kinases in cancer. EMBO J 2004 Jul 21;23(14):2707-12.

(215) Gur G, Rubin C, Katz M, Amit I, Citri A, Nilsson J, et al. LRIG1 restricts growth factor signaling by enhancing receptor ubiquitylation and degradation. EMBO J 2004 Aug 18;23(16):3270-81.

(216) Laederich MB, Funes-Duran M, Yen L, Ingalla E, Wu X, Carraway KL, III, et al. The leucine-rich repeat protein LRIG1 is a negative regulator of ErbB family receptor tyrosine kinases. J Biol Chem 2004 Nov 5;279(45):47050-6.

(217) Hedman H, Nilsson J, Guo D, Henriksson R. Is LRIG1 a tumour suppressor gene at chromosome 3p14.3? Acta Oncol 2002;41(4):352-4.

(218) Thomasson M, Wang B, Hammarsten P, Dahlman A, Persson JL, Josefsson A, et al. LRIG1 and the liar paradox in prostate cancer: A study of the expression and clinical significance of LRIG1 in prostate cancer. Int J Cancer 2010 Dec 2.

(219) Ljuslinder I, Malmer B, Golovleva I, Thomasson M, Grankvist K, Hockenstrom T, et al. Increased copy number at 3p14 in breast cancer. Breast Cancer Res 2005;7(5):R719-R727.

(220) Satterthwaite A, Witte O. Genetic analysis of tyrosine kinase function in B cell development. Annu Rev Immunol 1996;14:131-54.

(221) Fleming HE, Paige CJ. Cooperation between IL-7 and the pre-B cell receptor: a key to B cell selection. Semin Immunol 2002 Dec;14(6):423-30.

(222) Middendorp S, Dingjan GM, Hendriks RW. Impaired precursor B cell differentiation in Bruton's tyrosine kinase-deficient mice. J Immunol 2002 Mar 15;168(6):2695-703.

(223) Gauld SB, Cambier JC. Src-family kinases in B-cell development and signaling. Oncogene 2004 Oct 18;23(48):8001-6.

(224) Ogawa M, ten BE, Melchers F. Identification of CD19(-)B220(+)c-Kit(+)Flt3/Flk-2(+)cells as early B lymphoid precursors before pre-B-I cells in juvenile mouse bone marrow. Int Immunol 2000 Mar;12(3):313-24.

(225) Ogawa M, Sugawara S, Kunisada T, Sudo T, Hayashi S, Nishikawa S, et al. Flt3/Flk-2 and c-Kit are not essential for the proliferation of B lymphoid progenitor cells in the bone marrow of the adult mouse. Exp Hematol 1998 Jun;26(6):478-88.

(226) Li LX, Goetz CA, Katerndahl CD, Sakaguchi N, Farrar MA. A Flt3- and Ras-dependent pathway primes B cell development by inducing a state of IL-7 responsiveness. J Immunol 2010 Feb 15;184(4):1728-36.

(227) Coppola V, Barrick CA, Southon EA, Celeste A, Wang K, Chen B, et al. Ablation of TrkA function in the immune system causes B cell abnormalities. Development 2004 Oct;131(20):5185-95.

(228) van d, V, Taher TE, Keehnen RM, Smit L, Groenink M, Pals ST. Paracrine regulation of germinal center B cell adhesion through the c-met-hepatocyte growth factor/scatter factor pathway. J Exp Med 1997 Jun 16;185(12):2121-31.

(229) Weimar IS, de JD, Muller EJ, Nakamura T, van Gorp JM, de Gast GC, et al. Hepatocyte growth factor/scatter factor promotes adhesion of lymphoma cells to extracellular matrix molecules via alpha 4 beta 1 and alpha 5 beta 1 integrins. Blood 1997 Feb 1;89(3):990-1000.

(230) Gordin M, Tesio M, Cohen S, Gore Y, Lantner F, Leng L, et al. c-Met and its ligand hepatocyte growth factor/scatter factor regulate mature B cell survival in a pathway induced by CD74. J Immunol 2010 Aug 15;185(4):2020-31.

(231) Khnykin D, Troen G, Berner JM, Delabie J. The expression of fibroblast growth factors and their receptors in Hodgkin's lymphoma. J Pathol 2006 Feb;208(3):431-8.

(232) Renne C, Willenbrock K, Kuppers R, Hansmann ML, Brauninger A. Autocrine- and paracrine-activated receptor tyrosine kinases in classic Hodgkin lymphoma. Blood 2005 May 15;105(10):4051-9.

(233) Renne C, Hinsch N, Willenbrock K, Fuchs M, Klapper W, Engert A, et al. The aberrant coexpression of several receptor tyrosine kinases is largely restricted to EBV-negative cases of classical Hodgkin's lymphoma. Int J Cancer 2007 Jun 1;120(11):2504-9.

(234) Renne C, Minner S, Kuppers R, Hansmann ML, Brauninger A. Autocrine NGFbeta/TRKA signalling is an important survival factor for Hodgkin lymphoma derived cell lines. Leuk Res 2008 Jan;32(1):163-7.

(235) Pinto A, Gloghini A, Gattei V, Aldinucci D, Zagonel V, Carbone A. Expression of the c-kit receptor in human lymphomas is restricted to Hodgkin's disease and CD30+ anaplastic large cell lymphomas. Blood 1994 Feb 1;83(3):785-92.

(236) Aldinucci D, Poletto D, Nanni P, Degan M, Gloghini A, Di FR, et al. Hodgkin and Reed-Sternberg cells express functional c-kit receptors and interact with primary fibroblasts from Hodgkin's disease-involved lymph nodes through soluble and membrane-bound stem cell factor. Br J Haematol 2002 Sep;118(4):1055-64.

(237) Canioni D, Deau-Fischer B, Taupin P, Ribrag V, Delarue R, Bosq J, et al. Prognostic significance of new immunohistochemical markers in refractory classical Hodgkin lymphoma: a study of 59 cases. PLoS One 2009;4(7):e6341.

(238) Rassidakis GZ, Georgakis GV, Younes A, Medeiros LJ. c-kit is not expressed in Hodgkin disease and anaplastic lymphoma kinase (ALK)-positive anaplastic large cell lymphoma. Blood 2003 Dec 15;102(13):4619-20.

(239) Re D, Wickenhauser C, Ahmadi T, Buchdunger E, Kochanek M, Diehl V, et al. Preclinical evaluation of the antiproliferative potential of STI571 in Hodgkin's disease. Br J Cancer 2002 Apr 22;86(8):1333-5.

(240) Lamprecht B, Walter K, Kreher S, Kumar R, Hummel M, Lenze D, et al. Derepression of an endogenous long terminal repeat activates the CSF1R proto-oncogene in human lymphoma. Nat Med 2010 May;16(5):571-9, 1p.

(241) Naldini L, Vigna E, Narsimhan RP, Gaudino G, Zarnegar R, Michalopoulos GK, et al. Hepatocyte growth factor (HGF) stimulates the tyrosine kinase activity of the receptor encoded by the proto-oncogene c-MET. Oncogene 1991 Apr;6(4):501-4.

(242) Ferracini R, Longati P, Naldini L, Vigna E, Comoglio PM. Identification of the major autophosphorylation site of the Met/hepatocyte growth factor receptor tyrosine kinase. J Biol Chem 1991 Oct 15;266(29):19558-64.

(243) Longati P, Bardelli A, Ponzetto C, Naldini L, Comoglio PM. Tyrosines1234-1235 are critical for activation of the tyrosine kinase encoded by the MET proto-oncogene (HGF receptor). Oncogene 1994 Jan;9(1):49-57.

(244) Naldini L, Vigna E, Ferracini R, Longati P, Gandino L, Prat M, et al. The tyrosine kinase encoded by the MET proto-oncogene is activated by autophosphorylation. Mol Cell Biol 1991 Apr;11(4):1793-803.

(245) Bardelli A, Longati P, Williams TA, Benvenuti S, Comoglio PM. A peptide representing the carboxyl-terminal tail of the met receptor inhibits kinase activity and invasive growth. J Biol Chem 1999 Oct 8;274(41):29274-81.

(246) Trusolino L, Bertotti A, Comoglio PM. MET signalling: principles and functions in development, organ regeneration and cancer. Nat Rev Mol Cell Biol 2010 Dec;11(12):834-48.

(247) Thien CB, Langdon WY. Cbl: many adaptations to regulate protein tyrosine kinases. Nat Rev Mol Cell Biol 2001 Apr;2(4):294-307.

(248) Abella JV, Peschard P, Naujokas MA, Lin T, Saucier C, Urbe S, et al. Met/Hepatocyte growth factor receptor ubiquitination suppresses transformation and is required for Hrs phosphorylation. Mol Cell Biol 2005 Nov;25(21):9632-45.

(249) Peschard P, Fournier TM, Lamorte L, Naujokas MA, Band H, Langdon WY, et al. Mutation of the c-Cbl TKB domain binding site on the Met receptor tyrosine kinase converts it into a transforming protein. Mol Cell 2001 Nov;8(5):995-1004.

(250) Shattuck DL, Miller JK, Laederich M, Funes M, Petersen H, Carraway KL, III, et al. LRIG1 is a novel negative regulator of the Met receptor and opposes Met and Her2 synergy. Mol Cell Biol 2007 Mar;27(5):1934-46.

(251) Trusolino L, Comoglio PM. Scatter-factor and semaphorin receptors: cell signalling for invasive growth. Nat Rev Cancer 2002 Apr;2(4):289-300.

(252) Rong S, Segal S, Anver M, Resau JH, Vande Woude GF. Invasiveness and metastasis of NIH 3T3 cells induced by Met-hepatocyte growth factor/scatter factor autocrine stimulation. Proc Natl Acad Sci U S A 1994 May 24;91(11):4731-5.

(253) Giordano S, Maffe A, Williams TA, Artigiani S, Gual P, Bardelli A, et al. Different point mutations in the met oncogene elicit distinct biological properties. FASEB J 2000 Feb;14(2):399-406.

(254) Michieli P, Basilico C, Pennacchietti S, Maffe A, Tamagnone L, Giordano S, et al. Mutant Met-mediated transformation is ligand-dependent and can be inhibited by HGF antagonists. Oncogene 1999 Sep 16;18(37):5221-31.

(255) Onozato R, Kosaka T, Kuwano H, Sekido Y, Yatabe Y, Mitsudomi T. Activation of MET by gene amplification or by splice mutations deleting the juxtamembrane domain in primary resected lung cancers. J Thorac Oncol 2009 Jan;4(1):5-11.

(256) Jucker M, Schaadt M, Diehl V, Poppema S, Jones D, Tesch H. Heterogeneous expression of proto-oncogenes in Hodgkin's disease derived cell lines. Hematol Oncol 1990 Jul;8(4):191-204.

(257) Jucker M, Gunther A, Gradl G, Fonatsch C, Krueger G, Diehl V, et al. The Met/hepatocyte growth factor receptor (HGFR) gene is overexpressed in some cases of human leukemia and lymphoma. Leuk Res 1994 Jan;18(1):7-16.

(258) Pons E, Uphoff CC, Drexler HG. Expression of hepatocyte growth factor and its receptor c-met in human leukemia-lymphoma cell lines. Leuk Res 1998 Sep;22(9):797-804.

(259) Teofili L, Di Febo AL, Pierconti F, Maggiano N, Bendandi M, Rutella S, et al. Expression of the c-met proto-oncogene and its ligand, hepatocyte growth factor, in Hodgkin disease. Blood 2001 Feb 15;97(4):1063-9.

(260) Mathas S, Hinz M, Anagnostopoulos I, Krappmann D, Lietz A, Jundt F, et al. Aberrantly expressed c-Jun and JunB are a hallmark of Hodgkin lymphoma cells, stimulate proliferation and synergize with NF-kappa B. EMBO J 2002 Aug 1;21(15):4104-13.

(261) Gaudino G, Follenzi A, Naldini L, Collesi C, Santoro M, Gallo KA, et al. RON is a heterodimeric tyrosine kinase receptor activated by the HGF homologue MSP. EMBO J 1994 Aug 1;13(15):3524-32.

(262) Follenzi A, Bakovic S, Gual P, Stella MC, Longati P, Comoglio PM. Cross-talk between the proto-oncogenes Met and Ron. Oncogene 2000 Jun 22;19(27):3041-9.

(263) Cheng HL, Liu HS, Lin YJ, Chen HH, Hsu PY, Chang TY, et al. Co-expression of RON and MET is a prognostic indicator for patients with transitional-cell carcinoma of the bladder. Br J Cancer 2005 May 23;92(10):1906-14.

(264) Maggiora P, Lorenzato A, Fracchioli S, Costa B, Castagnaro M, Arisio R, et al. The RON and MET oncogenes are co-expressed in human ovarian carcinomas and cooperate in activating invasiveness. Exp Cell Res 2003 Aug 15;288(2):382-9.

(265) Vogel W, Brakebusch C, Fassler R, Alves F, Ruggiero F, Pawson T. Discoidin domain receptor 1 is activated independently of beta(1) integrin. J Biol Chem 2000 Feb 25;275(8):5779-84.

(266) Abdulhussein R, Koo DH, Vogel WF. Identification of disulfide-linked dimers of the receptor tyrosine kinase DDR1. J Biol Chem 2008 May 2;283(18):12026-33.

(267) L'hote CG, Thomas PH, Ganesan TS. Functional analysis of discoidin domain receptor 1: effect of adhesion on DDR1 phosphorylation. FASEB J 2002 Feb;16(2):234-6.

(268) Alves F, Saupe S, Ledwon M, Schaub F, Hiddemann W, Vogel WF. Identification of two novel, kinase-deficient variants of discoidin domain receptor 1: differential expression in human colon cancer cell lines. FASEB J 2001 May;15(7):1321-3.

(269) Foehr ED, Tatavos A, Tanabe E, Raffioni S, Goetz S, Dimarco E, et al. Discoidin domain receptor 1 (DDR1) signaling in PC12 cells: activation of juxtamembrane domains in PDGFR/DDR/TrkA chimeric receptors. FASEB J 2000 May;14(7):973-81.

(270) Kamohara H, Yamashiro S, Galligan C, Yoshimura T. Discoidin domain receptor 1 isoform-a (DDR1alpha) promotes migration of leukocytes in three-dimensional collagen lattices. FASEB J 2001 Dec;15(14):2724-6.

(271) Perez JL, Shen X, Finkernagel S, Sciorra L, Jenkins NA, Gilbert DJ, et al. Identification and chromosomal mapping of a receptor tyrosine kinase with a putative phospholipid binding sequence in its ectodomain. Oncogene 1994 Jan;9(1):211-9.

(272) Sakuma S, Saya H, Tada M, Nakao M, Fujiwara T, Roth JA, et al. Receptor protein tyrosine kinase DDR is up-regulated by p53 protein. FEBS Lett 1996 Dec 2;398(2-3):165-9.

(273) Abdulhussein R, McFadden C, Fuentes-Prior P, Vogel WF. Exploring the collagen-binding site of the DDR1 tyrosine kinase receptor. J Biol Chem 2004 Jul 23;279(30):31462-70.

(274) Hachehouche LN, Chetoui N, Aoudjit F. Implication of discoidin domain receptor 1 in T cell migration in three-dimensional collagen. Mol Immunol 2010 May;47(9):1866-9.

(275) Wang CZ, Hsu YM, Tang MJ. Function of discoidin domain receptor I in HGF-induced branching tubulogenesis of MDCK cells in collagen gel. J Cell Physiol 2005 Apr;203(1):295-304.

(276) Flynn LA, Blissett AR, Calomeni EP, Agarwal G. Inhibition of collagen fibrillogenesis by cells expressing soluble extracellular domains of DDR1 and DDR2. J Mol Biol 2010 Jan 22;395(3):533-43.

(277) Koo DH, McFadden C, Huang Y, Abdulhussein R, Friese-Hamim M, Vogel WF. Pinpointing phosphotyrosine-dependent interactions downstream of the collagen receptor DDR1. FEBS Lett 2006 Jan 9;580(1):15-22.

(278) Yang SH, Baek HA, Lee HJ, Park HS, Jang KY, Kang MJ, et al. Discoidin domain receptor 1 is associated with poor prognosis of non-small cell lung carcinomas. Oncol Rep 2010 Aug;24(2):311-9.

(279) Shimada K, Nakamura M, Ishida E, Higuchi T, Yamamoto H, Tsujikawa K, et al. Prostate cancer antigen-1 contributes to cell survival and invasion though discoidin receptor 1 in human prostate cancer. Cancer Sci 2008 Jan;99(1):39-45.

(280) Chiaretti S, Li X, Gentleman R, Vitale A, Wang KS, Mandelli F, et al. Gene expression profiles of B-lineage adult acute lymphocytic leukemia reveal genetic patterns that identify lineage derivation and distinct mechanisms of transformation. Clin Cancer Res 2005 Oct 15;11(20):7209-19.

(281) Tomasson MH, Xiang Z, Walgren R, Zhao Y, Kasai Y, Miner T, et al. Somatic mutations and germline sequence variants in the expressed tyrosine kinase genes of patients with de novo acute myeloid leukemia. Blood 2008 May 1;111(9):4797-808.

(282) Das S, Ongusaha PP, Yang YS, Park JM, Aaronson SA, Lee SW. Discoidin domain receptor 1 receptor tyrosine kinase induces cyclooxygenase-2 and promotes chemoresistance through nuclear factor-kappaB pathway activation. Cancer Res 2006 Aug 15;66(16):8123-30.

(283) Kim HG, Hwang SY, Aaronson SA, Mandinova A, Lee SW. DDR1 receptor tyrosine kinase promotes prosurvival pathway through Notch1 activation. J Biol Chem 2011 Mar 13.

(284) Weinstein IB, Joe A. Oncogene addiction. Cancer Res 2008 May 1;68(9):3077-80.

(285) Felsher DW, Bishop JM. Reversible tumorigenesis by MYC in hematopoietic lineages. Mol Cell 1999 Aug;4(2):199-207.

(286) Pegram MD, Lipton A, Hayes DF, Weber BL, Baselga JM, Tripathy D, et al. Phase II study of receptor-enhanced chemosensitivity using recombinant humanized anti-p185HER2/neu monoclonal antibody plus cisplatin in patients with HER2/neu-overexpressing metastatic breast cancer refractory to chemotherapy treatment. J Clin Oncol 1998 Aug;16(8):2659-71.

(287) Druker BJ. Translation of the Philadelphia chromosome into therapy for CML. Blood 2008 Dec 15;112(13):4808-17.

(288) Druker BJ, Guilhot F, O'Brien SG, Gathmann I, Kantarjian H, Gattermann N, et al. Five-year follow-up of patients receiving imatinib for chronic myeloid leukemia. N Engl J Med 2006 Dec 7;355(23):2408-17.

(289) O'Brien SG, Guilhot F, Larson RA, Gathmann I, Baccarani M, Cervantes F, et al. Imatinib compared with interferon and low-dose cytarabine for newly diagnosed chronic-phase chronic myeloid leukemia. N Engl J Med 2003 Mar 13;348(11):994-1004.

(290) Bixby D, Talpaz M. Seeking the causes and solutions to imatinib-resistance in chronic myeloid leukemia. Leukemia 2011 Jan;25(1):7-22.

(291) Xu AM, Huang PH. Receptor tyrosine kinase coactivation networks in cancer. Cancer Res 2010 May 15;70(10):3857-60.

(292) Stommel JM, Kimmelman AC, Ying H, Nabioullin R, Ponugoti AH, Wiedemeyer R, et al. Coactivation of receptor tyrosine kinases affects the response of tumor cells to targeted therapies. Science 2007 Oct 12;318(5848):287-90.

(293) Krause DS, Van Etten RA. Tyrosine kinases as targets for cancer therapy. N Engl J Med 2005 Jul 14;353(2):172-87.

(294) Demetri GD, von MM, Blanke CD, Van den Abbeele AD, Eisenberg B, Roberts PJ, et al. Efficacy and safety of imatinib mesylate in advanced gastrointestinal stromal tumors. N Engl J Med 2002 Aug 15;347(7):472-80.

(295) Rix U, Hantschel O, Durnberger G, Remsing Rix LL, Planyavsky M, Fernbach NV, et al. Chemical proteomic profiles of the BCR-ABL inhibitors imatinib, nilotinib, and dasatinib reveal novel kinase and nonkinase targets. Blood 2007 Dec 1;110(12):4055-63.

(296) Diehl V, Kirchner HH, Burrichter H, Stein H, Fonatsch C, Gerdes J, et al. Characteristics of Hodgkin's disease-derived cell lines. Cancer Treat Rep 1982 Apr;66(4):615-32.

(297) Wolf J, Kapp U, Bohlen H, Kornacker M, Schoch C, Stahl B, et al. Peripheral blood mononuclear cells of a patient with advanced Hodgkin's lymphoma give rise to permanently growing Hodgkin-Reed Sternberg cells. Blood 1996 Apr 15;87(8):3418-28.

(298) Drexler HG, Leber BF, Norton J, Yaxley J, Tatsumi E, Hoffbrand AV, et al. Genotypes and immunophenotypes of Hodgkin's disease-derived cell lines. Leukemia 1988 Jun;2(6):371-6.

(299) Falk MH, Tesch H, Stein H, Diehl V, Jones DB, Fonatsch C, et al. Phenotype versus immunoglobulin and T-cell receptor genotype of Hodgkin-derived cell lines: activation of immature lymphoid cells in Hodgkin's disease. Int J Cancer 1987 Aug 15;40(2):262-9.

(300) Schaadt M, Diehl V, Stein H, Fonatsch C, Kirchner HH. Two neoplastic cell lines with unique features derived from Hodgkin's disease. Int J Cancer 1980 Dec 15;26(6):723-31.

(301) Kamesaki H, Fukuhara S, Tatsumi E, Uchino H, Yamabe H, Miwa H, et al. Cytochemical, immunologic, chromosomal, and molecular genetic analysis of a novel cell line derived from Hodgkin's disease. Blood 1986 Jul;68(1):285-92.

(302) Ben-Bassat H, Goldblum N, Mitrani S, Goldblum T, Yoffey JM, Cohen MM, et al. Establishment in continuous culture of a new type of lymphocyte from a "Burkitt like" malignant lymphoma (line D.G.-75). Int J Cancer 1977 Jan;19(1):27-33.

(303) Lenoir GM, Vuillaume M, Bonnardel C. The use of lymphomatous and lymphoblastoid cell lines in the study of Burkitt's lymphoma. IARC Sci Publ 1985;(60):309-18.

(304) Bertrand S, Berger R, Philip T, Bernheim A, Bryon PA, Bertoglio J, et al. Variant translocation in a non endemic case of Burkitt's lymphoma: t (8;22) in an Epstein--Barr virus negative tumour and in a derived cell line. Eur J Cancer 1981 May;17(5):577-84.

(305) Denepoux S, Razanajaona D, Blanchard D, Meffre G, Capra JD, Banchereau J, et al. Induction of somatic mutation in a human B cell line in vitro. Immunity 1997 Jan;6(1):35-46.

(306) Menezes J, Leibold W, Klein G, Clements G. Establishment and characterization of an Epstein-Barr virus (EBC)-negative lymphoblastoid B cell line (BJA-B) from an exceptional, EBV-genome-negative African Burkitt's lymphoma. Biomedicine 1975 Jul;22(4):276-84.

(307) Lozzio CB, Lozzio BB. Human chronic myelogenous leukemia cell-line with positive Philadelphia chromosome. Blood 1975 Mar;45(3):321-34.

(308) Brattain MG, Fine WD, Khaled FM, Thompson J, Brattain DE. Heterogeneity of malignant cells from a human colonic carcinoma. Cancer Res 1981 May;41(5):1751-6.

(309) Livak KJ, Schmittgen TD. Analysis of relative gene expression data using real-time quantitative PCR and the 2(-Delta Delta C(T)) Method. Methods 2001 Dec;25(4):402-8.

(310) Rieseberg M, Kasper C, Reardon KF, Scheper T. Flow cytometry in biotechnology. Appl Microbiol Biotechnol 2001 Aug;56(3-4):350-60.

(311) Vanags DM, Porn-Ares MI, Coppola S, Burgess DH, Orrenius S. Protease involvement in fodrin cleavage and phosphatidylserine exposure in apoptosis. J Biol Chem 1996 Dec 6;271(49):31075-85.

(312) Takeda S, Shimizu T, Rodewald HR. Interactions between c-kit and stem cell factor are not required for B-cell development in vivo. Blood 1997 Jan 15;89(2):518-25.

(313) Brown RE, Nazmi RK. The Reed-Steinberg cell: molecular characterization by proteomic analysis with therapeutic implications. Ann Clin Lab Sci 2002;32(4):339-51.

(314) Moreau A, Praloran V, Berrada L, Coupey L, Gaillard F. Immunohistochemical detection of cells positive for colony-stimulating factor 1 in lymph nodes from reactive lymphadenitis, and Hodgkin's disease. Leukemia 1992 Feb;6(2):126-30.

(315) Giles FJ, Vose JM, Do KA, Johnson MM, Manshouri T, Bociek G, et al. Clinical relevance of circulating angiogenic factors in patients with non-Hodgkin's lymphoma or Hodgkin's lymphoma. Leuk Res 2004 Jun;28(6):595-604.

(316) Horikawa T, Sheen TS, Takeshita H, Sato H, Furukawa M, Yoshizaki T. Induction of c-Met proto-oncogene by Epstein-Barr virus latent membrane protein-1 and the correlation with cervical lymph node metastasis of nasopharyngeal carcinoma. Am J Pathol 2001 Jul;159(1):27-33.

(317) Bardelli A, Longati P, Gramaglia D, Stella MC, Comoglio PM. Gab1 coupling to the HGF/Met receptor multifunctional docking site requires binding of Grb2 and correlates with the transforming potential. Oncogene 1997 Dec 18;15(25):3103-11.

(318) Lu Y, Yao HP, Wang MH. Multiple variants of the RON receptor tyrosine kinase: biochemical properties, tumorigenic activities, and potential drug targets. Cancer Lett 2007 Nov 18;257(2):157-64.

(319) Brune V, Tiacci E, Pfeil I, Doring C, Eckerle S, van Noesel CJ, et al. Origin and pathogenesis of nodular lymphocyte-predominant Hodgkin lymphoma as revealed by global gene expression analysis. J Exp Med 2008 Sep 29;205(10):2251-68.

(320) Guo A, Villen J, Kornhauser J, Lee KA, Stokes MP, Rikova K, et al. Signaling networks assembled by oncogenic EGFR and c-Met. Proc Natl Acad Sci U S A 2008 Jan 15;105(2):692-7.

(321) Campbell TN, Robbins SM. The Eph receptor/ephrin system: an emerging player in the invasion game. Curr Issues Mol Biol 2008;10(1-2):61-6.

(322) Furge KA, Zhang YW, Vande Woude GF. Met receptor tyrosine kinase: enhanced signaling through adapter proteins. Oncogene 2000 Nov 20;19(49):5582-9.

(323) Deheuninck J, Goormachtigh G, Foveau B, Ji Z, Leroy C, Ancot F, et al. Phosphorylation of the MET receptor on juxtamembrane tyrosine residue 1001 inhibits its caspase-dependent cleavage. Cell Signal 2009 Sep;21(9):1455-63.

(324) Tulasne D, Deheuninck J, Lourenco FC, Lamballe F, Ji Z, Leroy C, et al. Proapoptotic function of the MET tyrosine kinase receptor through caspase cleavage. Mol Cell Biol 2004 Dec;24(23):10328-39.

(325) Follenzi A, Bakovic S, Gual P, Stella MC, Longati P, Comoglio PM. Cross-talk between the proto-oncogenes Met and Ron. Oncogene 2000 Jun 22;19(27):3041-9.

(326) Benvenuti S, Lazzari L, Arnesano A, Li CG, Gentile A, Comoglio PM. Ron Kinase Transphosphorylation Sustains MET Oncogene Addiction. Cancer Res 2011 Mar 1;71(5):1945-55.

(327) Park HS, Kim KR, Lee HJ, Choi HN, Kim DK, Kim BT, et al. Overexpression of discoidin domain receptor 1 increases the migration and invasion of hepatocellular carcinoma cells in association with matrix metalloproteinase. Oncol Rep 2007 Dec;18(6):1435-41.

(328) Perez JL, Jing SQ, Wong TW. Identification of two isoforms of the Cak receptor kinase that are coexpressed in breast tumor cell lines. Oncogene 1996 Apr 4;12(7):1469-77.

(329) Castro-Sanchez L, Soto-Guzman A, Navarro-Tito N, Martinez-Orozco R, Salazar EP. Native type IV collagen induces cell migration through a CD9 and DDR1-dependent pathway in MDA-MB-231 breast cancer cells. Eur J Cell Biol 2010 Nov;89(11):843-52.

(330) Ongusaha PP, Kim JI, Fang L, Wong TW, Yancopoulos GD, Aaronson SA, et al. p53 induction and activation of DDR1 kinase counteract p53-mediated apoptosis and influence p53 regulation through a positive feedback loop. EMBO J 2003 Mar 17;22(6):1289-301.

(331) Faraci-Orf E, McFadden C, Vogel WF. DDR1 signaling is essential to sustain Stat5 function during lactogenesis. J Cell Biochem 2006 Jan 1;97(1):109-21.

(332) Anderton JA, Bose S, Vockerodt M, Vrzalikova K, Wei W, Kuo M, et al. The H3K27me3 demethylase, KDM6B, is induced by Epstein-Barr virus and over-expressed in Hodgkin's Lymphoma. Oncogene 2011 Jan 17.

(333) Wang CZ, Su HW, Hsu YC, Shen MR, Tang MJ. A discoidin domain receptor 1/SHP-2 signaling complex inhibits alpha2beta1-integrin-mediated signal transducers and activators of transcription 1/3 activation and cell migration. Mol Biol Cell 2006 Jun;17(6):2839-52.

(334) Smyth GK, Michaud J, Scott HS. Use of within-array replicate spots for assessing differential expression in microarray experiments. Bioinformatics 2005 May 1;21(9):2067-75.

(335) Jonsson M, Andersson T. Repression of Wnt-5a impairs DDR1 phosphorylation and modifies adhesion and migration of mammary cells. J Cell Sci 2001 Jun;114(Pt 11):2043-53.

(336) Ikeda K, Wang LH, Torres R, Zhao H, Olaso E, Eng FJ, et al. Discoidin domain receptor 2 interacts with Src and Shc following its activation by type I collagen. J Biol Chem 2002 May 24;277(21):19206-12.

(337) Yoshida D, Teramoto A. Enhancement of pituitary adenoma cell invasion and adhesion is mediated by discoidin domain receptor-1. J Neurooncol 2007 Mar;82(1):29-40.

(338) Joos S, Kupper M, Ohl S, von BF, Mechtersheimer G, Bentz M, et al. Genomic imbalances including amplification of the tyrosine kinase gene JAK2 in CD30+ Hodgkin cells. Cancer Res 2000 Feb 1;60(3):549-52.

(339) Krause DS, Van Etten RA. Tyrosine kinases as targets for cancer therapy. N Engl J Med 2005 Jul 14;353(2):172-87.

(340) Weisberg E, Choi HG, Barrett R, Zhou W, Zhang J, Ray A, et al. Discovery and characterization of novel mutant FLT3 kinase inhibitors. Mol Cancer Ther 2010 Sep;9(9):2468-77.

(341) Day E, Waters B, Spiegel K, Alnadaf T, Manley PW, Buchdunger E, et al. Inhibition of collagen-induced discoidin domain receptor 1 and 2 activation by imatinib, nilotinib and dasatinib. Eur J Pharmacol 2008 Dec 3;599(1-3):44-53.

(342) Nam S, Williams A, Vultur A, List A, Bhalla K, Smith D, et al. Dasatinib (BMS-354825) inhibits Stat5 signaling associated with apoptosis in chronic myelogenous leukemia cells. Mol Cancer Ther 2007 Apr;6(4):1400-5.

(343) Ellis PM, Kaiser R, Zhao Y, Stopfer P, Gyorffy S, Hanna N. Phase I open-label study of continuous treatment with BIBF 1120, a triple angiokinase inhibitor, and pemetrexed in pretreated non-small cell lung cancer patients. Clin Cancer Res 2010 May 15;16(10):2881-9.

(344) Huynh H. Molecularly targeted therapy in hepatocellular carcinoma. Biochem Pharmacol 2010 Sep 1;80(5):550-60.

(345) Miknyoczki SJ, Chang H, Klein-Szanto A, Dionne CA, Ruggeri BA. The Trk tyrosine kinase inhibitor CEP-701 (KT-5555) exhibits significant antitumor efficacy in preclinical xenograft models of human pancreatic ductal adenocarcinoma. Clin Cancer Res 1999 Aug;5(8):2205-12.

(346) Hexner EO, Serdikoff C, Jan M, Swider CR, Robinson C, Yang S, et al. Lestaurtinib (CEP701) is a JAK2 inhibitor that suppresses JAK2/STAT5 signaling and the proliferation of primary erythroid cells from patients with myeloproliferative disorders. Blood 2008 Jun 15;111(12):5663-71.

(347) Knapper S, Mills KI, Gilkes AF, Austin SJ, Walsh V, Burnett AK. The effects of lestaurtinib (CEP701) and PKC412 on primary AML blasts: the induction of cytotoxicity varies with dependence on FLT3 signaling in both FLT3-mutated and wild-type cases. Blood 2006 Nov 15;108(10):3494-503.

(348) Weisberg E, Boulton C, Kelly LM, Manley P, Fabbro D, Meyer T, et al. Inhibition of mutant FLT3 receptors in leukemia cells by the small molecule tyrosine kinase inhibitor PKC412. Cancer Cell 2002 Jun;1(5):433-43.

(349) Holz M, Janning A, Renne C, Brauninger A. Effects of receptor tyrosine kinase inhibitors on Hodgkin's lymphoma. Haematologica . 2010.

(350) Marshall JL, Kindler H, Deeken J, Bhargava P, Vogelzang NJ, Rizvi N, et al. Phase I trial of orally administered CEP-701, a novel neurotrophin receptor-linked tyrosine kinase inhibitor. Invest New Drugs 2005 Jan;23(1):31-7.

(351) Angevin E, Lopez J.A., Pande A, Moldova C. TKI258 (dovitinib lactate) in metastatic renal cell carcinoma (mRCC) patients refractory to approved targeted therapies: A phase I/II dose finding and biomarker study. J.Clin.Oncol. 27, 3563. 2009.

(352) Lopes de Menezes DE, Peng J, Garrett EN, Louie SG, Lee SH, Wiesmann M, et al. CHIR-258: a potent inhibitor of FLT3 kinase in experimental tumor xenograft models of human acute myelogenous leukemia. Clin Cancer Res 2005 Jul 15;11(14):5281-91.

(353) Fathi A, Levis M. FLT3 inhibitors: a story of the old and the new. Curr Opin Hematol 2011 Mar;18(2):71-6.

(354) Dewan MZ, Watanabe M, Ahmed S, Terashima K, Horiuchi S, Sata T, et al. Hodgkin's lymphoma cells are efficiently engrafted and tumor marker CD30 is expressed with constitutive nuclear factor-kappaB activity in unconditioned NOD/SCID/gammac(null) mice. Cancer Sci 2005 Aug;96(8):466-73.

APPENDIX I

HISTOLOGY OF PARAFFIN EMBEDDED PAEDIATRIC SAMPLES

Centre/ ID code	*Pathological sub-classification*
Belfast (3)	
j05/6369	Nodular sclerosis (type II)
4638/99	Nodular sclerosis
j04/22990	Nodular sclerosis
j02/10600	Nodular sclerosis
j01/6150	Hodgkin's disease
j01/25554	Hodgkin's disease
BCH (4)	
234	Nodular sclerosis
252	Nodular sclerosis
22	Nodular sclerosis
251	Nodular sclerosis
186	Nodular sclerosis
409	Nodular sclerosis
512	Nodular sclerosis
140	Nodular sclerosis
210	Nodular sclerosis (cellular phase)
402	Nodular sclerosis (grade II)
499	Nodular sclerosis
340	Nodular sclerosis
53	Lymphocytic predominance cervical node
35	Nodular sclerosis (type I)
Cardiff (7)	
306	Nodular sclerosis
132	Nodular sclerosis
289	Hodgkin’s disease
291	Nodular sclerosis
404	Mixed cellularity
373	Nodular sclerosis
130	Nodular sclerosis
135	Nodular sclerosis (type I)
382	Nodular sclerosis (type I)
352	Nodular sclerosis
147	Nodular lymphocyte predominance HD
310	Nodular sclerosis

Liverpool (14)	
172	Nodular sclerosis
169	Nodular sclerosis
193	Nodular lymphocyte predominance HD
170	Nodular sclerosis
219	classical Hodgkin's disease
74	Nodular sclerosis
159	Mixed cellularity
223	Mixed cellularity
160	Nodular sclerosis
235	Nodular sclerosis
208	Nodular sclerosis
207	Nodular sclerosis
225	Mixed cellularity
224	Nodular sclerosis
71	Mixed cellularity
Newcastle (16)	
461	Mixed cellularity
457	Mixed cellularity
419	Nodular sclerosis (type I)
390	classical Hodgkin's disease
443	Nodular sclerosis
462	Lymphocytic predominance nodular
375	Nodular sclerosis (grade II)
Southampton (22)	
0519541k	Mixed cellularity
5249515	Mixed cellularity
s17602.03	Lymphocytic predominance nodular
s2489b.04	Lymphocytic predominance nodular